THE REGULATION AND ESSENTIAL FUNCTIONS OF MATRIX METALLOPROTEINASES DURING WOUND HEALING

By

Laura Jeanette Stevens

Dissertation

Submitted to the Faculty of the

Graduate School of Vanderbilt University

in partial fulfillment of the requirements

for the degree of

DOCTOR OF PHILOSOPHY

in

Cell and Developmental Biology

May, 2012

Nashville, Tennessee

Approved:

Professor Andrea Page-McCaw

Professor David Miller

Professor Laura Lee

Professor Jeff Davidson

Professor Jason Jessen

"Healing is a matter of time, but sometimes also a matter of opportunity"

-Hippocrates

ACKNOWLEDGEMENTS

As with any momentous undertaking, completion of a dissertation is never accomplished alone. I would like to take this opportunity to thank all those who have helped me during my academic pursuits and in the completion of my dissertation. First and foremost, I would like to thank my advisor, Prof. Andrea Page-McCaw, who not only provided the financial support for this work, but her guidance, patience, and attention to detail has allowed me to develop as a scientist. Without her scientific insight and extensive knowledge of the MMP field this project would not have been as successful.

I would like to thank all the past and present members of the Andrea Page-McCaw lab group for day-to-day comradery, as well as helpful scientific discussion. I would especially like to thank our amazing previous lab manager Bernadette Glasheen, without her dedication and organization, our lab at Rensselaer Polytechnic Institute would not have run remotely as smoothly, or be as pleasant to work in as it was. Bernie was also an irreplaceable resource for troubleshooting experiments and discussing experimental design, particularly when it came to molecular biology techniques. A special thank you also goes to our current lab technician, Kimi LaFever for her amazing ability to anticipate the needs of the lab, handling all the daily incidentals associated with a busy lab space. Kimi was also an invaluable resource for all information Vanderbilt and Nashville throughout my tenure at Vanderbilt. I also cannot thank my friend,

neighbor, and fellow graduate student in the Page-McCaw lab, Sarah Broderick, enough for always being available to discuss unexpected results, design new experiments, deal with the everyday stresses of graduate school, and for being a great friend and social relief from the daily grind of lab work and graduate school.

I would like to thank all of my committee members, both from my first thesis committee at Rensselaer Polytechnic Institute: Prof. Lee Ligon, Prof. Livingston Van De Water, and Prof. Fern Finger, as well as my current thesis committee at Vanderbilt: Prof. Laura Lee, Prof. Jeff Davidson, Prof. David Miller, and Prof. Jason Jessen, for their constructive feedback on my work. I would especially like to thank my current committee members for taking the time to critically read my thesis.

I would like to thank my parents, Mike and Jeanette Stevens, who have supported me through my seemingly endless career as a student. I would also like to thank my brother, Dennis Stevens, for providing frequent distractions. Without the never-ending love and support of my family, I could not have achieved this academic milestone.

Special thanks go out to all my friends who patiently provided emotional support and a social outlet during my time as a graduate student, without them I would not have been able to mentally and emotionally handle the stress of completing all my academic pursuits.

Lastly I would like to thank Dr. Carlton Hoyt for his insurmountable faith in my abilities, his continuous optimism, and for his patience while dealing with all my stress associated with both graduate school and transferring to Vanderbilt, as well as for convincing me to stop drinking coffee. It is hard to believe that I wrote the vast majority of this document un-caffeinated, but I am convinced that doing so made the anxiety associated with this process more manageable. I cannot image what graduate school would have been like, without Carlton's support and encouragement.

TABLE OF CONTENTS

Page

ACKNOWLEDGMENTS iv

LIST OF FIGURES xii

LIST OF ABBRVIATIONS xiv

Chapter

I. INTRODUCTION 1

Fundamentals of wound healing 2
Inflammation 2
Re-epithelialization 6
Scar Formation 10
Models to study wound healing 13
Matrix metalloproteinases 16
Structure 16
Function 19
MMPs in *Drosophila melanogaster* 21

II. A SECRETED MMP IS REQUIRED FOR RE-EPITHELIALIZATION DURING WOUND HEALING 25

Introduction 25
Methods 28
Fly lines 28
Wounding assays 29
Dissections, fixation, immunohistochemistry 30
Microscopy 31
Wound measurements 31
Expression analysis 32
Western blotting 34

Results....36
Both *Drosophila* MMPs are required for re-epithelialization....14
Mmp1 is required in the epidermis for re-epithelialization....41
Mmp1 is up-regulated in the epidermis in response to wounding....45
Mmp1 promotes assembly or maintenance of the basement membrane....48
Mmp1 is required for migration after wounding....53
Mmp1 promotes ERK activation....59
Mmp1 is regulated by JNK signaling during wound healing....63
Discussion....67
Mmp1 promotes assembly and repair of the basement membrane....67
Mmp1 levels are regulated by JNK in response to wounding....69

III. MATRIX METALLOPROTEINASES ARE REQUIRED FOR HEMOSTASIS IN *DROSOPHILA*....71

Introduction....71
Methods....75
Fly lines....75
Clotting kinetics....75
Scab formation analysis and quantification....76
Immunohistochemistry....77
Microscopy....78
Melanization inhibition assay....79
Wounding assays....79
Results....80
Mmp1 is required for hemostasis and scab formation....80
Mmp1 may be required in both hemocytes and epidermis for scab formation....83
Mmp1 and *Mmp2* function to regulate melanization....85
Mmp1 may function downstream of Spn27A during scab formation....88
Re-epithelialization is not dependent on scab formation....91

Mmp1 is required for re-epithelialization in pinch wounds 94
Discussion 98
Mmp1 and *Mmp2* regulate scab formation 98
Re-epithelialization is not dependent on scab formation 102

IV. *DROSOPHILA Mmp1* MAY FUNCTION IN HEMOCYTES TO REGULATE INFLAMMATION DURING WOUND HEALING 104

Introduction 104
Methods 109
Fly lines 109
Ex vivo bleeding assay 109
Wounding assay 110
Immunohistochemistry 110
Microscopy 111
Wound measurements 112
Expression analysis 112
Cell culture 113
Results 115
Mmp1 is up-regulated in hemocytes post-wounding 115
Hematopoietic *Mmp1.f2* may be required for re-epithelialization 118
Mmp1.f1 is up-regulated in response to wounding 125
Hematopoietic Mmp1 is regulated by JNK signaling 129
Mmp1 is only expressed in a subpopulation of hemocytes at the wound site 130
Mmp1 plays a role in regulating JNK signaling 136
Hematopoietic Mmp1 may function to restrict the area of ERK signaling 141
Discussion 145

V. *DROSOPHILA Mmp1, Mmp2,* AND *Timp* MAY FUNCTION TOGETHER DURING WOUND HEALING 153

Introduction 153
Methods 157
Fly lines 157

Wounding assays and *ex vivo* bleeds....158
Immunohistochemistry....158
Microscopy....159
Expression analysis....159
Wound measurements....161
Cell culture....161
Co-immunoprecipitation....162
Western blotting....164
Results....165
Mmp2 and *Timp* are required for Mmp1 localization....165
Mmp2 and *Timp* are required for re-epithelialization....171
The Mmp1 hemopexin domain is required for re-epithelialization....174
Mmp2 and *Timp* are required to promote cell elongation....176
Mmp1 and *Timp* function independent from *Mmp2* for ECM maintenance....178
Mmp2 and *Timp* are required for wound-induced Mmp1 up-regulation....187
Mmp1, Mmp2, and Timp do not co-localize in S2 cultured cells....190
Discussion....195
An Mmp2/Mmp1/Timp tri-molecular complex may be required *in vivo* for wound healing....196
Mmp1 and Mmp2 function independently during normal ECM maintenance....200

VI. CONCLUSIONS & DISCUSSION....203
VII. FUTURE DIRECTIONS....209

Appendix

A. SEQUENCE COMPARISON BETWEEN *MMP1* ISOFORMS....217
Methods....221
Sequence analysis....221

B. ECM DEFECTS MAY NOT BE SUFFICIENT TO INDUCE RE-EPITHELIALIZATION DEFECTS 222
Introduction 222
Methods 223
Fly lines 223
Wounding assays and immunohistochemistry 223
Microscopy 224
Wound area measurements 224
Results and Discussion 225

REFERENCES 230

LIST OF FIGURES

Figure Page

Chapter I

1.1 Inflammation 6
1.2 Re-epithelialization 10
1.3 Scar formation 12
1.4 *Drosophila* larval epidermis 16
1.5 Basic structure of MMPs 17
1.6 Domain structure of *Drosophila* MMPs 22

Chapter II

2.1 Each *Drosophila* MMP is required for re-epithelialization 40
2.2 Epidermal *Mmp1* is required for re-epithelialization 43
2.3 Mmp1-dsRNA knock-down efficiency 44
2.4 Mmp1 is up-regulated at the wound site 47
2.5 Mmp1 is up-regulated in pinch wounds 48
2.6 Mmp1 is required for ECM remodeling and maintenance 52
2.7 Wound-induced cell elongation changes 55
2.8 *Mmp1* is required for leading edge cell migration 57
2.9 Mmp1 co-localizes with β-integrin post-wounding 59
2.10 Wound-induced changes in wild-type dpERK intensity 61
2.11 Mmp1 promotes wound-induced ERK activation 62
2.12 Mmp1 is positively regulated by JNK signaling during wound healing 66

Chapter III

3.1 *Mmp1* is required for scab formation 83
3.2 Mmp1 expression is required in both hemocytes and epidermis for melanization 85
3.3 Scab phenotype is not indicative of re-epithelialization phenotype 88
3.4 Mmp1 may function downstream of Spn27A during scab formation 91
3.5 Re-epithelialization is not dependent on scab formation 94
3.6 *Mmp1* is required for re-epithelialization after pinch wounding 97

Chapter IV

4.1 Mmp1 is up-regulated in hemocytes post-wounding 117
4.2 Mmp1.f2 is required for re-epithelialization in hemocytes 124
4.3 Re-epithelialization comparison: *He-GAL4* v. *Hml-GAL4* 125
4.4 Anti-Mmp1 isoform specificity in S2 cultured cells....127
4.5 Mmp1.f1 is up-regulated in both epidermis and hemocytes post-wounding 128
4.6 Hematopoietic Mmp1 is up-regulated by JNK signaling 130
4.7 Mmp1 is expressed only in a subpopulation of hemocytes at the wound site....135
4.8 *Mmp1* plays a role in regulating JNK signaling....140
4.9 *Mmp1* promotes dpErk accumulation....144

Chapter V

5.1 *Mmp2* and *Timp* are required for Mmp1 localization in the epidermis 170
5.2 *Mmp2* and *Timp* are required for re-epithelialization....173
5.3 Mmp1 hemopexin domain is required for re-epithelialization....176
5.4 *Mmp2* and *Timp* are required for cell elongation....178
5.5 *Mmp1* and *Timp* are required for ECM maintenance....185
5.6 *Mmp1* is required for collagen deposition in ECM 186
5.7 Wound-induced Mmp1 up-regulation requires *Mmp2* and *Timp* 190
5.8 Mmp1, Mmp2, and Timp do not co-localize in S2 cells 194
5.9 Model: Mmp2, Timp, and Mmp1 may form a tri-molecular complex *in vivo* 197

Appendix A

A.1 Sequence comparison between predicted *Mmp1* isoforms 219

Appendix B

B.1 ECM defects may not be sufficient to cause re-epithelialization defects....227

ABBREVIATIONS

A	Alanine
aa	Amino acid
Bc	*Black cell*
Bsk	*Basket*
C. elegans	*Caenorhabditis elegans*
Ca^{2+}	Calcium ion
$CaCl_2$	Calcium chloride
CFP	Cyan fluorescent protein
Cg25C	*Collagen at 25C*
ColIV	Collagen type IV
$CuSO_4$	Copper (II) sulfate
Cy3	Cyanine 3
CyO	*Curly O*
Cys	Cysteine
DAPI	4′, 6-diamidino-2-pheynlindole
Dm	*Drosophila melanogaster*
DMSO	Dimethyl sulfoxide
DN	Dominant-negative
DNA	Deoxyribonucleic acid
Dom	*Domino*
dpErk	di-phosphorylated extracellular signal-related kinase
DSHB	*Drosophila* Studies Hybridoma Bank

dsRNA	Double-stranded RNA
E	Glutamic acid
ECM	Extracellular matrix
EDTA	Ethylenediaminetetraacetic acid
EGF	Epidermal growth factor
Egr	*Eiger*
Egr	*Eiger*
EM	Electron microscopy
EMS	Ethyl methanesulfonate
ERK	Extracellular signal-related kinase
EST	Expressed sequence tag
FasIII	Fasciclin-III
FITC	Fluorescein isothiocyanate
GAPDH	Glyceraldehyde 3-phosphate dehydrogenase
GFP	Green fluorescent protein
GPI	Glycosylphosphatidylinisotol
h	Hour(s)
He	*Hemese*
HEPES	4-(2-hydroxyethyl)-1-piperazineethanesulfonic acid
Hid	*Head involution defective*
Hml	*Hemolectin*
IGF	Insulin-like growth factor
IgG1	Immunoglobulin G, subclass 1
IgG2a	Immunoglobulin G, subclass 2a

IgG2b	Immunoglobulin G, subclass 2b
IL-1	Interleukin-1
IL-4	Interleukin-4
INF-γ	Interferon-gamma
IP	Immunoprecipitation
JNK	Jun N-terminal kinase
KCl	Potassium chloride
LUT	Look-up table
$MgCl_2$	Magnesium chloride
min	Minute(s)
MMP	Matrix metalloproteinase
Na_2HSO_4	Disodium hydrogen phosphate
NaCl	Sodium chloride
$NaHCO_3$	Sodium bicarbonate
NaN_3	Sodium azide
NCBI	National Center for Biotechnology Information
PAGE	Polyacrylamide gel electrophoresis
PBS	Phosphate buffered saline
Pcan	Perlecan
PDGF	Platelet-derived growth factor
PO	Phenoloxidase
PPEA	Prophenoloxidse activating enzyme
PPO	Prophenoloxidase
PTU	Phenylthiourea

Puc	Puckered
Puc	*Puckered*
Pvf-1	PDGF / VEGF –related factor 1
Pxn	*Peroxidasin*
RNA	Ribonucleic acid
RNAi	RNA interference
ROI	Region of interest
ROS	Reactive oxygen species
RTK	Receptor tyrosine kinase
Spn27A	*Serpin 27A*
Syn	*Synapsin*
TBS	Tris-buffered saline
TGFβ	Transforming growth factor-beta
TIMP	Tissue inhibitor of metalloproteinases
TNF	Tumor necrosis factor
TNFα	Tumor necrosis factor-alpha
Trol	*Terribly reduced optic lobes*
Tub	*Tubulin*
Tx	TritionX-100
VDRC	Vienna *Drosophila* RNAi Center
Vkg	*Viking*
w	*white*
YFP	Yellow fluorescent protein
Zn^{2+}	Zinc ion

CHAPTER I

INTRODUCTION

Since the days of the first humans, man has been developing remedies to heal wounds. Artifacts describing treatment for an assortment of wound types date back to ancient Mesopotamia with the world's oldest medical text being a description of poultices inscribed on a Sumerian tablet dating to about 2158-2008B.C. (Majno, 1975). Throughout the ages a variety of methods were employed to stimulate healing from washing wounds in vinegar, as prescribed by Galen (court physician to Marcus Aurelius), to "allowing the wound to rot a bit," common in the Middle Ages, where wounds were left untreated until infection and pus developed, to the use of maggots to debride the wound of necrotic tissue (Broughton et al., 2006), a technique actually still used to treat some chronic wounds today. Even with all the medical advances afforded to physicians and patients of the 21st century, treatment of wounds, particularly chronic wounds, pose a serious health concern conferring a cost just in the United States of approximately $10 billion annually (Murphy, 2011), with chronic wounds affecting approximately 1-2% of the population (Hess and Kirsner, 2003; Murphy, 2011). A better understanding of the biological mechanisms involved

in wound healing will lead the development of novel therapeutic approaches, leading to an improvement in wound care.

Fundamentals of Wound Healing

Wound healing involves the precise orchestration of numerous cell types and signaling events in order to efficiently and effectively restore a continuous tissue. There are three basic, overlapping, phases of wound healing: inflammation, re-epithelialization, and scar formation (Singer and Clark, 1999). Impairments during any of these three phases can have deleterious consequences including sustained infection, prolonged inflammation, persistent open wounds or ulcerated wounds, and / or excessive fibrosis leading to formation of keloids or hypertrophic scars (Singer and Clark, 1999).

Inflammation.

Tissue injury is typically accompanied by a rapid inflammatory response, which is characterized by an influx of platelets and leukocytes that primarily function to facilitate hemostasis, neutralize external pathogens, and phagocytose damaged or dying cells (Singer and Clark, 1999). Within minutes of wounding the clotting cascade is activated, leading to the recruitment, aggregation, and degranulation of platelets forming the thrombus (Furie and Furie, 1992). The alpha granules released from activated platelets at wound sites function to provide the requisite membrane surface that facilitates the coordination of

clotting factors leading to the production of fibrin, and formation the fibrin clot, thus sealing the wound (Furie and Furie, 1992). Additionally, platelets stimulate the inflammatory response by releasing growth factors, such as platelet-derived growth factor (PDGF), transforming growth factor-beta (TGF-β), as well as pro-inflammatory cytokines such as interleukin-1 (IL-1) (modeled in Fig1.1), which promotes infiltration of immune responsive cells (Barrientos et al., 2008).

Wounding induces a rapid release of hydrogen peroxide, which has been shown in zebarafish to initiate the inflammatory response, stimulating the rapid recruitment of leukocytes (Niethammer et al., 2009). Neutrophils, or polymorphonuclear leukocytes, are effector cells of the innate immune system that are rapidly recruited to areas of tissue damage. As quickly as one day post-wounding, neutrophils comprise roughly 50% of the leukocytes found at the wound site (Engelhardt et al., 1998), attracted by chemoattractant gradients of IL-1, tumor necrosis factor-alpha (TNF-α), and interferon-gamma (IFN-γ) released from platelets, or possibly attracted by the clot itself (Brandt et al., 2000; Eming et al., 2007; Gillitzer and Goebeler, 2001). Once at the wound site, neutrophils degranulate, releasing numerous cytotoxic factors including reactive oxygen species (ROS) in order to neutralize invading pathogens, which will be subsequently phagocytosed along with damaged epidermal cells. Release of ROS also functions in the recruitment of macrophages and the propagation of the inflammatory response (Weiss, 1989). Studies have also shown that

neutrophils transcriptionally up-regulate a number of other cytokines, proteases, and growth factors known to the involved in promoting extracellular matrix (ECM) remodeling, angiogenesis, as well as migration and proliferation of keratinocytes and fibroblasts, indicating that neutrophils may play an important role in facilitating tissue repair (Theilgaard-Monch et al., 2004). In addition to neutralizing any external pathogens found in the wound site, the degranulation of neutrophils often results in collateral damage to the surrounding tissue, as the cytotoxic molecules released by neutrophils are also toxic to the host cells. Interestingly, studies suggest that neutrophils may actually act to delay wound closure, as wounds in mice devoid of neutrophils have been shown to close faster relative to controls (Dovi et al., 2003).

Shortly following the influx of neutrophils into the wound site, monocytes infiltrate the wound site, where they are converted into macrophages, in response to cues found in the wound milieu (Barrientos et al., 2008). Longer lived than neutrophils, macrophages can be found at the wound site throughout the wound healing process, including the final tissue remodeling phases (Brancato and Albina, 2011). Isolation of macrophages from various time points throughout wound healing have suggested that there are multiple subpopulations of macrophages, whose phenotypic expression profiles differ temporally and spatially (Brancato and Albina, 2011; Daley et al., 2010). Macrophages isolated early post-wounding express high levels of pro-

inflammatory cytokines, such as TNF-α, while macrophages isolated later express higher levels for pro-repair growth factors, such as TGF-β. Granulocytes, such as neutrophils, basophils, and mast cells, found in the wound also contribute to the activation of resident macrophages by secreting IL-4, which leads to the production of collagen and polyamines through IL-4 induced arginase activity in the macrophage (Kreider et al., 2007; Mosser and Zhang, 2008). Similar to neutrophils, macrophages are also "professional" phagocytes that function to engulf pathogens and cell debris. As the wound ages, neutrophils undergo apoptosis and are cleared by wound macrophages (Meszaros et al., 2000). Growth factors, such as fibroblast growth factor (FGF), epidermal growth factor (EGF), PDGF, and TGF-β, are also released by macrophages at the wound site to stimulate cell migration, initiating the proliferative phase of wound healing (Barrientos et al., 2008). Despite all the evidence that macrophages play an integral role in wound healing, mice devoid of macrophages are able to close wounds at rates similar to controls. In fact these mice are reported to also have a reduced inflammatory response and less scarring (Martin et al., 2003), suggesting that while initially inflammation may play a role in minimizing infection and promoting repair, minimizing the inflammatory response may actually improve the outcome of tissue repair.

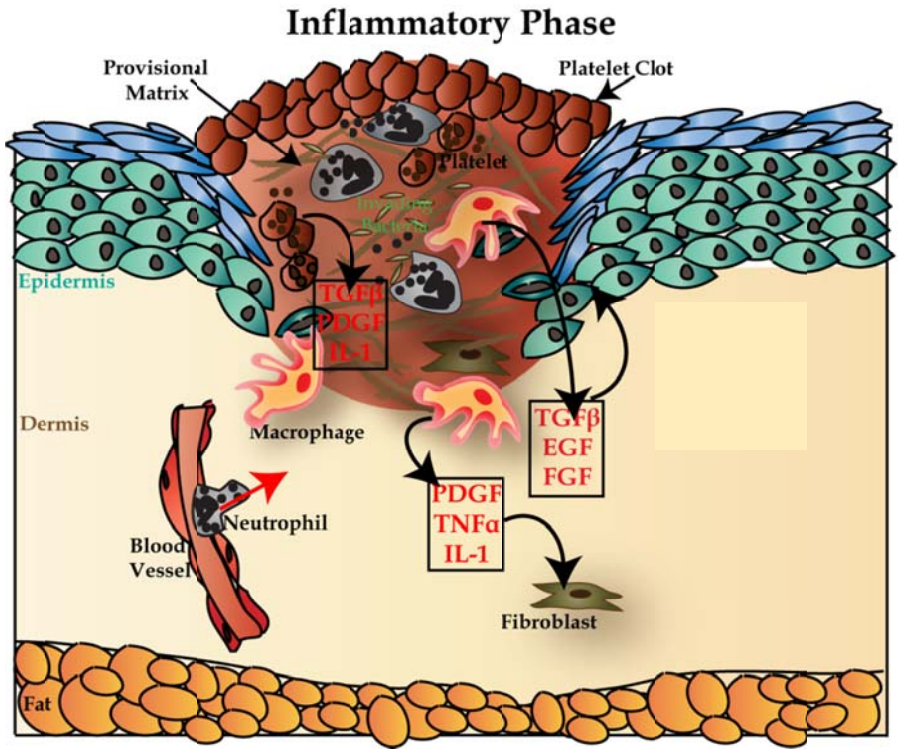

Figure 1.1: Inflammation.
Immediately following wounding platelets are recruited to the wound site, where they aggregate, degranulate, and form a clot, preventing further fluid loss. Platelets release pro-inflammatory cytokines, such as PDGF and IL-1, which activates local blood vessels, allowing for neutrophil extravasation, and recruitment to the wound site. At the wound site, neutrophils function to debride the wound of cell debris and pathogens by phagocytosis and the release cytotoxic granules and pro-inflammatory cytokines, to neutralize invading pathogens and propagate the inflammatory response, stimulating the recruitment of monocytes and macrophages. In addition to engulfing damaged epithelial cells, pathogens, and apoptotic neutrophils, macrophages secrete both pro-inflammatory cytokines and growth factors that stimulate epithelial cell migration and the recruitment of fibroblasts, thus promoting tissue repair. Red arrow represents direction of migration. Curved black arrows indicate the flow of signaling molecules from sources to targets. Model is for illustrative purposes only and is not drawn to scale.

Re-epithelialization.

Re-epithelialization, the second phase of wound healing, also known as the proliferative phase, is characterized by cell migration and proliferation with the purpose of restoring a complete and functional tissue (Fig1.2), as well as angiogenesis, to replace the damaged vasculature, and the formation of

granulation tissue, establishing a provisional matrix to support cell migration. In mammals, unwounded epidermis is a stratified tissue composed of multiple cell layers with older or dead cells, resting above younger cells, which sit on a layer of extracellular molecules, which compose the basement membrane (Silverthorn, 2004). Prior to epidermal cell migration into the wound bed, a matrix must be established, providing a scaffold to support migrating cells (Singer and Clark, 1999). Along with neutrophils and macrophages, fibrocytes, bone-marrow derived cells that have features of both monocytes and fibroblasts (Bucala et al., 1994), are recruited to the wound site where they function to promote angiogenesis, through secretion of vascular endothelial growth factor (VEGF) and PDGF, among other growth factors (Chesney et al., 1998; Hartlapp et al., 2001). In cell culture, fibrocytes have also been shown to promote ECM component production, aiding in granulation tissue formation (Abe et al., 2001; Bucala et al., 1994), although evidence of an *in vivo* function for fibrocytes remains unclear. Fibroblasts found in the wound bed respond to both growth factors secreted by macrophages (Fig. 1.1) and potentially signals released from the damaged ECM by producing collagen and other ECM components to establish a provisional matrix (Grinnell, 1994).

As cells move into the wound bed, they release matrix metalloproteinases (MMPs) to modify the provisional fibrin matrix and establish a collagen-based matrix to facilitate migration (Pilcher et al., 1997). Keratinocytes at the wound edge remodel their actin cytoskeleton to facilitate migration, as well as modify

cell-ECM adhesions, largely through modifications of integrins, heterodimeric transmembrane cell surface receptors that mediate cell-ECM adhesion (Cavani et al., 1993; Hynes, 2002; Juhasz et al., 1993). Integrins play a role in promoting cell proliferation as well, as seen in integrin α9 null mice, which have proliferation defects resulting in a thinner migrating epithelium following cutaneous wounding (Singh et al., 2009). Regulation of cell-cell and cell-ECM adhesion is critical for epithelial cell movement, as movement requires the generation of forces through actin polymerization coupled with cell adhesions (Lauffenburger and Horwitz, 1996; Mitchison and Cramer, 1996). If the cell is unable to generate enough force, it cannot progress forward.

As with all aspects of wound healing, re-epithelialization is a tightly regulated process. The signals that initiate cell migration are unclear; however, data, primarily from cell culture, have implicated several signaling cascades with promoting cell migration, including the receptor tyrosine kinase (RTK) and Jun N-Terminal kinase (JNK) signaling pathways (Galko and Krasnow, 2004a; Matsubayashi et al., 2004b; Sharma et al., 2003). Activated by growth factors, including PDGF and VEGF, RTK signaling activation leads to the activation of extracellular-related kinase (ERK) and promotes migration of epidermal cell sheets following scratch assays in cell culture (Lemmon and Schlessinger, 2010; Matsubayashi et al., 2004b), as well as *in vivo* in *Drosophila* larvae (Wu et al., 2009b). In mice, ERK-dependent cell migration is activated by an increase in calcium (Ca^{2+}), which is released by damaged keratinocytes and propagates in

waves through the epidermis surrounding the wound site (Leiper et al., 2006). On a side note, increases in intracellular calcium are also required for cell proliferation following injury (Sung et al., 2003). ERK has been shown to induce transcriptional activation of genes that promote cell motility and invasiveness (Doehn et al., 2009b), further implicating ERK signaling as an important regulator of cell migration, and presumably re-epithelialization. In a *Drosophila in vivo* model, JNK signaling has been shown to also be required for re-epithelialization as wounds in *Basket* (*Bsk*), or *Drosophila* JNK, fail to close (Galko and Krasnow, 2004a). While there is substantial evidence from both cell culture and *in vivo* models specifying signaling cascades that are involved in regulating re-epithelialization, further research is required to elucidate effectors of these pathways in order to understand precisely how re-epithelialization is regulated.

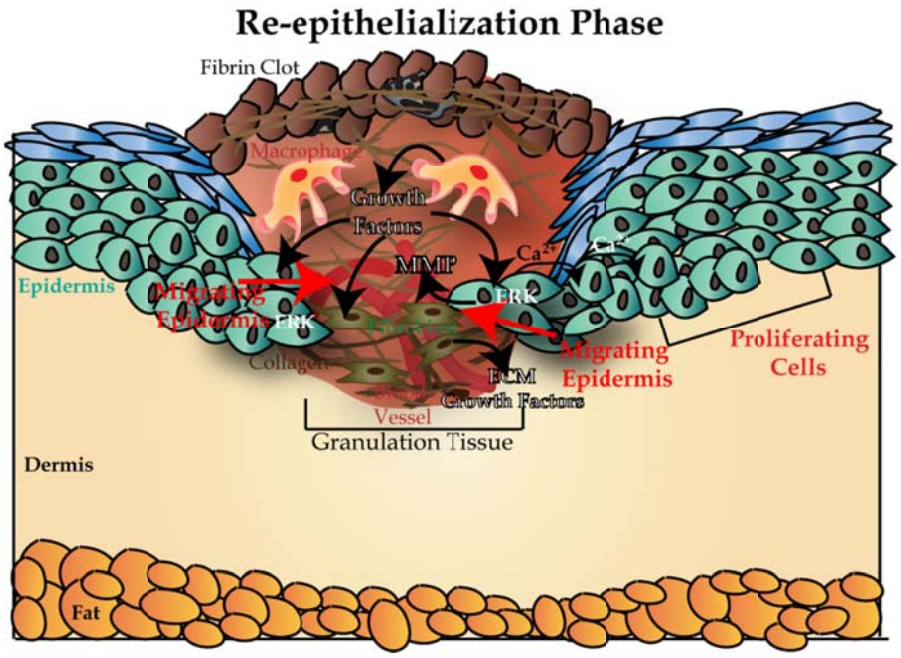

Figure 1.2: Re-epithelialization.
Re-epithelialization, the second phase of wound healing, is characterized by epidermal cell migration into the wound site in response to growth factors secreted by macrophages and ERK signaling. Keratinocytes behind the migratory front proliferate in response to cues from growth factors and Ca^{2+}. Fibroblasts found in the wound site, promote the formation of granulation tissue and provisional matrix formation by depositing ECM components into the wound bed. As epithelial cells migrate, they secrete MMPs, remodeling the provisional matrix and facilitating cell invasion. Factors produced by both macrophages and fibrocytes function to promote angiogenesis, thus restoring the blood vessels damaged during wounding. The red arrows indicate the direction of migration. The black arrows represent the flow of signaling molecules from sources to targets. Model is for illustrative purposes only and is not drawn to scale.

Scar formation.

The final phase of wound healing, or scar formation (fig 1.3), largely occurs once a continuous epithelium has been reestablished and functions to remodel the granulation tissue, increasing the tensile strength of the newly healed tissue. Interestingly, the resulting scar tissue typically only has approximately 70% of the tensile strength of unwounded tissue (Levenson et al., 1965; Singer and Clark, 1999). Once a continuous epithelium has been restored

epidermal cells cease migrating, reestablish cell-ECM adhesions and resume the quiescent phenotypes of unwounded epidermis (Gipson et al., 1988; Martin, 1997). Contraction of the wound bed is largely the function of myofibroblasts, fibroblasts with large α-smooth muscle actin (α-SMA) stress fibers (Desmouliere, 1995), which when stimulated by TGF-β, remodel the ECM by applying strong constrictive forces to the matrix, as well as release MMPs to cleave ECM components (Gill and Parks, 2008; Grinnell, 1994; Vyalov et al., 1993). Myofibroblast differentiation can be prevented in keratinocyte / fibroblast co-culture by exogenous application of IL-1 (Shephard et al., 2004), which has been shown to induce apoptosis in primary myofibroblasts, cultured from corneal epithelial wounds (Kaur et al., 2009), suggesting that cytokines are important regulators of myofibroblast differentiation and wound contraction. Delays in wound healing can occur as a result of failed wound contraction, as found in MMP-3 null mice (Bullard et al., 1999a), thus indicating that wound contraction and MMPs may play a critical role in enabling wound closure.

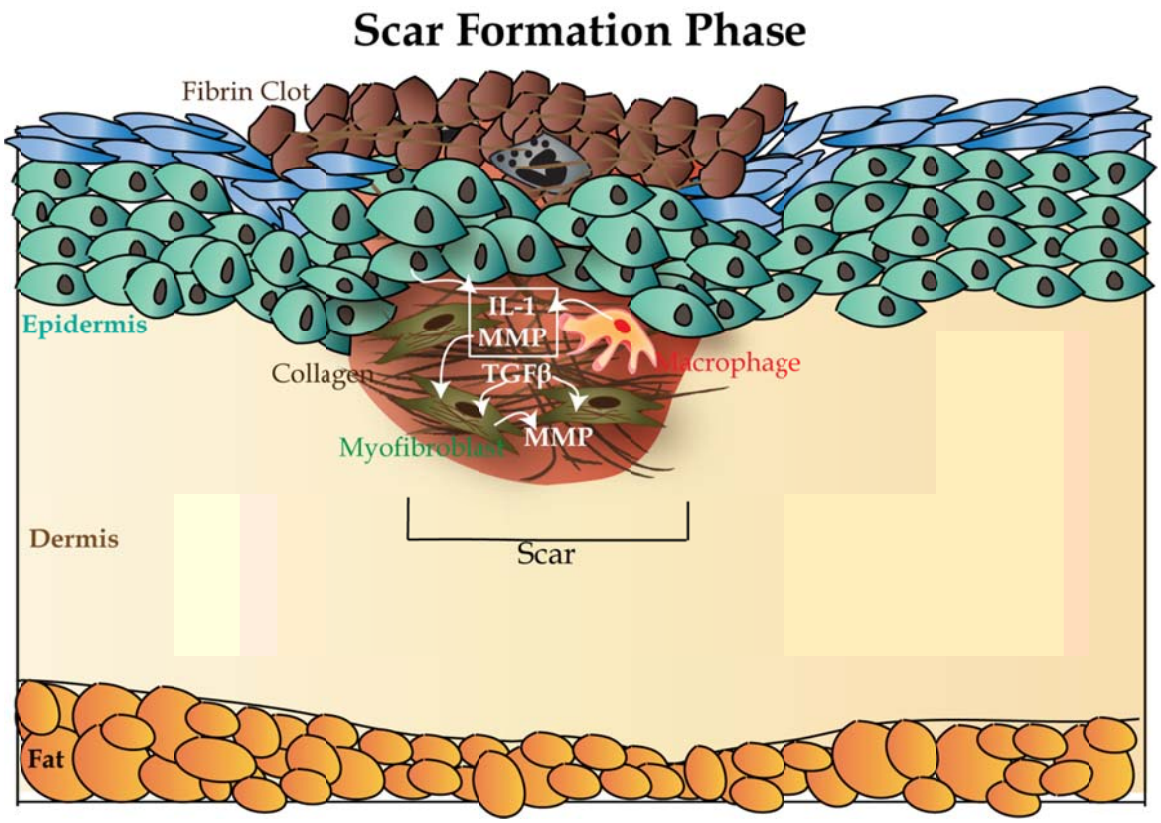

Figure 1.3: Scar Formation.
The third and final phase of wound healing, scar formation primarily occurs once a continuous epithelium has been reestablished. Cytokines, such as TGF-β and IL-1 are secreted from keratinocytes and macrophages, which play a role in promoting differentiation of myofibroblasts, characterized by the presence of α-SMA bundles. Myofibroblasts secrete MMPs and utilize contractile forces to contract the wound bed and remodel provisional matrix, increasing the tensile strength of the ECM underlying the newly reestablished tissue. White arrows designate the flow of signaling molecules involved during scar formation from source to target tissues. Model is for illustrative purposes only and is not drawn to scale.

Intriguingly, in embryos, scar formation does not occur and wounds are said to heal "perfectly" (Martin, 1997). Beyond being more aesthetically pleasing, understanding scar-less wound healing can potentially provide insights into mechanisms to minimize scar formation in adult tissues and prevent excessive scarring in disease states. The primary difference between embryonic wound healing and that in developed tissues is that the former heals by

regenerative processes, while the latter utilizes repair mechanisms (Larson et al., 2010). Wound healing in the early embryo induces minimal, if any, inflammatory response; whereas in tissues from older animals, a robust inflammatory response to wounding ensues (Krummel et al., 1987). Intriguingly, in PU.1 mice, mice with ineffective neutrophils and completely devoid of macrophages, not only are wounds able to heal within a similar timeframe as controls, but the wounds heal scarlessly (Martin et al., 2003). Mast cells are another immune response effecter cell that function at the wound site to secrete molecules that promote a variety of processes from inflammation to angiogenesis to collagen production (Hebda et al., 1993). Recent studies have implicated mast cells in inducing scar formation in E15 mice, a stage where wounds typically heal scarlessly, whereas ablation of mast cells in E18 mice, a stage where wounds typically scar, prevents scar formation (Wulff et al., 2012). These results suggest that by regulating the inflammatory response, it may be possible to induce scarless wound repair in adult tissues.

Models to study wound healing.

With a process as intricate as wound healing, naturally there are a myriad of models used to study it. Cultured cells represent the simplest model used to study wound healing, where scratch assays are used to study the events involved in wound healing on the level of a single cell. However, wound healing depends

on the interactions of multiple cell types, leaving cell culture models overly simplistic when it comes to trying to elucidate the regulatory mechanisms orchestrating the multiple cell types involved in wound healing. For that reason several *in vivo* models have been established for studying wound healing from using simple multicellular organisms, such as sponges, *Drosophila melanogaster*, and *Caenorhabditis elegans* (*C. elegans*) to vertebrate models such as amphibians, zebrafish and then of course mammals (Gurtner et al., 2008). Each system has a unique set of advantages and disadvantages, so choosing the proper model system should be determined by the question being asked, not simply by the tools at hand. Amphibians, particularly salamanders and planarians have the ability to completely regenerate amputated appendages through dedifferentiation of differentiated cells at the wound site, inducing blastema formation and the potential for regeneration of multiple cell types (Brockes and Kumar, 2002; Sanchez Alvarado, 2006). Elucidation of mechanisms that stimulate regeneration in models that naturally regenerate may provide insights as to how regeneration can be induced in organisms, such as humans, that employ repair mechanisms rather than regenerative mechanisms to heal wounds.

Genetically tractable organisms allow for *in vivo* characterization of biochemical pathways through genetic mutant analysis. Zebrafish larvae, as a genetically tractable model system, have the added advantage of being

translucent, a characteristic conducive to live-imaging experiments, which is particularly powerful for studying the events of wound healing in real time. For similar reasons, *Drosophila* embryos are also used to study wound healing in real-time (Stramer et al., 2005). Unlike vertebrates, *Drosophila* have an open circulatory system, so they cannot be used to study the signals involved in leukocyte extravasation or angiogenesis. However, *Drosophila* have a simple squamous epithelium (Fig. 1.4) (Martinez Arias, 1993a) that is beneficial for studying the mechanisms of re-epithelialization *in vivo* (Galko and Krasnow, 2004a; Wood et al., 2002b). As an established system for studying wound healing, *Drosophila* are also useful for studying the biochemical pathways involved in innate immune cell recruitment, hemostasis, and wound healing activation, as well as the *in vivo* dynamics of cell migration during wound healing on a cellular level (Razzell et al., 2011). At present there is no evidence for scar formation in *Drosophila*, but our data does indicate that ECM remodeling is required for re-epithelialization in *Drosophila* larvae.

Figure 1.4: *Drosophila* larval epidermis.
In *Drosophila* larvae the epidermis is a simple squamous epithelium with a single layer of thin epithelial cells resting on a extracellular basement membrane. The epidermal cells secrete a chitinous cuticle along the apical side that functions to provide rigidity to the body structure and protect the underlying epidermis. Cartoon is for illustrative purposes and is not drawn to scale.

Matrix Metalloproteinases

Structure.

Matrix metalloproteinases (MMPs) are zinc-dependent endopeptidases of the metzincin superfamily, characterized by a conserved methionine turn and a 3-histidine zinc binding motif in the catalytic site (Bode et al., 1993). Additionally, to be classified as an MMP, the protein at minimum must contain the conserved pro- and catalytic domains (Fig. 1.5A). Many MMPs also contain a hemopexin-like domain, structured as a 4-blade β-propeller (Fig. 1.5A), which functions as a substrate recognition domain (Bode et al., 1993; Ra and Parks, 2007). There are two types of MMP, a secreted type and a membrane anchored type (MT-MMP) (Fig. 1.5B). MMPs are anchored to the cell surface with either a transmembrane domain, or with a glycophophatidylinositol (GPI) anchor (Ra and Parks, 2007). In mammals, there are 24 MMPs (seventeen secreted and seven

membrane-anchored). Interestingly, two MMPs (MMP2 and MMP9) also contain three fibronectin type II repeats that bind collagens and gelatins (Allan et al., 1995; Massova et al., 1998; Steffensen et al., 1995).

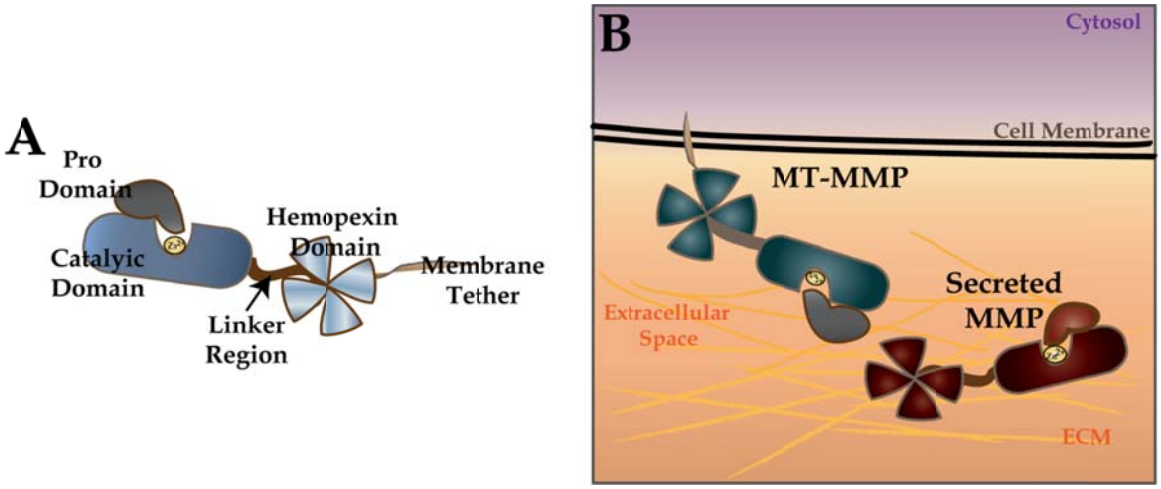

Figure 1.5: Basic structure of MMPs.
A) Typical domain structure of MMPs with a conserved pro-domain containing an N-terminal Cys that coordinates the Zn^{2+} ion found in the active site of the catalytic domain, also a conserved domain. Most MMPs also have a hemopexin-like domain that follows a flexible, proline-rich linker region. In membrane-anchored MMPs, a C-terminal membrane tether, either a transmembrane domain, or a GPI anchor, holds the protein at the cell surface. **B)** There are two types of MMP, a membrane-anchored type and a secreted type. Illustrations are not drawn to scale.

Secreted as zymogens, MMPs are regulated by four classic mechanisms: gene expression, compartmentalization (i.e. pericellular enzyme accumulation), zymogen activation, and enzyme inhibition / inactivation (Ra and Parks, 2007). In the latent form, an N-terminal Cysteine (Cys) residue on the pro-domain coordinates with the zinc ion (Zn^{2+}) found in the active-site of the catalytic domain, and functioning as a cysteine switch, inhibits the protease (Morgunova

et al., 1999; Sela-Passwell et al., 2010; Van Wart and Birkedal-Hansen, 1990). Membrane-anchored MMPs, and secreted MMP-11 and MMP-28, all contain a furin-cleavage consensus sequence, indicating that these MMPs can be activated intracellularly by furin, a proprotein convertase found in the Golgi (Massova et al., 1998; Santavicca et al., 1996; Thomas, 2002). For those MMPs that do not contain a furin cleavage site, there are several proposed activation mechanisms including homodimerization, or multidimerization, or interactions with other proteases (Lehti et al., 2002; Ra and Parks, 2007; Will et al., 1996b). *In vitro* assays have shown that MMP9 homodimer formation facilitates interactions with MMP3, leading to MMP9 activation (Goldberg et al., 1992; Olson et al., 2000). After wounding in mice, immunoprecipitation studies indicate that MMP9 and MMP8 are secreted from neutrophils as a heterodimer (Gutierrez-Fernandez et al., 2007a), suggesting that MMPs may function as complexes *in vivo*.

Once activated, one mechanism for MMP inhibition is through interactions with the endogenous inhibitors, Tissue inhibitor of metalloproteinases (TIMP). There are 4 TIMPs in vertebrates. TIMP, a wedge-shaped protein with a conserved N-terminal Cys, inhibits MMPs by binding to the MMP active site by chelating the Zn^{2+} ion (Fernandez-Catalan et al., 1998; Maskos and Bode, 2003; Olson et al., 2000). Functioning as an adaptor, TIMPs can also have non-inhibitory MMP interactions, by linking a membrane-anchored MMP to a secreted pro-MMP, through interactions with the hemopexin

domain of the secreted pro-MMP (Fernandez-Catalan et al., 1998; Gomis-Ruth et al., 1997; Itoh et al., 2001). While studies in cell culture suggest that an MT-MMP/TIMP/pro-MMP complex is required for pro-MMP activation and invasive cell behaviors (Itoh et al., 2001), *in vivo* evidence for the formation and functions of such a complex is unclear.

Function.

By definition, MMPs are able to cleave extracellular matrix (ECM) proteins, but that is not their exclusive function; MMPs have also been shown to process bioactive molecules, facilitating various cell signaling events (Gill and Parks, 2008; McQuibban et al., 2001). Up-regulated in virtually every type of human cancer, MMPs are associated with tumor progression and poor prognosis (Egeblad and Werb, 2002a). Recent studies have suggested that MT1-MMP may facilitate invasive tumor cell migration by degrading focal adhesions, thus allowing cell migration (Wang and McNiven, 2012). MMPs are also associated with other human diseases, such as arthritis, where MMP-1 and MMP-13, produced by synovial cells and chondrocytes, respectively, degrade collagen and aggrecan, a proteoglycan, leading to disease progression (Burrage et al., 2006). Due to their roles in disease states such as cancers and arthritis, MMPs are alluring therapeutic targets; however, more research is required to understand the normal physiological function of these versatile proteases before successful

drug candidates can be developed. Outside of disease states, MMPs have been shown to be required for the regulation of many tissue remodeling processes including bone formation, mammary formation, branching morphogenesis, and wound healing (Page-McCaw et al., 2007; Rebustini et al., 2009).

MMPs have been implicated to function during all three phases of wound healing (Gill and Parks, 2008). Beginning with hemostasis, studies in cultured platelets and *in vitro* have suggested that MMP-2 plays a role in platelet aggregation (Choi et al., 2008; Kazes et al., 2000), while MMP-12, -13, and -14 may play a role regulating clotting by cleaving the clotting factor, Factor XII (Hiller et al., 2000). Loss of the neutrophil collagenase (MMP-8) leads to an increased inflammatory response and delayed wound healing, as well as an increase in MMP-13 (Gutierrez-Fernandez et al., 2007a), suggesting that MMP-13 and MMP-8 may have redundant functions. MMP-13, under the control of the JNK signaling pathway, plays a role in mediating macrophage recruitment to wounds, as knockdown of MMP-13, in zebrafish, results in a dramatic reduction in the number of macrophages recruited to the wound site (Zhang et al., 2008). *In vitro* studies indicate that MMPs are able to proteolytically process chemokines, which are important for establishing the chemotactic gradients necessary for immune cell recruitment (McQuibban et al., 2001; McQuibban et al., 2000; McQuibban et al., 2002; Overall et al., 2002), suggesting that MMPs may play a key role in modulating the inflammatory response. Wound closure delays

are also observed in MMP-9 and MMP-13 null mice, which both cause a reduction in wound contraction and the formation of myofibroblasts (Hattori et al., 2009a). Interestingly, MMP-9/MMP-13 double mutants have an exacerbated wound closure phenotype (Hattori et al., 2009a), suggesting that MMP-13 and MMP-9 may have redundant functions. Work in cell culture has shown that MMP-1 functions to facilitate cell migration by modifying cell-ECM adhesions by cleaving integrins (Pilcher et al., 1997). MMP7 may play a similar role in facilitating re-epithelialization by modifying E-cadherin, as the migration rate of culture keratinocytes was accelerated when transfected with active MMP-7 (McGuire et al., 2003). However, as with the aforementioned MMPs, facilitating cell migration by cleaving E-cadherin, is not a function unique to MMP-7, as studies have shown that MMP-28 is also capable of cleaving cell-cell junctions in cultured keratinocytes (Saarialho-Kere et al., 2002). With such a high level of redundancy, determining the specific roles of MMPs is challenging in vertebrates, particularly during a multifaceted process like wound healing.

MMPs in *Drosophila melanogaster.*

To bypass the complexity of redundancy, we utilized the simple, genetically-tractable, model organism, *Drosophila melanogaster*, to study MMP function and regulation *in vivo.* In *Drosophila*, there are 2 genes encoding MMPs, one of each MMP class, secreted *Dm1-Mmp* (*Mmp1*), and membrane-anchored

Dm2-Mmp (*Mmp2*) (Llano et al., 2002; Llano et al., 2000). Both Mmp1 and Mmp2 have a domain structure similar to that of vertebrate MMPs, with an N-terminal signal sequence, followed by a pro-domain, a Zn^{2+} binding catalytic domain and a proline-rich hinge, or linker, region, followed by a C-terminal hemopexin domain (Fig. 1.6). Similar to vertebrate MT-MMPs, MMP-11, and MMP-28, both *Drosophila* Mmp1 and Mmp2 have a furin cleavage site (Llano et al., 2002; Llano et al., 2000), indicating that both Mmp1 and Mmp2 can be activated in the Golgi prior to secretion. Mmp2 also has a C-terminal GPI anchor, tethering Mmp2 to the plasma membrane (Llano et al., 2002). In *Drosophila*, as in vertebrates, MMPs are inhibited by an endogenous Tissue Inhibitor of Metalloproteinase, *DmTimp* (*Timp*), of which there is only one in *Drosophila* (Wei et al., 2003). While *Mmp1*, *Mmp2*, and *Timp* are orthologous to their vertebrate family members, they have no direct mammalian homologs (Page-McCaw et al., 2007).

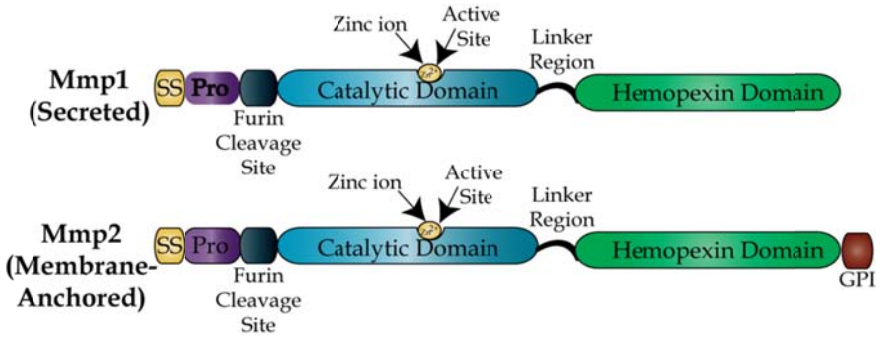

Figure 1.6: Domain structure of *Drosophila* MMPs.
Domain structure of Mmp1, the *Drosophila* secreted MMP, and Mmp2, the *Drosophila* membrane-anchored MMP. Both MMPs have an N-terminal signaling sequence, followed by a pro-domain, a furin cleavage consensus sequence, a Zn^{2+} binding catalytic domain, followed by a flexible linker region and a hemopexin domain. Membrane-anchored Mmp2, also has a C-terminal GPI anchor. Illustrations are not drawn to scale.

In *Drosophila*, MMPs are involved in many instances of tissue remodeling; however, they are not zygotically required for normal embryonic development, as both *Mmp1* and *Mmp2* mutants have been shown to survive at least until the late larval stages (Page-McCaw et al., 2003b). Similar to vertebrate MMPs, *Drosophila Mmp1* plays a role during tumor metastasis and invasion (Beaucher et al., 2007b; Uhlirova and Bohmann, 2006). Interestingly, *Mmp1* expression exclusively in the tumor microenvironment is not sufficient for metastasis. *Mmp1* is also required in the host tissue, indicating that the Mmp1-dependent signals released from the tissue surrounding the tumor is required to induce migration (Beaucher et al., 2007b). Invasive cell migration is also a critical step during eversion of the wing disc during *Drosophila* metamorphosis, a process that requires basement membrane remodeling and *Mmp1* (Srivastava et al., 2007). Growth of complex organ systems, such as the trachea and the dendritic arbor, is a process that not only requires remodeling of the growing tissue, but also of the surrounding extracellular matrix. During tracheal development, *Mmp1* is required both for degradation of old cuticle during molts, as well as the expansion of the ECM to accommodate the growing trachea (Glasheen et al., 2010a). *Mmp2* is also involved in tracheal development, functioning to restrict FGF signaling to the immediate vicinity of the growing air sac during branching morphogenesis (Guha et al., 2009; Wang et al., 2010). Similarly, during neural development, both *Mmp1* and *Mmp2* are involved in motor neuron guidance and defasciculation (Miller et al., 2008). Additionally, *Mmp2* plays role in reshaping

sensory neuron dendrites via degradation of the ECM locally, around the growing dendrite (Yasunaga et al., 2010). A common theme amongst all the various functions of MMPs in both *Drosophila* and vertebrates seems to be ECM remodeling and modification of signaling molecules in order to facilitate tissue growth, migration, and remodeling.

By combining the simplicity of *Drosophila* as a model system to study both wound healing and MMP functions *in vivo*, we have found that both *Mmp1* and *Mmp2*, as well as their endogenous inhibitor, *Timp*, play a critical role during wound healing, where all three molecules are required for re-epithelialization under the control of the JNK signaling pathway. Additionally, *Mmp1*, *Mmp2*, and *Timp* may also facilitate hemostasis and scab formation. In response to wounding, *Mmp1* is required for type IV collagen (*Viking* in *Drosophila*) accumulation at the wound margin, suggesting that *Mmp1* is required for wound-induced ECM modifications. The role of *Mmp1* in ECM deposition extends beyond wound healing, as we find that *Mmp1* and *Timp*, but not *Mmp2*, are required for ECM organization and secretion from epithelial cells in unwounded epidermis. From the redundant phenotypes that we have identified in *Mmp1*, *Mmp2*, and *Timp* mutants, along with our results that *Mmp2* and *Timp* are required for Mmp1 localization, we hypothesize that Mmp2, Mmp1, and Timp function as a tri-molecular complex to promote wound healing *in vivo*.

CHAPTER II

A SECRETED MMP IS REQUIRED FOR RE-EPITHELIALIZATION DURING WOUND HEALING

(Adapted from Stevens and Page-McCaw (2012))

Introduction

Healing a human skin wound requires a complex interplay of cells and extracellular matrix (ECM) within a tissue architecture that directs and restricts molecular interactions. In the hemostasis phase, platelets form a plug, which is replaced by a temporary fibrin matrix; in the inflammatory phase, white blood cells neutralize pathogens and phagocytose cell and ECM debris; in the re-epithelialization stage, epidermal epithelial cells migrate onto the restored wound bed, as collagen-based scar tissue replaces the fibrin matrix; and in the resolution phase white blood cells are cleared, and provisional ECM is replaced (Goldberg and Diegelmann, 2010; Gurtner et al., 2008; Shaw and Martin, 2009; Singer and Clark, 1999). These stages are controlled by many growth factors and extracellular signals including PDGF, EGF, TNFα, TGFβ, and IGF. In healthy individuals small wounds heal without intervention, but clinical wound-healing challenges remain for surgical patients, diabetic patients, and burn victims. Pathologies of wound healing can be roughly grouped into two categories: excessive wound-healing leading to fibrotic scarring; and incomplete wound

healing leading to ulcers and persistent inflammation (Goldberg and Diegelmann, 2010).

Matrix metalloproteinases are a large family of extracellular proteases, at least ten of which are up-regulated during wound healing by epidermal, dermal, fibroblast, or blood cells in mammals (reviewed by Gill and Parks, 2008). MMPs can be subdivided into two classes: secreted MMPs (seventeen mammalian family members) and membrane-anchored MMPs (seven mammalian family members). Their endogenous inhibitors are TIMPs (tissue inhibitors of metalloproteinases), which sterically hinder the active site in a one-to-one stoichiometry (Gomis-Ruth et al., 1997). *In vitro* and in cell culture, MMPs are capable of cleaving most ECM components and proteolytically modifying many signaling molecules important for wound healing (Bergers et al., 2000; Egeblad and Werb, 2002b; Gearing et al., 1995; Gill and Parks, 2008; Koshikawa et al., 2004; Levi et al., 1996; Li et al., 2002; Mott and Werb, 2004; Parks et al., 2004; Rebustini et al., 2009; Suzuki et al., 1997; Tholozan et al., 2007; Yu and Stamenkovic, 2000). MMPs are widely considered to be pro-inflammatory during the wound healing process because of the high levels of MMP expression in chronic wounds (Goldberg and Diegelmann, 2010; Menke et al., 2007; Schultz and Wysocki, 2009). However, MMPs may have larger roles as they sit at the nexus of inflammation, ECM remodeling and cell signaling (reviewed in Parks et al., 2004). Mouse MMP knockouts have limited utility in defining MMP functions because of redundancy within the MMP family (Page-McCaw et al.,

2007). Knock-out mice for each of four secreted MMPs (*MMP-3, MMP-8, MMP-9* and *MMP-13*) display a mild delay in closing excisional wounds, indicating that MMPs have a functional role in wound healing. *MMP-3* (stromelysin-1) mutants have defects in wound contraction (Bullard et al., 1999b); *MMP-8* mutants have prolonged inflammation (Gutierrez-Fernandez et al., 2007b); *MMP-9* and *MMP-13* mutants have delays in epithelial migration (Hattori et al., 2009b; Kyriakides et al., 2009a). These mild phenotypes probably belie the role of MMPs in wound healing, as the vertebrate MMP family displays significant redundancy. The ~24 mammalian MMPs have overlapping substrate specificity and expression patterns (Egeblad and Werb, 2002b). Indeed, MMP redundancy in wounding has been reported: *MMP-9/-13* double mutants have longer wound healing delays than the single mutants (Hattori et al., 2009b), yet even these mice still have a large number of intact MMP genes that may be masking other MMP wound-healing functions. This genetic redundancy clouds a mechanistic understanding of wound healing *in vivo*.

Drosophila is an established model system for wound healing (Galko and Krasnow, 2004b; Wood et al., 2002a), and in *Drosophila* there are only two MMPs: one secreted (DmMmp1) and one membrane-anchored (DmMmp2) (Llano et al., 2002; Llano et al., 2000; Page-McCaw et al., 2003a). Additionally, the *Drosophila* MMPs are inhibited by a single endogenous TIMP (DmTimp) (Godenschwege et al., 2000a; Wei et al., 2003), in contrast to the four TIMPs in mammals. This simplicity allows us to identify the roles of the secreted and membrane-anchored

MMPs as a class *in vivo*, including their tissue sources and regulatory mechanisms. *Drosophila* wound healing involves the same wound healing phases as vertebrates (hemostasis, inflammation, re-epithelialization, and resolution)(Galko and Krasnow, 2004b), including the migratory re-epithelialization phase. We report here that *Mmp1* and *Mmp2* are each required for re-epithelialization during wound healing, as puncture wounds remain open in the mutants. Focusing on the secreted MMP, Mmp1, we report that it facilitates re-epithelialization by promoting ECM assembly, cell elongation, actin cytoskeletal reorganization, and extracellular signal-regulated kinase (ERK) activation. The wound-induced up-regulation of Mmp1 is controlled by jun N-terminal kinase (JNK), and when JNK is ectopically activated by TNFα to produce high levels of Mmp1, wound closure is accelerated in an Mmp1-dependent manner.

Methods

Fly lines.

The following lines are described in Page-McCaw et al (2003): $Mmp1^{2}$ and $Mmp2^{Df(2R)Uba1\text{-}Mmp2}$ (imprecise *P* excision alleles resulting in deletions of most or all of the coding region); $Mmp1^{Q112*}$ and $Mmp2^{W307*}$ (EMS-induced nonsense alleles resulting in premature truncations); *UAS-Timp* and *tubP-GAL4* (Flybase ID FBtp0002651). The dominant-negative *Mmp1* line used was *UAS-Mmp1.f1*^{E225A} (Glasheen et al., 2009b; Zhang et al., 2006). Other fly lines used were *A58-Gal4*

(M. Galko), *UAS-Bsk^{DN}* (Flybase ID FBti0074418) and *He-Gal4* (Flybase ID FBti0064641) both from the Bloomington *Drosophila* Stock Center, two lines of *UAS-Mmp1-dsRNA* (D. Bohmann and the Vienna Drosophila RNAi Center insertion 101505), *Vkg-GFP^{G205}* (Yale Flytrap), *UAS-egr* (M. Muiro, shorter RB isoform (Igaki et al., 2002b), and *UAS-GFP-actin5C* (D. Kiehart,). *w^{1118}* was used as wild type.

It has not been possible to perform rescue experiments using standard *Mmp1* constructs because *Mmp1* over-expression is lethal when widely expressed (even under permissive temperatures with a heat-shock promoter, or under *GAL4/GAL80^{ts}* control). As an alternative approach, a non-complementation screen in an independent genetic background was performed in Page-McCaw et al (2003a) to identify new *Mmp1* alleles to show genetic specificity for *Mmp1*. Phenotypes in trans-heterozygotes (carrying a *P*-generated allele and an EMS allele) have been used to establish *Mmp1* specificity in previous reports (Glasheen et al., 2009b; Glasheen et al., 2010a; Page-McCaw et al., 2003a), a strategy we employ in this study as well.

Wounding assays.

3rd instar larvae were impaled with a 0.1mm steel needle (Fine Science Tools) on the dorsal side between segments A3-5, on molasses plates on ice. For pinch wounds, #5 dissecting forceps were used to gently pull / pinch the cuticle for about 5s, without puncturing, on the dorsal side of 3rd instar larvae. Both

assays were adapted from Galko and Krasnow (2004). After wounding, animals recovered on agar plates with access to wet yeast and water at 25°C.

Dissection, fixation, immunohistochemistry.

To excise the epidermis, larvae were decapitated at the cerebral tracheal branch and filleted along the right lateral side, followed by removal of the posterior end at approximately segment A7. Dissections were done in PBS + 1%BSA or directly in fixative. Tissue was pinned flat and fixed in PBS + 4% formaldehyde at RT for 30 min. Fixed samples were washed and permeabilized in PBS + 0.2% Triton X-100, blocked in PBS + 5% goat serum + 0.02% NaN_3, incubated in 1^o antibody (diluted in PBS + 1% goat serum + 0.02%NaN_3) overnight at 4°C, washed and incubated in 2^o antibodies for 1.5 h at RT in the dark, and mounted in Vectashield mounting media with DAPI (Vector Labs). Anti-Mmp1 catalytic domain (a 1:1:1 cocktail of mouse monoclonal IgG1 antibodies 3B8, 5H7, and 23G, generated by Page-McCaw et al (2003) and obtained from the Developmental Studies Hybridoma Bank (DSHB)), was used at 1:100. Anti-FasIII (a mouse monoclonal IgG2a from the DSHB) was used at 1:10. Rabbit anti-GFP (Molecular Probes) was pre-absorbed against larval epidermis and used at 1:100. Mouse anti-Integrin-βPS (a monoclonal IgG2b from DSHB) was used at 1:10. Mouse monoclonal IgG1 anti-diphosphorylated-ERK 1&2 (Sigma) was used at 1:200. Mouse monoclonal anti-collagen IV (gift of Lisa and John Fessler) was used at 1:25. Cy3 or FITC labeled goat anti-mouse IgG1

(Jackson ImmunoResearch), DyeLight649 labeled goat anti-mouse IgG2a (Jackson ImmunoResearch), Cy3 labeled goat anti-mouse (Jackson ImmunoResearch), FITC-labeled donkey anti-rabbit (Jackson ImmunoResearch) were all used at 1:300.

Microscopy.

Optical sectioning was performed with a Zeiss Apotome mounted on an Axio imager Z1 or M2, with the following objectives: 20X/0.8 Plan-Apochromat, 40X/1.3 oil EC Plan-NeoFluar, or 63X/1.4 oil Plan-Apochromat. Fluorescent images were acquired with an Axiocam MRm (Zeiss) camera paired with Axiovision 4.8 (Zeiss). Z-stacks were compressed into 2-deminsional projections using the Orthoview function in Axiovision. All images were exported from their acquisition programs as 16-bit, grayscale, TIFF files for post-processing in Adobe Photoshop CS4, or ImageJ v.1.43u.

Wound measurements.

Closure and wound area were assessed based on the presence of both FasIII staining at cell borders and epidermal polyploid nuclei as stained with DAPI. To calculate wound area, the outline tool in Axiovision (Zeiss) was used to manually outline the wound edge. This feature automatically calculates the area of the outlined region using image acquisition specifications. In Figure 2.1E-F, the wounded animals are as follows. Wild type (n=19): w^{1118}. *Mmp1* (n=6): 4

Mmp1$^{Q112*/2}$ and 2 *Mmp1*^{2}. *Mmp2* (n=7): 4 *Mmp2* $^{W307*/Df(2R)Uba1\text{-}Mmp2}$ and 3 *Mmp2*^{W307*}. *A58>Timp* (n=5). Student's t-tests were performed with the analysis tools available in GraphPad Prism v. 5.01 to compare mutant and wild-type wound area within each time point.

To measure aspect ratios (Fig. 5 and S3), wounded epidermal samples were fixed at varying times post-wounding (0h is immediately after wounding) and stained for FasIII and DAPI. XY projections of wounds were generated from optical sections taken at 20X. On each leading edge cell a line was drawn manually with ImageJ on the longest axis determined by FasIII staining, and then the longest perpendicular axis was drawn. The ImageJ measurement tool measured the lines, and aspect ratios were calculated in Microsoft Excel. Since this method ignores cell orientation, the long axis was used as the numerator, so that the smallest possible ratio was 1.0. Only cells with FasIII on all edges were measured. n≥29 cells from 3 different animals for each column. *Mmp1* was the transheterozygous *Mmp1*$^{Q112*/2}$. The mean aspect ratio for each genotype at each time point was calculated and graphed using GraphPad Prism v. 5.01 (GraphPad Software). Error bars represent the standard error of the mean. Student's t-test was used to determine the statistical significance between pairs of columns.

Expression analysis.

To generate heat maps of pixel intensity from fluorescent images, single channel 16-bit grayscale 2D projection from Z-stacks were converted to 8-bit

images in ImageJ v1.43u. The "fire" look-up table (LUT) was then applied to the image to pseudo-color pixels based on intensity, white = 256 and dark navy blue = 0.

To measure relative dpERK expression between genotypes over time, 2D projection images were opened in ImageJ and the ellipse tool was used to mark nuclei at the leading edge of the wound based on DAPI staining and anti-FasIII expression, while the dpERK channel was hidden. The multi-measure tool was then used to calculate an integrated intensity density for each region of interest (ROI, representing each nucleus) for the dpERK channel. Each integrated density value was imported into GraphPad Prism v5.01, where GraphPad Prism analysis tools were used to perform Student's t-test to compare mutant intensity to wild-type intensity at each time point and to compare wild-type wounded intensity to wild-type unwounded intensity at each time point.

For Vkg-GFP intensity analysis in unwounded tissue, XY images of Vkg-GFP taken at 63X during seven blindly-scored, independent trials were opened in ImageJ and automatically sized to 9.25in x 6.93in. A 1 in^2 square grid was applied to the image and integrated density was calculated within each square using the ImageJ measure tool. Squares that contained only basement membrane were measured; squares that contained folds in the tissue or ECM from other tissue types were excluded. All intensity measurements were imported in a Microsoft Excel spreadsheet and the average pixel intensity for each sample (each animal) was calculated along with the overall average intensity for each

genotype within each experimental replicate. To calculate relative expression intensity between *Mmp1* mutants and wild type, the ratio of mutant versus wild-type intensity was calculated for each sample within experimental replicate. The negative inverse was calculated for all ratios less than 1. Ratios for each mutant and wild-type sample were imported in GraphPad Prism and plotted on a box and whiskers plot, with wild type ranging from -1 to 1. Student's t-test was used to assess the differences between genotypes. A similar method was used to quantify anti-collagen IV staining intensity, except that the grid squares were ½ in^2.

Western blots.

Third instar larvae (1-3 *Vkg-GFP/CyO* larvae or 2-5 *Vkg-GFP* $Mmp1^2/Mmp1^{Q112*}$ larvae) were homogenized in 30µl 2X Laemmli buffer with mini-complete protease inhibitors (Roche). 20µl of each lysate was loaded in each lane of a 4-15% tris-glycine PAGE gradient gel (BioRad). Blots were washed in PBS + 0.1% Tween-20, blocked in Odyssey Blocking Buffer (BioRad) and probed with rabbit anti-GFP (Molecular Probes) used at 1:1,000, or mouse anti-actin (Abcam) used at 1:5,000, overnight at 4°C. Secondary antibody incubations were 1h at RT with goat anti-mouse labeled with IRdye800 (Li-Cor) at 1:7,500, or donkey anti-rabbit tagged with IRDye680 (Li-Cor) at 1:5,000, followed by developing with the Odyssey Infrared Imaging System (Li-Cor). Integrated fluorescence intensity was calculated for the top bands (shown in Fig. 4K) using

ImageJ v. 1.43u, as these had no corresponding background bands in non-GFP containing wild-type lanes; the intensities of these bands were summed to find total expression. Expression was normalized against integrated fluorescence intensity of the actin loading control. Fold change of anti-GFP expression in *Mmp1* mutants was calculated relative to that in wild type. No statistically significant difference was found between *Mmp1* mutants and wild type over 3 independent trials.

For the *Mmp1-dsRNA* knock-down efficiency blots (Fig. S2), third instar larvae (2 *Tub>Mmp1-dsRNA* of both the DB line and the VDRC line, 4 $Mmp1^{2}$, or 2 *Tub-Gal4*) were homogenized in 30ul 2X Laemmli buffer. 20µl of each lysate was loaded in each lane of a 10% tris-glycine PAGE gel (BioRad). Blots were washed in PBS + 0.1% Tween-20, blocked in Odyssey Blocking Buffer (BioRad) and probed overnight at 4°C with 1:1:1 cocktail of monoclonal mouse anti-Mmp1 antibodies 3B8, 5H7, and 3A6 (DSHB) used at 1:100 and with rat anti-α-Tubulin (AbD Serotec) used at 1:5000. Secondary antibody incubations were at RT for 1h in donkey anti-mouse labeled with IRdye800 (Li-Cor) at 1:5,000, or donkey anti-rat tagged with IRDye680 (Li-Cor) at 1:7,500, followed by developing with the Odyssey Infrared Imaging System (Li-Cor). Three independent trials were performed and results were quantified following the methods outlined for the Vkg-GFP blots, with Mmp1 expression normalized against α-Tubulin expression within each lane. Normalized intensity values were imported into GraphPadPrismv5.01, where the mean and standard error of the mean was

plotted for each genotype and the p-value was calculated by a Student's t-test comparing each mutant/knockdown expression level to wild type.

Results

Both *Drosophila* MMPs are required for re-epithelialization.

Mmp1, the secreted *Drosophila* MMP, is required for developmental tissue remodeling during tracheal growth and metamorphosis (Glasheen et al., 2009b; Glasheen et al., 2010a; Srivastava et al., 2007). We asked if *Mmp1* is required for the tissue remodeling required during wound healing of the larval epidermis. Larval epidermis is a monolayer squamous epithelium, protected on the apical side by a chitinous cuticle, and overlying a basal basement membrane (Martinez Arias, 1993b). Most larval epidermal cells are highly polyploid and incapable of proliferation (Smith and Orr-Weaver, 1991). To assess wound healing, we punctured larval epidermis in wild-type and *Mmp1* null mutants with a fine needle, using the procedure of Galko and Krasnow (2004b). We used third instar animals; $Mmp1^{2}$ null mutants die during a prolonged third instar, almost never entering metamorphosis (Page-McCaw et al., 2003a). After puncture, the animals were allowed a recovery period for healing, and then we dissected, fixed and stained the epidermis with anti-FasIII and DAPI to visualize cell borders and nuclei. In wild-type larvae 5h after wounding, epidermal cells at the wound edge had elongated and begun spreading into the wound; by 14h wounds had

typically closed, often forming syncitia over the center of the wound, as previously reported (Galko and Krasnow, 2004b). Assessing wound closure by location of nuclei and cell borders, we found that 79% of wild-type animals closed their wounds by 14h (n=19, Fig. 2.1A, E).

In contrast, re-epithelialization failed to occur in 100% of wounded *Mmp1* null animals, both homozygous null $Mmp1^{2}$ larvae, and transheterozygous null $Mmp1^{2/Q112*}$, demonstrating specificity for *Mmp1* (Fig. 2.1B, E). The *Mmp1* wounds gapped open by 1h (Fig. 2.1G) and remained larger than the size of the original puncture (Fig. 2.1F, G). These were not simply delays in wounding, as *Mmp1* wounds never closed: even at 50h post-wounding, the rare surviving *Mmp1* mutants still had open wounds (n=2) whereas all wild type wounds were closed (n=4).

There are only two MMPs in *Drosophila*, so we asked whether the predicted GPI-anchored MMP, *Mmp2* was also required for wound healing. In both $Mmp2^{W307*}$ and $Mmp2^{W307*/\ Df(2R)Uba1\text{-}Mmp2}$ animals, wounds failed to close (Fig. 2.1C, E, F). We overexpressed the catalytic inhibitor Timp throughout the larval epidermis using the *A58-GAL4* driver (Galko and Krasnow, 2004b), and the expression of this endogenous inhibitor recapitulated the failure of re-epithelialization in the MMP mutants with very large wounds (Fig. 2.1D-F). Thus each *Drosophila* MMP is involved in wound closure in a non-redundant manner.

To further test for redundant roles, we administered puncture wounds to double mutant *Mmp2 Mmp1* animals. Both single MMP mutants had an incompletely penetrant clotting defect, such that many of the animals died after puncturing (discussed further in chapter 3). In double mutants, the clotting defect was pronounced and fully penetrant: all the animals bled out and died shortly after wounding, indicating that they have clot formation defects (n=84). Thus *Drosophila* MMPs appear to act redundantly in the hemostasis phase of wound healing, but are each required for re-epithelialization. The remainder of this chapter is focused on Mmp1. Mmp2 and Timp will be discussed further in chapter 5.

Figure 2.1. Each *Drosophila* MMP is required for re-epithelialization.
A-D) Wounded larval epidermis 14h post-wounding from indicated genotypes. Anti-FasIII (yellow) labels cell borders and DAPI (blue) labels the nuclei. The white arrow (**A**) indicates the center of the closed wound, while the white dashed lines outline open wounds (B-D). Scale bar on (A) represents 20μm for A-D. **E)** Percent of wounds open versus closed 14 h post-wounding. The numbers on each bar (E-F) indicate the number of animals for each sample set. **F)** Mean wound area 14h post-wounding (including all wounds, open and closed). The red dashed line represents the area of the needle used to induce wounds (~8,000μm^2). Mutants are significantly different from wild type, as calculated by t-test: *Mmp1* (p=0.0004), *Mmp2* (p=0.011), *A58>Timp* (p<0.0001). **G)** Graph of wound area over time in wild type (black line) and *Mmp1* mutants (blue line). At 1h (*Mmp1* n = 4, wild type n=21), 5h (*Mmp1* n=14, wild type n=23), and 14h (*Mmp1* n=6, wild type n=19) post-wounding, mutant wounds are significantly larger than wild type (p=0.003, p=0.032, and p=0.0001, respectively). There is no significant difference in wound area between *Mmp1* mutants and wild type at 0h (*Mmp1* n=4, wild type n=8) and 0.5h (*Mmp1* n=5, wild type n=15) post-wounding. Error bars (F-G) represent standard error of the mean. See Materials and Methods for alleles used. (Adapted from Stevens and Page-McCaw 2012).

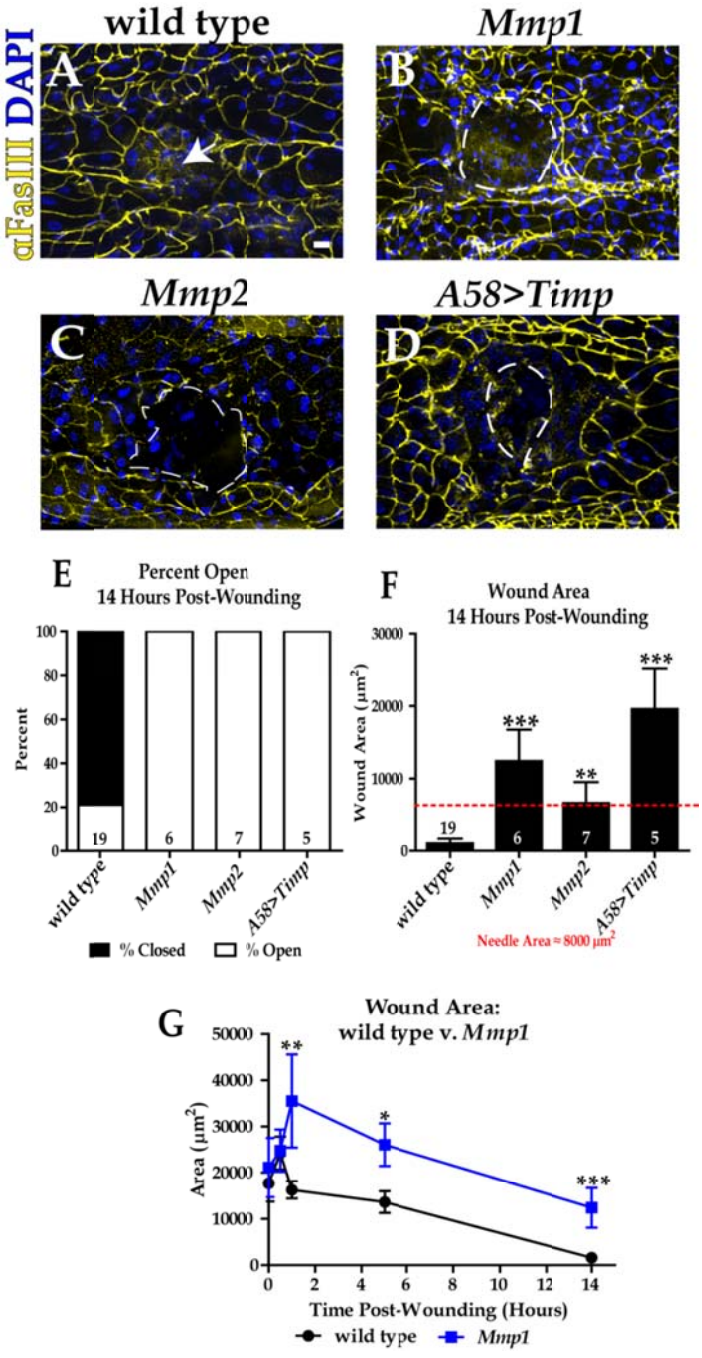
wild type
Mmp1
αFasIII DAPI
A
B
Mmp2
A58>Timp
C
D
E
Percent Open
14 Hours Post-Wounding
Percent
100
80
60
40
20
0
19
6
7
5
wild type
Mmp1
Mmp2
A58>Timp
% Closed
% Open
F
Wound Area
14 Hours Post-Wounding
Wound Area (μm²)
30000
20000
10000
0
***
**
***
19
6
7
5
wild type
Mmp1
Mmp2
A58>Timp
Needle Area ≈ 8000 μm²
G
Wound Area:
wild type v. Mmp1
Area (μm²)
50000
40000
30000
20000
10000
0
**
*
***
0
2
4
6
8
10
12
14
Time Post-Wounding (Hours)
wild type
Mmp1

***Mmp1* is required in the epidermis for re-epithelialization.**

Epidermal wound healing involves the coordination of at least two different tissue types: epidermal epithelial cells and hemocytes (innate immune cells of the blood). To elucidate which tissue(s) require *Mmp1* during re-epithelialization, we knocked down *Mmp1* using an inducible RNAi targeting construct (Uhlirova and Bohmann, 2006) under the control of tissue-specific GAL4 drivers *A58-GAL4* (epidermis) and *He-GAL4* (hemocytes). By 18h post-wounding, wounds closed in 86% of wild-type animals (Fig. 2.2A, E). Similar to the whole animal *Mmp1* mutants (Fig. 2.1B), when *Mmp1* was knocked down specifically in the epidermis (*A58>Mmp1-dsRNA*) wounds remained open in 100% of animals 18h post-wounding (Fig. 2.2C, E), with an average wound area that was significantly larger than wild type (Fig. 2.2F). In contrast, when *Mmp1* was knocked down in hemocytes *(He>Mmp1*-dsRNA), healing was similar to wild-type (Fig. 2.2B, E, F). To ensure specificity of the RNAi, we used an *Mmp1-dsRNA* line targeting another region of the transcript (from the VDRC), with similar results (unpublished data). An anti-Mmp1 western blot confirmed both lines reduced protein levels, with the Bohmann line more effective (Fig. 2.3). These results demonstrate that *Mmp1* expression in the epidermis is required for re-epithelialization.

To test whether the catalytic activity of Mmp1 was required for wound closure, we expressed in the epidermis a catalytically inactive Mmp1, *UAS-Mmp1*^{E225A}, which harbors an alanine mutation at a conserved glutamic acid in

the active site and acts as a dominant-negative (Glasheen et al., 2009b; Zhang et al., 2006). In animals expressing *Mmp1*^{E225A} in the epidermis, wounds remained open in 100% of the animals tested 18h post-wounding (Fig. 2.2D, E), with an average wound area that is similar to the RNAi-mediated knock-down of Mmp1 (Fig. 2.2F). Our results indicate that Mmp1 catalytic activity is required for re-epithelialization.

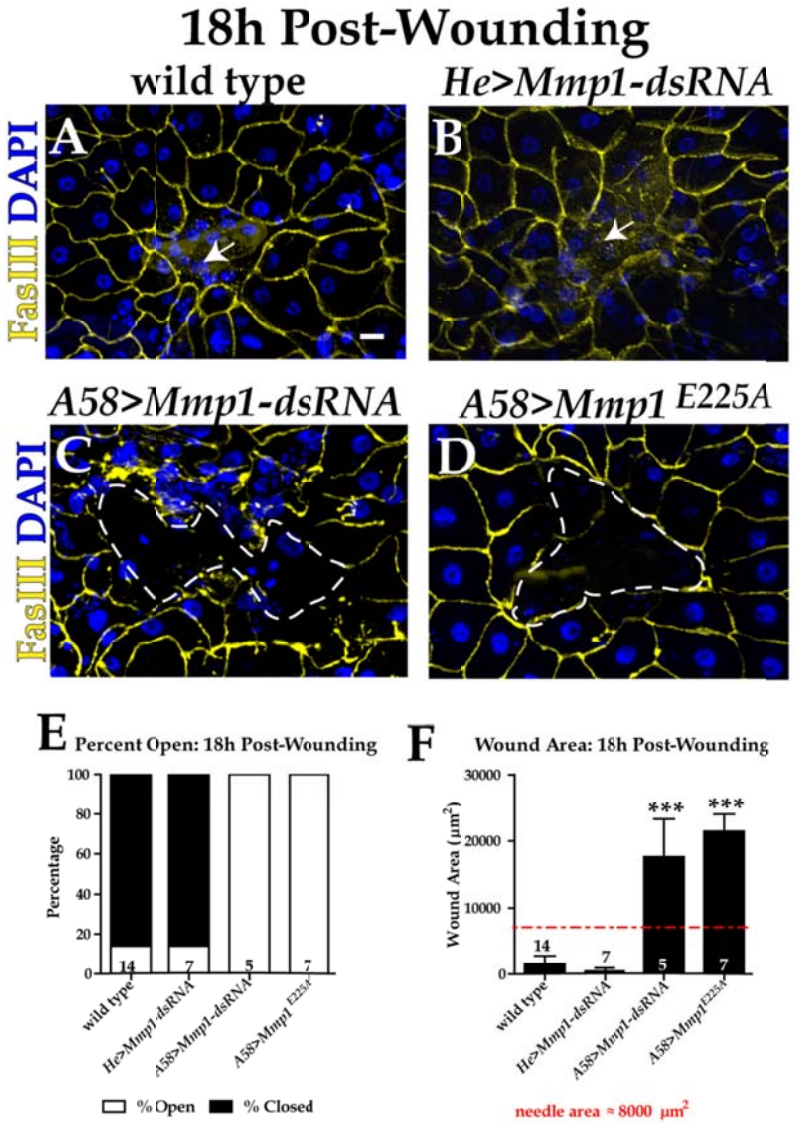

Figure 2.2: Epidermal *Mmp1* is required for re-epithelialization.
A-D) Wounded epidermis 18h post-wounding from the designated genotypes. The white arrows (A-B) point to the region of the closed wounds. White dashed lines (C-D) outline open wounds. Scale bar (A) represents 20μm for A-D. **E)** Graph showing percentage of wounds open versus closed 18h post-wounding in each genotype. **F)** Graph of the wound area 18h post-wounding. The numbers above the X-axis indicate the number of animals examined for each group. Wound areas in *A58>Mmp1-dsRNA* ($p=0.0007$) and *A58>Mmp1*^{E225A} ($p<0.0001$) mutants are significantly larger than wild type by Student's t-test. Error bars (F) show the standard error of the mean. (Adapted from Stevens and Page-McCaw 2012).

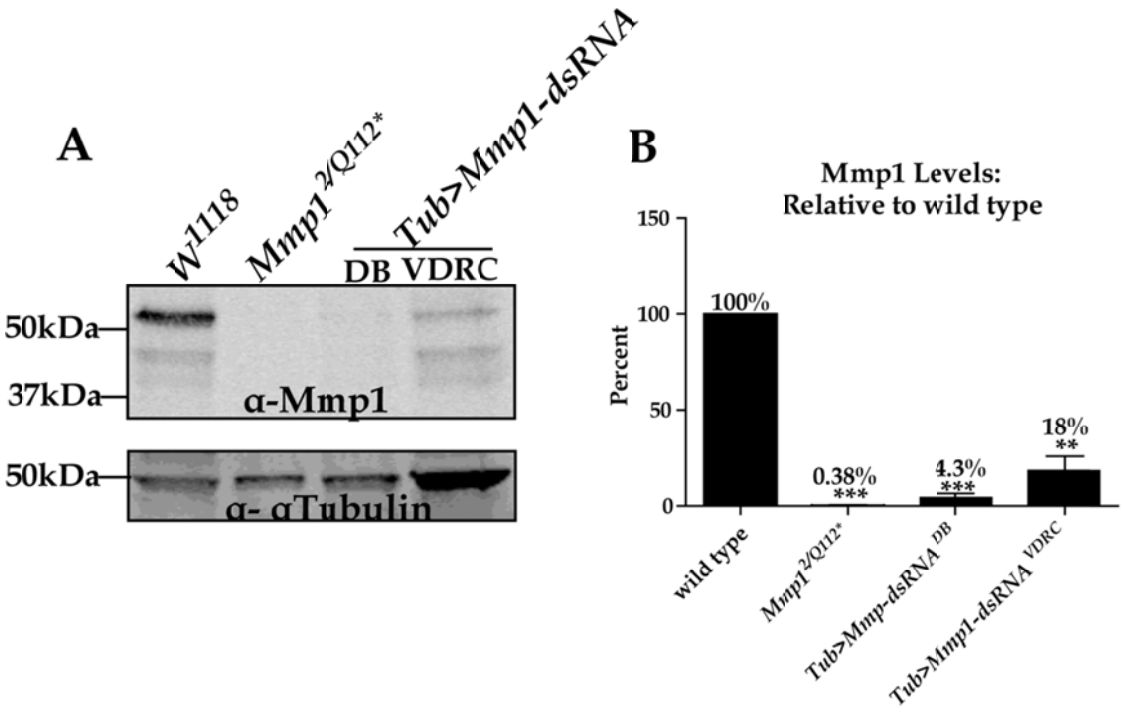

Figure 2.3: Mmp1-dsRNA knock-down efficiency.
A) Western blot comparing RNA-interference mediated knock-down of Mmp1 from two different constructs. An *Mmp1* null line (*2/Q112**) demonstrates the specificity of the antibody. DB indicates the *UAS-Mmp1-dsRNA* line from D. Bohmann (Uhlirova, M, & Bohmann, D., 2006) and VDRC indicates the *UAS-Mmp1-dsRNA* line from Vienna RNAi Stock Center. Lysates were made from whole 3rd instar larvae (see Materials and Methods). Anti-αTubulin was used as a loading control. **B)** Quantification of western blots showing the mean level of Mmp1 expression compared to wild-type of *Mmp1* null mutants (0.38%, $p<0.0001$), *Tub>Mmp1-dsRNA*^{DB} (4.3%, $p=0.0006$), and *Tub>Mmp1-DsRNA*^{VDRC} (18%, $p=0.0082$). Error bars represent standard error of the mean for 3 independent replicates, p-values calculated by Student's t-test comparing each genotype to wild-type. (Adapted from Stevens and Page-McCaw 2012).

Mmp1 is up-regulated in the epidermis in response to wounding.

To test if there is a local response to wounding, we analyzed wound-induced Mmp1 expression changes in the epidermis. To accommodate the large dynamic range of Mmp1 expression, we visualized Mmp1 expression changes by pseudo-coloring anti-Mmp1 images based on pixel intensity, generating heat maps (see Fig. 2.4 and Methods for this chapter). Using specific monoclonal antibodies that recognize the catalytic domain of Mmp1 (Glasheen et al., 2010a; Page-McCaw et al., 2003a), we found that Mmp1 was expressed at low levels throughout the unwounded epidermis (Fig. 2.4A, B). In XY projections, Mmp1 appeared localized to the cell-cell borders (Fig. 2.4A), but in XZ projections it was clear that Mmp1 also lines the basal surface of the epidermal cells, where it could come in contact with the basement membrane (Fig. 2.4B, B'). A half-hour after wounding Mmp1 expression had not changed at the wound site (Fig. 2.4C), but by three hours after wounding Mmp1 was up-regulated in the epidermal cells specifically around the wound site (Fig. 2.4D), with no detectable changes in expression in cells more than 4-5 cell diameters away from the wound. Maximal up-regulation was observed at 5h post wounding (Fig. 2.4E and data not shown). Elevated Mmp1 levels persisted in the syncytia and surrounding epithelial cells even after the wound was closed (Fig. 2.4F). In pinch wounds, where the cuticle remains intact, Mmp1 was also up-regulated (Fig. 2.5), suggesting that Mmp1 up-regulation is triggered by damage rather than by the introduction of pathogens. We found that Mmp1 is generally up-regulated in a gradient highest

in the cells at the wound margin (see Fig. 2.4D, E). Although Mmp1 is generally up-regulated throughout these cells (Fig. 2.4E-G), we observe an accumulation of Mmp1 at the distal edge (Fig. 2.4E white box, G, H; white arrows indicate distal accumulation), as well as high levels of Mmp1 proximal to the wound margin (Fig. 2.4H, H′ yellow arrow).

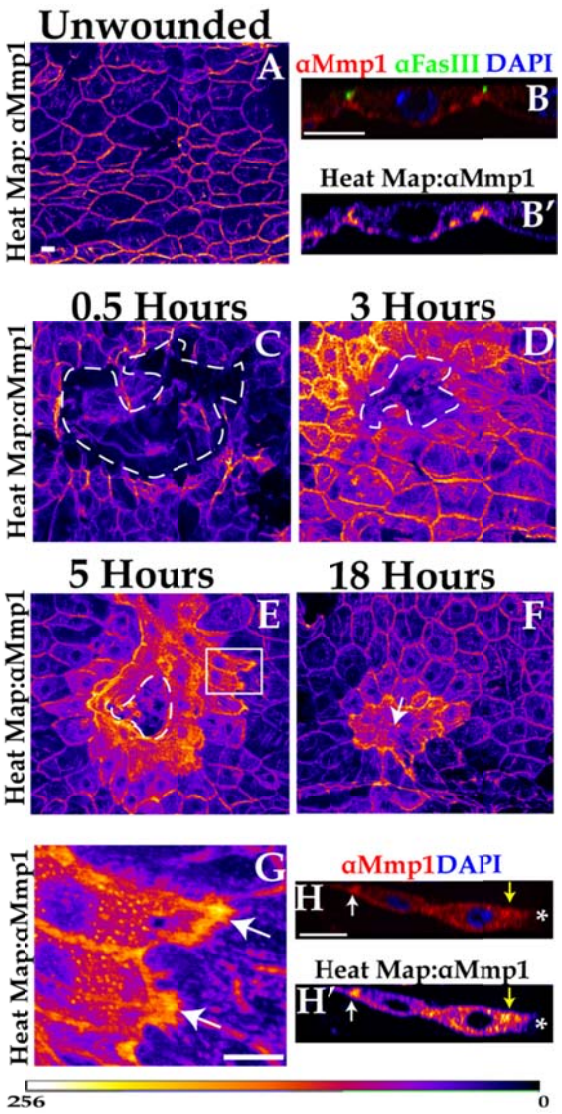

Figure 2.4: Mmp1 is up-regulated at the wound site.
A) Heat map showing Mmp1 localization in unwounded larval epidermis, pseudo-colored based on pixel intensity, intensity scale for A-G displayed at bottom of figure. **B, B′)** XZ images of epidermis showing anti-Mmp1 staining (red in B, heat map in B′), the cell border marker FasIII (green in B), and DAPI (blue in B). Apical is up. **C-F)** Heat maps showing anti-Mmp1 staining after wounding. The white dashed lines in C-E outline the wound bed, and the white arrow in F indicates the closed wound. Comparison of Mmp1 intensity levels can be made between A, C-F, as images were taken at matched exposure settings. **C)** Mmp1 0.5h post-wounding. **D)** Mmp1 3h post-wounding. **E)** Mmp1 5h post-wounding. **F)** Mmp1 18h post-wounding. **G)** Close-up of epidermal cells near the leading edge 5h post-wounding (white box in E) with white arrows pointing to distal-edge accumulation of Mmp1. **H, H′)** XZ images of Mmp1 (red in H, heat map in H′) and DAPI (blue in H) in two epidermal cells at the leading edge of a 5h wound. Apical is up. White asterisk indicates the wound bed. Yellow arrows designate proximal Mmp1 accumulation around leading edge and white arrow indicates distal Mmp1 accumulation. All scale bars represent 20μm. Scale bar in A also for C-F. (Adapted from Stevens and Page-McCaw 2012).

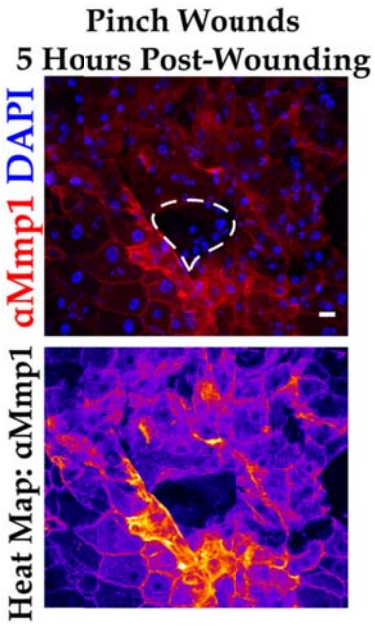

Figure 2.5: Mmp1 is up-regulated in pinch wounds.
Mmp1 up-regulation in pinch wounds 5h post-wounding, in a gradient radiating from the leading edge. Top: Mmp1 shown in red. Bottom: Mmp1 shown as a heat map. The white dashed lines (top) outline the wound bed. Scale bar (top panel) represents 20μm. (Adapted from Stevens and Page-McCaw 2012).

Mmp1 promotes assembly or maintenance of the basement membrane.

To heal mammalian puncture wounds, two kinds of extracellular matrix (ECM) must be repaired, both stromal ECM and the basement membrane. Although insects use an exoskeleton in place of most stromal ECM, the basement membrane of *Drosophila* is a collagen IV-containing matrix highly homologous to that of vertebrates (Hynes and Zhao, 2000). *Drosophila* has two conserved subfamilies of collagen IV, α1-like encoded by *cg25C* and α2-like encoded by *vkg* (Yasothornsrikul et al., 1997), and both are found in basement membranes (Murray et al., 1995; Noselli, 1998; Pastor-Pareja and Xu, 2011a). As MMPs derive their name from their ability to degrade ECM, we compared the basement

membrane during wound healing in wild-type and *Mmp1* mutant larvae. We used a Vkg-GFP (collagen IV α2) protein trap expressed under its endogenous promoter to visualize the basement membrane (Morin et al., 2001). By 1h post-wounding in wild-type animals there was no detectable Vkg-GFP accumulation along the wound edge (data not shown); however, by 5h post-wounding in wild-type larvae there was dramatic Vkg-GFP accumulation at, or directly in front of, the leading edge (n=6, Fig. 2.6A, A', C). In the *Mmp1* null mutants, there was no accumulation of Vkg-GFP at the leading edge (n=8, Fig. 2.6B, B', D). Notably, Mmp1 is expressed heavily around the leading edge by 5h after wounding (Fig. 2.6E, G) at the site where Vkg is assembled. Our data suggests that *Mmp1* promotes the assembly of collagen IV at wound sites, rather than promoting widespread degradation of collagen IV. It is likely that without new basement membrane, *Mmp1* mutant wounds are unable to close because the epidermal cells lack a substrate upon which to migrate.

As *Mmp1* is needed for wound-induced basement membrane assembly, we asked if it is necessary for basement membrane maintenance in unwounded epidermis, especially considering that Mmp1 protein is localized to the basal side of these cells (Fig. 2.6B). We used the Vkg-GFP protein trap to analyze baseline collagen IV levels and structure in unwounded tissue (Fig. 2.6E, F). In wild-type basement membrane underlying unwounded epidermis, Vkg-GFP appeared as a fibrous mesh, slightly concentrated around the cell nuclei (Fig. 2.6E, E'). In *Mmp1* mutants, the overall Vkg-GFP fibrous pattern was similar to wild type, but

the intensity was significantly lower than wild-type (Fig. 2.6F, F', I), as scored in seven blind experiments. As an independent confirmation of collagen IV localization in the unwounded basement membrane, we stained epidermal samples with a monoclonal antibody raised against cg25C (collagen IV α1); this antibody has been used previously for immunostaining (Murray et al., 1995). We again observed reduced levels of collagen IV in the *Mmp1* unwounded epidermal basement membrane (Fig. 2.6H, H', J) compared to wild type (Fig. 2.6G, G', J). These data suggest that either *Mmp1* is necessary for assembling collagen IV into the basement membrane, or that *Mmp1* is required for the expression or stability of collagen IV proteins. To test the latter hypothesis, we compared Vkg-GFP protein levels in whole larvae on western blots probed for GFP (Fig. 2.6K). We found no significant differences in Vkg-GFP levels between wild-type and *Mmp1* mutants (Fig. 2.6K, K'). Our data suggest that Mmp1 is required to facilitate Vkg-GFP deposition into the basement membrane, both at wound sites and during normal growth, but not for overall Vkg-GFP expression or stability.

Figure 2.6: Mmp1 is required for ECM remodeling and maintenance.
A-B) Vkg-GFP at wound margin 5h post-wounding (green), with nuclei (blue, DAPI) and cell borders (red, anti-FasIII) in *Vkg-GFP/+* (A, n=6 animals) and in *Vkg-GFP Mmp1^{Q112*}/Mmp1^{2}* (B, n=8 animals). White asterisk indicates wound bed. **A'-B')** Heat maps of Vkg-GFP from panels A, B. **C-D)** XZ image of Vkg-GFP (green), fasIII (red) and DAPI (blue) at the wound edge 5h post-wounding in control (C) and *Mmp1* mutants (D). White asterisks designate wound beds. **E-F)** Vkg-GFP localization in unwounded epidermis in control (E) and *Mmp1$^{2/Q112*}$* mutants (F). **E'-F')** XZ image of Vkg-GFP in unwounded control (E') and *Mmp1* mutants (F'). **G-H)** Anti-collagen IV (Cg25C) staining in unwounded epidermis in wild type (G) and in *Mmp1* mutants (H), n=6 animals for each genotype. **G'-H')** XZ images of anti-collagen IV staining in wild type (G') and *Mmp1* mutants (H'). All scale bars represent 20μm; scale bar in A for A-D; scale bar in F for E-H; scale bar in F' for E'-H'. **I-J)** Box-and-whiskers plot of Vkg-GFP intensity (J) or collagen IV staining intensity (K) in unwounded basement membrane in control and *Mmp1* mutants. Numbers in the boxes on graph indicate the number of animals measured. By Student's t-test, Vkg-GFP intensity (p=0.0051) and anti-collagen IV staining intensity (p=0.0054) are significantly lower in *Mmp1* mutants relative to wild type. **K)** Western blot of anti-GFP in unwounded whole *Vkg-GFP/+* and *Vkg-GFP Mmp1^{Q112*}/Mmp1^{2}* larvae, anti-actin as a loading control. **K')** Quantification of 3 western blots (as in K) showing no significant difference between Vkg-GFP protein levels in whole *Mmp1* mutant larvae versus wild-type by paired t-test (p=0.87). The fluorescence intensity of the bands was normalized to the loading control. Error bars represent standard error of the mean. (Adapted from Stevens and Page-McCaw 2012).

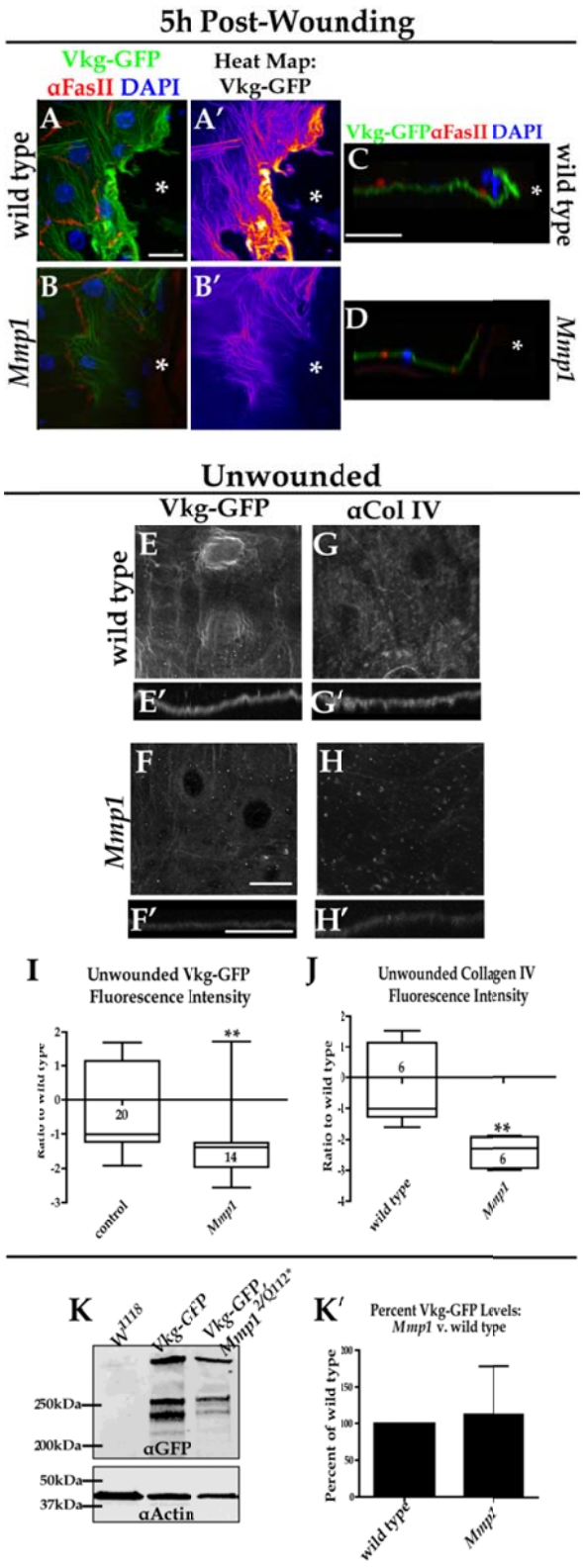
5h Post-Wounding
Vkg-GFP
αFasII DAPI
Heat Map:
Vkg-GFP
Vkg-GFPαFasII DAPI
wild type
Mmp1
Unwounded
Vkg-GFP
αCol IV
I
Unwounded Vkg-GFP
Fluorescence Intensity
Ratio to wild type
control
Mmp1
J
Unwounded Collagen IV
Fluorescence Intensity
wild type
Mmp1
K
250kDa
200kDa
αGFP
50kDa
37kDa
αActin
K′
Percent Vkg-GFP Levels:
Mmp1 v. wild type
Percent of wild type

***Mmp1* is required for migration after wounding.**

Cell migration is required to close wounds, so we asked whether cells at the leading edge of *Mmp1* mutant wounds were able to migrate. As cells migrate, they elongate in the direction of migration (reviewed in Mogilner and Keren, 2009a). We measured the aspect ratio of epidermal cells at the leading edge of the wound site (see Materials and Methods), comparing cell shape in healing wounds to initial cell shape in wounds that were immediately fixed after puncture, reasoning that the cell elongation represents a measure of migration. In wild-type wounds, we found that cell aspect ratios appeared to increase gradually over time, but that by 5h after wounding cells had clearly elongated (Fig. 2.7C). By 5h post-wounding, wild-type leading edge cells were almost twice as elongated as they were immediately post-wounding (Fig. 2.8A, A', C).

In contrast, leading edge cells failed to elongate by 5h in *Mmp1* mutants (Fig. 2.8B, B', C), and the aspect ratio remained fairly constant after wounding (Fig. 2.7D). In these mutants, cells maintained the aspect ratio they took on immediately after injury. We noticed that *Mmp1* epidermal cells are smaller than wild-type cells (see Figs. 2.8A, B and 2.7A, B), which may be secondary to the pronounced tracheal defects in the mutant that causes hypoxia (Beaucher et al., 2007a; Glasheen et al., 2010a). Epidermal cells knocked down for *Mmp1* (*A58>Mmp1-dsRNA*, Fig. 2.8C) did not exhibit marked changes in cell size, and these cells also failed to elongate after wounding (Fig. 2.8D), demonstrating that

Mmp1 is specifically required for cell elongation and migration. Similarly, when we overexpressed *Timp* in the epidermis, leading-edge cells failed to elongate (Fig. 2.8D). These data demonstrate that *Mmp1* in the epidermis is required for cells to elongate, the first step of migration.

Another characteristic of migrating cells is the presence of actin-rich projections in the direction of migration (reviewed in Mogilner and Keren, 2009a). As a second indicator of cell migration, we analyzed wound-induced actin changes in leading-edge epidermal cells using an Actin5C-GFP fusion protein (Verkhusha et al., 1999) expressed specifically in the epidermis with *A58-GAL4*. In wild-type tissue 1h after wounding we observed actin accumulation along the proximal side of leading edge cells, along with small, thin actin-rich projections extending into the wound bed (data not shown). By 5h post-wounding, wild-type cells had dense actin mesh along the proximal side of the leading edge cells with long, thick actin-rich projections extending into the wound bed (Fig. 2.8E), suggesting that these cells were actively migrating. In contrast, in *Mmp1* mutants 5h post-wounding we observed actin accumulation in stress fibers along the leading edge, but no projections extending into the wound bed (Fig. 2.8F), suggesting that leading edge cells in *Mmp1* mutants do not migrate to close the wound.

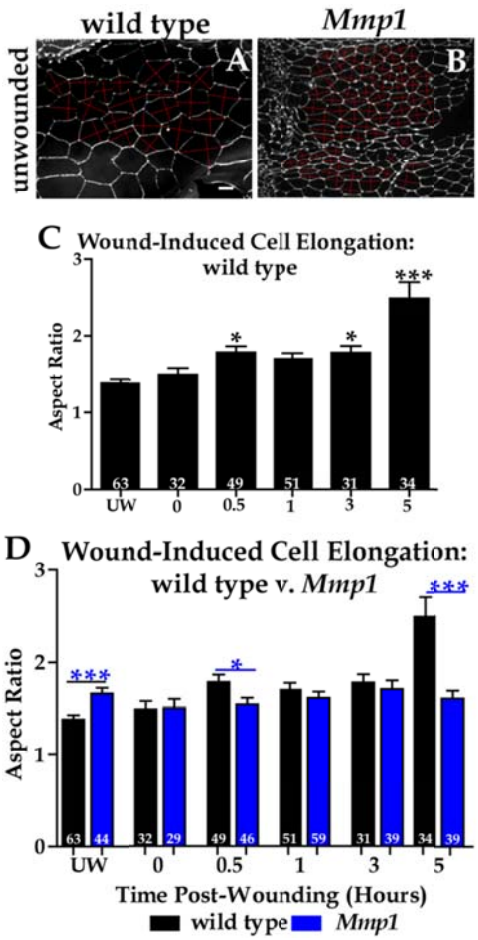

Figure 2.7: Wound-induced cell elongation changes.
A-B) Representative images of unwounded epidermis in wild type (A) and *Mmp1* mutants (B) with perpendicular red lines highlighting axes measured for aspect ratio calculations. Scale bar (A) represents 20μm. **C)** Quantification of wild-type wound-induced cell aspect-ratio changes over time in leading edge cells. Aspect ratios at each time point were compared to that at 0h post-wounding. Aspect ratios showed modest changes (with significant differences at 0.5h, p=0.017, and 3h, p=0.023) until 5h when ratios showed clear elongation that was highly significantly different from 0h ($p<0.0001$). **D)** Bar graph comparing aspect ratios between wild type and *Mmp1* mutants showing that *Mmp1* mutant cells are significantly different from wild-type in unwounded epidermis (p=0.0004), as well as at 0.5h (p=0.030) and 5h (p=0.0001) post-wounding. There is no significant difference between wild-type and *Mmp1* mutant cell elongation at 0h, 1h, and 3h post-wounding. Numbers on bars designate the number of cells measured within each genotype. Error bars represent the standard error of the mean (C-D). (Adapted from Stevens and Page-McCaw 2012).

Figure 2.8: *Mmp1* is required for leading edge cell migration.
A-B) Aspect ratios of wild-type (A,A') and *Mmp1* (B,B') leading edge cells were calculated by measuring perpendicular axes (shown in red), at 0h (A,B) and 5h (A',B') after wounding. See Materials and Methods for details. **C)** Aspect ratio analysis for wild type (black bars) and *Mmp1* mutants (blue bars). Black stars indicate that wild-type cells at 5h are significantly different from wild-type cells at 0h post-wounding ($p<0.0001$) by Student's t-test. Blue stars show that *Mmp1* mutant cells are significantly different from wild type at 5h ($p=0.0001$) post-wounding by Student's t-test. There is no significant difference in aspect ratio between wild-type and *Mmp1* mutant cells 0h post-wounding, and similarly cells in *Mmp1* mutants show no significant change in aspect ratio between 0 and 5h after wounding. **D)** Aspect ratio 5h post-wounding. Leading edge cells in *Mmp1* mutants ($p=0.0001$), *A58>Mmp1-dsRNA* ($p=0.0015$), *A58>Timp* ($p=0.041$), and *A58>Bsk^{DN}* ($p=0.0043$) are significantly less elongated than wild-type at 5h post-wounding. Numbers in the base of each bar (C-D) denote the number of cells measured. Error bars represent the standard error of the mean. **E, F)** Actin-GFP localization around control *A58>Actin-GFP* (E) and mutant *Mmp1^{2} A58>actin-GFP* (F) wounds (n=3 for each genotype). White arrows (E) indicate actin-rich protrusions into the wound bed. Asterisk indicates a wound bed (A-B, E-F). All scale bars are 20μm: A-B' scale bar in A', E-F scale bar in F. (Adapted from Stevens and Page-McCaw 2012).

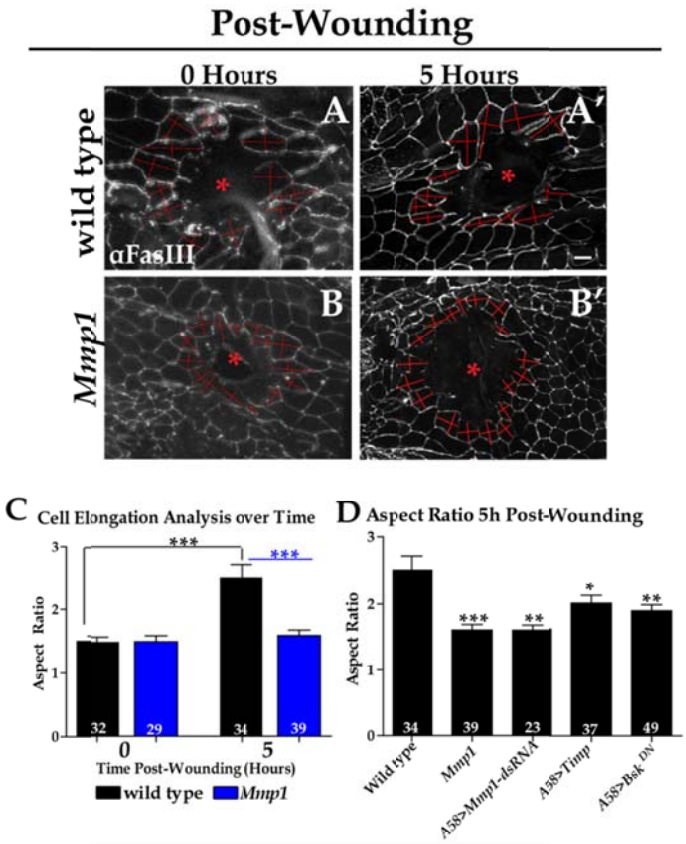
Post-Wounding
0 Hours
5 Hours
wild type
Mmp1
αFasIII
A
A′
B
B′
C
Cell Elongation Analysis over Time
Aspect Ratio
Time Post-Wounding (Hours)
wild type
Mmp1
***
32
29
34
39
D
Aspect Ratio 5h Post-Wounding
Wild type
Mmp1
A58>Mmp1-dsRNA
A58>Timp
A58>Bsk DN
34
39
23
37
49
wild type
Mmp1
Actin-GFP DAPI
E
F

One possible explanation for the lack of cell elongation in *Mmp1* mutants is that Mmp1 may be required to release the adhesion of cells from the ECM. In cell culture models, integrins on the distal edges of migrating cells are released from the basement membrane, allowing cells to progress forward, and there are reports of MMPs cleaving integrins (Pal-Ghosh et al., 2011; Vaisar et al., 2009). We examined βPS integrin localization at wild-type wounds by antibody staining, and we found that Mmp1 protein co-localized with βPS integrin at the distal edges of cells at the wound (Fig. 2.9). Although this co-localization suggested that Mmp1 may have a role in releasing β-integrins after wounding, we did not observe changes to integrin localization in our fixed wild-type samples at any time points during re-epithelialization (data not shown). Similarly, no changes in β-integrin staining were evident in *Mmp1* mutant wounds relative to wild-type wounds (data not shown). Although these negative results do not rule out the hypothesis that Mmp1 releases integrin-based adhesion, it seems unlikely that a failure to release adhesion at the distal edge would result in the observed failure of cell elongation (Fig. 2.8A-D); rather, persistent integrin adhesion at the distal edge would be expected to result in perpetually elongated cells that are non-motile, a phenotype not observed.

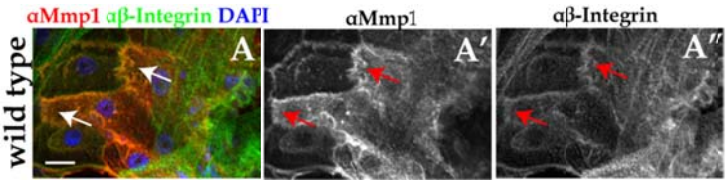

Figure 2.9: Mmp1 co-localizes with β-integrin post-wounding.
A-A″) Antibody staining against Mmp1 (A′) and against β-integrin (A″) showing co-localization (A) at the distal tips of leading edge cells 5h post-wounding, as indicated by arrows (n≥15). Scale bar in A represents 20μm. (Adapted from Stevens and Page-McCaw 2012).

Mmp1 promotes ERK activation.

In addition to functioning to remodel ECM, MMPs are also known to process components of signaling pathways, both activating and inactivating them (reviewed by Gill and Parks, 2008; Page-McCaw et al., 2007). In mammalian cell culture studies, ERK activation is necessary to induce epithelial cell motility and invasiveness (Doehn et al., 2009a; Matsubayashi et al., 2004a). It has been reported that ERK, a kinase that mediates receptor tyrosine kinase signaling, is activated in larval epidermal wounds (Wu et al., 2009a). To determine if *Mmp1* is required for signaling through receptor tyrosine kinase pathways, we examined the activation of ERK (encoded by *rolled*) in *Mmp1* mutants compared to wild type. Upon pathway activation, ERK is phosphorylated on two residues (called dpERK) and is translocated to the nucleus where it can be detected by a diphospho-ERK specific antibody (Gabay et al., 1997; Helman and Paroush, 2010). To examine the intensity of ERK activation in leading edge nuclei, we used DAPI to blindly identify nuclei in the leading edge cells, which we outlined and then measured the intensity of ERK

staining within the marked areas (see Materials and Methods). In wild-type animals, we found that dpERK activation is nearly undetectable in unwounded epidermis and increases modestly at 0.5h and 1h after wounding; but by 3h and 5h after wounding, dpERK levels are much greater in nuclei at the leading edge of wounds (Fig. 2.10 and Fig. 2.11). In contrast, in *Mmp1* mutant animals, ERK activation does not change appreciably after wounding (Fig. 2.11B, D). Similarly, in epidermal knock-downs of *Mmp1* (*A58>Mmp1-dsRNA*), dpERK activation is significantly decreased after wounding (Fig. 2.11C, D), although not as completely as in the *Mmp1* null animals, perhaps because of the residual leakiness of the knock-down (Fig. 2.3), or because of Mmp1 contributions from other unaffected tissues. Our data demonstrate that *Mmp1* is required to promote ERK signaling in epidermal cells after wounding.

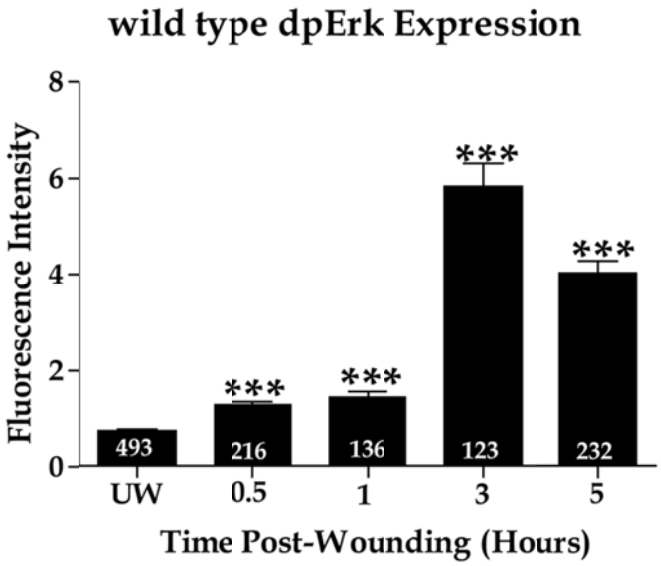

Figure 2.10: Wound-induced changes in wild-type dpErk intensity.
Quantification of wound-induced dpErk expression at the leading edge over time in wild-type animals (see Materials and Methods). dpErk is significantly upregulated, relative to unwounded expression, in all time points tested ($p<0.0001$ at each time point by Student's t-test). Error bars represent standard error of the mean. (Adapted from Stevens and Page-McCaw 2012).

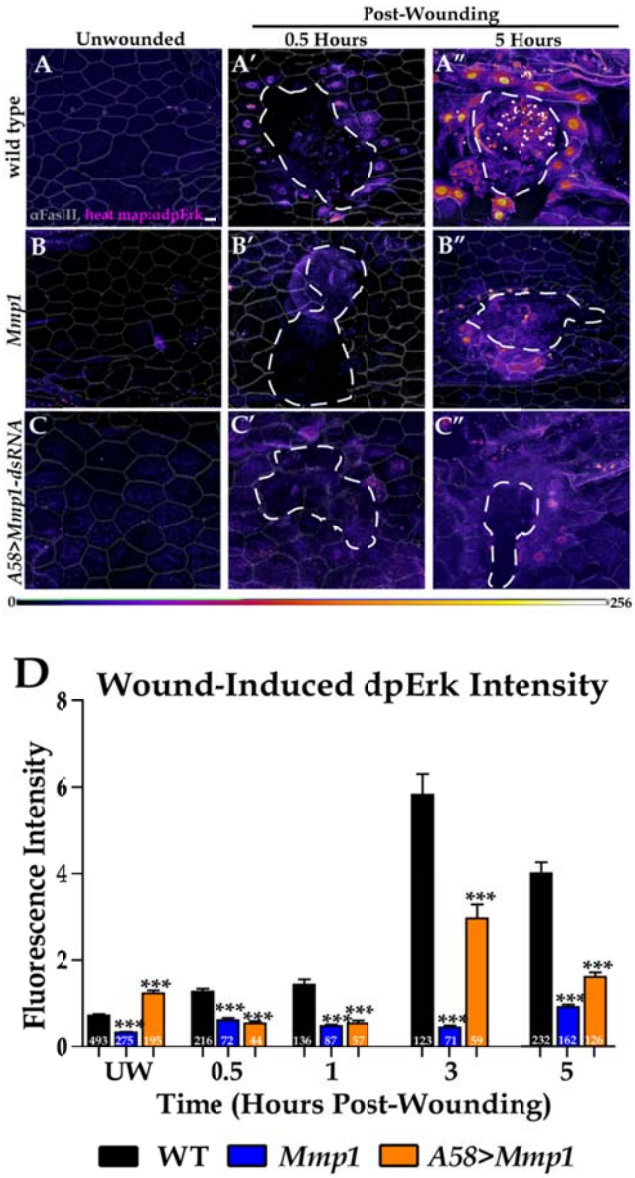

Figure 2.11: Mmp1 promotes wound-induced ERK activation.
A-C) Heat maps of anti-dpERK staining (color scale below panel C) in the indicated genotypes in unwounded (A-C), 0.5h (A′-C′), or 5h (A″-C″) post-wounding (n≥4 for all genotypes and time points). The cell border marker, FasIII (grey lines), is overlaid onto each image (A-C″) to outline cells. White dashed lines (A′-C′ and A″-C″) outline the wound bed. Scale bar (A) represents 20μm for all images. **D)** Quantification of anti-dpErk fluorescence intensity in leading edge cells over time (see Materials and Methods). At all time points tested after wounding dpErk intensity is significantly lower in both *Mmp1* and *A58>Mmp1-dsRNA* mutants relative to wild type ($p<0.001$ for all mutant to wild type comparisons) by Student's t-test. Numbers on each bar indicate the number of cells measured. Error bars represent the standard error of the mean. (Adapted from Stevens and Page-McCaw 2012).

***Mmp1* is regulated by JNK signaling during wound healing.**

Another pathway known to be required for wound healing is the JNK pathway (Galko and Krasnow, 2004b; Ramet et al., 2002; Wu et al., 2009a). Previous studies have shown that Mmp1 is regulated by JNK signaling during tumor invasion and wing disc eversion (Srivastava et al., 2007; Uhlirova and Bohmann, 2006). We asked if JNK signaling regulates Mmp1 activity during re-epithelialization by using a JNK *(Bsk)* dominant-negative construct (*UAS-Bsk^{DN}*) to interfere with JNK signaling specifically in the epidermis (*A58>Bsk^{DN}*). In unwounded tissue, there was no apparent difference in Mmp1 expression or localization in wild type compared with *A58>Bsk^{DN}* (compare Fig. 2.12A to B). After wounding, however, Mmp1 was not up-regulated in the epidermis of *A58>Bsk^{DN}* mutants as it was in wild-type (compare Fig. 2.12B to D). Furthermore, the re-epithelialization defects seen in the *Mmp1* mutants are also observed in the *A58>Bsk^{DN}* mutants including cell elongation failures (Fig. 2.12D) and wound closure failures (Galko and Krasnow, 2004b; our data not shown).

Ectopic up-regulation of the JNK pathway resulted in the up-regulation of Mmp1. Previous studies have shown that tumor necrosis factor-alpha (TNFα) stimulates JNK activation in mammalian cells and in *Drosophila* (Brenner et al., 1989; Igaki et al., 2009). When we over-stimulated the JNK pathway by overexpressing *Drosophila* TNF, *eiger* (*egr)*, in the epidermis (*A58>egr)*, Mmp1 expression in unwounded *A58>egr* epidermis was similar to wild-type (compare Fig. 2.12A to E). In contrast, 5h after wounding *A58>egr* epidermis, we observed

dramatic Mmp1 up-regulation not only in the epidermal cells at the wound site, but extending to epidermal cells about 5 cell-lengths from the wound (compare Fig. 2.12B to F). Importantly, *egr* overexpression in the epidermis caused accelerated wound closure. Five hours post-wounding, *A58>egr* wounds are significantly smaller than wild-type (Fig. 2.12B, F, G-G", H-H", I, J). To determine if the accelerated wound closure is *Mmp1*-dependent, we generated mutants that simultaneously overexpressed *egr* and knocked down *Mmp1* in the epidermis (A58>*egr, Mmp1-dsRNA*). We found that by 5h post-wounding, the average wound area in *A58>egr, Mmp1-dsRNA* mutants was not only significantly larger than both wild-type and *A58>egr* alone, but the wound areas were similar between *A58>egr, Mmp1-dsRNA* compared to *A58>Mmp1-dsRNA* (Fig. 2.12J). Taken together with the expression data, these results indicate that Mmp1 is downstream of and required for the accelerated healing function of egr. Although our data are consistent with the hypothesis that Mmp1 levels determine the rate of closure, it is also possible that other targets of egr signaling accelerate healing, and Mmp1 is simply a permissive factor. Unfortunately we could not test if increased Mmp1 directly accelerates healing because all animals ectopically expressing (GAL4-mediated) epidermal Mmp1 were lethal before third instar, even in the presence of GAL80 (not shown). As a whole, our results demonstrate that the *Drosophila* secreted MMP, Mmp1, is up-regulated in wounded epidermis where it promotes epidermal re-epithelialization, basement membrane repair, and wound signaling.

Figure 2.12: Mmp1 is positively regulated by JNK signaling during wound healing.
A-F) Heat map showing Mmp1 expression in the epidermis in unwounded (A,C,E) and 5h post-wounding (B,D,F) in the designated genotypes, pseudo-colored based on pixel intensity (intensity scale shown on right). A white dashed line (B,D) outlines the open wound beds. The white arrow (F) indicates the very small wound bed in *A58>egr* wounded epidermis. n≥5 for each genotype. Scale bar in E represents 20μm for A-F. **G-H)** Images of wounds at 0h (G,H), 3h (G′,H′), and 5h (G″,H″) post-wounding in wild type (G-G″) and *A58>egr* (H-H″) labeled with FasIII (yellow) and DAPI (blue). White dashed lines outline the wound bed. Scale bar in G represents 20μm for G-H″. **I)** Quantification of wound area over time in *A58>Mmp1-dsRNA* (orange line), wild type (black line), and *A58>egr* (purple line). *A58>Mmp1-dsRNA* wounds are significantly larger than wild type at 0.5h ($p=0.032$), 1h ($p=0.0005$) and 5h ($p=0.0027$) by Student's t-test. *A58>egr* wounds are significantly smaller than wild type at 5h ($p=0.031$) by t-test. There is no significant difference in wound area between mutants and wild type in initial wound area (0h). Areas of ≥3 wounds were measured for each time point. **J)** Wound area 5h post-wounding for the indicated genotypes. By t-test, wounds in *A58>Mmp1-dsRNA* ($p = 0.021$), *A58>egr* ($p = 0.031$) and *A58>egr, Mmp1-dsRNA* ($p = 0.017$) are all significantly different from wild type. Additionally, by t-test *A58>egr* wounds are significantly smaller than *A58>egr, Mmp1-dsRNA* ($p= 0.0024$) wounds at 5h post-wounding. There is no significant difference in wound area 5h post-wounding between *A58>Mmp1-dsRNA* and *A58>egr, Mmp1-dsRNA* mutants ($p=0.77$) by t-test. All error bars represent the standard error of the mean. (Adapted from Stevens and Page-McCaw 2012).

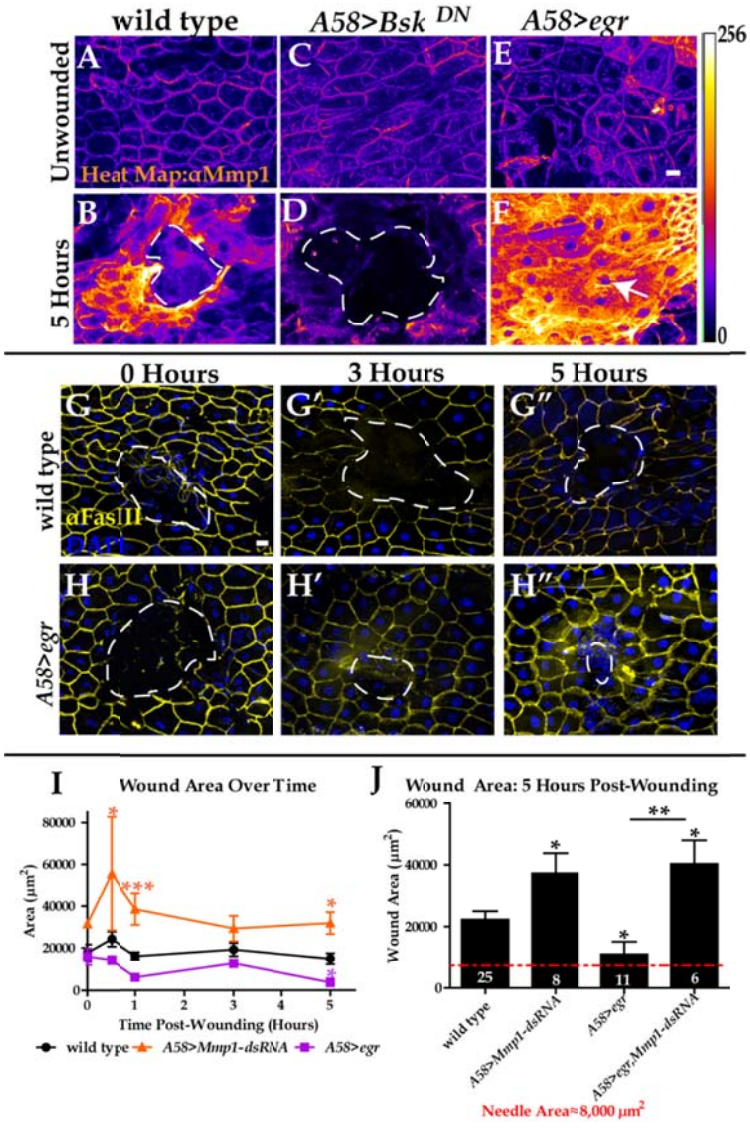
wild type
A58>Bsk DN
A58>egr
Unwounded
5 Hours
A
B
C
D
E
F
Heat Map:αMmp1
256
0
0 Hours
3 Hours
5 Hours
wild type
A58>egr
G
G′
G″
H
H′
H″
αFasIII
I
Wound Area Over Time
Area (μm²)
Time Post-Wounding (Hours)
wild type
A58>Mmp1-dsRNA
A58>egr
J
Wound Area: 5 Hours Post-Wounding
Wound Area (μm²)
25
8
11
6
wild type
A58>Mmp1-dsRNA
A58>egr
A58>egr,Mmp1-dsRNA
Needle Area≈8,000 μm²

Discussion

To bypass the complexities of the large and redundant set of MMPs expressed in mammalian wounds, we utilized the simple model organism, *Drosophila*, to analyze MMP function in wound healing. We find that both *Mmp1* and *Mmp2* null mutants display not just delays in wound healing, but a complete failure of re-epithelialization. Interestingly, wounding the double MMP mutants identifies the first instance of MMP redundancy in *Drosophila*: the two MMPs are redundant for clotting, as the double mutants bleed out within a few hours after wounding. Thus both MMPs are required for re-epithelialization and either MMP is required for hemostasis. Focusing on the role of the secreted MMP, we find that *Mmp1* is required in the epidermis for re-epithelialization, and that *Mmp1* is required for cell elongation, reorganizing the actin cytoskeleton, repairing the basement membrane, and promoting ERK signaling.

Mmp1 promotes assembly and repair of the basement membrane

Of the many defects observed in the *Mmp1* mutant wounds, it is possible that the defects in the basement membrane are primary, with the other phenotypes as consequences. Not only do leading edge cells fail to deposit collagen IV at the wound, but even unwounded basement membrane appears abnormal with respect to collagen IV levels. These data lead to the surprising conclusion that a secreted MMP is required not for matrix degradation, but to promote matrix assembly. Although this may seem paradoxical, we envision

MMPs contributing to ECM assembly by cleaving the existing basement membrane in order to insert new molecules, a step that may be required for matrix expansion as the animal grows. We note that the *MMP-14* (MT1-MMP) knock-out mouse has weakened tendons, suggesting a precedent for MMPs in promoting extracellular matrix assembly (Holmbeck et al., 1999), although the matrices of fibrillar collagen and basement membrane are very different.

The inability to deposit basement membrane could lead to severe consequences for wound healing. If the wound cannot repair the basement membrane, the cells could lack a scaffold to support cell migration, resulting in cell elongation failures and open wounds, as observed. It seems likely that the compromised basement membrane in the mutants is weaker than wild-type. The *Mmp1* mutant wounds were much larger than wild-type wounds, suggesting that they gap open after puncture. The actin stress-fibers observed in *Mmp1* mutant wounds may simply be a compensatory mechanism for the weak basement membrane, as the tissue attempts to increase stability with actin cables, similar to the actin cable formed in *Drosophila* embryos closing wounds (Wood et al., 2002a). As cells migrate they pull on their surrounding matrix, and a weak basement membrane may lack the resistance necessary for cell migration (Discher et al., 2005a; Kirmse et al., 2011b). Additionally, we note that the Mmp1 epidermal samples are much more fragile during dissection than the wild-type controls, possibly because of weakened basement membranes.

Mmp1 levels are regulated by JNK in response to wounding.

Wound healing is a tightly regulated processes, involving the orchestration of several signaling cascades including JNK signaling, which has previously been shown to be required for wound healing (Galko and Krasnow, 2004b; Ramet et al., 2002). MMPs have been shown to be regulated by JNK signaling in *Drosophila* during imaginal disc morphogenesis (Srivastava et al., 2007), in *Drosophila* tumor models (Uhlirova and Bohmann, 2006), and in zebrafish during the inflammatory phase of wound healing (Zhang et al., 2008); and JNK-regulation of MMPs has been observed in mammalian cell culture (Gum et al., 1997). We find that the dramatic Mmp1 up-regulation in wounded epidermis is dependent on JNK signaling. However, in unwounded epidermis, Mmp1 is expressed independently of JNK signaling, suggesting that only wound-induced expression of Mmp1, but not homeostatic expression of Mmp1, are under JNK control. Animals misexpressing TNF (*eiger*) in the epidermis and hyper-activating JNK had dramatically increased Mmp1 expression after wounding, and they displayed accelerated re-epithelialization. Importantly, this accelerated healing was dependent on *Mmp1*.

In mammals, *MMP-3, MMP-8, MMP-9,* and *MMP-13* knock-out mice have defects in wound healing. Although all these are secreted MMPs, the wounding phenotypes observed in fly *Mmp1* mutants, which lack all secreted MMPs, are most similar to *MMP-9* -/- mice. These mice have delayed re-epithelialization attributed to reduced mobility of their keratinocytes, which migrate more slowly

ex vivo (Kyriakides et al., 2009a). Interestingly, these mice also have abnormal deposition of collagen fibers. The main phenotypic difference between the *MMP-9 -/-* mice and the *Mmp1* mutant flies is that the fly wounds do not heal at all. By taking advantage of the many genetic tools available in *Drosophila,* our data demonstrates that *Mmp1*, under the control of the JNK pathway, functions during re-epithelialization *in vivo* to promote basement membrane deposition, cell elongation and migration, actin cytoskeletal reorganization, and ERK signaling.

CHAPTER III

MATRIX METALLOPROTEINASES ARE REQUIRED FOR HEMOSTASIS IN *DROSOPHILA*

Introduction

The initial step to wound healing, hemostasis, functions to seal the wound area, prevent further fluid loss and neutralize invading external pathogens (Singer and Clark, 1999). This initial step is critical to the success of the wound healing process, as well as for the survival of the organism, as clotting failures, such as those caused by hemophilia, lead to excessive fluid loss and often death after injury. In mammals, the components of the blood coagulation pathways are well understood. The components are quiescent under normal physiological conditions and only become activated in response to injury (Furie and Furie, 1992). Activation of clotting factors begins with the activation of tissue factor, a membrane protein found only on nonvascular, activated, cell surfaces (Osterud and Rapaport, 1977; Spicer et al., 1987), which leads to the activation of factor IXa and factor VIIIa creating the tenase complex, which converts factor X to factor Xa. Factor Xa will then interact with factor Va to form the prothrombinase complex (Mann et al., 1988). The thrombinase complex converts membrane-bound pro-thrombin to thrombin, releasing it from the membrane. To this point, all steps of the coagulation pathway occur at the cell membrane of activated

platelets (Mann et al., 1988). The clot is then formed by thrombin cleaving fibrinogen to create fibrin, which auto-polymerizes to form a fibrin clot, sealing the wound (Furie and Furie, 1992).

Injury promptly elicits the recruitment and activation of platelets, small cells that circulate in an inactive form in the blood. Upon activation, platelets will aggregate and adhere to the wound site (Furie and Furie, 1992). Activated platelets shed plasma membrane-derived microparticles (Ando et al., 1988; Sims et al., 1988) to provide the extensive volume of plasma membrane surface required for coagulation. These microparticles highly express factor VIII binding sites which promote prothrombinase complex formation and facilitates fibrin plug generation (Gilbert et al., 1991).

Like vertebrates, effective hemostasis is a critical initial step to the wound healing process in arthropods, particularly in light of the fact that arthropods have open circulatory systems. In insect larvae in particular, efficient clotting is especially important because the open circulatory system not only maintains body shape by hydrostatic pressure, but it also facilitates locomotion (Martinez Arias, 1993a). The components of the clotting mechanisms of mammals and arthropods share only functional similarity, with very few actual orthologs (Theopold, Schmidt et al. 2004). However, the end result of these pathways is similar: blood is coagulated to form a plug at the wound site, preventing fluid loss and neutralizing pathogens. In *Drosophila melanogaster,* as with other insects, there are two basic steps of hemostasis. First is the formation of a soft clot, which

is followed by activation of phenoloxidase (PO) to form a cross-linked, optically dense hard clot (Bidla et al., 2005; Galko and Krasnow, 2004a; Goto et al., 2003). Soft clot formation is mediated by hemocytes (*Drosophila* blood cells) that adhere to extracellular matrix (ECM) fibers, and then extend filopodia and membrane blebs across the wound area forming a clot matrix (Bidla et al., 2005). This fibrous matrix also ensnares hemocytes, which aid in clearing the wound site of pathogens (Scherfer et al., 2004). Formation of the soft clot is Ca^{2+}-dependent (Bidla et al., 2005) and is believed to involve hemolectin (Hml), a *Drosophila* protein with a domain structure similar to mammalian clotting factors, factor V, factor VIII, and von Willebrand factor (Goto et al., 2003; Goto et al., 2001). This initial clot formation is independent of the following melanization steps, clotting is observed in mutants that lack the key melanization cascade component, prophenoloxidase (PPO) (Scherfer et al., 2004).

A hallmark of the second phase of insect clot formation is the activation of melanization cascade through activation of the the zymogen, prophenoloxidase by the serine protease, prophenoloxidsae activating enzyme (PPAE) to create phenoloxidase (PO) (Cerenius and Soderhall, 2004). Once activated, PO functions to catalyze the oxidation of tyrosine-derived phenols to form quinones, which non-enzymatically polymerize to form melanin, a cytotoxic polymer that is deposited to seal wounds and encapsulate pathogens (Cerenius and Soderhall, 2004; Nappi et al., 2005). PPO is primarily produced by a specialized type of hemocyte called crystal cells, named for the crystalline inclusions observed

within these cells (Lanot et al., 2001; Meister and Lagueux, 2003). The melanization cascade is tightly regulated by the serine protease inhibitor, Serpin 27A (Spn27A) that functions to inhibit activated-PPAE (De Gregorio et al., 2002). In response to injury, or immune challenge, *Spn27A* mutants display profuse melanization, often form ectopic melanotic masses, and a have reduced ability to encapsulate pathogens during natural infections (De Gregorio et al., 2002; Ligoxygakis et al., 2002; Nappi et al., 2005), demonstrating the importance of maintaining precise control over the melanization cascade. In the absence of either PPO, such as in *Black cell* (*Bc*) mutants, or in the absence of hemocytes all together, as is the case in *Domino* (*Dom*) mutants, there are marked melanization failures, as well as diminished immune response following septic injury (Braun et al., 1998; Rizki and Rizki, 1959); indicating that PPO, and the hemocytes, from where it is primarily produced, play a vital role during wound healing and in the *Drosophila* innate immune response.

From our preliminary studies of MMPs during *Drosophila* wound healing, we have observed pronounced clotting and melanization defects in both *Mmp1* and *Mmp2* mutants, suggesting that both *Mmp1* and *Mmp2* may be required for hemostasis and scab formation following wounding. We also show that both the hemopexin and the catalytic domains of Mmp1 may be required for melanization. Interestingly, we find that re-epithelialization is not dependent on scab formation, as even wounds with light melanization successfully re-

epithelialize. Furthermore, in wounds lacking scabs, such as those induced by a pinch wound, *Mmp1* is required for re-epithelialization.

Methods

Fly lines.

The following lines are described in Page-McCaw et al (2003): $Mmp1^{2}$ and $Mmp2^{Df(2R)Uba1\text{-}Mmp2}$ (imprecise *P* excision alleles resulting in deletions of most or all of the coding region); $Mmp1^{Q112*}$, $Mmp1^{Q273*}$, $Mmp1^{W439*}$, and $Mmp2^{W307*}$ (EMS-induced nonsense alleles resulting in premature truncations); *UAS-Timp*. The dominant-negative $Mmp1^{\Delta Cat}$ line, which lacks the catalytic domain, used was *UAS-Mmp1.f1*$^{\Delta cat}$ (Glasheen et al., 2009b; Zhang et al., 2006). Other fly lines used were *A58-Gal4* (M. Galko), and *He-Gal4* (Flybase ID FBti0064641) both from the Bloomington *Drosophila* Stock Center, *UAS-Mmp1-dsRNA* (D. Bohmann), Bc^{1} (Flybase ID FBgn0261382) from the Bloomington *Drosophila* stock center, *Domino* (K.V. Anderson), $Spn27A^{1}$ (B. LeMaitre). For epistasis experiments, we generated Bc^{1} $Mmp1^{2}$ and *Spn27A* $Mmp1^{2}$ double mutant flies. w^{1118} was used as wild type.

Clotting kinetics.

The clotting kinetics assay was adapted from Goto, Kadwaski, et al (2003). Third instar larvae were impaled through the dorsal side between abdominal segments A3-A5 with a 0.1mm steel needle (Fine Science Tools) and left to heal on apple juice plates for the designated amount of time (5-30minutes). Wounded

larvae were then transferred to Whatman filter paper soaked in hemolymph-like solution (70mM NaCl + 5mM KCl + 1.5mM $CaCl_2$ + 20mM $MgCl_2$ + 10mM $NaHCO_3$ + 5mM Trehalose + 5mM HEPES, pH 7.2) at 5m intervals beginning at t=0; with animals transferred from wounding needle directly to filter paper (n=7 w^{1118}; n=2 $Mmp1^{2}$; n=2 $Mmp1^{Q273*}$ animals tested at each time point). Animals were left on wet filter paper, on ice, for 3h. Animals were then removed and the filter paper was incubated at 25C overnight to induce melanization of the collected hemolymph. Appearance of a melanized spot of hemolymph indicated that the wound had not undergone hemostasis prior to transferring the animal to the filter paper.

Scab formation analysis and quantification.

To assess scab formation phenotypes, 3rd instar larvae were impaled on the dorsal side between abdominal segments A3-A5 with a 0.1mm steel needle (Fine Science Tools) and allowed to heal at 25C for desired amount of time. For initial scab formation analysis (t = 0-30m post-wounding) bright field images were then taken of the dorsal wound on whole larvae (11 w^{1118} at 5m, 5 w^{1118} at 10m; at 30m: 28 w^{1118}, 30 $Mmp1^{2}$ or $Mmp1^{2/Q1112*}$, 3 *Dom*, 24 $Mmp1^{Q27*3/W439*,}$ 10 *He>Mmp1-dsRNA,* 13 *A58>Mmp1-dsRNA,* 7 *He>*$Mmp1^{\Delta Cat}$, 7 *A58>*$Mmp1^{\Delta Cat}$, 7 Bc^{1}, 21 $Spn27A^{1}$, *9* Bc^{1} $Mmp1^{2}$, 3 $Spn27A^{1}$ $Mmp1^{2}$).

For scab phenotype relative to wound area correlation experiments, animals were wounded and dissected according to procedures outlined in

Chapter II and Stevens and Page-McCaw (2012), and allowed to heal for 14h at 25C. DIC images at 20X were taken of scabs 14h post-wounding. Scab formation was classified as discrete (melanization formed neatly over wound area), profuse (melanization extends beyond wound bed and / or there are sites of ectopic melanization), or incomplete (discontinuous, lightly colored melanization, or very small melanin deposits near the wound site). The distribution of scab phenotypic class within genotype was plotted as percentage of total animals examined within genotype with GraphPad Prism v 5.01.

For wound area versus scab formation phenotype correlation studies, the wound area corresponding to each scab was calculated by Axiovision v.4.8 using the outline tool to specify the wound edge, as defined by FasIII and DAPI expression (see Methods from chapter II for more details regarding wound area measurements). Average wound area was calculated within each scab formation phenotypic class for each genotype and plotted, along with the standard error of the mean, using GraphPad Prism v.5.01.

Immunohistochemistry.

Fixed samples were washed and permeabilized in PBS + 0.2% Triton X-100, blocked in PBS + 5% goat serum + 0.02% NaN_3, incubated in 1^o antibody (diluted in PBS + 1% goat serum + 0.02%NaN_3) overnight at 4°C, washed and incubated in 2^o antibodies for 1.5 h at RT in the dark, and mounted in Vectashield mounting media with DAPI (Vector Labs). Anti-Mmp1 catalytic

domain (a 1:1:1 cocktail of mouse monoclonal IgG1 antibodies 3B8, 5H7, and 23G, generated by Page-McCaw et al (2003) and obtained from the Developmental Studies Hybridoma Bank (DSHB), was used at 1:100. Anti-FasIII (a mouse monoclonal IgG2a from the DSHB) was used at 1:10. Cy3 labeled goat anti-mouse IgG1 (Jackson ImmunoResearch), DyeLight649 labeled goat anti-mouse IgG2a (Jackson ImmunoResearch) were all used at 1:300.

Microscopy.

Bright field images of whole larvae were acquired on a Zeiss SteREO Lumar. V12 mircoscope equipped with a NeoLumar S 0.8X FWD 8mm objective, using an additional ~22.5X digital zoom to acquire color bright field images of the dorsal wound site using an AxioCam MR3 color camera and Axiovision v4.8 acquisition software (Zeiss). Images were collected using AxioVision v4.8 software (Ziess). Fourteen hour scab formation images were obtained with a Zeiss Axio imager Z1 microscope using the 20X/0.8 Plan Apochromat objective. DIC images were acquired with an Axiocom MRc color camera using Axiovision v4.8 acquisition software (Zeiss). Optical sectioning was performed with a Zeiss Apotome mounted on an Axio imager Z1 or M2, with the 20X/0.8 Plan Apochromat objective. Fluorescent images were acquired with an Axiocam MRm (Zeiss) camera paired with Axiovision 4.8 (Zeiss). Z-stacks were compressed into 2D XY projections using the orthoview function in Axiovision. All DIC images were exported from Axiovision v.4.8 as 16-bit, color, TIFF files.

All fluorescent images were exported from their acquisition programs as 16-bit, grayscale, TIFF files. All post-processing was done in either in Adobe Photoshop CS4, or ImageJ v.1.43u.

Melanization inhibition assay.

3rd instar larvae were anaesthetized by exposure to diethyl ether for approximately 2 minutes in a closed chamber. A nanoinject was used to inject 27.6nl of 1mM Phenylthiourea (PTU) in PBS + 20%DMSO, or 27.6nl of vehicle only (PBS + 20%DMSO), in larvae on the dorsal side between abdominal segments A3-A5 with a glass needle. Larvae were transferred to apple juice plates and animals were allowed to recover for 14h at 25C. The injection site served as the wound site for all subsequent analysis. Wounded epidermis was dissected and collected according to protocol outlined in Chapter II (Stevens and Page-McCaw, 2012).

Wounding assays.

Both puncture and pinch wounding assays were adapted from Galko and Krasnow (2004a) and are described in detail in chapter II, as well as in Stevens and Page-McCaw (2012). For puncture wound suturing, 3rd instar larvae (12 w^{1118} and 15 Bc^{1}) were wounded with a 0.1mm steel needle through the dorsal side. Immediately after wounding, a flat toothpick was used to apply a small

amount of Krazy® Glue to the wound site. Animals were left to heal at 25C for a desired amount of time.

Results

Mmp1 is required for hemostasis and scab formation.

In mammals, the secreted MMP, MMP-2, has been shown to be secreted by activated platelets and to play a role in platelet aggregation *in vitro* (Kazes et al., 2000; Sawicki et al., 1997). In *Drosophila,* as in mammals, hemostasis is a critical first step in the wound healing process, so we asked if MMPs were involved in clotting in our *in vivo* wound healing model. First we characterized wild-type clotting kinetics using a bleeding assay developed by Goto, et al. (2003). In wild-type larvae, evidence of clotting is observed as early as 10min post-wounding (Fig 3.1A). After 30min post-wounding, wild type animals have successfully completed hemostasis, with no detectable hemolymph spots in the filter paper (Fig. 3.1A). Using brightfield microscopy to analyze melanization of the wound site on the animal, we found a slight darkening of the wild-type wound site at 5min (fig. 3.1B; n=10) and 10min (Fig. 3.1B'; n=5) with a very dark melanin deposit observed by 30min post-wounding (fig. 3.1B"; n=28), similar to that observed by Galko and Krasnow (2004a). The clotting kinetic assay showed only minimal hemolymph in the absence of *Mmp1* 5min post-wounding (fig3.1C). While there appears to be some variability, the general lack of melanized hemolymph spots on the filter paper, suggests that either loss of

Mmp1 may induce accelerated clotting relative to wild type, or that these mutants have may have defects in the melanization cascade. By this assay a wound that has successfully completed hemostasis and defective melanization appear the same. It is important to note that these are preliminary results and need to be repeated.

To determine if *Mmp1* mutants have melanization defects, we analyzed melanin deposition at the wound site 30min post-wounding. In *Dom* mutants, which lack hemocytes, 30min post-wounding wounds are have no detectable melanization and in most cases have failed to form the initial soft clot (Fig. 3.1E, n=2), as these mutants often bleed out shortly after wounding, indicating that both hemostasis and scab formation require hemocytes. Similarly, in *Mmp1* mutants (fig. 3.1F; n=40) we observe only very light melanization, often forming a halo pattern around the wound site. Additionally, in *Mmp1* mutants we often find hemolymph and internal organs forming a bleb out of the wound site (an example is shown in fig 3.1F).

During tracheal development, the *Mmp1* hemopexin and catalytic domains have independent functions (Glasheen et al., 2009a), so to determine which domain of *Mmp1* is required for hemostasis, we measured clotting kinetics in $Mmp1^{Q273*}$ ($Mmp1^{\Delta Pex}$) mutants, which lack the hemopexin, or substrate recognition, domain (Glasheen et al., 2009a). In $Mmp1^{\Delta Pex}$ mutants, hemolymph spots were observed as late at 30min post-wounding (fig. 3.1D), which may suggest that the Mmp1 hemopexin domain is required for clot formation, but not

melanization as hemolymph collected by our bleeding assays does darken similar to that from wounded wild-type animals. Similar to both the *Dom* and *Mmp1* mutants, when we analyzed melanization of the wound site on the whole animals 30min post-wounding, we observed only very light melanization, again often forming a halo pattern, along what we presume are the wound edges (fig 3.1G; n=23). Together, these results suggest that *Mmp1*, and the *Mmp1* hemopexin domain specifically, are required for melanization of the wound site. Additionally, our preliminary clotting experiments, suggest that *Mmp1* may play a role in hemostasis.

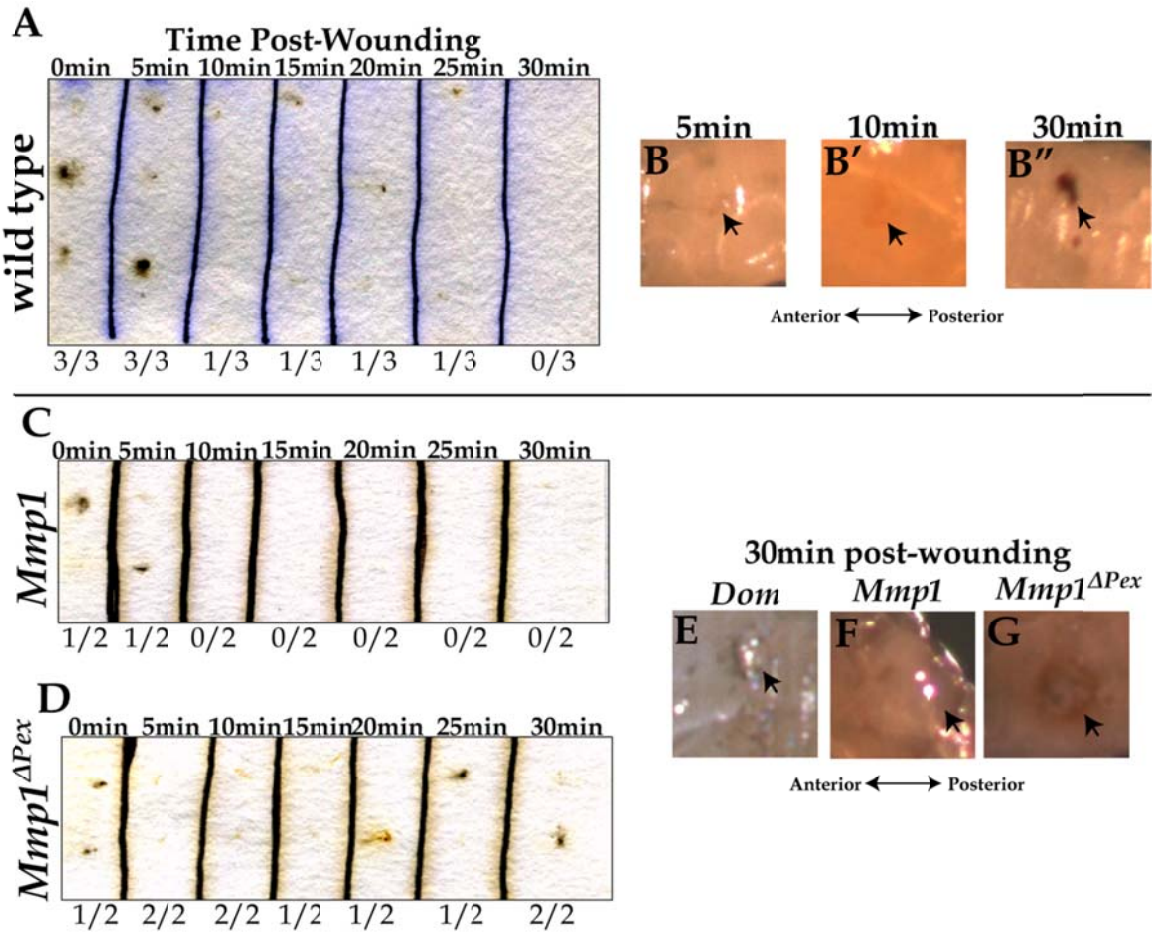

Figure 3.1: *Mmp1* is required for scab formation.
A)Time course for wild type clotting measured by amount of melanization after time specified above each lane (n=3 larvae at each time point). **B-B″)** Representative DIC images of scab at 5m (B) 10m (B′) and 30m (B″) post-wounding in wild type larvae (n ≥ 5 at each time point). **C)** Clotting time course for *Mmp1* mutants (n=2 larvae at each time point). **D)** Clotting time course for $Mmp1^{\Delta Pex}$ (n=2 larvae at each time point; see methods for allelic designations). Numbers under clotting panels (A, C, D) indicate the number of melanized spots observed over the total number of animals tested in at each time point. **E-G)** Representative DIC images of scab formation 30m post-wounding in *Dom* (E), *Mmp1* (F), and $Mmp1^{\Delta Pex}$ (G) (n ≥ 6 for each genotype). See methods for allelic designations. In B-B″, E-G anterior is to the left, as shown in diagram below B′ and F.

Mmp1 may be required in both hemocytes and epidermis for scab formation.

The melanization cascade is primarily carried out in crystal cells, a type of hemocyte (Meister, 2004), so we asked if *Mmp1* is required in the hemocytes for melanization post-wounding using an inducible *UAS-Mmp1-dsRNA* construct

driven with *Hemese-Gal4* (*He-Gal4*) specifically in the hemocytes (*He>Mmp1-dsRNA*). Unlike wild-type animals (fig. 3.2A; n=28), wounds in *He>Mmp1-dsRNA* animals are incompletely melanized (Fig 3.2B; n=10) 30min post-wounding, often with the halo pattern similar to that seen in *Mmp1* mutants (Fig. 3.1F); thus suggesting that *Mmp1* expression specifically in the hemocytes is required for melanization post-wounding. As Mmp1 is a secreted protease, we asked if other tissues are involved in wound healing, namely the epidermis. Interestingly, when we knocked down Mmp1 expression specifically in the epidermis with the epidermal driver *A58-Gal4*, we saw less melanization at the wound site than wild type (compare fig 3.2C to 3.2A; n=6), suggesting that epidermal Mmp1 expression may also promote melanization at the wound site. By utilizing an Mmp1 construct lacking the catalytic domain (*UAS-Mmp1$^{\Delta Cat}$*), which functions as a dominant-negative (Glasheen et al., 2009a), we can determine if Mmp1 catalytic activity is required for melanization. Expression of the catalytically-deleted Mmp1 in either the hemocytes (*He>Mmp1$^{\Delta Cat}$*), or in the epidermis (*A58>Mmp1$^{\Delta Cat}$*) resulted in incomplete melanization 30m post-wounding (Fig. 3.2D, E; n=7 for both genotypes), indicating that catalytically-active Mmp1 is necessary to facilitate melanization of the wound. However, as Mmp1 is a secreted protein, overexpression of the dominant-negative, catalytically-inactive Mmp1 could interfere with endogenous Mmp1 release from other tissue sources as well; as a consequence we are unable to draw any

conclusions regarding the tissue source in which the Mmp1 catalytic domain is required to promote melanization.

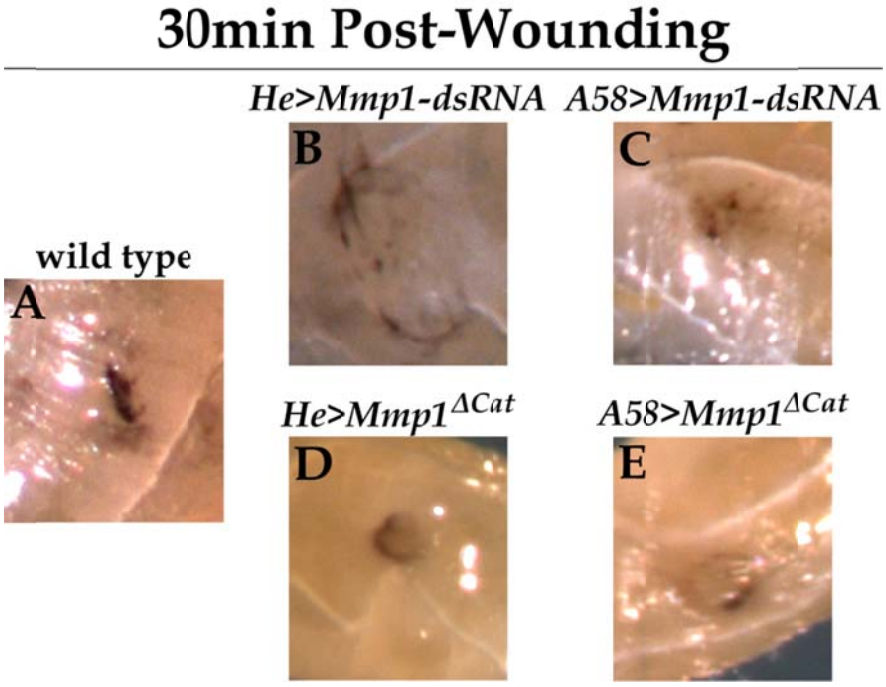

Figure 3.2: Mmp1 expression is required in both hemocytes and epidermis for melanization. **A-E)** DIC images of scab formation 30min post-wounding in designated genotypes (n ≥ 7 larvae, for all genotypes). For all images, anterior is to the left.

Mmp1 and *Mmp2* function to regulate melanization.

Fourteen hours after wounding, a time point when most wild-type animals have completed re-epithelialization (Fig. 2.1 and Stevens and Page-McCaw (2012)), we find three classes of scab formation: discrete scabs, with a solid, optically dense, melanin deposit limited to the area of the initial wound, such as that seen in Fig. 3.3A; profuse melanization, which we define as large

scabs that cover an area much larger than the initial wound size, often accompanied by regions of ectopic melanization near, but not at the wound site (see example in Fig. 3.3D); and incomplete melanization, characterized by light, often discontinuous melanization near the area of the wound (Fig. 3.3B), or very small melanin deposits in the wound bed. In wild type animals, 14h post-wounding, the melanin plug can be described as a discrete scab with melanin deposited exclusively in the immediate vicinity of the wound in 46% of animals tested (Fig 3.3A, E). In *Mmp1* mutants, on the other hand, there is generally very little melanization of the wound site (66% of animals) and what is present is typically lightly colored and discontinuous (Fig. 3.3B, E), suggesting that *Mmp1* may function to promote melanization of the wound site. Interestingly, some *Mmp1* mutants (33% of animals) are able to form what appear to be discrete scabs, suggesting that there may be compensatory mechanisms to overcome the loss of *Mmp1.*

One possible candidate is the other *Drosophila* membrane-anchored MMP, *Mmp2*. Scab formation in *Mmp2* mutants 14h post-wounding appears similar to wild type, but with a higher propensity to form profusely melanized scabs (42% in *Mmp2* compared to only 15% in wild type; Fig. 3.3C, E), indicating that *Mmp2* may have a role in limiting the melanization cascade. Unfortunately, this analysis could not be performed on *Mmp1 Mmp2* double mutants, as these animals have severe clotting defects and bleed out within hours of wounding.

The exacerbation of the *Mmp1* melanization and clotting phenotypes in the *Mmp1 Mmp2* double mutants not only indicates that MMPs play a pivotal role in regulating scab formation, but suggests that *Mmp1* and *Mmp2* may function redundantly, or additively, to facilitate re-epithelialization.

Drosophila MMP's are inhibited by an endogenous inhibitor, *Timp* (*Tissue Inhibitor of Metalloproteinase*). In the absence of *Timp*, both *Mmp1* and *Mmp2* would presumably be able to act on their substrate unchecked, leading to excessive melanization of the wound site. Indeed, that is exactly what we find. Unlike the *Mmp1* mutants, scab formation in *Timp* mutants ranges from discrete to profuse melanization (Fig 3.3D, E), with a much higher incidence of profuse melanization than seen in wild type (50% in *Timp* compared to 15% in wild type). The *Mmp1*-dependent melanization phenotypes are recapitulated when *Timp* is over-expressed in the epidermis (*A58>Timp*), leading to primarily incomplete scab formation (Fig. 3.3E); thus indicating that overexpression of the endogenous inhibitor blocks *Mmp1* function and prevents proper scab formation. Together, these results suggest that both *Mmp1* and *Mmp2*, under the regulation of *Timp*, function to regulate the melanization cascade. Additionally, these results suggest that *Mmp1* may function to promote melanization, while *Mmp2* may functions to inhibit melanization.

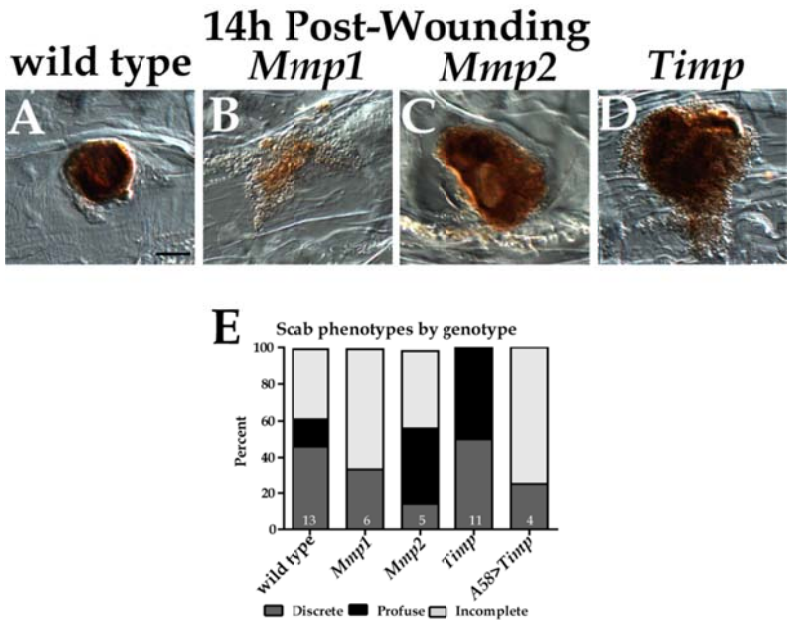

Figure 3.3: Scab phenotype is not indicative of re-epithelialization phenotype.
A-D) DIC images of scab formation 14h post-wounding in designated genotypes. Scale bar in (A) represents 50μm. **E)** Graph showing the percent representation of each scab phenotypic class within genotype. Dark grey shows discrete class (example shown in (A)), black represents profuse melanization class (example depicted in (D)), and light grey represents incomplete melanization class (example shown in (B)). Numbers on each bar indicate the total number of animals tested of each genotype. The percentage of animals within each phenotypic class is dependent on genotype based on Chi-squared analysis (X^2=207.5; df=8; p<0.0001).

Mmp1 may function downstream of Spn27A during scab formation.

One of the benefits of *Drosophila* as a model organism is that it is genetically tractable, an ideal characteristic for elucidating biochemical pathways *in vivo*. To understand how Mmp1 is involved in facilitating melanization, we performed two epistasis tests to try to position Mmp1 in the melanization cascade. Injury induces activation of serine protease cascades, which subsequently lead to the activation of PPAE, a key protease necessary for the activation of the oxidase, PPO, which leads to oxidation of the cytotoxic melanin

pre-cursors, quinones. Polymerization of quinones, analogous to fibrin polymerization in mammals, forms a plug at the wound site, sealing the wound (diagramed in fig 3.4A and reviewed in Cerenius and Soderhall (2004). The melanization cascade is regulated by serpin27A (spn 27A), which directly inhibits PPAE (De Gregorio et al., 2002; Leclerc et al., 2006; Ligoxygakis et al., 2002). *Black cell* (*Bc*) mutants have a mutation that causes crystal cells to spontaneously melanize, presumably by a mutation in PO (Gajewski et al., 2007; Rizki and Rizki, 1959). When wounded, melanization at the wound site fails in Bc^{1} and the animals often bleed out post-wounding (Fig. 3.4C). Conversely, loss of the inhibitor, *Spn27A*, results in profuse melanization at the wound site (Fig. 3.4D, black arrow), as well as formation of ectopic melanotic masses that are generally found posterior to the wound site (Fig 3.4D, red arrow; and observed by De Gregorio, Han et al. (2002)). To determine if *Mmp1* was directly involved in the melanization cascade we generated Bc^{1} $Mmp1^{2}$ double mutants and *Spn27A* $Mmp1^{2}$ double mutants and assayed scab formation 30m post-wounding (Fig. 3.4 B-G). Similar to Bc^{1} mutants (Fig. 3.4C), Bc^{1} $Mmp1^{2}$ double mutants we find a complete failure in melanin deposition at the wound site (Fig. 3.4F). As this phenotype is more severe than that observed in the *Mmp1* mutant alone (Fig. 3.4E), we predict that *Mmp1* functions downstream of *Bc* in the melanization cascade. However, as both the Bc^{1} and *Mmp1* single mutants have a similar melanization phenotype, the results from the Bc^{1} *Mmp1* double mutants are difficult to interpret. In the *Spn27A Mmp1* double mutant there is minimal

melanization at the wound site 30m post-wounding (Fig3.4G, black arrow); suggesting that even in the absence of the inhibitor, melanin is unable to be produced without Mmp1. However, this is a preliminary result, as only 3 *Spn27A Mmp1* double mutants were tested. As shown in Fig. 3.3, there is some variability in melanization even in wild type, so a larger number of *Spn27A Mmp1* mutants should be analyzed to confirm the presented result. Interestingly, in the *Spn27A Mmp1* double mutants we observe an occasional small ectopic melanotic mass, similar to that seen in *Spn27A* mutants (compare fig 3.4D to 3.4F, yellow arrows), suggesting that the formation of ectopic melanotic masses and melanin deposition at a wound site may be under the regulation of two independent mechanisms, one that requires Mmp1, and one that does not.

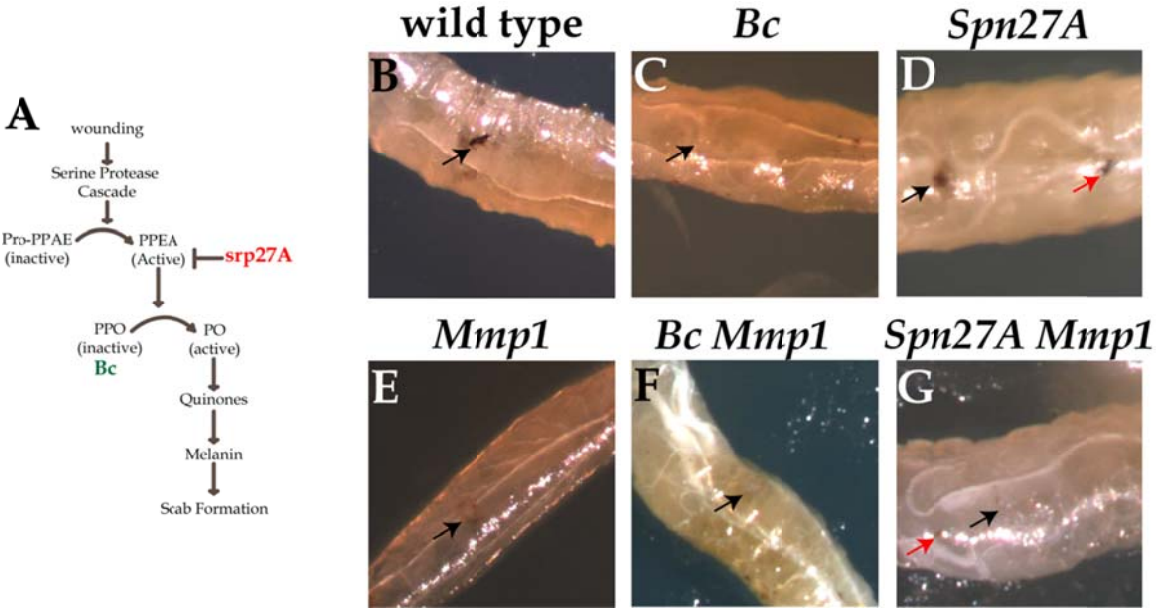

Figure 3.4: Mmp1 may function downstream of Spn27A during scab formation.
A) Schematic of the melanization cascade. Wounding induced serine protease cascades to activate prophenoloxdase activating enzyme (PPAE), which then converts prophenoloxidase (PPO) to phenoloxidase (PO), or Bc, leading to the production of quinones, which polymerize to form melanin, facilitating scab formation. PO is inhibited by Spn27A. **B- G)** DIC images of scab formation 30m post-wounding in wild type (B), *Bc* (C), *Spn27A* (D), *Mmp1* (E), *Bc Mmp1* (F), and (G). Black arrows indicate wound site. Red arrows (D, G) indicate ectopic melanotic masses. n ≥ 3 for all genotypes.

Re-epithelialization is not dependent on scab formation.

In vertebrates, the fibrin clot functions as a scaffold to facilitate mesenchymal cell migration into the wound bed (Singer and Clark, 1999). In the absence of the clot, cells lack a scaffold to support migration and re-epithelialization fails. To determine if the re-epithelialization defects that we have reported in *Mmp1, Mmp2,* and *Timp* mutants (Chapters II, V, and Stevens and Page-McCaw (2012) are secondary to melanization defects, we first asked if

scab formation defects were sufficient to cause re-epithelialization defects. We attempted to measure wound area in *Dom* or Bc^{1} mutants, which are unable to produce melanin due to a lack of hemocytes. While *Bc* is presently a mutation that is not mapped to the genome, it is hypothesized to be a mutation in PPO (Gajewski et al., 2007). Unfortunately, we were unsuccessful analyzing re-epithelialization in either mutant because these animals bleed out shortly after wound induction due to clotting defects.

Cyanoacrylate adhesives, or superglue, were first used on human patients on battle fields during the Vietnam war to stop severe hemorrhaging, seal wounds, and save lives (Coover, 1959). In an attempt to assess re-epithelialization in *Dom* or *Bc* mutants, we applied small amounts of Krazy® Glue to wound sites immediately following stabbing. Unfortunately, this was unsuccessful, as animals either died, or the superglue affixed too much other tissue to the wound site, obstructing our view of the epidermis after infection (data not shown; n=24 wild type and n=15 *Bc* mutants).

Finally to determine if scab formation correlated with re-epithelialization, we compared wound area to melanization phenotype, within wild type only, 14h post-wounding using the melanization classification system defined above. By this analysis, we find no differences in wound area between scab formation classes in wild type (Fig 3.5A), indicating that re-epithelialization is not dependent on scab formation. To confirm these results, we tried to inhibit

melanization in wild type animals by injecting the melanization inhibitor, Phenylthiourea (PTU), at the time of wounding, allowing the animals to heal for 18h, then measured wound area. At 1mM PTU viability was unaffected compared to vehicle only controls (data not shown), while still inducing mild melanization defects; 4 of 5 animals tested showed incomplete melanization 14h post-wounding (compare fig 3.5B to 3.5B'). Despite these scab formation defects, these animals have no re-epithelialization defects, both control and 1mM PTU animals complete re-epithelialization within 14h post-wounding (Fig. 3.5C), indicating that re-epithelialization is not dependent on scab formation.

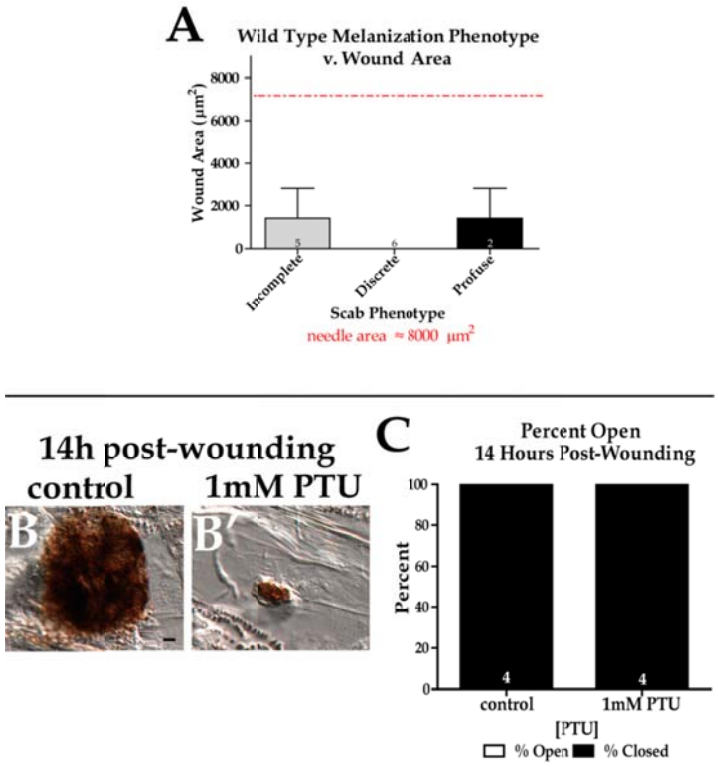

Figure3.5: Re-epithelialization is not dependent on scab formation.
A) Graph of average wound area within each scab phenotypic class in wild type animals 14h post-wounding. Error bars represent the standard error of the mean. There is no significant difference in wound area between the phenotypic classes by one-way ANOVA. **B,B')** DIC images of scab formation in wild type control (B) compared to wild type + 1mM PTU (B′) samples. Scale bar in (B) represents 20μm. **C)** Graph showing that percentage of closed versus open wounding in animals treated with 1mM PTU relative to controls. All wounds in both treatment groups closed by 14h post-wounding. Numbers on bars on graphs (A, C) indicate the n-value for that group. All images taken at 20X.

Mmp1 is required for re-epithelialization in pinch wounds.

Previous studies in our lab have shown that *Mmp1* is required for re-epithelialization after puncture wounding (Chapter II, and Stevens and Page-McCaw 2012). While our data indicate that scab formation in general is not required for re-epithelialization, we asked if *Mmp1* is necessary for re-epithelialization in wounds that do not require either the initial hemostasis steps

or scab formation, namely pinch wounds. In a pinch wound, the overlying cuticle remains intact while extensive damage is inflicted upon the underlying epidermis. Presumably the basement membrane is also damaged in the pinch wounding process, but this should be confirmed by closer examination of basement membrane in general by electron microscopy (EM), or at the analysis of individual ECM components, such as Collagen IV, perhaps by simple IHC techniques, following pinch wounding. Wild type and *Mmp1* mutants were pinched on the dorsal side with #5 dissecting forceps then left to heal at 25C (assay adapted from Galko and Krasnow (2004a)). Eighteen hours post-wounding, pinch wounds in wild-type animals have completely re-epithelialized (Fig 3.6A, C). However, in the absence of *Mmp1*, pinch wounds remain open (Fig. 3.6B, C), with an average wound area 18h post-wounding that is significantly larger than wild type (Fig 3.6D); thus, demonstrating that *Mmp1* is required for re-epithelialization regardless of the need for hemostasis. Interestingly, open wounds in *Mmp1* mutants typically have a large number of hemocytes congregating in the wound bed (small nuclei in the wound bed in Fig. 3.6B), often expressing low levels of the cell junction protein, Fasciclin III (FasIII). In fact, pinch wounds in *Mmp1* mutants can be identified by this characteristic concentration of hemocytes within a hole in the epidermal sheet. The edge of the wound is also often lined with numerous, of what appear to be, epidermal cells unable to migrate into the wound bed (Fig 3.6B). Together, these observations suggest that perhaps in the absence of *Mmp1*-induced epidermal cell migration

(see Chapter II); hemocytes attempt to compensate by infiltrating the wound bed, adopting an adhesive morphology, and forming aggregates to hold the weakened epidermis together. The presence of a large population of hemocytes in the wound additionally suggests that pinch wounding elicits an inflammatory response in addition to re-epithelialization, which may contribute to pinch wound healing.

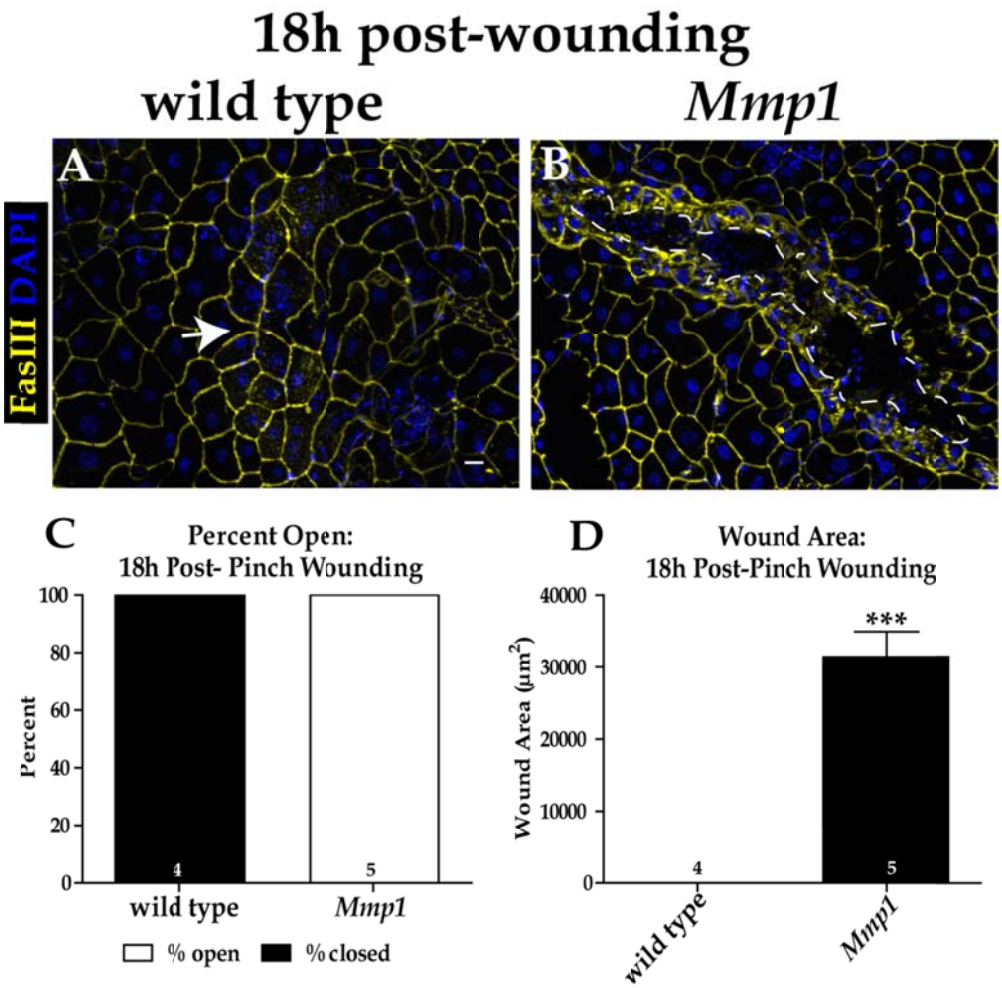

Figure 3.6: *Mmp1* is required for re-epithelialization after pinch wounding.
A-B) 20x XY projections of pinch wounds 18h post-wounding in wild type (A) and $Mmp1^{2/Q112*}$ mutants (B). The white arrow (A) indicated the location of the closed wound in wild type animals. White dashed line (B) outlines the open wound of *Mmp1* mutants. Scale bar (A) represents 20µm. Cell borders are labeled with anti-FasIII (yellow) and nuclei are labeled with DAPI (blue). **C)** Graph of percent of wounds remaining open versus closed 18h post-pinch wounding. **D)** Graph of average wound area 18h post-wounding in wild type and *Mmp1* mutants. Error bars represent standard error of the mean. Wounds are significantly larger in *Mmp1* mutants relative to wild type 18h post-wounding by Student's T-test ($p = 0.0009$). Numbers on, or above, each bar in graphs (C-D) specify the number of animals / wounds measured.

Discussion

Mmp1 and *Mmp2* regulate scab formation.

Hemostasis is a critical first step in the wound healing process. Clotting failure often leads to hemorrhaging and, in mammals, prevents the subsequent re-epithelialization process. While this important initial step in wound healing is well characterized in mammals, it is often overlooked in arthropods, leaving much to be learned about the regulation of the clotting and the subsequent scab formation process, as well as the function of the melanization cascade during wound healing in arthropods. Our preliminary studies indicate that both the secreted extracellular protease, *Mmp1,* as well as the membrane-anchored protease, *Mmp2*, under the control of *Timp*, functions during both soft clot formation and melanization in response to wounding.

During the initial clotting phases, our data suggest that *Mmp1* is play a role in promoting clotting, as we observe clotting delays in the *Mmp1* mutant background. It is possible that these clotting defects are secondary to the basement membrane defects that we find in *Mmp1* mutants (Stevens and Page-McCaw, 2012). The clot matrix that is established during *Drosophila* hemostasis is composed primarily of ECM strands and filipodia projected into the clot by hemocytes (Bidla et al., 2005); therefore it is plausible that without *Mmp1* to promote proper basement membrane integrity and to modify ECM components, the ability of hemocytes to extend those filopodia into the clot would be

compromised, as there would not be the cell would be unable to form the requisite cell-ECM adhesions that facilitate such cell morphology changes, leading to the impaired clotting phenotypes that we observed in the *Mmp1* mutant background.

Previous studies in our lab have suggested that the different domains of Mmp1 may have independent functions during tissue remodeling (Glasheen et al., 2009a). This does not appear to the case during scab formation, where we have demonstrated that both the hemopexin and catalytic domains of Mmp1 are required. When we disrupt the catalytic activity of Mmp1 by driving the expression of a dominant-negative $Mmp1^{\Delta Cat}$ construct in either the hemocytes or the epidermis, we find decreased melanization at the wound site, suggesting that the catalytic domain of Mmp1 is required to facilitate scab formation. Similarly, $Mmp1^{\Delta pex}$ mutants, which lack the hemopexin domain, show slowed clotting and incomplete melanization. In cultured activated platelets, the hemopexin-like domain of MMP-2 facilitates platelet aggregation in wound sites by binding to integrin $\alpha_{IIb}\beta_3$ (Choi et al., 2008). In *Drosophila*, melanization is mediated by activated crystal cells, which facilitate clotting by extending filopodia that will adhere to extracellular matrix and other crystal cells forming a clot matrix (Bidla et al., 2005). If the function of the hemopexin domain in *Drosophila* Mmp1 is similar to that of mammalian MMP-2, then, as we observe, loss of the hemopexin domain would result in hemostasis defects, due to an impaired ability for crystal

cells to form adhesions, suggesting that the Mmp1 hemopexin domain may play a role in promoting hemolymph coagulation.

Melanization of the soft clot that forms within minutes of wounding (our results and Galko and Krasnow (2004a)) is the final outcome of the melanization cascade. Our epistasis test in *Spn27A*^{1} *Mmp1*^{2} double mutant, while preliminary, may suggest that Mmp1 functions downstream of the PPAE inhibitor, *Spn27A*, to promote formation of the melanin plug. This would be the first evidence that MMPs participate, either directly or indirectly in the scab formation. *In vitro* studies have shown that the catalytic domain of mammalian MMPs, MMP-8, MMP-12, MMP-13, and MT1-MMP cleave both fibrinogen and clotting factor XII, which leads to impaired fibrin clot formation (Hiller et al., 2000; Tschesche et al., 2000). If *Drosophila* MMPs have a similar function *in vivo*, we would expect the loss of an MMP to elicit excessive melanization, such as that seen in *Mmp2* mutants. Perhaps *Mmp2* plays a role in the proteolysis of an enzyme required to inhibit either directly, or indirectly inhibit PO activity, such as Spn27A; as such, loss of *Mmp2* would prevent inactivation of PO, resulting in unchecked PO activity, melanin polymerization and deposition at the wound site. In *Mmp1* mutants, however, we find the opposite phenotype, incomplete melanization, indicating that the membrane-anchored *Mmp2* and the secreted *Mmp1* may have independent functions during scab formation, either to inhibit, or to promote melanization, respectively. However, the exacerbation of the clotting defects

observed in the *Mmp1 Mmp2* double mutants, suggests that *Mmp1* and *Mmp2* may have redundant functions as well.

On activated platelets, a membrane-anchored MMP, MT1-MMP, forms a complex with a TIMP, TIMP-2, and a secreted MMP, MMP-2, on the cell surface to promote platelet aggregation (Kazes et al., 2000). Our results can also be explained if Mmp1, Mmp2, and Timp formed a similar tri-molecular complex on the surface of hemocytes, more specifically crystal cells, which would then function to hold Mmp1 at the cell surface and promote melanization. In this model, disruption of the complex by loss of either Mmp2, or Timp, could result in the excessive, ectopic melanization phenotypes, as we observe in both *Mmp2* and *Timp* mutant wounds; thus leaving the secreted *Mmp1* free to promote melanization on targets outside the immediate vicinity of the wound. Overexpression of *Timp* would similarly disrupt the Mmp2/Mmp1/Timp complex, but in this case the excess inhibitor would prevent all Mmp1 function, resulting in the observed incomplete melanization phenotypes. More evidence suggesting that Mmp2, Mmp1, and Timp may form a tri-molecular complex, as well as additional *in vivo* functions of the complex, is provided in chapter IV.

Re-epithelialization is not dependent on scab formation.

In mammals, the fibrin clot functions to seal the wound, preventing further fluid loss (Singer and Clark, 1999) and is a critical initial step in the wound healing process. Analogously, a melanin plug rapidly forms at wound sites in arthropods, which, as in mammals, functions to seal the wound. As previous studies have suggested that the hemocytes, the cells primarily responsible for hemostasis in *Drosophila*, are not required for re-epithelialization (Babcock et al., 2008; Stramer et al., 2005; Wu et al., 2009b), we asked if melanization is necessary for re-epithelialization. Our results show that there is no correlation between melanization plug size and wound area 14h post-wounding in wild-type larvae. While scab formation is not necessary for re-epithelialization, *Mmp1* is required. To expand on our previous studies (discussed in chapter II), which showed that *Mmp1* is required in the epidermis for re-epithelialization following puncture wounding (Stevens and Page-McCaw 2012), here we demonstrate that *Mmp1* is also required for re-epithelialization following pinch wounding. Together, these results demonstrate the re-epithelialization defects are not secondary to scab formation defects and *Mmp1* plays a pivotal role in both hemostasis and re-epithelialization.

Mechanisms of hemostasis in mammals are well understood, but the same cannot be said for the mechanisms of hemostasis in arthropods, such as *Drosophila melanogaster*. Further research is needed to understand both the

components and the regulatory mechanisms involved in scab formation. Our studies have shown that both *Drosophila Mmp1* and *Mmp2* play a role in hemostasis functioning during both initial soft clot formation, as well as formation of the melanin plug. However, we do not understand specifically what role MMPs have in the melanization cascade, whether they directly or indirectly effect scab formation. Additionally, our data suggest that *Mmp1* and *Mmp2* may function redundantly during hemostasis, the first redundant function identified for MMPs in *Drosophila.* While the components of the hemostasis mechanisms between *Drosophila* and human are different, the end result is the same: the formation of plug to seal a wound preventing excess fluid loss and invasion of pathogens. Comprehension of how MMPs are involved in hemostasis and scab formation in a simple system, such as *Drosophila*, may provide insight into how MMPs influence during hemostasis and scab formation in higher organisms.

CHAPTER IV

DROSOPHILA Mmp1 MAY FUNCTION IN HEMOCYTES TO REGULATE INFLAMMATION DURING WOUND HEALING

Introduction

Inflammation is the initial response of an organism to tissue damage and infection (Medzhitov, 2008). In the normal physiological state, inflammation is an acute response, occurring exclusively at the source of a noxious stimulus. However, if an acute inflammatory response is not sufficient to mitigate the threat, to neutralize the pathogen, and to repair the damaged tissue, chronic inflammation develops. Chronic inflammation occurs in many disease states, such as type II diabetes, ulcerated chronic wounds, and autoimmune disorders (Medzhitov, 2008). The mechanisms that lead to the development of chronic inflammation are not well understood.

Acute inflammation is characterized by an influx of leukocytes into the damaged area, which function to engulf pathogens and cell debris, as well as secrete a number of cytokines, chemokines, proteases, and growth factors to stimulate repair (Eming et al., 2007; Singer and Clark, 1999). The inflammatory pathway is initiated following clotting, with degranulating platelets establishing chemoattractant gradients that lead to the extravasation of leukocytes from blood vessels and recruitment to the wound site (Larsen et al., 1989). Among the first

responders to tissue damage are neutrophils, or polymorphonuclear leukocytes (PMN), which migrate from activated, leaky blood vessels to invade the wound site, where they phagocytose pathogens, as well as release reactive oxygen species (ROS), proteases, such as matrix metalloproteinases, and other pro-inflammatory molecules, such as chemokines and cytokines, to amplify the inflammatory response, recruit macrophages, and stimulate repair (Werner and Grose, 2003). Macrophages, the other leukocytes predominantly found at wound sites, are "professional" phagocytes that function during wound healing to engulf foreign particles, cell debris, and neutrophils that have undergone apoptosis (Luster et al., 2005; Martin and Leibovich, 2005; Zhang et al., 2008). In zebrafish, macrophage migration to wound sites is dependent on MMP-13, under the regulation of the Jun N-Terminal Kinase (JNK) signaling pathway (Zhang et al., 2008).

MMPs have been shown to play diverse roles during inflammation, functioning both to promote, as well as dampen, the inflammatory response (Gutierrez-Fernandez et al., 2007a; McQuibban et al., 2000; McQuibban et al., 2002; Zhang et al., 2008). MMP-8 -/- mice have an increased inflammatory response post-wounding and yet these mice also have delayed re-epithelialization (Gutierrez-Fernandez et al., 2007a), indicating that MMP-8 functions to dampen the inflammatory response. However, it is unclear if the re-epithelialization delays are a secondary result of an excessive inflammatory

response, or an independent result of the loss of MMP-8. Similarly, MMP-2 has also been shown to dampen the inflammatory response by generating anti-inflammatory chemokines through proteolytic processing (McQuibban et al., 2000; McQuibban et al., 2002). MMPs in vertebrates are highly redundant, with one MMP sometimes up-regulated to compensate for the loss of a different MMP family member (Rudolph-Owen et al., 1997). In mice, for example, MMP-13 is up-regulated in MMP-8-/- mice, suggesting a compensatory mechanism for the loss of MMP-8 (Hartenstein et al., 2006). Redundancy of this nature adds an additional level of complexity to an already complex process, rendering it difficult to elucidate MMP functions during inflammation in vertebrates.

For that reason, we turned to a simpler model, namely *Drosophila melanogaster*, whose genome only encodes two MMPs, one secreted and one membrane-anchored, to examine the *in vivo* functions of MMPs during tissue-damage-induced inflammation. Just as in higher organisms, tissue damage induces a rapid, localized inflammatory response involving recruitment of the *Drosophila* innate immunity effector cells, hemocytes to the wound site (Galko and Krasnow, 2004a; Stramer et al., 2005). *Drosophila* is an established model used to study wound healing and inflammation; however, one limitation is that *Drosophila* have an open circulatory system, so diapedesis, or hemocyte extravasation, is not required for hemocyte recruitment to wound sites. As a genetically-tractable organism, however, *Drosophila* is still useful for studying

other aspects of the inflammatory response, such as inflammation resolution and hemocyte recruitment, *in vivo* at a cellular and molecular level (Razzell et al., 2011). Studies of inflammation in a simple genetically-tractable system, such as *Drosophila*, may provide insight into the mechanisms of inflammation in more complex organisms.

There are three basic types *Drosophila* hemocyte: crystal cells, plasmatocytes, and lamellocytes (Meister and Lagueux, 2003). The most abundant population of hemocytes is plasmatocytes, comprising roughly 95% of the circulating hemocyte population (Meister, 2004). Functionally equivalent to neutrophils and macrophages, these small cells circulate throughout the animals, functioning as a surveillance system, engulfing foreign objects, and apoptotic cells (Babcock et al., 2008; Franc et al., 1996; Franc et al., 1999). Crystal cells are named for the crystalline inclusions found within the cells, which are important for melanization. Crystal cells are believed to mediate clotting and melanization (Rizki and Rizki, 1959). The third hemocyte class, lamellocytes, are large flat cells that function during an innate immune response to encapsulate and neutralize pathogens, such as parasitic wasp eggs, that are too large for phagocytosis (Crozatier et al., 2004). Within minutes of wounding, hemocytes are recruited to the damaged area in response to chemotactic gradients established by damaged cells (Stramer et al., 2005; Wood et al., 2006). Once at the wound site, hemocytes are captured at the wound surface, where they become tightly adherent,

aggregate, then disperse throughout the wound bed, becoming phagocytically-active (Babcock et al., 2008). In addition to debriding the wound site of pathogens and debris, hemocytes have also been shown to secrete Pvf-1 (platelet-derived growth factor (PDGF) / vascular endothelial growth factor (VEGF)-related factor-1), which activates receptor tyrosine kinase (RTK) signaling, and promotes re-epithelialization. Further investigation is needed to fully comprehend the precise mechanisms that regulate the inflammatory response to tissue damage *in vivo*.

In this chapter, we discuss our findings that the *Drosophila* secreted MMP, *Mmp1*, is highly up-regulated in response to wounding in hemocytes, via JNK signaling, and possibly accumulated in secretory vesicles. Mmp1 may function to dampen JNK signaling in the epidermis, limit the extent of the inflammatory response to the immediate vicinity of the wound site, and facilitate epidermal migration by promoting RTK signaling. Mmp1 up-regulation is observed in hemocytes after both pinch and puncture wounds, indicating that tissue-damage alone is sufficient to activate hemocytes and induce inflammation. We show that catalytically-active *Mmp1.f2* may be required in the hemocytes to promote re-epithelialization, while catalytically-active *Mmp1.f1* is required for re-epithelialization in the epidermis. These preliminary results represent the first indications of independent functions for individual MMP isoforms *in vivo*. Together these results indicate that *Mmp1* may have a complex role during

wound healing, functioning simultaneously to modulate the inflammatory response and promote re-epithelialization.

Methods

Fly lines.

The following lines are described in Page-McCaw et al (2003): *Mmp1*^{2} (imprecise *P* excision alleles resulting in deletions of most or all of the coding region). The dominant-negative catalytically-inactive *Mmp1* lines, *UAS-Mmp1.f1*^{E225A} and *UAS-Mmp1.f2*^{E225A}, which have a glutamate to alanine mutation at amino acid 225 in the catalytic domain (Glasheen et al., 2009b; Zhang et al., 2006). Other fly lines used were *A58-Gal4* (M. Galko), *He-Gal4* (Flybase ID FBti0064641) and *He-Gal4, UAS-GFP* both from the Bloomington *Drosophila* Stock Center, *Hml-Gal4,UAS-eGFP* (J. Royet), *UAS-Mmp1-dsRNA* (D. Bohmann), *Puc*^{LacZ} (B. Stronach), *Domino* (K.V. Anderson), and *UAS-preproANF-GFP (Rao et al., 2001)*. Two *UAS-Erg-dsRNA* lines were used (Vienna *Drosophila* RNAi Center (VDRC)). *w*^{1118} was used as wild type.

***Ex vivo* bleeding assay.**

To collect hemolymph samples, 3rd instar larvae were wounded according to the protocol described in Chapter II and allowed to heal for a specified amount of time at 25C. Wounded animals were washed once in PBS + 0.1%

Tween-20 and then twice in 70% ethanol. On a Sylgard® plate, a small hole was made in the posterior of the larvae with #5 dissecting forceps. Hemolymph was gently squeezed out of animal and the carcass was discarded. Hemolymph was immediately transferred with a fine glass needle to glass multi-well microscope slides (MP Biomedical, Cat# 096041205) with a small volume of complete Schneider's culture media. Cells were left to adhere to the slide for approximately 1h at room temperature in a humid chamber. Cells were fixed and stained according to protocol described below. For all *ex vivo* bleeding experiments n≥3 animals for condition / genotype tested.

Wounding assay.

Both puncture and pinch wounding assays were adapted from Galko and Krasnow (2004a) and are described in detail in chapter II, and Stevens and Page-McCaw (2012).

Immunohistochemistry.

Wounded epidermal samples were extracted from larvae according to procedure described in Chapter II, as well as in Stevens and Page-McCaw (2012). Tissue was fixed in PBS + 4% formaldehyde at RT for 30 min. Fixed samples were washed and permeabilized in PBS + 0.2% Triton X-100, blocked in PBS + 5% goat serum + 0.02% NaN_3, incubated in 1^o antibody (diluted in PBS + 1% goat serum + 0.02%NaN_3) overnight at 4°C, washed and incubated in 2^o antibodies for

1.5 h at RT in the dark, and mounted in Vectashield mounting media with DAPI (Vector Labs). Anti-Mmp1 catalytic domain (a 1:1:1 cocktail of mouse monoclonal IgG1 antibodies 3B8, 5H7, and 23G, generated by Page-McCaw et al (2003) and obtained from the Developmental Studies Hybridoma Bank (DSHB)), was used at 1:100. Anti-Mmp1 hemopexin domain (a mouse monoclonal IgG1 from DSHB) was used at 1:100, Anti-FasIII (a mouse monoclonal IgG2a from the DSHB) was used at 1:10. Mouse monoclonal IgG1 anti-diphosphorylated ERK 1&2 (Sigma, Cat# M8159) was used at 1:200. Rabbit anti-GFP (Abcam, Cat#ab6556) was pre-absorbed against larval epidermis and used at 1:100. Rabbit anti-β-Galactosidase (Cappal/ICN, Cat#55976), pre-absorbed against larval epidermis, used at 1:100. Cy3 or FITC labeled goat anti-mouse-IgG1 (Jackson ImmunoResearch), DyeLight649, or FITC labeled goat anti-mouse-IgG2a (Jackson ImmunoResearch), Cy3 labeled goat anti-mouse (Jackson ImmunoResearch), Cy3, or FITC-labeled donkey anti-rabbit (Jackson ImmunoResearch) were all used at 1:300.

Microscopy.

Optical sectioning was performed with a Zeiss Apotome mounted on an Axio imager Z1 or M2, with the following objectives: 20X/0.8 Plan-Apochromat, 40X/1.3 oil EC Plan-NeoFluar, or 63X/1.4 oil Plan-Apochromat. Fluorescent images were acquired with an Axiocam MRm (Zeiss) camera paired with Axiovision 4.8 (Zeiss). Z-stacks were compressed into 2-diminsional XY

projections using the Orthoview function in Axiovision. All images were exported from their acquisition programs as 16-bit, grayscale, TIFF files for post-processing in Adobe Photoshop CS4, or ImageJ v.1.43u.

Wound measurements.

Closure and wound area were assessed based on the presence of both FasIII staining at cell borders and epidermal polyploid nuclei as stained with DAPI. To calculate wound area, the outline tool in Axiovision (Zeiss) was used to manually outline the wound edge. This feature automatically calculates the area of the outlined region using image acquisition specifications. One-way ANOVA, followed by Tukey post-hoc tests were performed with the analysis tools available in GraphPad Prism v5.01 to compare mutant and wild-type wound area within each time point. Chi-squared analysis was performed to determine significant of closure phenotypes between genotypes using the analysis tools available in GraphPad Prism v.5.01. For all statistical analysis, results were considered significant if they were within a 95% confidence interval, or had a p-value less than 0.05. Error bars represent the standard error of the mean.

Expression analysis.

To generate heat maps of pixel intensity from fluorescent images, single channel 16-bit grayscale 2D projection from Z-stacks were converted to 8-bit images in ImageJ v1.43u. The "fire" look-up table (LUT) was then applied to the

image to pseudo-color pixels based on intensity, white = 256 and dark navy blue = 0.

To measure relative Puc^{LacZ} or dpErk expression between genotypes over time, 2D projection images were opened in ImageJ and the ellipse tool was used to mark nuclei at the leading edge of the wound based on DAPI staining and anti-FasIII expression, while the Puc^{LacZ} or dpErk channel was hidden. The multi-measure tool was then used to calculate the integrated intensity density for each region of interest (ROI, representing each nucleus) for the Puc^{LacZ}, or dpErk, channel. Each integrated density value was imported into Orign v8.6 software, where statistical analysis tools were used to perform repeated-measure two-way ANOVA to determine if either time or genetype significantly influenced expression intensity. Two-way ANOVA analysis was followed-up by Bonferroni post-hoc tests to compare expression intensity both within genotype over time and between genotypes at each time point. For all statistical analysis, results were considered significant if they were within the 95% confidence interval, or had a p-value less than 0.05. Error bars represent the standard error of the mean.

Cell culture.

Drosophila S2 cells were cultured at 27°C in Schneider's *Drosophila* medium (Gibco) + 10% heat-inactivated FBS (BioWest, Lot #B51217) + 50U/ml penicillin G + 50µg/ml streptomycin sulfate (Gibco). Gene expression from the *pRMHa-3* metallothionine promoter was induced by adding 2M $CuSO_4$ to a final

concentration of 500µM. Cells were transiently transfected with a total of 19µg plasmid DNA in 2M $CaCl_2$ + 50mM HEPES, pH 7.1 + 1.5mM Na_2HPO_4 + 280mM NaCl. Transfected plasmids included: *pRmHa-3.Gal4*, *pUASt.GFP*, *pUASt.Mmp1.f1*, *pUASt.Mmp1.f1*^{E225A}, *pUASt.Mmp1.f2*, *pUASt.Mmp1.f2*^{E225A}. For immunocytochemistry, 100µl of S2 cells were plated on 12-well multi-well slides (MP Biomedical, Cat# 096041205) and allowed to settle for about 1h. Cells were fixed in 4% formaldehyde in PBS for 25m at RT and then stained according to immunohistochemistry protocol described above.

Results

Mmp1 is up-regulated in hemocytes post-wounding.

In response to wounding, Mmp1 is dramatically up-regulated in the epidermis (Stevens and Page-McCaw 2012), so we asked if Mmp1 is also up-regulated in hemocytes post-wounding. To assess Mmp1 expression changes, we bled 3rd instar larvae after wounding onto glass slides and stained with anti-Mmp1. In unwounded animals, Mmp1 is expressed at low levels in the hemocytes with no distinct pattern (Fig. 4.1A). As early as 30m post-wounding Mmp1 is slightly up-regulated and localized to punctae (white arrows in Fig. 4.1B). By 1h post-wounding, Mmp1 is dramatically up-regulated in hemocytes primarily in a punctate pattern throughout the cell (Fig. 4.1C). By pseudo-coloring Mmp1 expression based on pixel intensity (scale below Fig 4.1E'-F'), we can see that Mmp1 expression becomes continuously more intense through 2h post-wounding relative to that seen earlier time points (Fig. 4.1D compared to Fig. 4.1A-C). As Mmp1 is a secreted protein, we asked whether the Mmp1-rich punctae were localized on the cell surface, or contained within the cell. Hemolectin (Hml) is a protein produced exclusively by a sub-class of plasmatocytes (Goto et al., 2003). By using *Hml-Gal4* to drive eGFP expression, functioning as a transcriptional reporter, we are able to localize GFP within the cell in permeabilized samples (Fig. 4.3E); however in non-permeabilized samples we observe no GFP expression (Fig. 4.1F), indicating that our permeability assay

is working. When we compared Mmp1 expression in permeabilized versus non-permeabilized hemocytes in *ex vivo* bleeds from larvae 2h post-wounding, Mmp1 is sequestered in a punctate pattern within the cell (Fig. 4.1E'), with only minimal, if any Mmp1 expression on the cell surface (white arrows in Fig. 4.1F'). The punctate expression pattern of Mmp1, which is only found within the cell, strongly suggests that in response to wounding Mmp1 is being sequestered in granules, presumably in preparation for Mmp1 secretion at the wound site. To determine if Mmp1 is localized to vesicles within hemocytes, we looked for co-localization between Mmp1 and a vesicle marker. Atrial natriuretic factor precursor (ANF) is a marker of dense-core vesicles often used in neurons to study the transport of neuropeptides (Pack-Chung et al., 2007; Rao et al., 2001). To identify vesicles in hemocytes we used *He*-Gal4 to drive expression of *UAS-preproANF-GFP* fusion protein in hemocytes stained with anti-Mmp1. One hour after wounding Mmp1 is up-regulated and co-localizes with the vesicle marker, ANF-GFP in hemocytes (Fig. 4.1G-G"), suggesting that up-regulated Mmp1 is localized to secretory vesicles within the hemocytes in response to wounding.

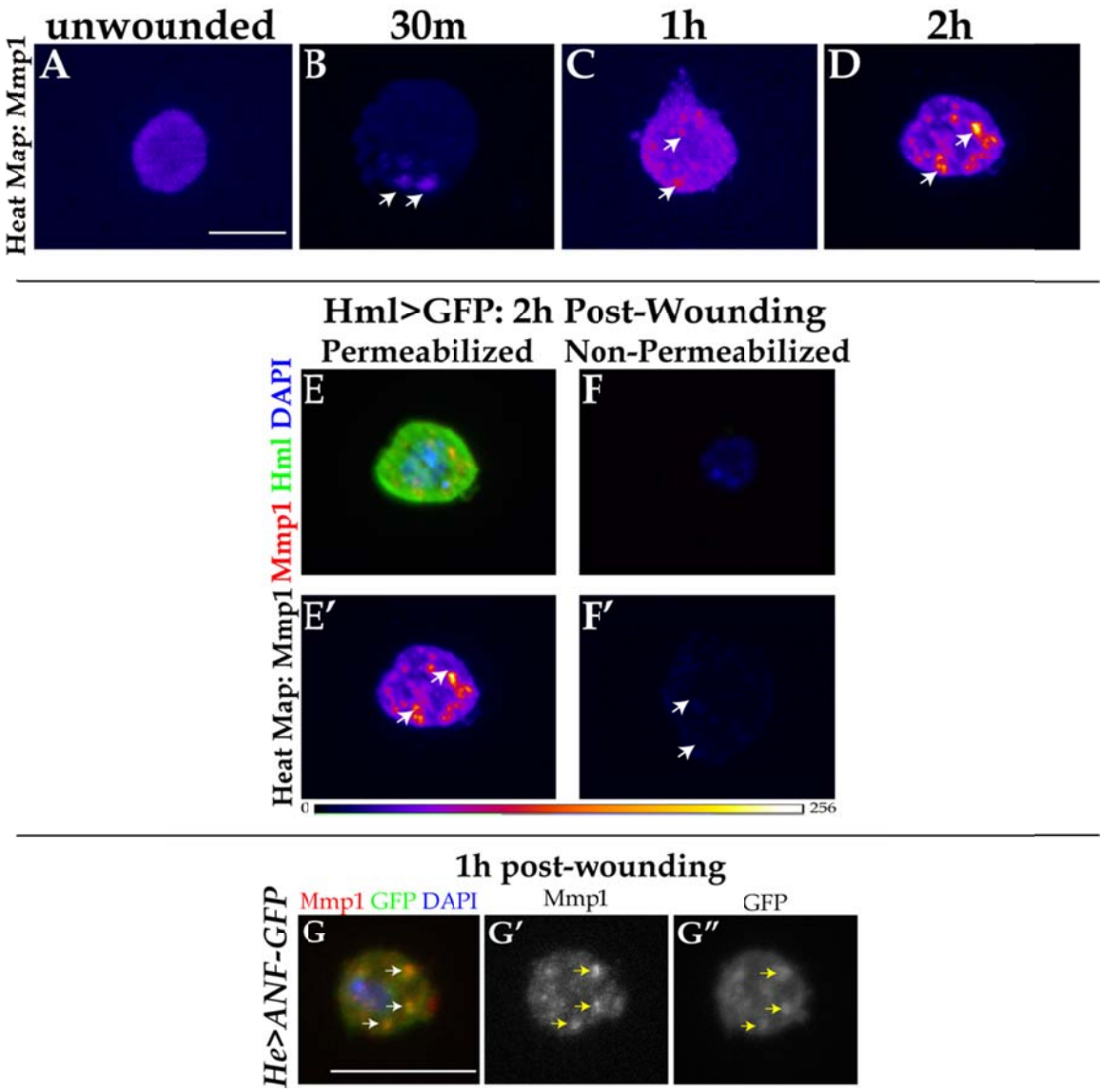

Figure 4.1: Mmp1 is up-regulated in hemocytes post-wounding.
A-D) XY projections of Mmp1 expression from *ex vivo* bleeds of wild-type hemocytes at designated time points post-wounding. Mmp1 expression (A-D, E′, F′) has been pseudo-colored based on pixel intensity (color intensity scale below E′-F′). White arrows (B-D) indicate Mmp1 localization in punctae. **E-F)** XY projections of permeabilized (E, E′) and non-permeabilized (F, F′) hemocytes from *ex vivo* bleeds 2h post-wounding in *Hml>GFP* animals. GFP expression, stained with anti-GFP (green in E-F), was used as a permeabilization control and DAPI (Blue in E-F) labels the nuclei and identifies cells. Mmp1 (red in E-F and heat map based on pixel intensity E′-F′) is found in punctae (white arrows in E′-F′). **G-G″)** *Ex vivo* bleeds 1h post-wounding in *He>ANF-GFP* showing co-localization between Mmp1 (Red in G, gray in G′) and vesicle marker ANF-GFP (green in G, gray in G″). Arrows (white in G, yellow in G′-G″) indicate Mmp1 co-localization with ANF-GFP in vesicles. Images A-F′ were acquired at 40X (scale bar in A). Images G-G″ were acquired at 63X (scale bar in G). All images are representative of hemocytes collected from individual whole larvae bleeds (n≥3 larvae bled for each condition). All scale bars represent 20µm.

Hematopoietic *Mmp1.f2* may be required for re-epithelialization.

Previous studies in our lab have demonstrated that *Mmp1* is required in the epidermis for re-epithelialization (Stevens and Page-McCaw (2012); and Chapter II). Successful wound healing requires the orchestration of both the epidermis and the hemocytes, so we asked if *Mmp1* is required in the hemocytes to facilitate re-epithelialization. We attempted to measure re-epithelialization in the hemocytes-deficient mutant, *Domino* (*Dom*), but as discussed in chapter III, these mutants have clotting defects that cause the animals to bleed out prior to a time point sufficient for wound closure analysis. As this would be a recurring obstacle, we decided to focus on the requirement of Mmp1 expression specifically in the hemocytes during re-epithelialization, as opposed to the broader question of the necessity of hemocytes in general for re-epithelialization.

Drosophila Mmp1 is predicted to have nine isoforms (National for Biotechnology Information (NCBI) database); however, after comparative sequence analysis we can break those into four groups of isoforms encoding five unique polypeptides (for details see Appendix A). In all groups, the only differences between each Mmp1 isoform are at the C-terminus of the hemopexin domain (Fig 4.1B, Appendix A), the putative MMP substrate recognition domain (Ra and Parks, 2007). This suggests that the various Mmp1 isoforms recognize a unique set of substrates, which possibly serve as a mechanism to finely regulate Mmp1 activity. For a more in-depth discussion of the differences between the

various predicted Mmp1 isoforms see Appendix A. The remainder of this chapter will focus exclusively on Mmp1.f1 (40 unique amino acids) and Mmp1.f2 (11 unique amino acids), as we currently only have reagents available to study these two isoforms *in vivo*.

Eighteen hours post-wounding, the majority of wild-type wounds have completely re-epithelialized (Fig. 4.2A, I-J, and chapter II). To test if the catalytic activity of Mmp1 is required for re-epithelialization in either hemocytes, or the epidermis, we expressed a catalytically-inactive Mmp1 construct, *UAS-Mmp1*^{E225A}, which harbors an alanine mutation at a conserved glutamic acid in the active site and acts as a dominant-negative (Glasheen et al., 2009b; Zhang et al., 2006). As mentioned above, Mmp1.f1 and Mmp1.f2 differ only at the C-terminal region of the hemopexin domain (Fig. 4.2B), so to determine if one, or both, of these isoforms is required for re-epithelialization, we expressed either catalytically-inactive Mmp1.f1 (*UAS-Mmp1.f1*^{E225A}) or catalytically-inactive Mmp1.f2 (*UAS-Mmp1.f2*^{E225A}) in the epidermis, using *A58-Gal4,* or in the plasmatocytes, using *Hemese-Gal4 (He-Gal4*), and measured wound area 18h post-wounding. In animals expressing *Mmp1.f1*^{E225A} in the hemocytes (*He>Mmp1.f1*^{E225A}) wounds closed in 50% of the animals tested (Fig. 4.2C, I), with an average wound area at 18h post-wounding that was not significantly different from wild type (Fig. 4.1J). However, when the same construct was driven specifically in the epidermis (*A58>Mmp1.f1*^{E225A}) wounds failed to close within

18h post-wounding in 100% of the animals tested (Fig. 4.2D, I), with an average wound area that is significantly larger than wild type, similar to the RNAi-mediated knock-down of Mmp1 (Fig. 4.2J). Conversely, expression of catalytically-active Mmp1.f2 in the hemocytes (*He>Mmp1.f2*^{E225A}) resulted in re-epithelialization failure in 100% of animals tested (Fig. 4.2E, I). Interestingly, while the wounds remained open in *He>Mmp1.f2*^{E225A} mutants, the average wound area 18h post-wounding was not significantly larger than wild-type (Fig. 4.2J), suggesting that re-epithelialization in *He>Mmp1.f2*^{E225A} may simply be delayed and wounds in these mutants will close, provided enough time. To test this hypothesis, wound area should be measured in *He>Mmp1.f2*^{E225A} mutants at time points greater than 18h post-wounding. If wounds in this mutant background eventually close, then these data suggest that wound healing is merely delayed when we over-express an Mmp1.f2 dominant-negative construct in the hemocytes. Disruption of Mmp1.f2 catalytic activity in the epidermis (*A58>Mmp1.f2*^{E225A}), however, resulted in no re-epithelialization impairment, as wounds closed in all animals tested (Fig. 4.2F, I-J). Together, these results suggest that Mmp1.f1 and Mmp1.f2 may have unique, tissue-specific functions during wound healing. The simplest explanation of these results is that Mmp1.f1 is required in the epidermis, while Mmp1.f2 may play a role in the hemocytes to facilitate re-epithelialization.

Interestingly, when we used a double-stranded RNA construct to knockdown all Mmp1 isoforms in either the hemocytes (*He>Mmp1-dsRNA*), or the epidermis (*A58>Mmp1-dsRNA*), we recapitulated only the *Mmp1.f1*^{E225A} phenotypes. Eighteen hours post-wounding, wounds in *He>Mmp1-dsRNA* mutants closed (Fig. 4.2G,I-J), while *A58>Mmp1-dsRNA* mutant wounds failed to re-epithelialize (Fig. 4.2H, I), leaving an average wound area 18h post-wounding that was significantly larger than wild type (Fig. 4.2J and Stevens and Page-McCaw (2012)). These results suggest that Mmp1 in general may not be required for re-epithelialization; calling into question our finding that catalytically-active Mmp1.f2 may be required in the hemocytes to promote re-epithelialization. It is important to note however, that *He-Gal4* is only expressed in approximately 70% of hemocytes (data not shown).

To determine if our mild re-epithelialization phenotypes were an artifact of the weakness of the *He-GAL4* driver, we repeated the re-epithelialization experiments with a second plasmatocyte-specific driver, *Hemolectin-Gal4* (*Hml-Gal4*), and found a similar result (Fig. 4.3). Fourteen hours post-wounding, there was no significant difference in wound area in *Hml>Mmp1-dsRNA* mutants relative to wild type, despite an observation that wounds remained open in 66% of animals tested (Fig. 4.3A-B). When *He-GAL4* is used to knock-down Mmp1 expression (*He>Mmp1-dsRNA*), wounds are significantly larger than wild type 14h post-wounding and, like the *Hml>Mmp1-dsRNA* animals, there is a 66% re-

epithelialization failure rate in this mutant background (Fig. 4.3A-B). As with the *He-GAL4* driver, it is important to note that the *Hml-Gal4* again only drives expression in a sub-population of hemocytes (our observations and Goto, Kadowaki, et al. (2003). It is also possible that an n-value of 3 (the sample size of both *He>Mmp1-dsRNA* and *Hml>Mmp1-dsRNA* at 14h post-wounding) it not large enough to adequately account for the variability within the population and our results could change with a larger sample size. Together with our 18h re-epithelialization data, these findings suggest that knocking down Mmp1 in only a subpopulation of hemocytes may be sufficient to cause re-epithelialization delays, but insufficient to induce complete re-epithelialization failure; perhaps if given enough time, wounds in either *He>Mmp1-dsRNA* or *Hml>Mmp1-dsRNA* mutants will close. Conceivably, if we were to use the *He-GAL4* and *Hml-GAL4* drivers in combination to interfere with Mmp1 expression we would observe stronger phenotypes.

Figure 4.2: Mmp1.f2 is required for re-epithelialization in hemocytes.
A-H) XY projections of wound sites 18h post-wounding in the designated genotypes. Anti-FasIII (yellow) labels the cell borders and cell nuclei are labeled in DAPI (blue). White arrows (A, C, F, and G) indicate the closed wounds and dashed lines (D, E, and H) outline open wounds. Scale bar (A) represents 20μm. **I)** Graph showing percentage of open versus closed wounds 18h post-wounding. By Chi-squared analysis, genotype significantly influences the percentage of wounds that are open versus closed 18h post-wounding ($p<0.0001$). **J)** Graph of average wound area 18h post-wounding. By one-way ANOVA genotype significantly influences wound area ($F = 17.26$, R ($p<0.0001$). By Tukey post-hoc tests wounds are significantly larger than wild type in *A58>Mmp1-dsRNA* ($p<0.005$, 95%CI[-24590,-7449]) and *A58>Mmp1.f1*^{E225A} ($p<0.005$, 95%CI[-27460,-12370]). Red dashed line (J) indicates approximate initial wound area (8000μm). Numbers on each bar represent number of animals measured in each group.

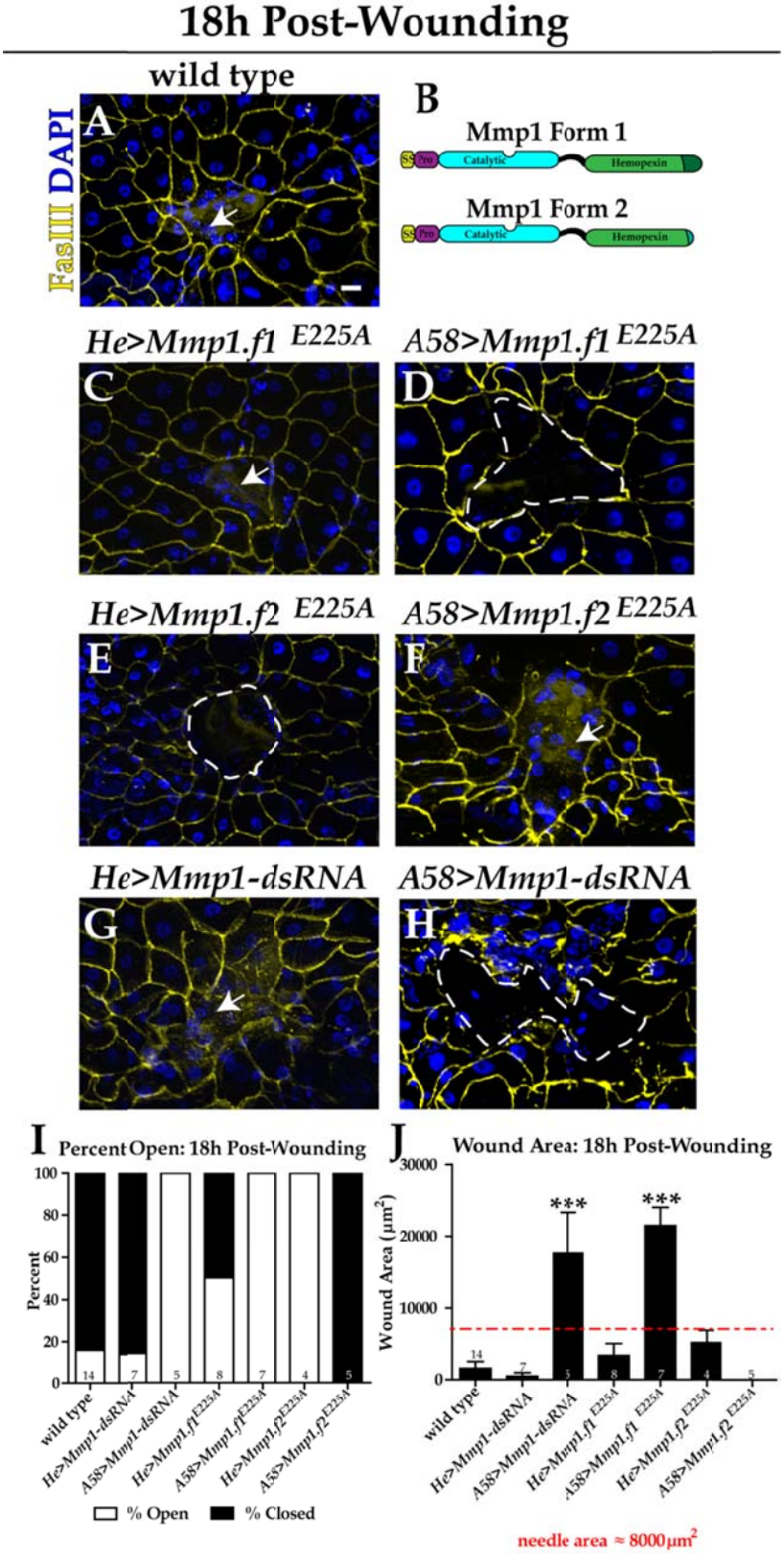
18h Post-Wounding
wild type
FasIII DAPI
A
B
Mmp1 Form 1
SS
Pro
Catalytic
Hemopexin
Mmp1 Form 2
He>Mmp1.f1 E225A
A58>Mmp1.f1 E225A
C
D
He>Mmp1.f2 E225A
A58>Mmp1.f2 E225A
E
F
He>Mmp1-dsRNA
A58>Mmp1-dsRNA
G
H
I Percent Open: 18h Post-Wounding
Percent
100
80
60
40
20
0
14
7
5
8
7
4
5
wild type
He>Mmp1-dsRNA
A58>Mmp1-dsRNA
He>Mmp1.f1E225A
A58>Mmp1.f1E225A
He>Mmp1.f2E225A
A58>Mmp1.f2E225A
% Open
% Closed
J Wound Area: 18h Post-Wounding
Wound Area (μm²)
30000
20000
10000
0
***
***
14
7
5
8
7
4
5
wild type
He>Mmp1-dsRNA
A58>Mmp1-dsRNA
He>Mmp1.f1 E225A
A58>Mmp1.f1 E225A
He>Mmp1.f2 E225A
A58>Mmp1.f2 E225A
needle area ≈ 8000μm²

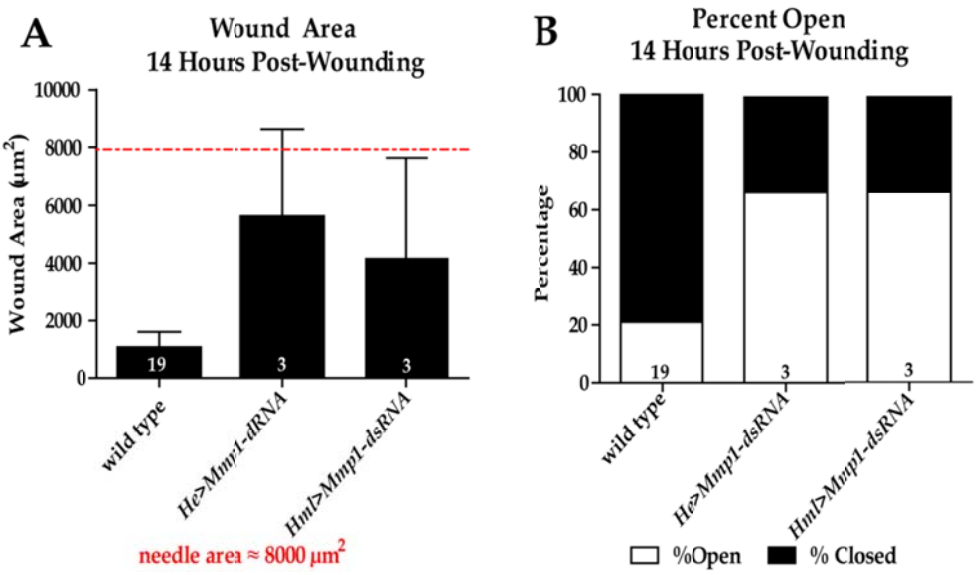

Figure 4.3: Re-epithelialization comparison: *He-GAL4* v. *Hml-GAL4*.
A) Graph of wound area 14h post-wounding in designated genotypes. Red dashed line represents approximate initial wound area (~8000µm²). By one-way ANOVA genotype does significantly influence the mean area at 14h post-wounding ($F = 3.464$, $R^2 = 0.2396$, $p = 0.0492$). However, by Tukey post-hoc tests there is no significant difference in wound area between with mutant genotype and wild type. **B)** Graph indicating percent of open versus closed wounds 14h post-wounding in designated genotypes. The numbers on each bar (A-B) represent the number of wounded animals measured in each group. The percentage of wounds that are open versus closed is contingent upon genotype, by Chi-squared analysis ($P<0.0001$). Error bars represent the standard error of the mean.

Mmp1.f1 is up-regulated in response to wounding.

To begin to understand how Mmp1.f1, or Mmp1.f2, may be involved in facilitating re-epithelialization, we analyzed wound-induced isoform-specific Mmp1 expression changes using an anti-Mmp1 antibody generated against the Mmp1 hemopexin domain (Page-McCaw et al., 2003b). As mentioned above, the differences between Mmp1.f1 and Mmp1.f2 are at the C-terminal end of the hemopexin domain, so to test the specificity of the anti-hemopexin antibody to either Mmp1.f1 or Mmp1.f2 we used *Drosophila* S2 cultured cells that were

transiently transfected to overexpress either Mmp1.f1 or Mmp1.f2, or the catalytically-inactive constructs of each isoform (Fig 4.4). Cells were also transfected with a plasmid containing GFP, as a transfection control. In mock transfected cells we detect only very low levels of endogenous Mmp1 expression with either the anti-Mmp1 catalytic domain, or the anti-Mmp1 hemopexin domain antibodies (Fig. 4.4 A-A′ and F-F′). In cells expressing both Mmp1.f1 and Mmp1.f1^{E225A}, high levels of both anti-Mmp1 catalytic domain (Fig. 4.4B-B′, D-D′) and anti-Mmp1 hemopexin domain antibodies (Fig. 4.4G-G′, I-I′) are detected. However, in cells overexpressing either Mmp1.f2, or Mmp1.f2^{E225A}, Mmp1 expression is only detected with the anti-Mmp1 catalytic domain antibodies (Fig. 4.4 C-C′, E-E′), not the anti-Mmp1 hemopexin domain antibody (Fig. 4.4H-H′, J-J′); thus demonstrating that the anti-Mmp1 hemopexin domain antibody (hereafter referred to as anti-Mmp1.f1) is specific for Mmp1.f1 and does not detect Mmp1.f2.

Before wounding, Mmp1.f1 is expressed at the low levels in unwounded epidermis (Fig. 4.5A) and, in response to wounding, Mmp1.f1 is up-regulated in cells at the leading edge of the wound site (Fig. 4.5B); further suggesting that Mmp1.f1 plays a role in the epidermis during re-epithelialization. In the hemocytes, 2h post-wounding Mmp1.f1 is expressed in a pattern similar to that detected with the general anti-Mmp1 antibody (compare Fig. 4.5C to D) with Mmp1 concentrated in punctae, presumably in vesicles (Fig. 4.5C′-D′). Hemocytes were also labeled for actin (green in Fig. 4.5C-D) and DAPI (blue in

Fig. 4.5C-D) to clearly define the shape of the hemocytes. Together, these results suggest that Mmp1.f1 may play a role during the inflammatory phases of wound healing in the hemocytes, in addition to being required in the epidermis to facilitate re-epithelialization.

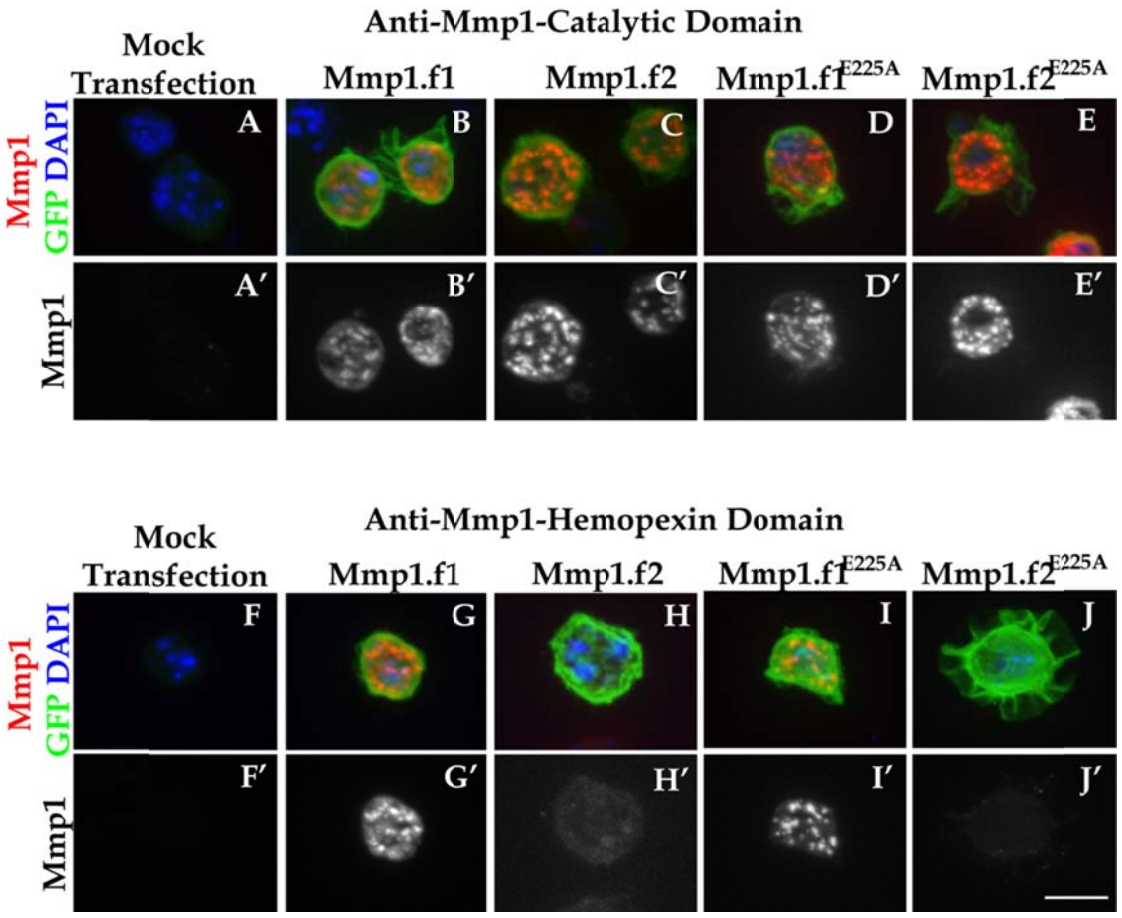

Figure 4.4: Anti-Mmp1 isoform specificity in S2 cultured cells.
A-E) *Drosophila* S2 cells showing that anti-catalytic domain (red in A-E, grayscale A′-E′) antibodies recognize both Mmp1.f1 and Mmp1.f2. **F-J)** Anti-hemopexin domain antibodies (red in F-J, grayscale F′-J′) only recognize Mmp1.f1 (G-G′ and I-I′), not Mmp1.f2 (H-H′ and J-J′). GFP expression is a transfection control (green in A-J) and DAPI (blue in A-J) labels the DNA. The white scale bar (J′) represents 10μm.

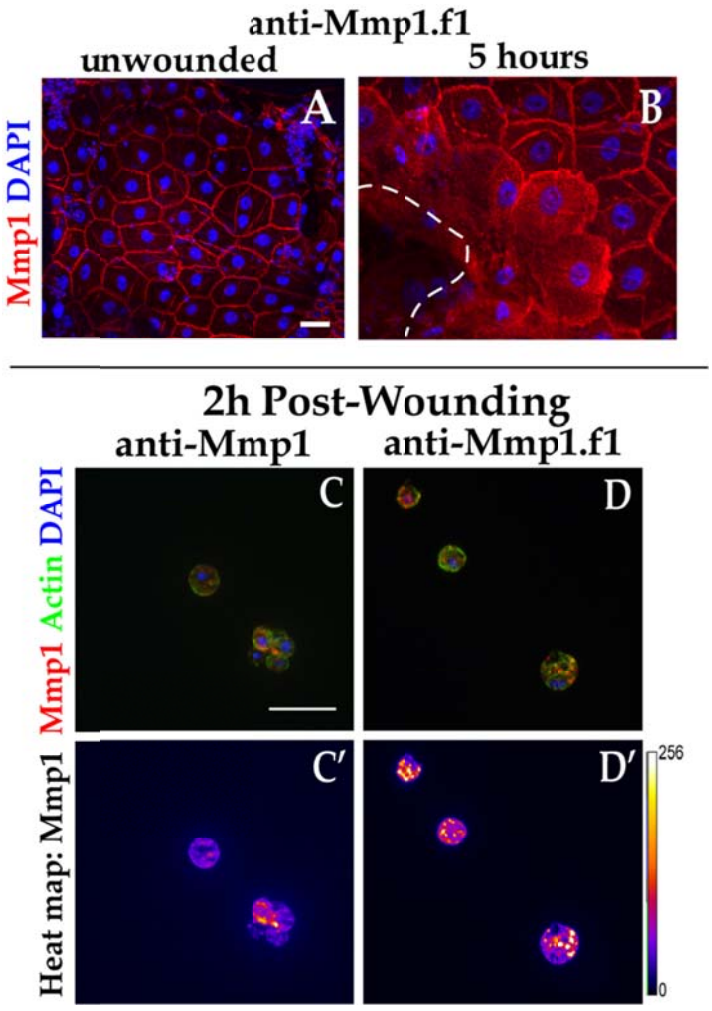

Figure 4.5: Mmp1.f1 is up-regulated in both epidermis and hemocytes post-wounding.
A-B) XY projections of Mmp1.f1 expression (Red) in unwounded (A) and 5h post-wounded epidermis (B). DAPI (blue A-B) labels DNA. White dashed line (B) outlines the wound edge. **C-D)** XY projections of hemocytes 2h post-wounding from *ex vivo* bleeds stained with general anti-Mmp1 (red in A) or anti-Mmp1.f1 (red in B). Anti-β-Actin (green in A-B) and DAPI (blue in A-B) show shape and location of cells. **C′-D′)** Mmp1 expression pseudo-colored based on pixel intensity (scale to right of D′) highlighting Mmp1 concentrated in punctae. Scale bars (A, C) represent 20μm.

Hematopoietic Mmp1 is regulated by JNK signaling.

In the epidermis, Mmp1 up-regulation in response to wounding is regulated by the Jun N-terminal Kinase (JNK) pathway (Stevens and Page-McCaw 2012), so we asked if a similar mechanism regulated Mmp1 expression in the hemocytes. One hour post-wounding, Mmp1 is dramatically up-regulated in vesicles in wild-type hemocytes (Fig. 4.6A). However, when we interfere with JNK signaling by overexpressing a dominant-negative *Drosophila* JNK, or *Basket* (*Bsk*), construct (*UAS-Bsk^{DN}*) with *He-GAL4* (*He>Bsk^{DN}*), Mmp1 up-regulation is markedly reduced by 1h post-wounding in *ex vivo* bleeds (Fig. 4.6B), suggesting the JNK signaling is required for wound-induced Mmp1 up-regulation in the hemocyte, as well as the epidermis. Tumor necrosis factor (TNF), or *Eiger* (*Egr*) in *Drosophila*, is a pro-inflammatory cytokine that, when released stimulates the JNK pathway (Barrientos et al., 2008; Igaki et al., 2011; Igaki et al., 2002a; Kauppila et al., 2003). Using two independent double-stranded RNA constructs to interfere with *Egr* expression in the hemocytes (*He>Egr-dsRNA*) we blocked Mmp1 up-regulation in response to wounding, recapitulating the impaired wound-induced Mmp1 up-regulation phenotypes of the *He>Bsk^{DN}* mutants (Fig. 4.6C). *Egr* knockdown in hemocytes actually appears to cause a greater reduction of Mmp1 response to wounding, relative to *He>Bsk^{DN}*, suggesting that the Erg-dsRNA construct has some off target effects or could function in a positive-feedback loop to enhance the inhibition of Mmp1 up-regulation post-wounding. Alternatively, perhaps *Egr* stimulates other signaling pathway that is

capable of inducing Mmp1 up-regulation in the absence of JNK signaling; without Egr as an initial signal, other pathways are not activated. It is also plausible that *UAS-Bsk^{DN}* does not completely ablate JNK signaling, thus allowing slight Mmp1 up-regulation after wounding. Together, these results suggest that wound-induced Mmp1 up-regulation in the hemocytes is primarily regulated by JNK signaling during wound healing.

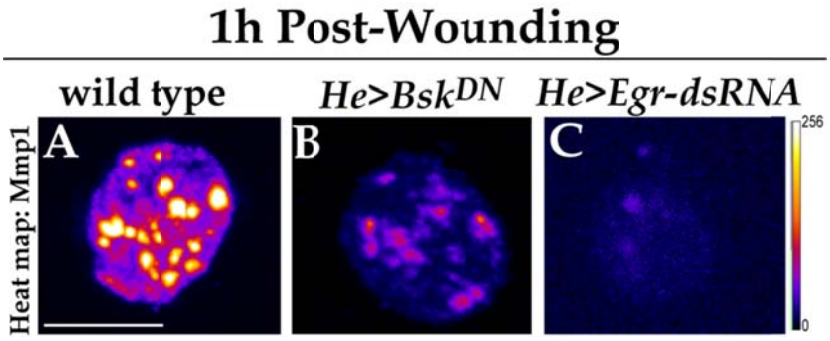

Figure 4.6: Hematopoietic Mmp1 is up-regulated by JNK signaling.
A-C) XY projections of hemocytes 1h post-wounding from *ex vivo* bleeds in designated genotypes. Mmp1 expression shown as a heat map with pixels pseudo-colored based on intensity in genotypes specified (intensity scale to right of C). Images show a representative plasmatocyte from the population of cells collected within each genotype. For all genotypes, n≥3 animals tested. Scale bar (A) represents 10µm.

Mmp1 is only expressed in a subpopulation of hemocytes at the wound site.

Similar to the *ex vivo* bleeds, hemocytes found at wound sites *in vivo* also express Mmp1 in a punctae pattern (Fig. 4.7). Not only is Mmp1 up-regulated in hemocytes after puncture wounding (Fig. 4.7A, A'), Mmp1 is also up-regulated in hemocytes after pinch wounding (Fig. 4.7B, B'), a wounding method in which

the protective cuticle remains intact, preventing influx of external pathogens and development of infection. Together, these results demonstrate that immune challenge, such as that induced by invading pathogens during puncture wounding, is not required for hemocytes activation, defined in this case by an up-regulation of Mmp1, or hemocyte recruitment to areas of tissue damage.

While analyzing Mmp1 expression in the plasmatocytes recruited to the wound, we observe at least two types of hemocytes in the wound bed, a class of hemocytes expressing high levels of Mmp1 (white arrows in Fig 4.7A', B') and a class of smaller hemocytes that are not expressing Mmp1 (yellow arrows in Fig. 4.7A', B'). This observation could be an indication that there are multiple subpopulations of hemocytes recruited to the wound site. Alternatively, Mmp1 may be released from hemocytes at the wound site; thus resulting in the appearance of a subpopulation of hemocyte lacking Mmp1 expression and a subpopulation with high levels of Mmp1 expression, when in reality we are looking at the same population of hemocytes simply pre- or post-Mmp1 release. To distinguish between these two models, the Mmp1 localization pattern in hemocytes at the wound site should be assayed in a secretion mutant, an animal with a defective secretory system. If hemocytes are releasing Mmp1-positive granules into the wound site, then in mutants where vesicles cannot be released, we would not expect to find any hemocytes lacking Mmp1-positive punctae.

When we use *He-Gal4* to drive expression of a *UAS-GFP*, labeling plasmatocytes, we again find multiple subpopulations of hemocytes in the wound bed: a class expressing Mmp1 and He>GFP (yellow double-headed arrows in Fig. 4.7C), a class expressing Mmp1, but not He>GFP (cyan arrows in Fig. 4.7C), and a third class expressing *He>GFP*, but not Mmp1 (white double-headed arrows in Fig. 4.7C). This third class of hemocytes (GFP-positive / Mmp1-negative), could also simply be mature plasmatocytes that have degranulated, releasing their store of Mmp1 into the wound bed. When we use *He>GFP,* to simultaneously knock down Mmp1 expression (*He>GFP, Mmp1-dsRNA*), we find a large number of plasmatocytes in the wound site that are *He>GFP* positive and Mmp1 negative, as expected (white double-headed arrows in Fig. 4.7D); however, we also find many hemocytes in the wound bed that are *He>GFP* negative and Mmp1 positive (cyan arrows in Fig. 4.7D). Together, these results could suggest that there may be multiple sub-types of plasmatocytes recruited to the wound site.

While hematopoietic Mmp1 appears to be involved during the damage-induced inflammatory response, we find no reduction in hemocyte recruitment to the wound site by 2h post-wounding between wild type animals (Fig. 4.7C) and *He>Mmp1-dsRNA* animals (Fig. 4.7D), indicating that Mmp1 is not required for hemocyte recruitment to an area of tissue damage. However, although very preliminary, we observe a larger number of hemocytes, particularly at later time

points, in Mmp1-deficient samples relative to wild type (Fig. 4.7D and data not shown), suggesting that Mmp1 may play a role in hemocyte release from the wound site, or that Mmp1 plays a role in limiting the extent of the inflammatory response during wound healing. It is also possible the hemocyte retention in the wound site is secondary to the re-epithelialization defects in *Mmp1* mutants, as previous studies have suggested that hemocyte release from the wound site is dependent on epidermal cells invasion into the wound bed, presumably displacing hemocytes (Babcock et al., 2008).

Figure 4.7: Mmp1 is expressed only in a subpopulation of hemocytes at the wound site.
A-B) XY projections of wound sites 5h after either puncture (A-A′) or pinch (B-B′) wounding in wild-type larvae with anti-Mmp1 pseudo-colored red and DAPI to label cell nuclei in blue. White dashed lines indicate the wound edge and white boxes (A-B) demarcate the area shown at higher magnification below (A′-B′). **A′-B′)** The same wound sites shown in A-B, but at higher magnification. Yellow arrows indicate hemocytes with up-regulated Mmp1 and white arrows indicate hemocytes without increased Mmp1. **C-D)** XY projections of wounds 2h post-puncture wounding in *He>GFP* (wild type, C) and *He>GFP, Mmp1*-dsRNA (D) animals. Hemese (He)-expressing hemocytes are labeled with GFP (green, C-D), Mmp1 is shown in red (C-D), and DAPI is shown in blue (C-D). Cyan arrows indicate examples of hemocytes expressing Mmp1, but not He-GFP (C-D), yellow double-headed arrows indicate hemocytes expression Mmp1 and He-GFP (C only) and white double-headed arrows point out examples of cells expressing He-GFP, but not Mmp1 (C-D). Hemocytes are the small nuclei in each frame, relative to the large polyploid epidermal nuclei in all panels. All scale bars (A, A′, and C) represent 20μm. For all conditions n ≥ 4 animals examined.

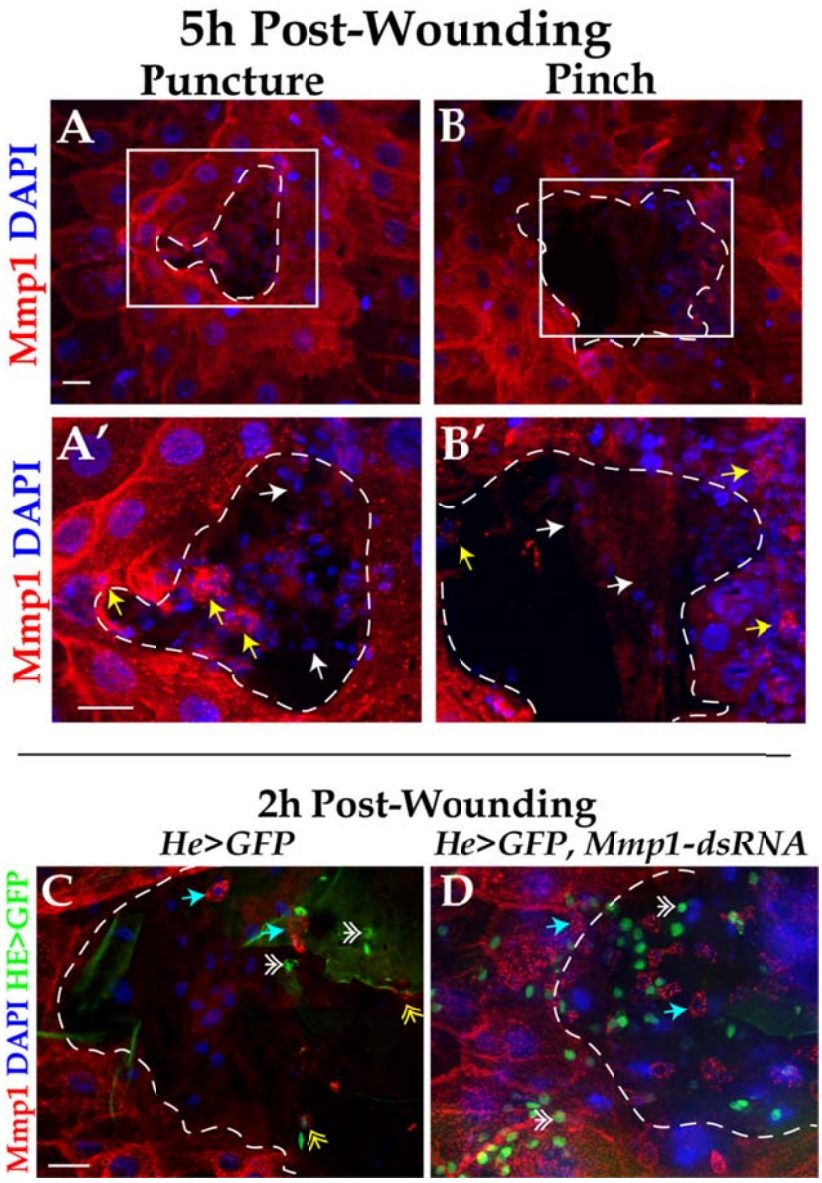
5h Post-Wounding
Puncture
Pinch
A
B
Mmp1 DAPI
A′
B′
Mmp1 DAPI
2h Post-Wounding
He>GFP
He>GFP, Mmp1-dsRNA
C
D
Mmp1 DAPI HE>GFP

Mmp1 plays a role in regulating JNK signaling.

The JNK pathway has been implicated in many processes that require tissue remodeling in both *Drosophila* and vertebrates, such as dorsal and thorax closure during development (Sluss et al., 1996; Zeitlinger and Bohmann, 1999), tumorgenesis (Uhlirova and Bohmann, 2006), and of course wound healing (Galko and Krasnow, 2004a; Martin and Nobes, 1992; Ramet et al., 2002). In *Drosophila* mutants that are devoid of crystal cells, the cell type that facilitates scab formation, wounding leads to super-induction of the JNK pathways (Galko and Krasnow, 2004a). In Chapter III we have shown that *Mmp1* is required for complete scab formation post-wounding, so we asked if JNK signaling was affected when Mmp1 is knocked down in either the plasmatocytes, or the epidermis. A common readout of JNK pathway activation is induction of a *lacZ* transcriptional reporter for *puckered* (*Puc*), a JNK phosphatase and JNK feedback inhibitor, downstream of the transcription factors Jun and Fos (Martin-Blanco et al., 1998; Ramet et al., 2002). Following wounding, in wild type Puc^{lacZ} is expressed in a gradient pattern originating at the leading edge of the wound and can be detected by 3h post-wounding (Fig. 4.8A', D), with a significant increase in expression intensity observed by 5h post-wounding (Fig. 4.8A", D). Minimal, if any, Puc^{lacZ} can be detected in unwounded epidermis (Fig. 4.8 A-C, D). When we knock down Mmp1 expression in the epidermis (*A58>Mmp1-dsRNA*) Puc^{lacZ} intensity can be detected by 3h post-wounding in the epidermal cells at the leading edge (Fig. 4.8B', D), with a significant increase in expression intensity by

5h post-wounding (Fig. 4.8B", D), similar to that seem in wild type samples. In fact there is no significant difference in Puc^{LacZ} expression intensity between wild type and *A58>Mmp1*-dsRNA mutants at any of the time points that we examined (Fig. 4.8D); indicating that Mmp1 expression in the epidermis is not required for wound-induced Puc expression.

In contrast to the *A58>Mmp1-dsRNA* mutants, knockdown of Mmp1 in the hemocytes (*He>Mmp1-dsRNA*) causes no change in Puc^{LacZ} expression intensity at the leading edge within genotype over time (Fig. 4.8C-C", D). Additionally, Puc^{lacZ} expression at *He>Mmp1-dsRNA* wound sites is significantly lower than wild type 5h post-wounding (Fig. 4.8C" compared to A", D). It is important to note that while we do find some variability in Puc^{lacZ} intensity, with some leading edge cells in *He>Mmp1-dsRNA* mutants able to induce Puc^{lacZ} expression at levels that appear to be wild type (white arrow in Fig. 4.8C"), however, the overall intensity of Puc^{lacZ} in these animals is reduced relative to wild type 5h post-wounding. We also observe cells up to 4-5 cell lengths away from the wound site with activated JNK signaling, by expression of Puc^{lacZ} (yellow arrows in Fig. 4.8C"); thus suggesting that hematopoietic *Mmp1* may play a role in restricting the area of the JNK signaling, or inflammation, to the immediate vicinity of the wound site. However this is merely an observation (n=3 animals at 5h) and more detailed analysis is required to confirm these results. Together, these results suggest that Mmp1 expression in the hemocytes may be required to limit

the area in which the JNK pathway is activated, as well as possibly function in a feedback loop to potentiate JNK signaling. One caveat to consider is that Mmp1 is a secreted protein, making it difficult to unquestionably determine the tissue source of Mmp1 at the wound site; knockdown of Mmp1 expression from one tissue source could be compensated for by overexpression / secretion of Mmp1 from a different tissue source.

Figure 4.8: *Mmp1* plays a role in regulating JNK signaling.
A-C) XY projections of Puc^{LacZ} (purple) expression changes in unwounded (A-C) and at 3h (A'-C'), 5h (A"-C") post-wounding in designated genotypes. FasIII (green) labels the cell borders, white dashed lines outline the wound bed. White arrows (C") indicate cells that appear to have wild type Puc^{lacZ} expression. Yellow arrows (C") indicate cells with ectopic Puc^{lacZ}, or JNK signaling. Scale bar in A represents 20μm. **D)** Graph of mean Puc^{LacZ} fluorescence intensity. Both genotype and time significantly influence Puc^{LacZ} intensity by two-way ANOVA ($p<0.0001$). Bonferroni post-hoc comparison was used to determine significance both with genotype over time, and between genotypes within each time point. In unwounded tissue and by 3h post-wounding, there is no significant change in Puc^{LacZ} intensity between wild type and any of the mutant genotypes shown (in all cases $P>0.05$). By 5h post-wounding, the change in Puc^{LacZ} intensity at the leading edge is significant within genotype in both wild type (black star, $p<0.05$) and *A58>Mmp1-dsRNA* (purple star, $p<0.05$), but there is no significant difference in Puc^{LacZ} intensity between wild type and *A58>Mmp1-dsRNA* at 5h post-wounding. Within genotype, there is no change in Puc^{LacZ} intensity *in He>Mmp1-dsRNA* over time. Additionally, Puc^{LacZ} intensity at the leading edge *in He>Mmp1-dsRNA* mutants is significantly lower than wild type at 5h post-wounding (green star, $p<0.05$). Error bars represent the standard error of the mean. Numbers on each bar indicate the number of leading edge nuclei measured in each group.

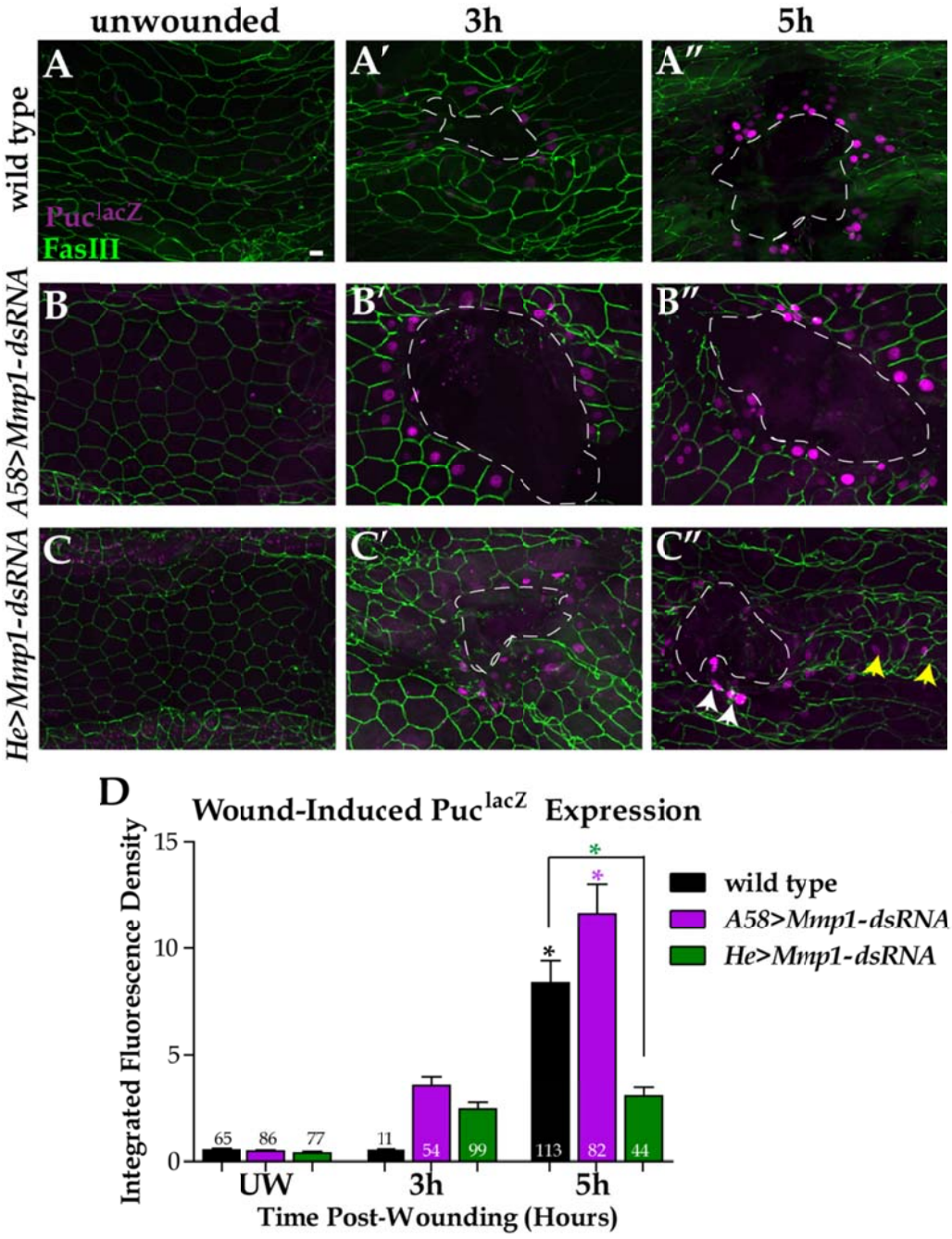
unwounded
3h
5h
wild type
A
A′
A″
Puc^lacZ
FasIII
A58>Mmp1-dsRNA
B
B′
B″
He>Mmp1-dsRNA
C
C′
C″
D
Wound-Induced Puc^lacZ Expression
Integrated Fluorescence Density
15
10
5
0
65
86
77
11
54
99
113
82
44
UW
3h
5h
Time Post-Wounding (Hours)
wild type
A58>Mmp1-dsRNA
He>Mmp1-dsRNA

Hematopoietic Mmp1 may function to restrict the area of Erk signaling.

In addition to clearing infectious agents and damaged cell, neutrophils and macrophages secrete growth factors and chemokines to stimulate keratinocyte proliferation and migration in response to wounding (reviewed by Eming et al. (2007). In fact, re-epithelialization delays are observed in mice lacking macrophages (Leibovich and Ross, 1975). In *Drosophila*, re-epithelialization is induced by the *Drosophila* the PDGF/VEGF-related factor, Pvf-1, which is secreted from the hemocytes (Wu et al., 2009b). PDGF, VEGF (vertebrates), and Pvf-1 (*Drosophila)* are secreted growth factors that activate receptor tyrosine kinase (RTK) signaling on epidermal cells, stimulating cell migration (Lemmon and Schlessinger, 2010; Wu et al., 2009b). Extracellular signal-regulated kinase (Erk), a common readout for RTK signaling pathway (Wu et al., 2009b), activation is necessary to induce epithelial cell motility and invasiveness (Doehn et al., 2009b; Matsubayashi et al., 2004b). Our previous studies have shown that *Mmp1* is required for di-phosphorylated Erk (dpErk) expression at the leading edge post-wounding (Stevens and Page-McCaw, 2012).

When we interfere with Mmp1 expression in the hemocytes with either an Mmp1 double-stranded RNA construct, or Mmp1.f2^{E225A} dominant-negative construct, we find delays in re-epithelialization (Fig. 4.2). We asked if these observed re-epithelialization delays are a result of a failure to induce RTK signaling in the epidermis. By 3h post-wounding dpErk is highly expressed in

the epidermal cells at the wound margin in wild type (Fig. 4.9A, E) and occasionally in hemocytes near the wound site (white arrows in Fig. 4.9A). As we have reported previously, *dpErk* expression is significantly reduced in both *Mmp1* null and *A58>Mmp1-dsRNA* mutants relative to wild type 3h post-wounding (Fig. 4.9B-C, Fig. 2.11 and Stevens and Page-McCaw (2012). While both time and genotypes do significantly influence dpErk intensity in the wounded epidermis by two-ANOVA analysis (Fig. 4.9E), there is no significant difference in dpErk expression intensity in the leading edge epidermal cells at 3h post-wounding when we knockdown Mmp1 in the hemocytes (*He>Mmp1-dsRNA*), relative to wild type (Fig. 4.9D-E), by Bonferroni post-hoc tests. The same caveat that accompanies all our data involving the *He-Gal4* driver applies here as well: Mmp1 is only knocked-down in a subpopulation of plasmatocytes with *He-GAL4*, suggesting that if we were able to knock down Mmp1 expression in all hemocytes we could potentially induce a more penetrant phenotype.

Interestingly, when we look at the expression pattern of dpErk in the *He>Mmp1-dsRNA* mutants we find dpErk expressed in epidermal cells 2-3 cell lengths from the wound site (yellow arrows in Fig. 4.9D), an area much more extensive than that observed in wild type. There is some variability in the number of epidermal cells ectopically expressing dpErk, so more research needs to done to quantify and confirm this observation (n=3 *He>Mmp1-dsRNA* wounded animals). Occasionally, we also find cells in the whole animal *Mmp1*

mutants that are expressing low levels of dpErk approximately 3 cell length from the wound site (yellow arrow in Fig. 4.9B, n=5 *Mmp1*$^{2/Q112*}$ mutant animals), but the expression pattern of dpErk in *Mmp1* mutants is difficult to interpret because the intensity of expression is so low. We do not observe ectopic dpErk expression in *A58>Mmp1-dsRNA* mutants. We also find no significant differences in dpErk expression in unwounded *Mmp1*, *A58>Mmp1-dsRNA*, or *He>Mmp1-dsRNA* mutant epidermis relative to wild type (Fig. 4.9E). Together, these results suggest that *Mmp1*, in the epidermis, is required to promote dpErk expression in epidermal cells at the wound margin; while hematopoietic *Mmp1* may be required to limit wound-induced signaling to the immediate wound vicinity.

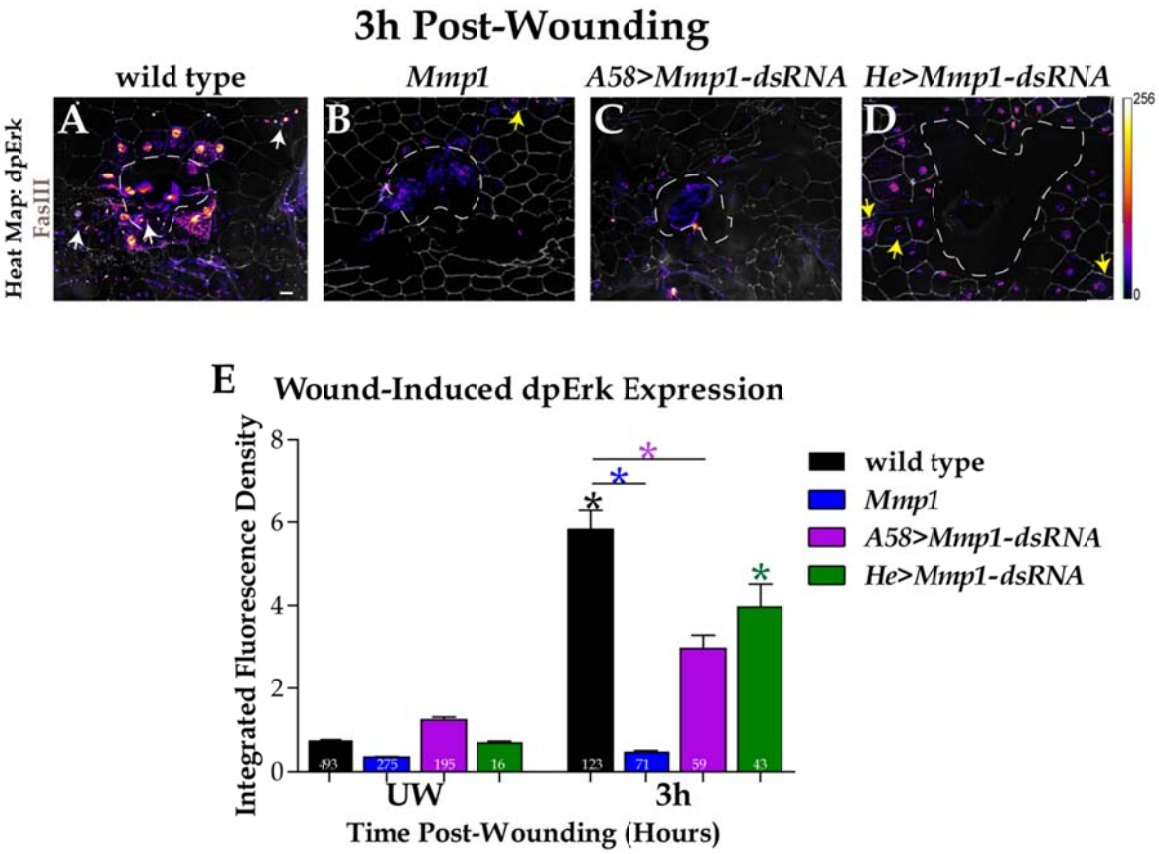

Figure 4.9: *Mmp1* promotes dpErk accumulation.
A-D) Heat map of dpErk expression 3h post-wounding with anti-FasIII (gray) overlay to indicate cell borders in designated genotypes. White dashed lines outline the wound bed. Pixel intensity scale to right of D. Scale bar (A) represents 20μm. White arrows in (A) indicate dpErk expression in hemocytes near wild-type wounds. Yellow arrows (B and D) indicate epidermal cells with ectopic dpErk. **E)** Graph of mean dpErk integrated fluorescence density in leading edge cells only, over time, in the designated genotypes. By two-way ANOVA both time and genotype significantly influence dpErk intensity ($p<0.0001$) and there is also a significant intereaction between time and genotype ($p<0.0001$). Bonferroni post-hoc comparisons were used to determine significance both within genotype over time and within time between genotypes. There is no significant difference in dpErk intensity in unwounded tissue between wild type and any of the mutant backgrounds shown here (in all cases $p>0.05$). However, by 3h post-wounding, dpErk intensity is significantly higher in wild type and *He>Mmp1-dsRNA* within genotype (black star and green star, respectively, $p<0.05$ for both genotypes), but there is no significant change within genotype in either *Mmp1* or *A58>Mmp1-dsRNA* mutants. At 3h post-wounding, dpErk expression in both *Mmp1* (underlined blue star) and *A48>Mmp1-dsRNA* (underlined purple star) is significantly different from wild type (for both $p<0.05$), but at 3h post-wounding, there is no significant difference in mean dpErk intensity at the leading edge between wild type and *He>Mmp1-dsRNA* mutants. Numbers on bars indicate the number of cells measured in each group. Error bars represent the standard error of the mean. Figure is adapted from Stevens and Page-McCaw (2012).

Discussion

Inflammation, induced within minutes of wounding, involves the recruitment of innate immune cells, neutrophils and macrophages, in vertebrates, or hemocytes in *Drosophila*, which function to rid the wound site of pathogens, clear damaged cells, and stimulate repair. In this chapter we have shown that the *Drosophila,* secreted MMP, *Mmp1*, may have a role in the hemocytes to promote re-epithelialization. More specifically, we have shown preliminary data that the Mmp1 isoform, Mmp1.f2, may function in the hemocytes for re-epithelialization, while *Mmp1.f1* does not. In the epidermis, however, the opposite seems to be the case: *Mmp1.f1* is required for re-epithelialization, while *Mmp1.f2* is not. This result is still preliminary, as it is possible that the dominant-negative constructs used to interfere with the Mmp1 isoforms may have off-target effects, or could cross-react with the other Mmp1 isoforms. Additionally, we are assuming that over-expression of a catalytically-inactive Mmp1 dominant-negative is functioning cell autonomously, but as Mmp1 is a secreted protein, it is possible that over-expression of the dominant-negative is acting non-cell autonomously, interfering with endogenous Mmp1 from other tissue sources. These results should be confirmed with rescue experiments, by over-expressing a wild-type version of each isoform, while simultaneously expressing the catalytically-inactive construct. Further confirmation could be obtained by knocking down each isoform individually by

isoform-specific RNAi. While experiments in cell culture have previously found that human MMP-11 (or stromelysin-3) has two isoforms, which have different localization patterns within the cell (Luo et al., 2002), our finding would be the first *in vivo* demonstration that different MMP isoforms have independent functions and suggests that a mechanism to finely tune MMP functions *in vivo* may be through alternative splicing.

Our data supports the hypothesis that hemocytes are required for re-epithelialization, as we find re-epithelialization delays when we knockdown Mmp1 specifically in the hemocytes, coupled with reduced Erk activation, which is involved in promoting cell migration. However, there are studies that suggest that hemocytes are not required for re-epithelialization in *Drosophila (Galko and Krasnow, 2004a; Razzell et al., 2011; Stramer et al., 2005).* This seemingly contradictory data could be a result of the developmental stage of the animals, as much of the wound healing research done in *Drosophila* is during the embryonic stages. In vertebrates during embryonic and fetal wound healing, wounds heal perfectly, or scar-less, and do not invoke an inflammatory response (Bullard et al., 2003), indicating that the inflammatory response is not necessary for re-epithelialization during early development. Perhaps, as with vertebrates, the wound healing process in *Drosophila* embryos also does not require an inflammatory response to induce re-epithelialization. As all of our wound healing research has been conducted on third instar larvae, it is plausible that at

this later developmental stage, as with older vertebrates, an inflammatory response is required for re-epithelialization.

Loss of crystal cells, in *lozenge*^{r15} (*lz*^{r15}) mutants, in *Drosophila* larvae has no effect on re-epithelialization, despite scab formation defects (Galko and Krasnow, 2004a). Similarly, when the plasmatocytes-specific driver, *peroxidasin-GAL4* (*Pxn-GAL4*) was used to drive expression of the apoptosis pathway component *Head involution defective* (*UAS-Hid*), resulting in apoptosis of all plasmatocytes expressing *Pxn-GAL4*, wounds in 3rd instar larvae were still able to close (Babcock et al., 2008), indicating that Pxn-positive plasmatocytes are not required for re-epithelialization. Interestingly, re-epithelialization is unaffected in neutrophil-depleted mice (Dovi et al., 2003). However, macrophages may be necessary for re-epithelialization (Leibovich and Ross, 1975). Our studies suggest that re-epithelialization may be delayed when we interfere with *Mmp1.f2* in a subset of plasmatocyte, using the *He-Gal4* driver, a plasmatocyte marker. Together these results suggest that while crystal cells are not required for re-epithelialization, plasmatocytes may play a role in promoting re-epithelialization in *Drosophila* larvae, but more research is required to clearly define the requirement and function of hemocytes during re-epithelialization.

In response to wounding, Mmp1 is up-regulated, via JNK signaling, in hemocytes systemically, as we find hemocytes with up-regulated Mmp1 throughout the hemolymph, as observed in both wounded larvae *in vivo* and by

ex vivo bleeds, including the hemocytes found at the wound site. Unlike the epidermis, which appears to up-regulate Mmp1 throughout the cells (Chapter II and Stevens and Page-McCaw (2012)), our data suggest that hematopoietic Mmp1 is localized in vesicles shortly after wounding. Additionally, wound-induced hematopoietic Mmp1 up-regulation is a systemic response; hemocytes with elevated Mmp1 levels in granules are found throughout the hemolymph of the wounded animals, thus suggesting that the Mmp1-positive vesicles are accumulating within the hemocytes prior to the arrival of the hemocyte at the wound site, perhaps to be released when the hemocyte reaches the wound bed. While we do find that Mmp1 co-localizes with *preproANF-GFP*, a marker of dense-core secretory vesicles, providing evidence for the former hypothesis that Mmp1 is accumulating in secretory vesicles, it does not dispel the alternative hypothesis that hemocytes are collecting Mmp1 from another tissue source, through endocytosis. Analysis of the Mmp1 expression pattern in secretory pathway mutants, as well as endocytosis mutants, could determine if Mmp1 was being secreted, or collected as hemocytes respond to the wound stimulus.

Interestingly, at the wound site we observe two classes of hemocyte, one with Mmp1-positive granules and a class without Mmp1-positive granules. This latter class could either represent a set of hemocytes that have released accumulated Mmp1 into the wound bed, or they could be a unique sub-set of hemocytes that either does not express Mmp1, or does not up-regulate Mmp1 in

response to wounding. Further investigation need to be conducted to understand how Mmp1, a secreted protease, is regulated in hemocytes.

In the process of neutralizing pathogens and clearing damaged cells, the inflammatory response releases cytotoxic molecules into the wound site, which subsequently leads to some collateral damage, inducing apoptosis in otherwise healthy cells (Stramer et al., 2007). As a result, the inflammatory response is highly regulated, with dampening inflammation being equally, if not more, important than activation. In *Mmp1* whole animal mutants, or any of our tissue-specific *Mmp1* mutants, we do not observe any defects in hemocyte recruitment to wound sites, suggesting that *Mmp1* is not required for activation of inflammation post-wounding, or accumulation of hemocytes at the wound site. However, we observe a large number of hemocytes remaining in and around wound sites in *Mmp1* mutants at late time points (time>5h). These preliminary, purely observational results, may suggest that *Mmp1* plays a role in releasing hemocytes from the wound site.

In both vertebrates and *Drosophila*, JNK signaling is required for wound healing (Galko and Krasnow, 2004a; Martin and Nobes, 1992; Zenz et al., 2003). In both mouse and zebrafish models, JNK has been shown to regulate the inflammatory response via activation of MMPs, specifically MMP-8 and MMP-13, and their endogenous inhibitors, tissue inhibitor of metalloproteinase (TIMP), where loss of MMP-13 leads to a decreased macrophage recruitment to the

wound site, while loss of either MMP-8 or TIMP-3 causes increased inflammation and delayed wound healing (Guinea-Viniegra et al., 2009; Gutierrez-Fernandez et al., 2007a; Mohammed et al., 2004; Zhang et al., 2008). Together these results implicate MMPs in both activation and inactivation of inflammatory signaling. Similar to the vertebrate models, our data also suggest that *Mmp1*, under the regulation of JNK signaling, may function in a feedback loop to limit JNK signaling in the epidermis to the vicinity of the wound site, as shown by ectopic expression of the JNK signaling reporter Puc^{lacZ} in cells not immediately at the wound edge. Interestingly, while Mmp1 expression in the epidermis does not appear to play a role in JNK signaling, hematopoietic Mmp1 may be required to potentiate JNK signaling in the epidermis as we significantly lower Puc^{LacZ} expression epidermal cells at the wound margin in *He>Mmp1-dsRNA* mutants compared to wild type at 5h post-wounding. Together, these results demonstrate the complexity of inflammation regulation and suggest that secreted MMPs may perform different functions during an inflammatory response, to both limit the area of JNK signaling, as well as promote JNK signaling at the wound edge.

In addition to neutralizing pathogens and clearing dead and dying cells, *Drosophila* hemocytes also function to promote tissue repair by secreting growth factors, such as Pvf-1 (Wu et al., 2009b). Pvf-1 promotes cell migration and re-epithelialization by activating RTK signaling in the epidermal cells at the wound

margin, as indicated by common readout out for RTK signaling, *dpErk* expression (Lemmon and Schlessinger, 2010; Wu et al., 2009b). Previous studies in our lab have shown that *Mmp1* expression in the epidermis promotes *dpErk* expression (Stevens and Page-McCaw, 2012). The present study indicates that Mmp1 expression in the hemocytes may also play a role in limiting RTK signaling to the epidermal cells at the wound margin, as is indicated by our preliminary data showing cells 2-3 cell lengths from the wound expressing *dpErk*, an area of expression greater than that observed at most wild-type wound sites.

By utilizing the genetic tools available in *Drosophila*, we have shown that *Mmp1* isoforms, *Mmp1.f1* and *Mmp1.f2* may have independent tissue-specific requirements and play unique roles during wound healing. Additionally, we have found that the hematopoietic *Mmp1* is up-regulated, via JNK signaling, and accumulates in vesicles; awaiting release once the hemocyte reaches the wound site. Once secreted from the hemocyte, *Mmp1* may function to finely regulate JNK signaling in a time-dependent manner, while simultaneously limiting the area of inflammation to the vicinity of the wound. Additionally, hemocytes may release Mmp1 to stimulate epidermal repair by promoting dpErk signaling in epidermal cells at the wound margin. Further research is required to fully understand the functions of *Mmp1* in hemocytes during wound healing, as some of the data discussed in this chapter is only preliminary. A better understanding of how secreted *Mmp1* functions during both the inflammatory and re-

epithelialization phases of wound healing in a simple *Drosophila* model, may provide insight into the functions of secreted MMPs during an inflammatory response in higher organisms, as well as the mechanisms involved in finely regulating inflammation during wound healing.

CHAPTER V

DROSOPHILA Mmp1, Mmp2, AND *Timp* MAY FUNCTION TOGETHER DURING WOUND HEALING.

Introduction

Matrix metalloproteinases (MMPs) have been implicated to function in almost every context that requires tissue remodeling from basic development, to cancer metastasis, to re-generation and wound healing (Page-McCaw et al., 2007). During wound healing, MMPs are known to be involved in all three phases: inflammation, re-epithelialization, and scar-formation (Gill and Parks, 2008). Mice deficient for MMP-8 have an increased inflammatory response and delayed re-epithelialization (Gutierrez-Fernandez et al., 2007a). Wound contraction delays in mice *in vivo,* as well as inefficient cell migration in cultured cells result from a loss of either *MMP-10, MMP-3*, or *MMP-13* (Hattori et al., 2009a; Krampert et al., 2004; Kyriakides et al., 2009b). Interestingly, *MMP-9* has been shown to play multiple roles during healing of corneal epithelial wounds, including delaying the inflammatory response, promoting cell proliferation and migration, and remodeling the provisional fibrin matrix (Mohan et al., 2002). Additionally, *MMP-9 MMP-13* double mutants show longer re-epithelialization delays compared to either single mutant (Hattori et al., 2009a), indicating that MMPs function redundantly during wound healing.

Understanding protein structure can suggest how a protein interacts with other molecules and how that protein might be regulated; as such, extensive research has gone into elucidating the structure of MMPs, as a means to shed light on MMP function. MMPs are enodpeptidases of the metzincin family that contain a Zn^{2+} ion and a conserved methionine turn in the active site (Bode et al., 1993). Translated as zymogens, MMPs contain a signaling sequence that targets MMPs to secretory vesicles were they will subsequently either be secreted or inserted into the plasma membrane (Bode et al., 1993). In vertebrates, there are 25 MMPs, all of which have conserved pro and catalytic domains, as well as a very similar 3-D structure (Massova et al., 1998). Most MMPs also have a hemopexin-like domain, which is thought to be the substrate recognition domain (Bode et al., 1993; Massova et al., 1998). The MMP family is comprised of two classes, the secreted type (of which there are seventeen family members in mice) and the membrane-anchored type (which includes seven family members in mice). MMPs are inhibited by four endogenous inhibitors, known as Tissue Inhibitors of Metalloproteinases (TIMP), which function by coordinating with the Zn^{2+} ion in the MMP active site via a conserved N-terminal cysteine residue (Fernandez-Catalan et al., 1998; Gomis-Ruth et al., 1997). TIMPs also been shown to have functions independent of MMP inhibition (Brew and Nagase, 2010). During liver regeneration, TIMP-3-/- mice have increased inflammation and excessive necrosis, despite no change in overall MMP activity (Mohammed et al., 2004), suggesting that TIMPs may have functions independent of MMPs during

regeneration and wound healing. While there is substantial evidence indicating that MMPs and TIMPs are involved in wound healing, due to the high level of redundancy between MMPs in mammalian systems, it is difficult to elucidate precise MMP functions and regulatory mechanisms in a complicated process, such as wound healing.

MMPs have been shown to be activated by several different mechanisms, including cleavage at a furin cleavage site prior to MMP secretion (Massova et al., 1998; Santavicca et al., 1996; Thomas, 2002), or through the formation of a homodimeric or multidimeric MMP complexes (Butler et al., 1998; Olson et al., 2000; Strongin et al., 1995). Work in primarily cultured cells, as well as *in vitro* studies, suggest that a membrane-anchored MMP (MMP-14), a TIMP (TIMP2), and a secreted pro-MMP (MMP2) form a tri-molecular complex, with TIMP2 binding in the active site of MMP-14 at the cell surface and functioning as an adaptor to localize MMP2 through interactions with the MMP2 hemopexin domain (Butler et al., 1998; Itoh et al., 2001; Kinoshita et al., 1998; Strongin et al., 1995). In cultured cells, an MMP-14/TIMP2/pro-MMP2 complex has been shown to be necessary for pro-MMP2 activation and invasive cell migration (Fernandez-Catalan et al., 1998; Ingvarsen et al., 2008; Itoh et al., 2001; Strongin et al., 1995; Will et al., 1996a). However, *in vivo* for the formation of a complex is unclear. While MMP-14, MMP2, and TIMP2 are all required to promote tail fin regeneration in zebrafish (Bai et al., 2005), as would be expected if they function

together as a complex, the phenotypes of *MMP-2, MMP-14,* and *TIMP-2* knock-out mice are not similar (Gill et al., 2010; Holmbeck et al., 1999; Kuzuya et al., 2003; Oblander et al., 2005; Zhou et al., 2000b). Additionally, pro-MMP2 does not require MMP-14 for activation (Miyamori et al., 2001; Overall et al., 2000; Wang et al., 2000) and MMP-14 can promote cell invasion in the absence of MMP2 (Hotary et al., 2006; Sabeh et al., 2009); thus suggesting that if such a complex does form *in vivo* it may only be required under specific circumstances.

To bypass the complications of redundancy, we utilized the simple model system, *Drosophila melanogaster,* to investigate the function and regulatory mechanisms of MMPs *in vivo* during wound healing. Aside from being an established model system in which to study wound healing *in vivo* (Galko and Krasnow, 2004a; Wood et al., 2002b), the *Drosophila* genome only encodes two MMPs: one secreted (*dmMmp1*) and one membrane-anchored (*dmMmp2*), as well as one TIMP (*dmTimp*) (Godenschwege et al., 2000b; Page-McCaw et al., 2003b; Wei et al., 2003). By taking advantage of the simplicity of this system we are able to identify the functions of each class of MMP *in vivo*, as well as their regulatory mechanisms. In this chapter we report that both *Mmp2* and *Timp* are required for re-epithelialization, where they play a role in promoting cell elongation post-wounding. Additionally, we find that *Mmp2* and *Timp* are required for Mmp1 localization in the epidermis, as well as in the hemocyte. From the combination of the shared re-epithelialization failure phenotypes and the requirement of

Mmp2 and *Timp* for Mmp1 localization, we hypothesize that Mmp1, Mmp2, and Timp may form a tri-molecular complex *in vivo*, which functions to localize Mmp1 and promote wound healing. During tracheal development, *Mmp1* is required to promote ECM remodeling and tissue growth, but a role for *Mmp2* has not been identified (Glasheen et al., 2010a), indicating that *Mmp1* and *Mmp2* also have independent functions *in vivo*. In this chapter, we also report that while *Mmp1* and *Timp* are required for ECM maintenance, *Mmp2* is not; indicating that *Mmp1* and *Mmp2* have both shared, as well as independent functions under normal physiological conditions. Together these results suggest that if an Mmp2/Mmp1/Timp complex does form *in vivo*, it is context-specific.

Methods

Fly lines.

The following lines are described in Page-McCaw et al (2003): $Mmp1^{2}$, $Mmp2^{Df(2R)Uba1\text{-}Mmp2}$ (imprecise *P* excision alleles resulting in deletions of most or all of the coding region); $Mmp1^{Q112*}$ and $Mmp2^{W307*}$ (EMS-induced nonsense alleles resulting in premature truncations). $Timp^{1}$ syn^{28} (imprecise *P* excision that removed all of *Timp* and the neighboring gene *synapsin* coding region (Godenschwege et al., 2000b). For most mutant analyses, trans-heterozygous mutants (combining a *P*-generated allele and an EMS allele) were used to ensure *Mmp1* or *Mmp2* specificity (Glasheen et al., 2009a; Glasheen et al., 2010b; Page-McCaw et al., 2003b). Other fly lines used were *UAS-Timp* (Godenschwege et al.,

2000b; Page-McCaw et al., 2003b), *A58-Gal4* (M. Galko), and *He-Gal4* (Flybase ID FBti0064641) from the Bloomington *Drosophila* Stock Center, *Vkg-GFP*^{G205} (Yale Flytrap). *w*^{1118} was used as wild type.

Wounding Assays and *ex vivo* bleeding assays.

The wounding assay protocol is described in detail in chapter II and Stevens and Page-McCaw (2012). *Ex vivo* bleeding assay for Mmp1 localization in *Mmp2* and *Timp* mutant hemocytes was performed as described in Chapter IV.

Immunohistochemistry.

Samples were dissected and fixed according to protocol described in Chapter II. For permeabilized immunohistochemistry experiments, fixed tissue was permeabilized by washing three times in PBS + 0.2% Triton-X100. For non-permeabilized immunohistochemistry experiments, samples were prepared in the absence of any detergents. Also for non-permeabilized samples, all washes were done in PBS. All samples were blocked in PBS + 5%goat serum + 0.02%NaN_3. Anti-Mmp1 catalytic domain (a 1:1:1 cocktail of mouse monoclonal IgG1 antibodies 3B8, 5H7, and 23G, generated by Page-McCaw et al (2003) and obtained from the Developmental Studies Hybridoma Bank (DSHB)), was used at 1:100. Anti-FasIII (a mouse monoclonal IgG2a from the DSHB) was used at 1:10. Rabbit anti-GFP (Abcam, Cat#ab6556) was pre-absorbed against larval epidermis and used at 1:100. Mouse monoclonal IgG2a anti-GFP (NeuroMab,

clone N86/38) was used at 1:100. Rabbit anti-perlecan (gift of S. Baumgartner) was used at 1:1000. Cy3 or FITC labeled goat anti-mouse IgG1 (Jackson ImmunoResearch), DyeLight649 or FITC labeled goat anti-mouse IgG2a (Jackson ImmunoResearch), Cy3 labeled goat anti-mouse (Jackson ImmunoResearch), DyeLight649 or FITC labeled donkey anti-rabbit (Jackson ImmunoResearch) were all used at 1:300.

Microscopy.

Optical sectioning was performed with a Zeiss Apotome mounted on an Axio imager Z1 or M2, with the following objectives: 20X/0.8 Plan-apochromat, 40X/1.3 oil EC Plan-NeoFluar, or 63X/1.4 oil Plan-apochromat. Fluorescent images were acquired with an Axiocam MRm (Zeiss) camera. All images were obtained in the dark at RT. Z-stacks were compressed into 2-diminsional projections using the orthoview function in Axiovision. All images were exported from their acquisition programs as 16-bit grayscale TIFF files for post-processing in Adobe Photoshop CS4, or ImageJ v.1.43u.

Expression analysis.

To generate heat maps of anti-Mmp1 pixel intensity from fluorescent images, single channel 16-bit grayscale from 2D XY projections from Z-stacks were converted to 8-bit images in ImageJ v1.43u. The "fire" look-up table (LUT)

was then applied to the image to pseudo-color pixels based on intensity, white = 256 and dark navy blue = 0.

To measure Pcan and Vkg-GFP expression in permeabilized versus non-permeabilized tissues between genotypes, 2D XY projections were made from Z-stacks acquired at 63X in Axiovision 4.8 and then exported as a stack of single channel grayscale TIFF images. Grayscale images for channels of interest were opened in ImageJ and automatically sized to 9.25in x 6.93in. A $0.5in^2$ grid was applied to each image and integrated density was calculated within each square using the ImageJ measure tool. Squares that contained only basement membrane were measured; squares that contained folds in the tissue or ECM from other tissue types were excluded. All intensity measurements were imported into a Microsoft Excel spreadsheet and the average pixel intensity for each sample (each animal) was calculated and imported into GraphPad Prism v5.01, which calculated and plotted the mean intensity for each experimental condition. The error bars all show the standard error of the mean. Two-way ANOVA was used to assess the impact of genotype and permeabilization on Pcan intensity, followed by Bonferroni post-hoc tests to determine if there are significant differences between mutant and wild type Pcan expression. Within genotype, Student's T-test was used to determine significance between permeabilization conditions. Student's t-test was used to determine significance between wild type and mutant intensity in non-permeabilized Vkg-GFP samples. For all statistical analysis, results were considered significant if $p<0.05$.

Wound measurements.

Closure and wound area were assessed based on the presence of both FasIII staining at cell borders and epidermal polyploid nuclei as stained with DAPI. To calculate wound area, the outline tool in Axiovision (Zeiss) was used to manually outline the wound edge. This feature automatically calculates the area of the outlined region using image acquisition specifications. Student's t-tests were performed with the analysis tools available in GraphPad Prism v5.01 to compare mutant and wild-type wound area within each time point. Error bars represent the standard error of the mean. Aspect ratios measurements were performed as outlined in Chapter II. Two-way ANOVA, followed by Bonferroni post-hoc tests were performed in OriginPro v8.6 to determine aspect ratios were significantly different over time in wild type versus *Mmp1, Mmp2,* and *Timp* mutants. Aspect ratios in *A58>Timp* mutants were only measured at 5h post-wounding, so to determine if genotype significantly influences aspect ratio 5h post-wounding, one-way ANOVA, followed by Tukey post-hoc tests were performed in GraphPad Prism v5.01. For all statistical analysis, results were considered significant if they were within a 95% confidence interval, or if $p<0.05$.

Cell culture.

Drosophila S2 cells (Schneider, 1972) were cultured at 27C in Schneider's *Drosophila* medium (Gibco) + 10% heat-inactivated FBS (BioWest, Lot #B51217) + 50U/ml penicillin G + 50µg/ml streptomycin sulfate (Gibco). Gene expression

from the *pRMHa-3* metallothionine promoter was induced by adding 2M $CuSO_4$ to a final concentration of 500µM. Approximately 3.5x10^6 cells (total volume = 3ml) were plated into wells of a 6-well plates (Corning, cat#3516), allowed to settle overnight at 27C, then were transiently transfected with a total of 18µg (6µg/plasmid) plasmid DNA in 2M $CaCl_2$ + 50mM HEPES, pH 7.1 + 1.5mM Na_2HPO_4 + 280mM NaCl. Transfected plasmids included: *pRmHa-3.Mmp1.f1*, *pRmHa3.Mmp1.f2, pRmHa3.Timp.c-Myc,* and two different *pRmHa3.Mmp2.GFP* plasmids (one with the GFP tag inserted immediately after the furin cleavage site and the second with the GFP tag inserted immediately before the GPI anchor). *pRmHa3.GFP* was used as a transfection control during parallel transient transfection experiments. For immunocytochemistry, 50µl of S2 cells were plated on 12-well multi-well slides and allowed to settle for about 20min. Cells were fixed in 4% formaldehyde in PBS for 25min at RT and then stained according to immunohistochemistry protocol described below.

Co-immunoprecipitation.

Drosophila S2, either wild-type or stably transfected with *Mmp1.f1*, cells were cultured and transfected as described above. When cells reached a density of approximately 2.0x10^6 cells/ml (about 2 days post-induction) 3ml cultured cells were collected (~6.0x10^6 cells), washed twice in 1ml cold PBS, then lysed in 500ul cold co-IP lysis buffer (20mM Tris-HCl, pH7.5 + 1mM EDTA + 10% glycerol + 0.5% tritonX-100 + 1 tablet/10ml mini complete protease inhibitors

(Roche)) by incubating at 4C for 30min with agitation. Cells were centrifuged in a microfuge at 16,110xg at 4C and supernatant was collected. Protein concentration was determined at A280 with the nanodrop. Lysates were then diluted to 1mg/ml in co-IP lysis buffer. Lysates were pre-cleared against ProteinG- conjugated Dynabeads® (Invitrogen).

The following antibodies were individually bound to ProteinG Dynabeads ® (Invitrogen): mouse monoclonal IgG1 anti-Mmp1 clones 3A6, 5H7, and 3B8 (DSHB), mouse monoclonal IgG1 anti-cMyc (DSHB), rabbit anti-GFP (Abcam, Cat#ab6556.), mouse monoclonal IgG2a anti-GFP (NeuroMab, clone N86/38). After binding, antibodies were cross-linked to beads in 0.2M triethanolamine + 25mM Dimethyl pimelidate dihydrochloride for 45min at RT, blocked in 0.1M ethanolamine for 1h at RT, then resuspended in PBS + 0.1% Tween-20 + 0.02% NaN_3. All washes during bead-antibody conjugation steps were done in 0.1M Na Phosphate buffer, pH8.0. Prior to mixing with lysate, beads cross-linked to Mmp1 monoclonal antibodies were mixed 1:1:1 (A36:5H7:3B8). For immunoprecipitation, 300µg protein from pre-cleared lysates was mixed with 30µl antibody cross-linked Dynabeads® and then incubated overnight at 4C with agitation, washed three times in co-IP lysis buffer, then resuspended in 30µl 3X Laemmli buffer. Protein was boiled off beads by incubating at 70C for 5min. Samples were then tested via western blot for presence of target proteins.

Western blotting.

Lysates were made from dissected 3rd instar larvae epidermis of genotypes w^{1118}, $Mmp1^{2/Q112*}$, $Mmp2^{W307/Df}$, and $Timp^{1}$ syn^{28}. Samples were homogenized in 2X Laemmli buffer with mini-complete protease inhibitors (Roche), and 3-8 epidermal sample equivalents loaded in each lane. Blots were washed in TBS + 0.05% Tween-20, blocked in TBS + 5% nonfat milk + 0.02% NaN_3, and probed with the following primary antibodies for 2h at RT: a 1:1:1 cocktail of mouse anti-Mmp1 monoclonal antibodies, 5H7, 3B8, 3AC used at 1:100, or goat anti-GAPDH (Imgenex, Cat# IMG-3073), used at 1:10,000. Secondary antibody incubations were for 2h at RT with HRP goat anti-mouse (Jackson ImmunoResearch) at 1:5000, or HRP donkey anti-goat (Jackson ImmunoResearch) at 1:10,000, followed by developing with ECL Plus Blotting Detection System (GE Healthcare).

For co-IP samples, 30µl of each sample was loaded onto either a 10% tris-glycine gel, or 4-15% tris-glycine gradient gel. Separated proteins were transferred onto nitrocellulose paper and blocked in Odyssey blocking buffer (Li-Cor). Blots were probed with a 1:1:1 cocktail of mouse anti-Mmp1 monoclonal antibodies A36, 5H7, 3B8 (DSHB) at 1:100, rabbit anti-cMyc (Abcam, Cat#ab9106) at 1:2000, rabbit anti-GFP (Abcam, Cat #ab6556), mouse anti-GFP (NeuroMab, Clone N86/38). Secondary antibodies incubations were for 1h at RT in the dark with goat anti-mouse labeled with IRdye800 (Li-Cor) at 1:7,500 and donkey anti-rabbit tagged with IRDye680 (Li-Cor) at 1:5,000, diluted in odyssey blocking

buffer (Li-Cor) + 0.02%NaN_3, followed by developing with the Odyssey Infrared Imaging System (Li-Cor). All blot images were exported as grayscale Tiff files for post-processing in Adobe Photoshop Cs4.

Results

Mmp2 and *Timp* are required for Mmp1 localization.

Results from cell culture and *in vitro* crystal structure studies have suggested that a membrane-anchored MMP (MT1-MMP), a secreted MMP (MMP-2), and a TIMP (TIMP-2) form a tri-molecular complex, which at least in cell culture, functions to localize the secreted MMP to the cell surface, which leads to the activation of the secreted pro-MMP, and promotes cell migration and invasiveness (Fernandez-Catalan et al., 1998; Itoh et al., 2001). To test this model with our *in vivo* system, we analyzed Mmp1 expression in unwounded epidermis in both permeabilized tissue, to assay total Mmp1 expression, as well as non-permeabilized tissue, to assess exclusively the extracellular contribution to Mmp1 localization. Expression of anti-αtubulin was used as a permeabilization control, as tubulin, being an intracellular protein, will only be detected in permeabilized cells (inset images in Fig. 5.1A-J). Focusing on total Mmp1 expression in unwounded wild-type epidermis, that observed in permeabilized samples, Mmp1 is localized primarily at the cell-cell borders, with

some low levels of Mmp1 detected in punctae throughout the cell and occasionally in a long fiber-like pattern across cells (Fig. 5.1A). From images in the XZ plane, we find that Mmp1 is primarily localized to the basal edge of the cell, with some staining seen in more apical regions, as well as at cell junctions (Fig. 5.1A'). In the absence of *Mmp2*, Mmp1 expression is reduced in permeabilized samples (Fig 5.1C), suggesting that *Mmp2* plays a role in either the localization, or the production, of Mmp1 in unwounded epidermis. A similar phenotype is observed in the absence of the MMP inhibitor, *Timp*, where again we find reduced Mmp1 localization in unwounded epidermis (Fig. 5.1E compared to A).

To confirm that the decreased expression of Mmp1 in both *Mmp2* and *Timp* mutants is a result of Mmp1 mislocalization, not a defect in Mmp1 translation, we analyzed Mmp1 expression via western blot in epidermal samples from 3rd instar larvae (Fig. 5.1K). By western blot, Mmp1 expression in both *Mmp2* and *Timp* mutants is similar to wild type. While this western blot was repeated three times, all with the same results, they were not done with a quantifiable protocol; as such, these western blot experiments should be repeated with a quantifiable technique in order to measure relative band intensity between genotypes.

TIMP has been shown to bind to MMPs with a 1:1 stoichiometry (Cao et al., 1996; Imai et al., 1996; Strongin et al., 1995). When we over-express *Timp* in

the epidermis, therefore disrupting the putative Mmp2/Timp/Mmp1 complex, Mmp1 localization appears similar to both that seen in *Mmp2* and *Timp* mutants, with reduced Mmp1 localization to cell-cell borders (Fig. 5.1G). This suggests that overexpression of Timp may also disrupt Mmp1 localization. The predicted tri-molecular complex is predicted to sequester the secreted MMP at the cell surface by TIMP interacting with the MMP hemopexin domain (Butler et al., 1998; Itoh et al., 2001; Kinoshita et al., 1998); it would then follow that without the hemopexin domain, the secreted MMP would not be properly localized. In the absence of the Mmp1 hemopexin domain ($Mmp1^{\Delta pex}$), there is a significant reduction in Mmp1 expression relative to wild type (Fig. 5.1I). In all genotypes tested, some Mmp1 can be properly localized to the cell-cell borders, as seen in the XY projections (Fig. 5.1A, C, E, G, I) and in varying degrees along the basal side of the cell, as seen in the XZ images (Fig. 5.1A′, C′, E′, G′, I′). Together these results suggest that *Mmp2* and *Timp* are required to localize Mmp1 in the epidermis, perhaps through formation of an Mmp2/Mmp1/Timp tri-molecular complex; however in the absence of either *Mmp2* or *Timp* there may be other mechanisms to localize at least a portion of Mmp1 in the epidermis.

To determine if Mmp1 trafficking also requires *Mmp2* and *Timp*; we analyzed Mmp1 expression in non-permeabilized unwounded epidermis, which allows us to visualize extracellular Mmp1 localization exclusively. Visualization of extracellular Mmp1 indicates that most of Mmp1 expression observed in

permeabilized samples, particularly that at cell-cell borders and along fibers, is extracellular and localized to the basal side of epidermal cells in wild type (Fig. 5.1B, B′). Similar, to that observed in permeabilized tissue, in the absence of *Mmp2*, Mmp1 expression is reduced in non-permeabilized samples, relative to wild type (Fig 5.1D). Interestingly, Mmp1 expression levels in non-permeabilized *Mmp2* epidermis appear to be lower when compared to permeabilized Mmp1 expression in the *Mmp2* mutant background by the XY projections (Fig. 5.1D compared to C), suggesting that *Mmp2* plays a role in facilitating Mmp1 secretion. While the intensity of Mmp1 expression in the XZ projections appears similar in non-permeabilized samples relative to both wild type and permeabilized *Mmp2*, the pattern of Mmp1 expression in the *Mmp2* mutant background appears slightly more diffuse than that seem in wild type (Fig. 5.1D′ compared to B′), again suggesting that *Mmp2* may be required for Mmp1 localization to the cell surface. In both *Timp* loss-of-function and *Timp* gain-of-function (*A58>Timp*) mutants, extracellular Mmp1 expression intensity is lower than that in non-permeabilized wild type (Fig. 5.1F, H compared to B), as well as to total Mmp1 expression seen within genotype (compare Fig. 5.1F to E and H to G). A similar trend is also observed in the *Timp* and *A58>Timp* mutants when we analyze Mmp1 expression in the XZ plane, where again we find reduced Mmp1 intensity along the basal cell surface relative to wild type, as well as within genotype when compared to permeabilized expression intensity (Fig. 5.1F′, H′). Together these results suggest that *Timp* may not only be required for

Mmp1 localization, but may also play a role in Mmp1 secretion from the epidermal cells. The intensity of Mmp1 expression in *Mmp1*$^{\Delta Pex}$ mutants is so low in permeabilized tissue, that it is difficult to assess extracellular Mmp1 localization in this mutant background, as in both permeabilized and non-permeabilized samples Mmp1 expression is nearly undetectable (Fig. 5.1J, J').

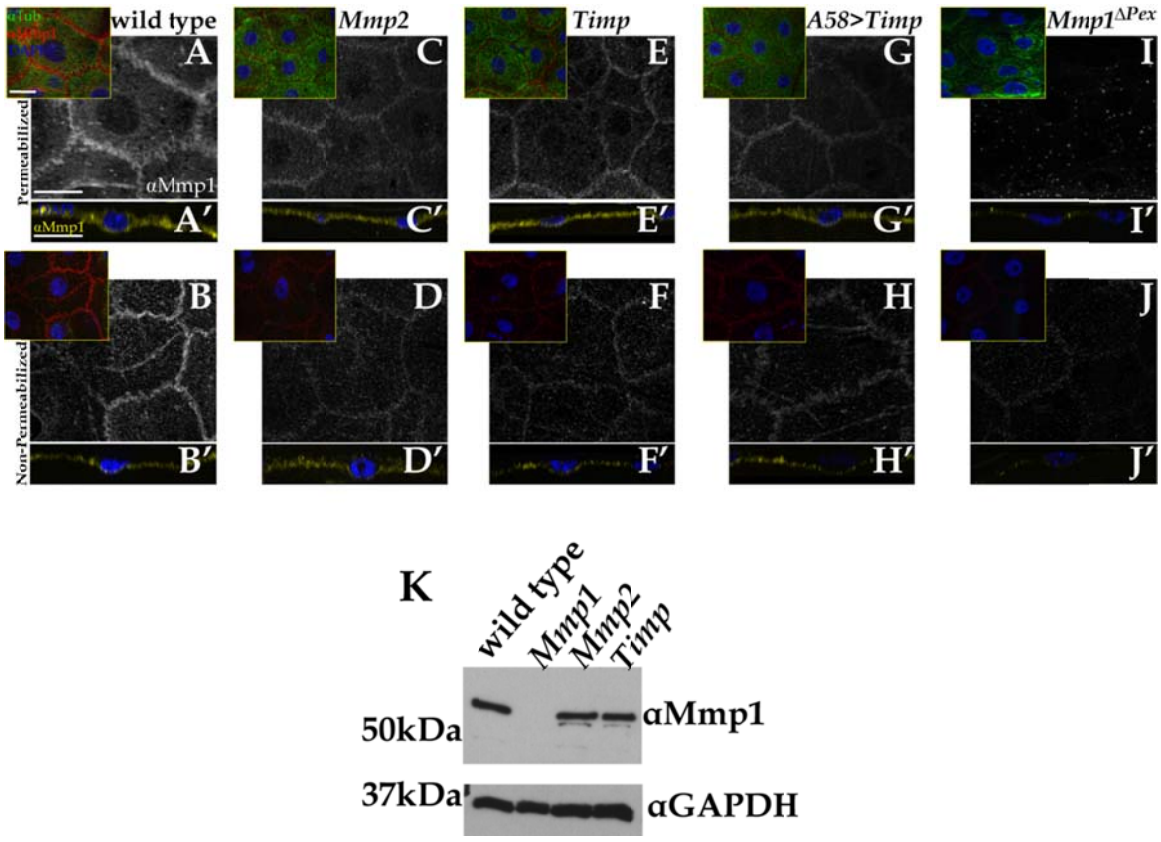

Figure 5.1: *Mmp2* and *Timp* are required for Mmp1 localization in the epidermis.
A-J) XY projections of anti-Mmp1 expression in unwounded 3rd instar larval epidermis in either permeabilized (A, C, E, G, I) or non-permeabilized (B, D, F, H, J) samples in designated genotypes. Yellow-framed inset images in upper left corner indicate permeabilized controls for the corresponding anti-Mmp1 XY image with anti-αTub (green), DAPI (blue) and Mmp1 (red). **A′-J′)** XZ images from single optical section with anti-Mmp1 (yellow) and DAPI (Blue) from either permeabilized (A′, C′, E′, G′, I′) or non-permeabilized (B′, D′, F′, H′, J′) samples in designated genotypes. For all XZ images basal side is down and apical side is up. White scale bars (A, A inset, and A′) represent 20μm. **K)** Western blot of anti-Mmp1 in whole larvae lysates from designated genotypes. Anti-GAPDH was used as a loading control.

***Mmp2* and *Timp* are required for re-epithelialization.**

Previous studies in our lab have shown that the *Drosophila* secreted MMP, *Mmp1*, is required during re-epithelialization to remodel the ECM and promote cell migration (Stevens and Page-McCaw, 2012). To determine if the membrane-anchored MMP, *Mmp2*, or the endogenous inhibitor, *Timp*, also function during wound healing, we punctured 3rd instar larvae with a fine needle. By 14h post-wounding, 79% of wild-type animals have closed their wounds (Fig 5.2A,F, and Stevens and Page-McCaw (2012)). In either *Mmp1* (Fig 5.1B), or *Mmp2* (Fig. 5.2C) mutants wounds fail to re-epithelialize in 100% of animals tested by 14h post-wounding (Fig. 5.2F), with an average wound area 14h post-wounding that is significantly larger than wild type ($p=0.001$, $p=0.007$, respectively). This re-epithelialization failure phenotype is recapitulated when we over-express the endogenous MMP inhibitor, *Timp,* in the epidermis, using the epidermal-specific Gal4 driver, *A58-Gal4* (Fig. 5.2E, F), again leading to a mean wound area that is significantly larger than wild type 14h post-wounding (Fig. 5.2G, $p<0.0001$). Interestingly, loss of the MMP inhibitor, in *Timp* mutants, also induces re-epithelialization defects in all animals tested, with wounds not only remaining open, but also with an average wound area that is significantly larger than wild type by 14h post-wounding (Fig. 5.2D, F-G, $p=0.0217$). Together, these results suggest that *Mmp1*, *Mmp2*, and *Timp* are all required to facilitate re-epithelialization. Unfortunately, we were unable to measure wound area in

either *Mmp1 Mmp2* or *Mmp1 Timp* double mutants as these animals have clotting defects and often bleed out shortly after wounding (n=84 $Mmp1^{2/Q112*}$ $Mmp2^{W307*/Df}$, with n=1 at 14h post-wounding; and n=6 $Mmp1^{2}$ $Timp^{1}$ syn^{28}, with n=2 at 14h post-wounding). In few*Mmp1 Mmp2* and *Mmp1 Timp* double mutants that did survive for 14h post-wounding, the wounds were open (data not shown). The enhancement of the single mutants clotting defects in these double mutants (see Chapter III for more details) suggests that *Mmp1, Mmp2*, and *Timp* may have function some redundant functions during wound healing.

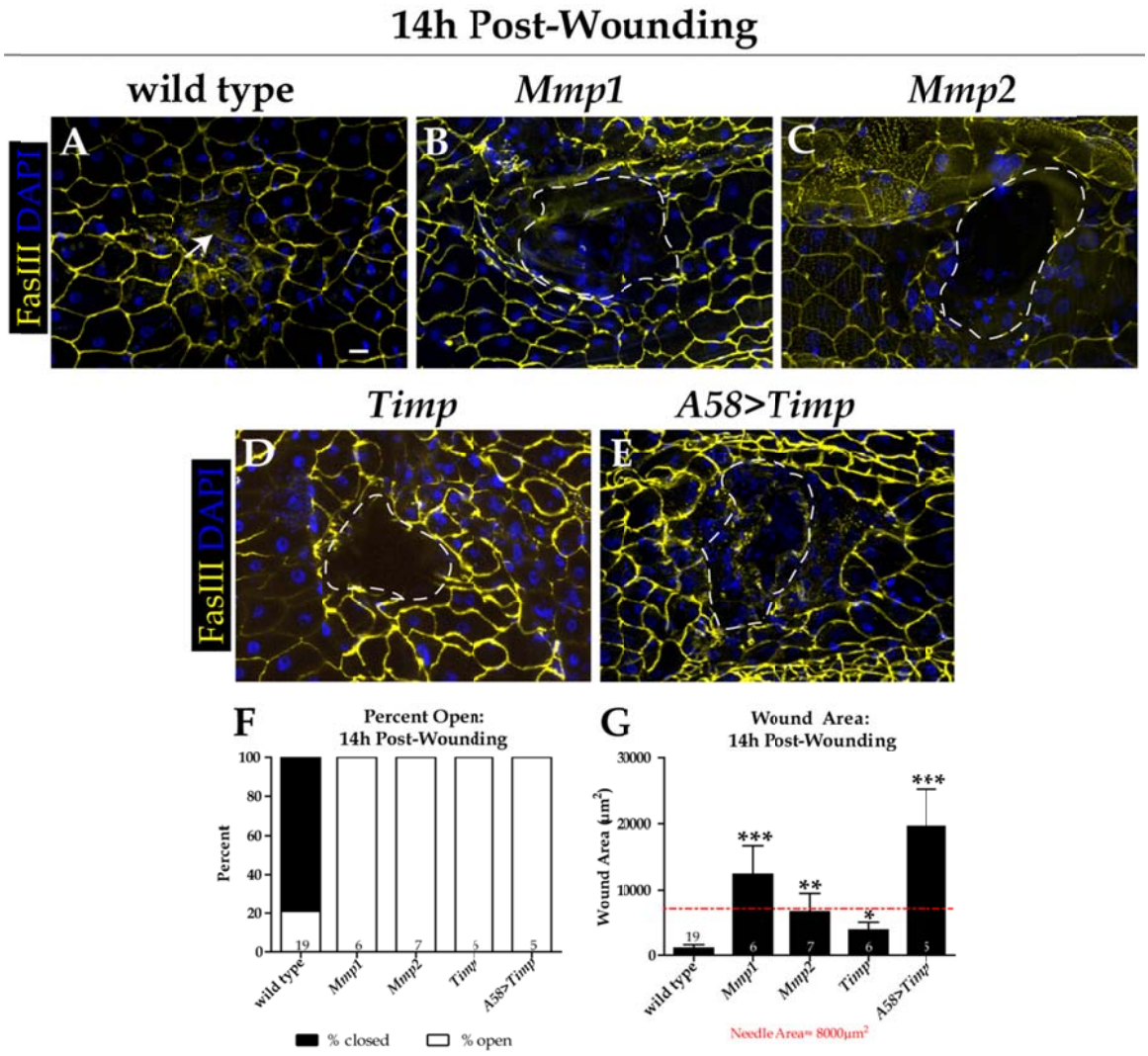

Figure 5.2: *Mmp2* and *Timp* are required for re-epithelialization.
A-E) XY projections of wounded epidermis 14h post-wounding in designated genotypes. FasIII (yellow) labels cell borders and DAPI (blue) stains nuclei. White dashed lines outline wound bed (B-C). White arrow (A) indicated closed wound. Scale bar represents 20µm². **F)** Graph showing percentage of wounds open versus closed 14h post-wounding. By Chi-squared analysis, genotype has a significant effect on the percentage of wounds that are open versus closed by 14h post-wounding ($p<0.0001$). **G)** Graph of mean wound area 14h post-wounding. Wound area is significantly larger than wild type in *Mmp1* ($p=0.0001$), *Mmp2* ($p=0.007$), *Timp* ($p=0.0217$), and *A58>Timp* ($p=0.0004$) by Student's t-test. Numbers on bars (F-G) indicates number of animals tested in each group. Error bars indicate the standard error of the mean.

The Mmp1 hemopexin domain is required for re-epithelialization.

Based on the crystallography evidence, the vertebrate MT1-MMP/TIMP2/MMP2 complex is predicted to form by N-terminal cysteine residues in TIMP-2 chelating the Zn^{2+} ion in the MT1-MMP active site. Serving as a bridge, the C-terminal domain of TIMP-2 will then bind to the outer edge of the MMP2 hemopexin domain (Overall et al., 1999; Overall et al., 2000; Strongin et al., 1995). If a similar complex forms between Mmp2, Mmp1, and Timp in *Drosophila* to promote wound healing, as suggested by our Mmp1 localization data (Fig. 5.1), we would predict that loss of the Mmp1 hemopexin domain would impair complex formation and recapitulate the re-epithelialization phenotypes that we observe in *Mmp1*, *Mmp2*, and *Timp* mutants. To test this hypothesis we measured wound closure 18h post-wounding in *Mmp1* mutants that are trans-heterozygous for two independent mutations in *Mmp1* (*Mmp1*^{Q273*} and *Mmp1*^{W439*}) that induces 2 premature stop codons and, when translated, a protein that lacks the *Mmp1* hemopexin domain (*Mmp1*$^{\Delta Pex}$) (Glasheen et al., 2009a). By 18h post-wounding, where 84% wild-type animals have closed their wounds (Fig. 5.3A, D), wounds in both *Mmp1* (Fig. 5.3B) and *Mmp1*$^{\Delta Pex}$ (Fig. 5.3C) mutants fail to undergo complete re-epithelialization in 100% of animals tested (Fig. 5.3D). Note, however, that only 3 *Mmp1*$^{\Delta Pex}$ mutants were tested 18h post-wounding, so this experiment should be repeated to increase the n-value. In both *Mmp1* and *Mmp1*$^{\Delta Pex}$ mutants, the mean wound area 18h post-wounding is

significantly larger than wild type (Fig. 5.3E); thus indicating that not only is *Mmp1* required for re-epithelialization, the *Mmp1* hemopexin domain, specifically, is also required to facilitate wound closure. However, as seen in Fig. 5.1, very little Mmp1 is detected in the $Mmp1^{\Delta Pex}$ mutant in general, so it is possible that the re-epithelialization defects in the $Mmp1^{\Delta Pex}$ mutant background may not be a result of loss of the Mmp1 hemopexin domain, but may instead simply be a consequence of insufficient levels of Mmp1 in general.

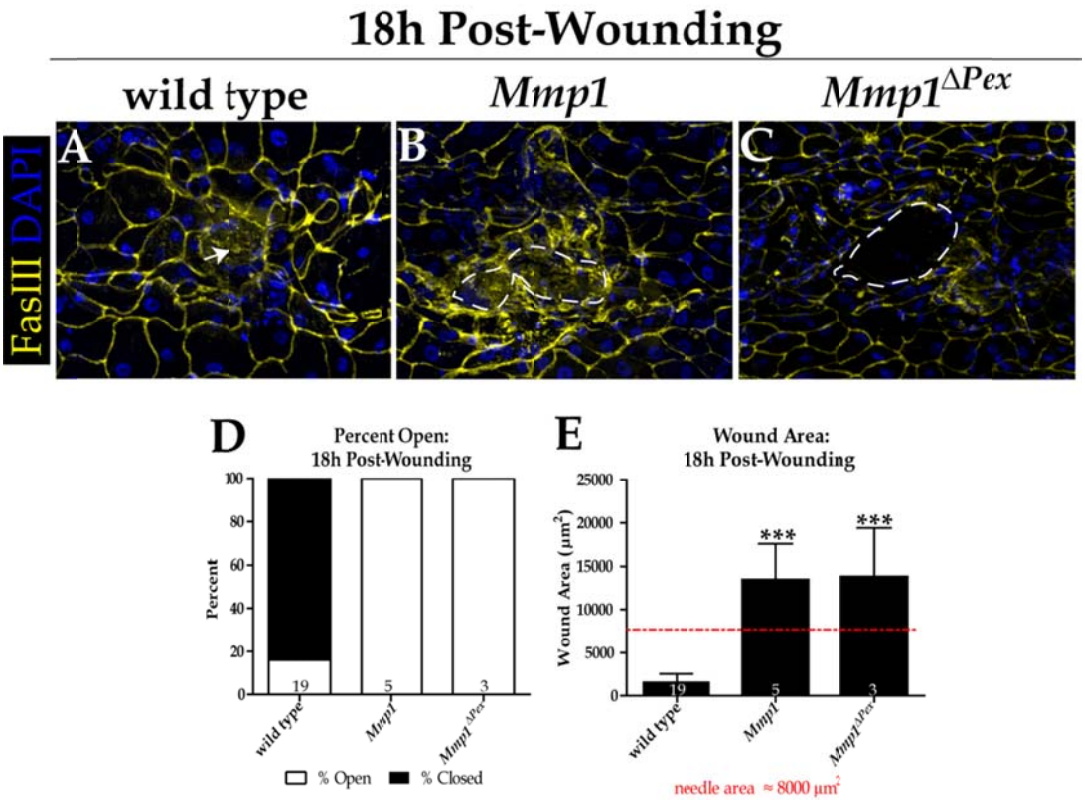

Figure 5.3: Mmp1 hemopexin domain is required for re-epithelialization.
A-C) XY projections of wounded epidermis 18h post-wounding in wild type (A), *Mmp1*$^{2/Q112*}$(B), and *Mmp1*$^{W439*/Q273*}$ (C). FasIII (yellow) labels cell borders and DAPI (blue) stains nuclei. White arrow (A) indicates closed wounds and white dashed lines outline wound bed (B-C). **D)** Graph showing percentage of wounds open versus closed 18h post-wounding. **E)** Graph of mean wound area 18h post-wounding. Wounds are significantly larger in *Mmp1* (p=0.0003) and *Mmp1*$^{\Delta Pex}$ (p=0.0009), relative to wild type by Student's t-test. Numbers on bars (D-E) indicate the number of animals tested in each group. Error bars represent the standard error of the mean.

Mmp2 and *Timp* are required to promote cell elongation.

Re-epithelialization is characterized by migration of the cells at the wound margin into the wound bed (Singer and Clark, 1999). As cells migrate, they rearrange the actin cytoskeleton and elongate in the direction of migration (Mogilner and Keren, 2009b). Our previous studies indicate that *Mmp1* is

required for cell elongation 5h post-wounding (Fig. 5.4E-F, chapter II and Stevens and Page-McCaw (2012)), a phenotype that we can replicate by over-expression of *Timp* specifically in the epidermis (Fig. 5.4D, E, F, chapter II and Stevens and Page-McCaw (2012)). As both *Mmp2* and *Timp* are required for re-epithelialization, we asked if they were also involved in promoting cell elongation. Similar to *Mmp1* mutants, in *Mmp2* mutants there is no significant difference in the aspect ratio of cells at the wound margin immediately post wounding, relative to wild type (Figure 5.4E). However, by 5h post-wounding leading edge epidermal cells are significantly less elongated in *Mmp2* mutants compared to wild type (compare Fig, 5.4B to A, quantified in Fig. 5.4F). Intriguingly, in *Timp* mutants leading edge epidermal cells are significantly longer than wild type wild type immediately post-wounding, but at 5h post-wounding leading edge cells in *Timp* mutants fail to elongate are significantly shorter than wild type at the same time point (Fig. 5.4C, F), this could imply that epidermal cells are initially longer than in *Timp* mutants relative to wild type, a hypothesis that could be tested by comparing cell aspect ratio in unwounded *Timp* mutants to wild type. Together these results suggest that *Mmp2* and *Timp* function, like *Mmp1*, to promote cell elongation, and presumably cell migration, in response to wounding.

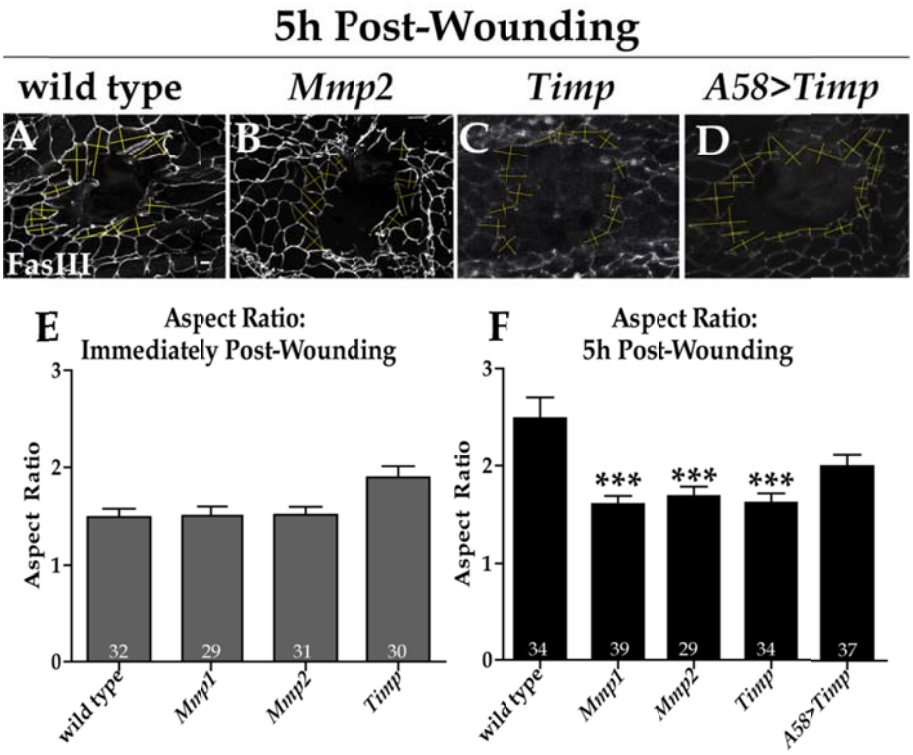

Figure 5.4: *Mmp2* and *Timp* are required for cell elongation.
A-D) XY projection of wounded epidermis 5h post-wounding in the designated genotypes, with cell borders labeled in FasIII (white). Yellow lines indicate the axis measured for aspect ratio calculations (see Methods). Scale bar (A) represents 20μm. **E-F)** Graphs of mean aspect ratio immediately post-wounding (E) and 5h post-wounding (F). By two-way ANOVA genotype and time significantly influence the mean aspect ratio ($p<0.05$). There is no significant difference immediately post-wounding between mutant and wild –type cells. Five hours post-wounding, aspect ratio is significantly different in *Mmp1*, *Mmp2*, *Timp* mutants relative to wild type by Bonferroni post-hoc tests ($p<0.001$ for all mutant / wild type pairs). Numbers on bars indicate the number of cells measured. Error bar represent the standard error of the mean.

Mmp1 and *Timp* function independent from *Mmp2* for ECM maintenance.

A characteristic of the MMP family is the ability to modify extracellular matrix (ECM) components (Page-McCaw et al., 2007). Perlecan (Pcan) is a heparan sulfate proteoglycan that is deposited within the basement membrane,

where it has been shown to function to sequester signaling molecules within the ECM and support cell polarity and tissue architecture (Schneider et al., 2006). We have previously reported that *Mmp1* is required for maintenance of the unwounded basement membrane (Stevens and Page-McCaw, 2012). *Mmp2* and *Timp* are required for Mmp1 localization (Fig. 5.1) and share the *Mmp1* re-epithelialization phenotypes (Fig. 5.2), so we asked if *Mmp2* and *Timp* were also required for organization of the basement membrane in unwounded epidermis. Using an antibody against domain V of *Drosophila* Pcan (Friedrich et al., 2000) as an indicator of ECM organization, we analyzed Pcan localization in the basement membrane of unwounded larval epidermis. In unwounded, wild-type tissue that was permeabilized prior to exposure to antibodies, we find Pcan homogenously expressed throughout the basement membrane with a slight concentration at the cell-cell borders (Fig. 5.5A). In the XZ plane, we find Pcan localized to the basal side of cells, as expected of an ECM protein (Fig. 5.5A'). To separate the extracellular from intracellular contributions to Pcan expression, we stained tissue in the absence of detergents, using loss of anti-αtubulin expression as a non-permeabilization control (inset panels Fig. 5.5A-K). Similar to the permeabilized samples, in non-permeabilized, wild-type tissue we find Pcan expressed homogenously throughout the sample and localized to the basal side of the epidermal cells, again with a slight concentration at the cell-cell borders (Fig. 5.5B, B'). When we compare Pcan expression intensity within wild-type samples we find that there is significantly less Pcan expressed in non-

permeabilized samples relative to permeabilized samples (Fig. 5.5M), indicating that the epidermal cells may be a source of Pcan, which is then secreted and deposited in the ECM.

Deposition of Pcan in the basement membrane appears to be dependent on *Mmp1*, as in the absence of *Mmp1,* we find significantly less extracellular Pcan expression when compared to either that in wild type samples, or to Pcan expression in permeabilized *Mmp1* mutant samples (Fig. 5.5C, D, M). Additionally, we observe a decrease in the complexity of the Pcan expression pattern, in that we a less distinct cell-cell border pattern, in the permeabilized *Mmp1* mutant samples relative to wild type; despite there being no significant difference in Pcan intensity between *Mmp1* mutants and wild type (compare Fig. 5.5C to A, quantified in M). Interestingly, from the images of Pcan expression in the XZ plane, Pcan appears to be localized to the basal side of the cells in *Mmp1* mutants, similar to wild type (Fig. 5.5C'); however the lack of Pcan expression in non-permeabilized *Mmp1* samples (Fig. 5.5D, D') suggests that *Mmp1* may be required for the secretion of Pcan from the epidermal cells.

As validation of our assay, we analyzed extracellular type IV collagen localization unwounded basement membrane using the collagen IV-GFP protein trap (*Vkg-GFP*) expressed in either a wild-type, or an *Mmp1* mutant background. Previously, we have shown that *Mmp1* is required for proper Vkg organization in unwounded basement membrane in permeabilized samples (Chapter II, fig.

2.6, published in Stevens and Page-McCaw (2012)). By utilizing an anti-GFP antibody to isolate the extracellular Vkg-GFP component from the total amount of Vkg-GFP expressed in our permeabilized versus non-permeabilized expression assay (see methods) we found that, as expected, Vkg-GFP is expressed extracellularly and localized to the basal side of the epidermal cells, presumably the basement membrane, in wild type (Fig. 5.6A, A'), confirming that without detergents, we are able to visualize ECM components. Recapitulating our previous results from permeabilized samples, loss of *Mmp1* leads to significantly less extracellular Vkg-GFP expression, as observed in non-permeabilized tissue (Fig. 5.6B, B', quantified in C), similar to that seen with Pcan expression. Together, these results suggest that *Mmp1* plays a critical role in facilitating ECM organization, and may facilitate extracellular Pcan insertion into the basement membrane. Studies suggest that Pcan insertion into the ECM follows polymerization of the type IV collagen matrix (Fessler et al., 1994), therefore, disruption of the collagen IV matrix, as seen in *Mmp1* mutants, could results in an inability to localize Pcan in the basement membrane. Cells are constantly aware of the consistency of their basement membrane (Discher et al., 2005b), suggesting that in response to mislocalized Pcan in *Mmp1* mutants, epidermal cells produce an increased amount of Pcan as an attempt to compensate for insufficient amounts of Pcan in the ECM. Alternatively, *Mmp1* could function to promote Pcan secretion, thus loss of *Mmp1* leads to Pcan retention within the cell. The outcome of either hypothesis would result in the

increased levels of intracellular Pcan relative to extracellular Pcan that we observe in *Mmp1* mutants.

Similar to the *Mmp1* mutants, loss of *Timp* impairs Pcan deposition, as we find significantly less extracellular Pcan expression relative to wild type (Fig. 5.4H, H', M). However, in permeabilized tissue there is no significant difference in Pcan expression intensity between *Timp* and wild type (Fig. 5.5G, G', M). These results suggest that *Timp* may also have a role in facilitating extracellular Pcan localization. However by this analysis it is unclear if *Timp* is directly required for Pcan insertion into the basement membrane, or if Timp has an indirect role, where it functions to inhibit a protease, such as Mmp2, that would otherwise degrade basement membrane and prevent proper Pcan localization. Interestingly, when we over-express *Timp* in the epidermis we find no statistically significant difference in Pcan levels, in either permeabilized or non-permeabilized tissue relative to wild type (Fig. 5.5I, J, M), or in the amount of Pcan found in non-permeabilized tissue versus that found in permeabilized *A58>Timp* samples within genotype (Fig. 5.5M). Together these data suggest that *Timp* overexpress does not affect Pcan localization in the basement membrane, which appears to be properly deposited into the ECM, as we observe Pcan expressed along the basal side of *A58>Timp* cells in both permeabilized and non-permeabilized XZ sections (Fig. 5.51'-J'). If *Mmp1, Mmp2,* and *Timp* are functioning together, as our re-epithelialization and Mmp1 localization data

suggests, then we would expect a loss of the *Mmp1* hemopexin domain (*Mmp1*$^{\Delta Pex}$) to phenocopy *Mmp1*, *Mmp2*, and *Timp* mutant phenotypes. However, there is no significant difference in Pcan intensity in either permeabilized or non-permeabilized tissue relative to wild type (Fig. 5.5K, K', L, L', M), suggesting that the hemopexin domain of *Mmp1* is not required for Pcan insertion into the basement membrane.

Next we asked if the *Mmp2* was involved in Pcan deposition into the basement membrane. Unlike *Mmp1* mutants, there is no significant difference between wild type and *Mmp2* mutants in Pcan intensity in either permeabilized (Fig. 5.5E) or non-permeabilized (Fig. 5.5F) samples (quantification in Fig. 5.4M). The localization pattern of Pcan in *Mmp2* mutants also appears to be similar to wild type, with Pcan localized to the basal surface of the cells with a concentration of Pcan at the cell-cell borders (Fig. 5.5E, E', F, F'), indicating that *Mmp2* is not required to for Pcan localization and that *Mmp1* and *Mmp2* do not function together to facilitate unwounded ECM organization.

Figure 5.5: *Mmp1* and *Timp* are required for ECM maintenance.
A-L) XY projections of Pcan expression in unwounded epidermis in designated genotypes. **A′-L′)** XZ images from a single frame from optically-sectioned, unwounded epidermis stained with Pcan (green), αTub (red) and DAPI (blue) from designated genotypes. Inset images on upper left of A-L are XY images of αTub, a permeabilization control (red) and DAPI (blue) corresponding to each grayscale Pcan image. Samples were permeabilized prior to immunohistochemistry in (A, A′, C′, C′, E, E′, G, G′, I, I′, K, K′). Samples were not permeabilized and immunohistochemistry was performed in the absence of detergents (see Methods) in (B, B′, D, D′, F, F′, H, H′, J, J′, L, L′). For all XZ images basal side is down and apical side is up. Scale bar for A-L (A) and A′-L′ (A′) represent 20μm. **M)** Graph of mean integrated Pcan fluorescence intensity associated with permeabilized (black bars) or non-permeabilized (gray bars) unwounded epidermis in designated genotypes. Pcan intensity is significantly different between permeabilized versus non-permeabilized tissue in wild type ($p=0.0175$) and *Mmp1* ($p=0.0312$) by Student's t-test. By two-way ANOVA, both genotype and permeabilization condition affect Pcan intensity. There are no significant differences in Pcan intensity between mutants and wild type in permeabilized tisuue by Bonferroni post-hoc tests. In non-permeabilized tissue, Pcan intensity is significantly different from wild type in *Mmp1*, *Timp* ($p<0.05$). Numbers on each bar indicate the number of samples measured within each class. Error bars represent standard error of the mean.

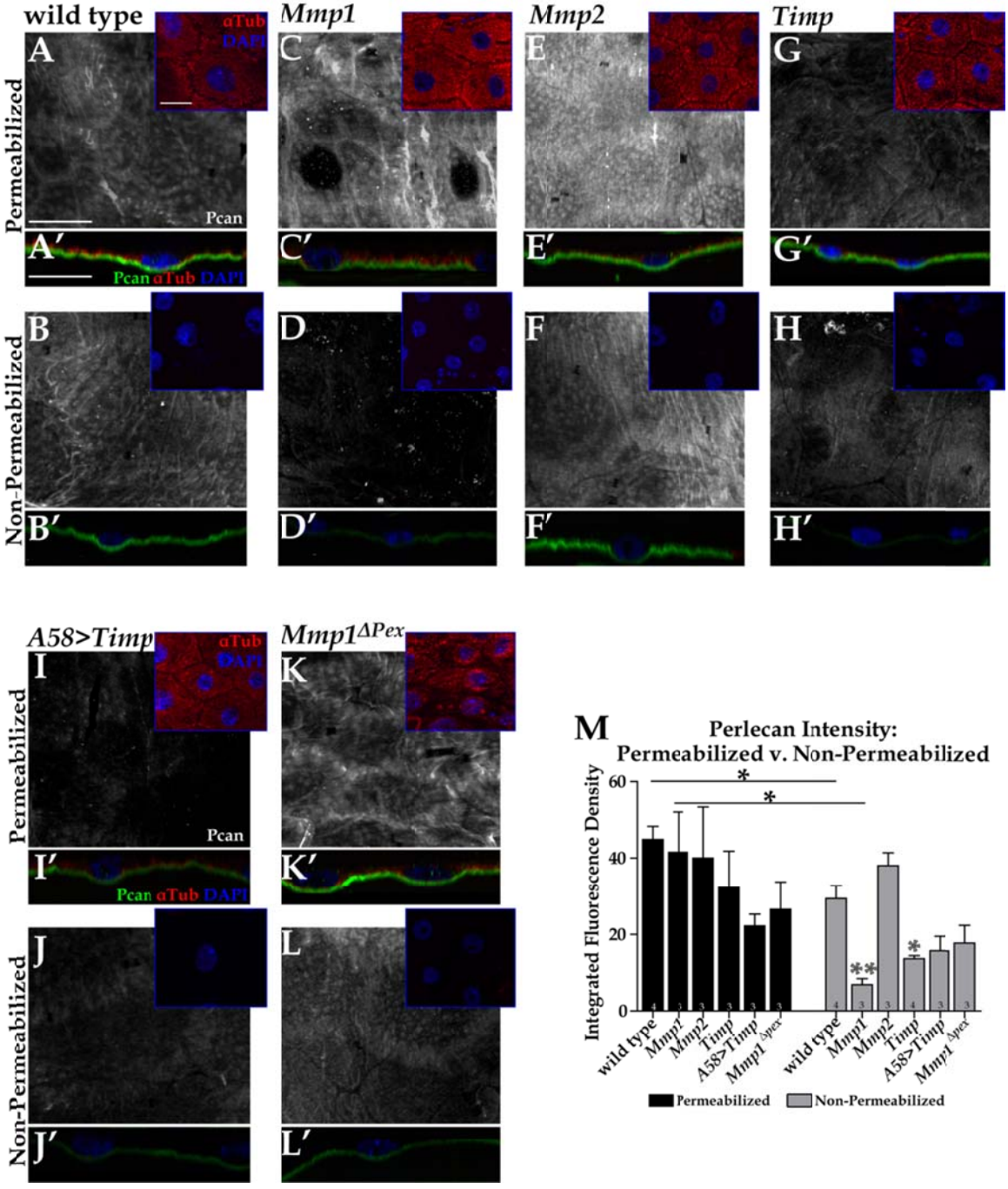
wild type
Mmp1
Mmp2
Timp
A58>Timp
Mmp1ΔPex
αTub
DAPI
Pcan
Permeabilized
Non-Permeabilized
A
A′
B
B′
C
C′
D
D′
E
E′
F
F′
G
G′
H
H′
I
I′
J
J′
K
K′
L
L′
M
Perlecan Intensity:
Permeabilized v. Non-Permeabilized
Integrated Fluorescence Density
60
40
20
0
*
*
**
*
wild type
Mmp1
Mmp2
Timp
A58>Timp
Mmp1 Δpex
Permeabilized
Non-Permeabilized

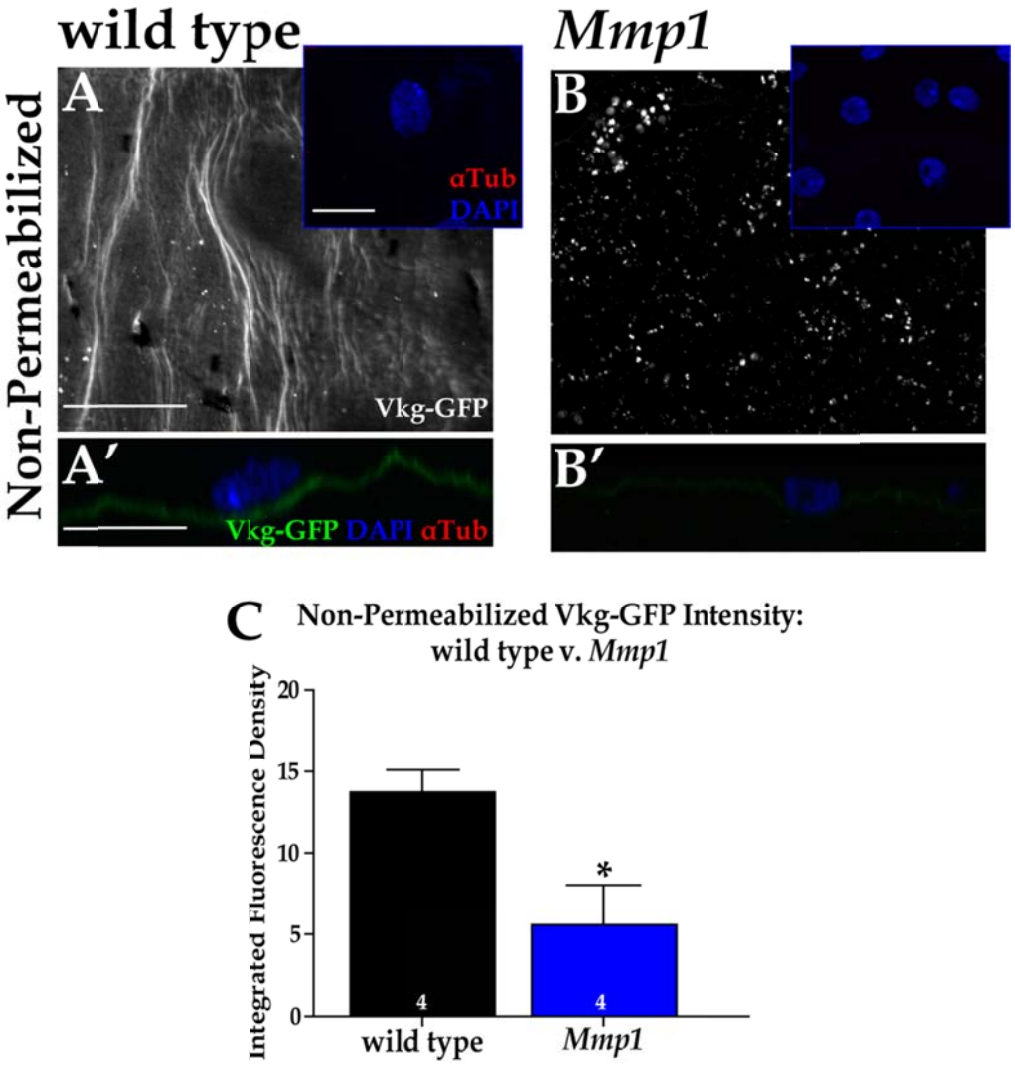

Figure 5.6: *Mmp1* is required for collagen deposition in ECM.
A-B) XY projections of Vkg-GFP expression in wild type (A) and *Mmp1* (B) unwounded epidermis in non-permeabilized samples. Small inset images show permeabilization control with αTub (red) and DAPI (blue) for the corresponding Vkg-GFP grayscale images. During image acquisition, exposure times were set so as to capture primarily the anti-GFP staining pattern only, but some GFP from the *Vkg-GFP* reported could have also been captured. **A′-B′)** XZ images from a single frame from optically-sectioned, unwounded epidermal samples shown Vkg-GFP (green), αTub (red), and DAPI (blue) in wild type (A′) or *Mmp1* (B′). For all XZ images basal side is down and apical side is up. Scale bars (A, A′) all represent 20μm. **C)** Graph showing mean integrated Vkg-GFP fluorescence intensity in wild type (black bar) and *Mmp1* (blue bar) non-permeabilized, unwounded epidermis. Vkg-GFP intensity if significantly lower in *Mmp1* mutants relative to wild type ($p=0.0274$). Numbers on each bar indicate the number of samples measured. Error bars represent the standard error of the mean.

***Mmp2* and *Timp* are required for wound-induced Mmp1 up-regulation.**

Our data suggest that *Mmp2* and *Timp* are required for re-epithelialization during wound healing, as well as Mmp1 localization in unwounded epidermis. We next asked if *Mmp2* and *Timp* are required for Mmp1 up-regulation in response to wounding. In wild type, Mmp1 is dramatically up-regulated by 5h post-wounding in the epidermal cells at the leading edge in a gradient pattern, as we see when we pseudo-color anti-Mmp1 staining based on pixel intensity (Fig. 5.7A, Chapter II; n=23). However, in the absence of *Mmp2* we observe only minimal, if any, Mmp1 up-regulation by 5h post-wounding (Fig. 5.7B; n=10). However, due the Mmp1 localization defects in unwounded epidermis that we observe in the *Mmp2* mutant background, this result is difficult to interpret; either Mmp1 is up-regulated, but without *Mmp2* is mislocalized, or Mmp2 is required on a transcriptional level for Mmp1 production post-wounding. Similarly, loss of *Timp* also results is a reduction of Mmp1 expression by 5h post-wounding (Fig. 5.7C, n=4), suggesting that like *Mmp2*, *Timp* is required for either Mmp1 up-regulation, or Mmp1 localization post-wounding. Interestingly, over-expression of *Timp* in the epidermis elicits a milder phenotype than either loss-of-function *Mmp2,* or *Timp* mutants, with slight Mmp1 up-regulation post-wounding (Fig. 5.7D; n=8), but Mmp1 up-regulation is not to the extent of that found in wild type 5h post-wounding (compare Fig. 5.7A to D), again suggesting that *Timp* is either required to promote wound-induced Mmp1 transcription or to facilitate Mmp1 localization in the epidermis. To distinguish between the two

proposed hypothesis, an Mmp1 transcriptional reporter should be used in *Mmp2, Timp,* and *A58>Tim*p mutant backgrounds to determine if *Mmp2* and / or *Timp* are influence Mmp1 transcription in response to wounding.

In chapter III we showed that *Mmp1* in the hemocytes plays a role in wound healing, so we analyzed Mmp1 up-regulation in hemocytes in *ex vivo* bleeds from both unwounded and 1h post-wounded 3rd instar larvae to determine if *Mmp2* and *Timp* also play a role in Mmp1 localization in the hemocytes (Fig. 5.7E-G). To clearly visualize the dynamic range of Mmp1 expression intensity, we pseudo-colored anti-Mmp1 staining based on pixel intensity. In hemocytes from unwounded larvae, Mmp1 is expressed at very low levels throughout the hemocyte in both wild type and *Mmp2* mutants (Fig. 5.7E, F). In hemocytes from *Timp* mutants, it is unclear if more Mmp1 is present in unwounded hemocytes, relative to wild type, or if the Mmp1 that is expressed is simply concentrated in foci within the cell (Fig. 5.7G, compared to Fig. 5.7E). By 1h post-wounding, Mmp1 is dramatically up-regulated in wild-type hemocytes (Fig. 5.7E'). However, in the absence of *Mmp2* (Fig. 5.7F'), hemocytes do not appear to up-regulate Mmp1, either due to a failure to induce Mmp1 up-regulation at a transcriptional level, or perhaps Mmp1 is up-regulated in hemocytes, but without *Mmp2*, Mmp1 cannot be properly localized. As Mmp1 is a secreted protein, once it is released from the hemocyte Mmp1 is undetectable by this assay. *Timp* mutant hemocytes have a slightly milder phenotype, with

Mmp1 slightly up-regulated by 1h post-wounding, but as in the epidermis, Mmp1 is not up-regulated to the extent of that in wild-type cells at the same time point, indicating that *Timp* plays a role in facilitating Mmp1 up-regulation post-wounding. As in *Mmp2* mutants, if Mmp1 in the *Timp* mutant background is up-regulated, but secreted, then we are unable to detect the full magnitude of the Mmp1 expression change in the hemocytes post-wounding. Further analysis, perhaps by a combination of qPCR and western blotting of hemolymph collected from wounded and unwounded animals, as well as expression of an Mmp1 transcriptional reporter in the hemocytes, is required to distinguish between a role for *Mmp2* and *Timp* in Mmp1 localization, or transcriptional up-regulation post-wounding.

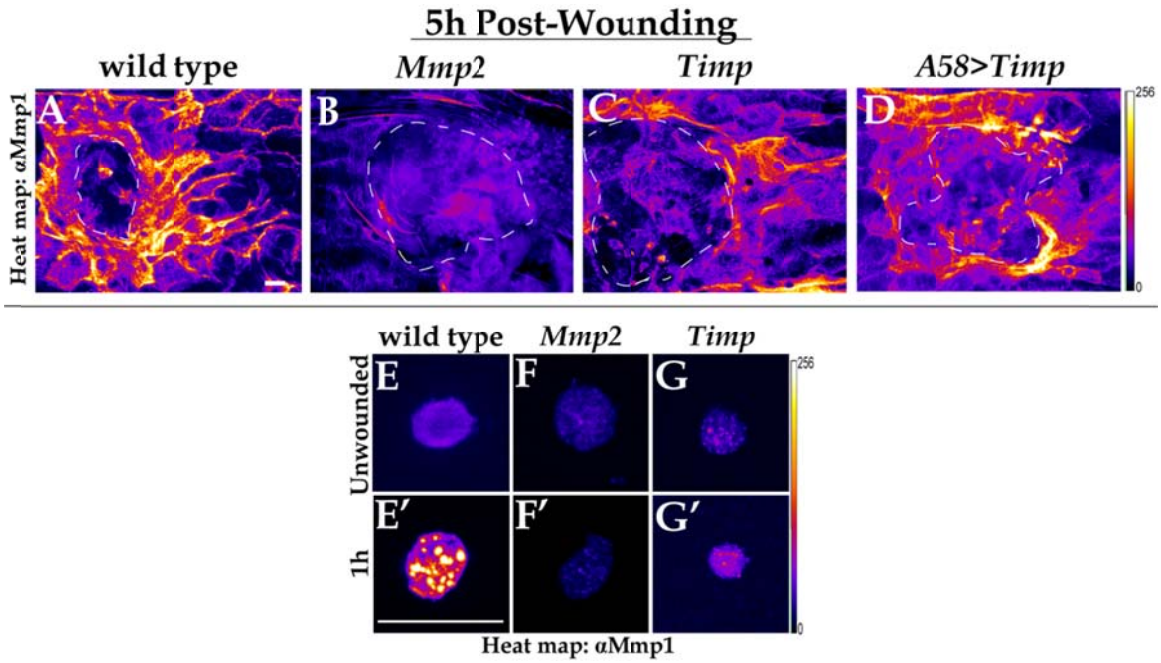

Figure 5.7: Wound-induced Mmp1 up-regulation requires *Mmp2* and *Timp*.
A-D) XY projections of wounded epidermis 5h post-wounding with Mmp1 expression pseudo-colored based on pixel intensity in designated genotypes. Pixel color scale to right of (D). White dashed lines outline wound bed. **E-G)** XY projection of unwounded hemocytes from *ex vivo* bleeds in designated genotypes with Mmp1 expression pseudo-colored based on pixel intensity. **E′-G′)** XY projections of hemocytes for *ex vivo* bleeds 1h post-wounding in designated genotypes. Pixel color intensity scale to right of (G, G′). All scale bars (A, E′) represents 20μm.

Mmp1, Mmp2, and Timp do not co-localize in S2 cultured cells.

The shared wound healing phenotypes in *Mmp1*, *Mmp2*, and *Timp* mutants, in conjunction with the Mmp1 mislocalization observed in *Mmp2* and *Timp* mutants supports the hypothesis that a tri-molecular complex forms in the epidermis between Mmp1, Mmp2, and Timp. Unfortunately, the reagents to test this hypothesis *in vivo* are currently unavailable for Mmp2 and Timp. We attempted to generate antibodies against Mmp2 and Timp, however these efforts

were unsuccessful (data not shown). To test if Mmp2, Mmp1, and Timp physically interact, we utilized *Drosophila* S2 cells transiently transfected with inducible Mmp2 tagged with GFP (Mmp2-GFP), and Timp tagged with c-Myc (Timp-cMyc) to do co-localization and co-immunoprecipitation studies. S2 cells endogenously express Mmp1 at very low levels, so in an attempt to preserve a balance between Mmp1, Mmp2, and Timp, which are predicted to bind in a 1:1:1 ratio (Cao et al., 1996; Strongin et al., 1995), we simultaneously transfected the cells with an inducible Mmp1 construct. Both Mmp.f1 and Mmp1.f2 were tested with similar results (data not shown), but only data from cells over-expressing Mmp1.f1 are shown. Two Mmp2-GFP constructs were generated, one with the GFP tag inserted towards the C-terminus, just before the GPI anchor (Mmp2-GFP^{GPI}), and the second with the GFP tag near the N-terminus (Mmp2-GFP^{Nterm}), immediately following the furin-cleavage site. For the tagged-Timp construct, the cMyc tag was added to the 3′ end of the protein. In cells transiently transfected with Mmp1, Mmp2-GFP^{Nterm}, and Timp-Myc we find all three proteins expressed in a punctae pattern in the cells (Fig. 5.8B-C), which are virtually undetectable in the mock transfected cells (Fig. 5.8A-A′″). As expected, Mmp2-GFP and Timp-cMyc co-localize (yellow arrows in Fig. 5.8B-B′″), just as Mmp1 and Timp-cMyc co-localize (cyan arrows in Fig. 5.8C-C′″). However, in our transfected S2 cells, we were unable to find cells where all three components, Mmp1, Mmp2-GFP, and Timp-cMyc, co-localized to the same punctae (Fig. 5.8B-C). In fact, the incidence of a cell that overexpressed Mmp1, while

simultaneously expressing Mmp2-GFP was very rare, despite a high transfection rate. Similar results were obtained when cells were transfected with Mmp2-GFP^{GPI} (data not shown). Together these results indicate that Mmp1, Mmp2-GFP, and Timp-cMyc do not co-localize in S2 cultured cells. Additionally, they suggest that, at least in this cell culture system, Mmp1 overexpression and Mmp2 overexpression may be mutually exclusive, a cell overexpressing Mmp1 will possibly down-regulate Mmp2 and vice versa.

In conjunction with the above co-localization experiments, we asked if Mmp1, Mmp2-GFP, and Timp-cMyc physically interact. When anti-Mmp1 was used as bait, we were able to pull down both Mmp1, as expected, as well as Timp-cMyc (Fig. 5.8D), but we were unable to pull-down Mmp2-GFP with anti-Mmp1 (Fig. 5.8D), thus confirming our co-localization results that Timp and Mmp1 physically interact, but Mmp1 and Mmp2-GFP do not. Further confirming that Mmp1 and Timp-cMyc physically interact, we were able to pull-down Mmp1 with antibodies against cMyc (Fig. 5.8E). Similarly, when we use anti-GFP as bait to ask if either Mmp1 or Timp-cMyc is associated with Mmp2-GFP, we are able to pull down Mmp2-GFP and Timp-cMyc, but not Mmp1 (Fig. 5.8F). While we are able to resolve a GFP-specific band when we IP with anti-cMyc, but at approximately 40kDa, the size of the Mmp2-GFP band is much smaller than predicted (predicted size of Mmp2-GFP is 116kDa), suggesting that we only recovered a portion of Mmp2-GFP (all of GFP (at~25kDa) +

approximately 135aa, or most of the catalytic domain only) with Timp-cMyc either as a results of experimental error, or due to some as yet unaccounted for post-translational modification of Mmp2. Interestingly, the predicted molecular weight of Timp-cMyc is approximately 25kDa, however, we consistently resolve Timp-cMyc at approximately 40kDa (Fig. 5.8D-F), suggesting that Timp may actually function as a dimer or Timp is post-translationally modified. Dimerization of TIMP-3 has been shown to occur in mammals and is associated with the retinal disorder, Sorsby fundus dystrophy, which leads in an accumulation of TIMP-3 in the ECM and results in age-related macular degeneration (Weber et al., 1994; Wei et al., 2003). Similarly, Mmp2-GFP also runs much higher than predicted, (at approximately 200kDa, Fig. 5.8F), suggesting the Mmp2 may also either form dimers, as has been suggested by cell culture studies of mammalian MMPs (Itoh et al., 2001), or has post-translational modifications. Together, the results from these cell culture experiments show that Mmp1 and Timp, as well as Mmp2 and Timp physically interact; however, we have no evidence that Mmp1, Mmp2, and Timp physically interact, at least in S2 cell culture.

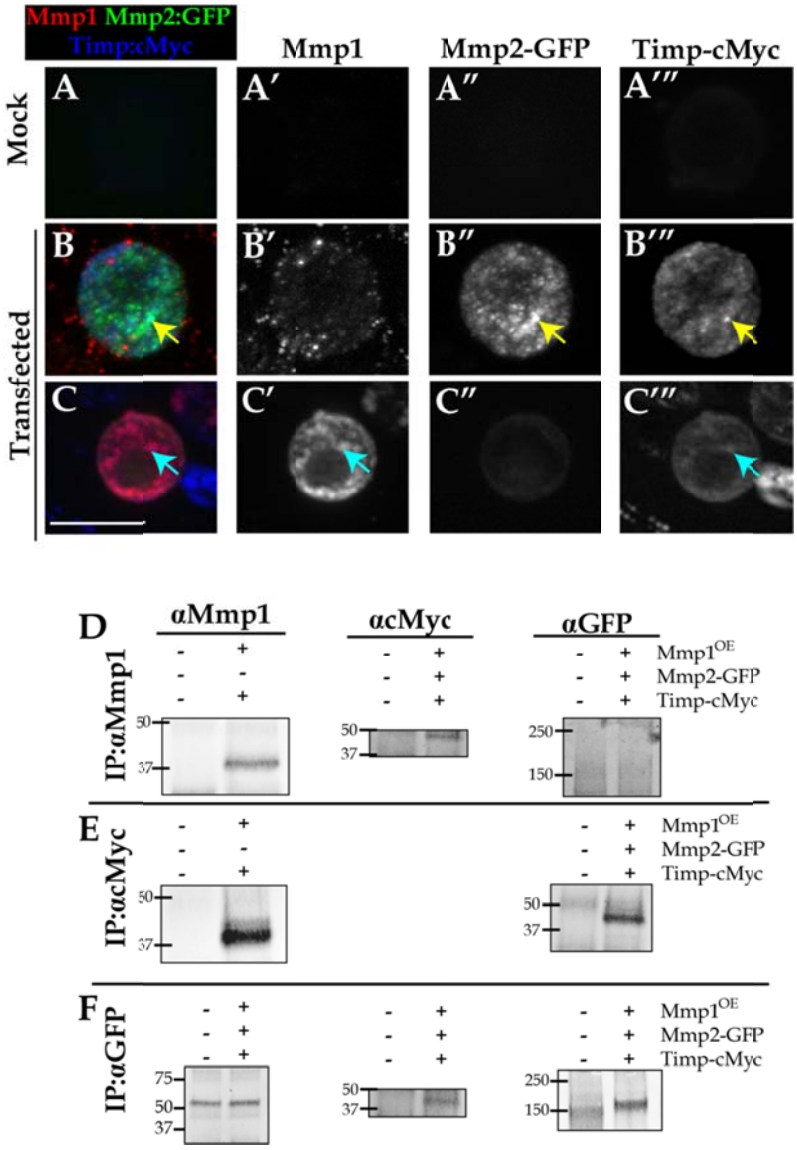

Figure 5.8: Mmp1, Mmp2, and Timp do not co-localize in S2 cells.
A-C) XY projections of mock transfected (A) or transiently transfected with Mmp1.f1, Mmp2-GFP^{NTerm}, and Timp-cMyc (B-C) S2 cells that are stained with anti- Mmp1(red in A-C, grayscale in A′-C′), anti-GFP (green in A-C, grayscale in A″-C″), and anti-cMyc (blue in A-C, grayscale in A‴-C‴). Yellow arrows (B, B″, B‴) indicate an example of a punctae with co-localized Mmp2-GFP and Timp-cMyc. Cyan arrows (C, C′, C‴) indicate example of a punctae with co-localized Mmp1 and Timp-cMyc. Scale bar (C) represents 10μm. **D-F)** Co-immunoprecipitation results from lysates generated from mock transfected (as indicated by (-)) or cells overexpressing Mmp1 (Mmp1^{OE}), Mmp2-GFP, and Timp-cMyc (as indicated by (+)). **D)** Co-immunoprecipitation with anti-Mmp1 as bait, probed with designated antibodies. **E)** Co-immunoprecipitation with anti-cMyc as bait, probed with designated antibodies. **F)** Co-immunoprecipitation with anti-GFP, probed with designated antibodies. No specific band is detected with anti-Mmp1 antibodies following IP with anti-GFP. Numbers with lines to right of each co-IP results indicate size (in kDa). N-value for each co-IP experimental combination ≥ 2. For all panels, the Mmp2-N-terminal GFP construct was used to tag Mmp2 and cells were overexpressing Mmp1.f1.

Discussion

Wound healing involves precise regulation of many factors, including matrix metalloproteinases. Through our studies using the simple model organism, *Drosophila melanogaster*, we have found that both classes of MMP, secreted (*Mmp1*) and membrane-anchored (*Mmp2*) are required for re-epithelialization, as well as the endogenous MMP inhibitor, *Timp*. Our data indicates that *Mmp1*, *Mmp2*, and *Timp* are all required to promote cell elongation, an indicator of cell migration, in response to wounding. Additionally, Mmp1 localization in unwounded epidermis, as well as up-regulation in both the epidermis and the hemocytes involves *Mmp2* and *Timp*. While the functions of *Mmp1*, *Mmp2*, and *Timp* appear to be redundant during the re-epithelialization phase of wound healing, our data suggests that they have independent functions during baseline ECM maintenance; where *Mmp1* and *Timp* are required for Pcan deposition into the ECM, but *Mmp2* is not.

An Mmp2/Mmp1/Timp tri-molecular complex may be required *in vivo* for wound healing.

Previous studies, primarily in cell culture have suggested that a membrane-anchored MMP, a TIMP, and a secreted MMP form a tri-molecular complex to localize the secreted MMP at the cell surface (Itoh et al., 2001). Interestingly, in zebrafish, when the putative MT1-MMP/MMP2/TIMP2

complex was disrupted by overexpression of the MT1-MMP hemopexin domain during tail fin regeneration, cell proliferation and subsequently the regenerative process failed (Bai et al., 2005). The shared re-epithelialization and cell elongation failure phenotypes observe in *Mmp1*, *Mmp2*, and *Timp* mutants, as well as the mis-localization of Mmp1 in the epidermis suggests that a similar complex forms between the *Drosophila* secreted MMP (*Mmp1*), the membrane-anchored MMP (*Mmp2*), and the *Timp* in the epidermis *in vivo* (modeled in Fig. 5.9A). Following this model then, in the absence of Mmp2 to serve as an anchor, an *Mmp1/Timp* complex could still form, but would not be held at the cell surface (Fig. 5.9B). Similarly, without Timp, to function as an adaptor, linking Mmp1 and Mmp2, Mmp1 would also be released into the extracellular space (Fig. 5.9C); just as an excess of Timp in *A58>Timp* mutants would disrupt the 1:1 MMP:TIMP stoichiometry, disrupt complex formation, and cause Mmp1 secretion into the extracellular space (Fig. 5.9D). To add to the complexity of Mmp1 regulation, our data also suggests that *Mmp2* and *Timp* may play a role in promoting Mmp1 release from epidermal cells, as we find higher Mmp1 expression in permeabilized *Mmp2* and *Timp* epidermis, than in non-permeabilized *Mmp2* and *Timp* epidermis, indicating that Mmp1 is being retained within the cells.

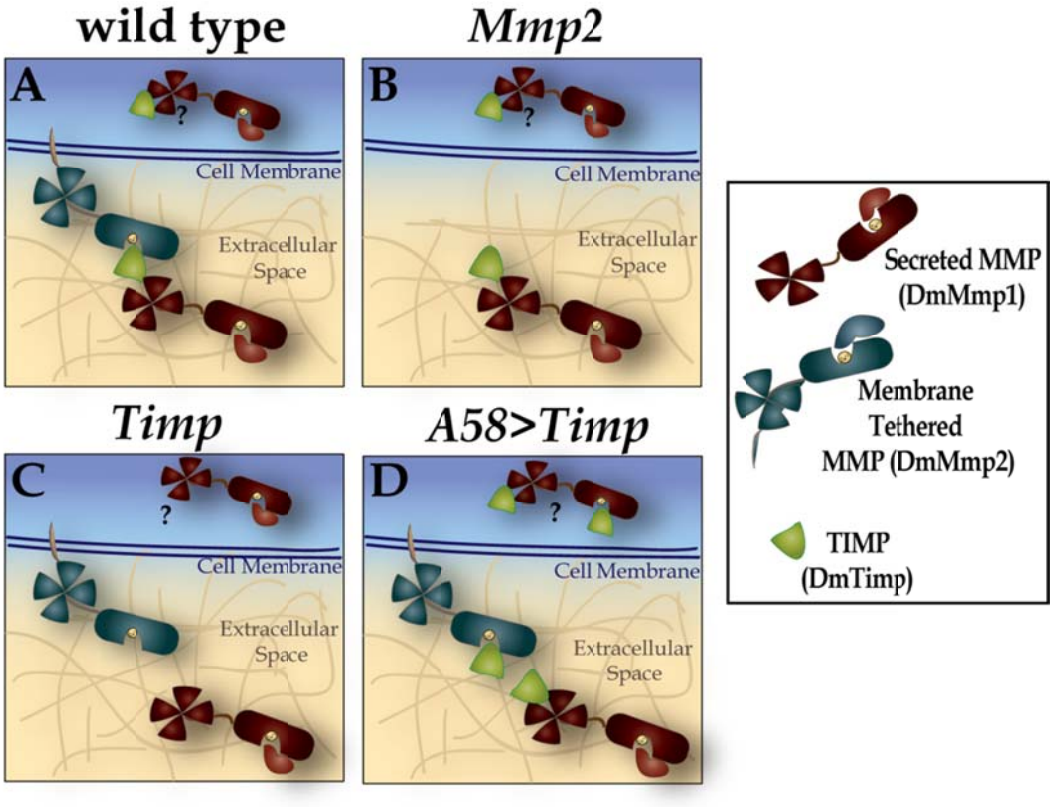

Figure 5.9: Model: Mmp2, Timp, and Mmp1 may form a tri-molecular complex *in vivo*.
A-D) Models illustrating the role of Mmp2/Mmp1/Timp tri-molecular complex formation in Mmp1 localization to the basal cell surface. In wild type (A), Mmp2 functions as an anchor, with Timp binding to the Mmp2 active-site functioning as an adaptor to hold Mmp1 through interactions with the Mmp1 hemopexin domain. In *Mmp2* (B), or *Timp* (C) mutants, Mmp1 is released into the extracellular space due to the absence of either the molecular anchor, or adaptor, respectively. Overexpression of *Timp* (D) interrupts the 1:1 stoichiometry of the interaction, thus prohibiting complex formation. Our results also indicate that *Mmp2* and *Timp* may play a role in Mmp1 secretion from the cells (A), as we find Mmp1 retention within epidermal cells in *Timp* mutants (C). Models are for illustrative purposes only and are not drawn to scale. Key identifying individual components is to the right of panels B and D.

MMPs are regulated on many levels, two of which are access to substrates and / or through proteolysis by either another protease, such as furin, or another activated MMP (Ra and Parks, 2007; Sela-Passwell et al., 2010). Perhaps the re-epithelialization defects that we observe in *Mmp2* and *Timp* mutants are a consequence of disruption of Mmp2/Mmp1/Timp complex formation, leading

to disruption of Mmp1 localization. In cell culture, pro-MMP2 is activated by MT1-MMP, which forms an MT1-MMP homodimer with an adjacent MT1-MMP. When MT1-MMP homodimer formation is disrupted, pro-MMP2 cannot be activated (Itoh et al., 2001; Lehti et al., 2002). It is plausible that a similar mechanism regulates *Drosophila* MMP activation during wound healing, where Mmp2, while in a complex with Mmp1 and Timp, may form a homodimer with a free Mmp2, which could function to activate Mmp1 to promote re-epithelialization. However, Mmp1 contains furin consensus sequence, allowing or Mmp1 autoactivation (Llano et al., 2000), thus negating the need for the formation of an Mmp2/Mmp1 complex to activate Mmp1.

A simple mechanism in which to prevent protease function is simply to prevent protease/substrate interactions. We have shown that *Mmp1* is required for wound healing, and as such it is conceivable that mislocalization of Mmp1 would interfere with access of Mmp1 to its substrates, precluding Mmp1 functions during wound healing. A putative Mmp2/Mmp1/Timp complex may simply function as a mechanism to localize secreted Mmp1 to the cell surface, thus promoting Mmp1/substrate interactions. While our data might support the hypothesis that formation of an Mmp2/Timp/Mmp1 complex in the epidermis is required to facilitate wound healing; at this point the actual formation of an Mmp2/Timp/Mmp1 tri-molecular complex *in vivo* is speculative. Our work in S2 cell culture indicates that both Mmp1 and Mmp2 physically interact with

Timp, but the three components do not co-localize or co-IP together. Just as we find both shared and independent phenotypes of *Mmp1* and *Mmp2* that suggest that formation of a tri-molecular complex is context-specific *in vivo*, it is possible that in cell culture as well, Mmp2/Mmp1/Timp complex formation is also context specific. While the formation of an MT1-MMP/proMMP2/TIMP2 complex has been shown to be required for proMMP2 activation in cell culture (Itoh et al., 2001), MT1-MMP is not required for MMP2 activation *in vivo* (Wang et al., 2000; Zhou et al., 2000a), leaving the tri-molecular complex without a precise function *in vivo.* Precisely how and when this tri-molecular complex functions *in vivo* to facilitate re-epithelialization during wound healing remains elusive. However, until evidence of physical interaction between Mmp2, Mmp1, and Timp is established *in vivo* the re-epithelialization failure phenotypes in *Mmp1* and *Mmp2* mutants may simply represent a shared phenotype between *Mmp1* and *Mmp2* in *Drosophila*. As an alternative hypothesis to explain the shared *Mmp1, Mmp2,* and *Timp* phenotypes as well as our Mmp1 localization data, we propose that *Mmp2* may function to process some unknown molecule that is necessary to promote Mmp1 localization at the cell surface. By this model, in conjunction with our data, *Timp* would still function as an adaptor, a hypothesis that our data cannot disprove, perhaps functioning to enhance Mmp1 localization by promoting interactions between Mmp1 and an unknown factor.

Mmp1 and Mmp2 function independently during normal ECM maintenance.

Previously we reported that *Mmp1* is required for baseline ECM maintenance, where we found that in the absence of *Mmp1* there is significantly less type IV collagen present in the basement membrane (Stevens and Page-McCaw, 2012). The present study expands on those results to show that *Mmp1* is required for Vkg (*Drosophila* type IV collagen α2) deposition into the ECM. Our data also indicates that proper secretion and deposition of the heparin-sulfate proteoglycan, Perlecan, from the epidermal cells into the ECM is dependent on *Mmp1*. This result could implicate *Mmp1* in mediating Pcan localization directly, or disruption of Pcan localization in *Mmp1* mutants could be a secondary to the defects in Vkg deposition. Previous studies have suggested that type IV collagen matrix is established, followed by Pcan insertion into that matrix (Fessler et al., 1994; Pastor-Pareja and Xu, 2011b); therefore, disruption in the initial type IV collagen matrix would lead to mislocalization of Pcan. An alternative hypothesis is then that Pcan is produced, released from the epidermis, but without *Mmp1* to facilitate type IV collagen matrix formation, Pcan cannot be effectively deposited into the ECM and simply mixes into hemocol of the animal. Cells are actively aware of the composition of the basement membrane (Discher et al., 2005b) and may respond to Pcan mislocalization by continuously producing and secreting Pcan as a mechanism to compensate for the disorganized ECM. While it is not too surprising that over-expression of the endogenous MMP inhibitor, *Timp,*

recapitulates this phenotype, as we would expect overexpression of an *Mmp1* inhibitor to interfere with *Mmp1* function, it was surprising to discover that loss of *Timp* also prohibited extracellular Pcan localization. This phenotype could be a secondary defect to the Mmp1 mislocalization defects that we observe in *Timp* mutants, or indicate that *Timp* itself directly plays a role in facilitating ECM organization. During *Drosophila* development, loss of *Timp* results in wing blisters and gut malformations that cause tissue autolysis (Godenschwege et al., 2000b), both of which are phenotypes that could develop due to an impairment in ECM organization, further implicating *Timp* with a role in promoting ECM maintenance under normal physiological conditions.

Unlike either *Mmp1* or *Timp, Mmp2* is not required for extracellular Pcan localization in the ECM, suggesting that Mmp1 and Mmp2 function independently during baseline ECM maintenance. Additionally, independent phenotype suggests that an Mmp2/Timp/Mmp1 tri-molecular complex is not required for ECM maintenance, which is further validated by our results that suggest that the Mmp1 hemopexin domain is also not required for Pcan localization. *Mmp1* and *Mmp2* have been shown to function independently during other tissue remodeling processes, such as trachea development, air sac development, dendritic arbor modifications, as well as other instances of tissue remodeling during *Drosophila* development and morphogenesis (Glasheen et al., 2010b; Page-McCaw et al., 2003b; Wang et al., 2010; Yasunaga et al., 2010).

The appearance of both independent and shared functions of *Mmp1* and *Mmp2* suggest that if a tri-molecular complex may form between Mmp1, Mmp2, and Timp *in vivo*, but if it does it is context-specific. In the context of wound healing, our data suggests that the *Drosophila* membrane-anchored MMP, *Mmp2*, the secreted MMP, *Mmp1*, and their endogenous inhibitor, *Timp*, function together to promote re-epithelialization, presumably by facilitating cell migration. However, in a context that does not require cell migration, such as ECM maintenance and organization, *Mmp1, Mmp2*, and *Timp* are not required to function together, allowing *Mmp1* and *Mmp2* play independent roles. Further elucidation of the mechanisms that regulate MMPs during normal physiological processes may provide insight into how these versatile proteases function during disease states.

CHAPTER VI

CONCLUSIONS & DISCUSSION

By utilizing a simple *in vivo* model to study wound healing, we have found that both classes of MMP, secreted and membrane-anchored, as well as the inhibitor, *Timp*, are required for wound healing in *Drosophila*. During re-epithelialization, our data indicate that *Mmp1*, *Mmp2*, and *Timp* are required to promote cell elongation, an indicator of cell migration. *Mmp1* is also required for *Vkg* accumulation at the wound margin, in addition to promoting dpERK expression in leading edge epidermal cells, signaling cell migration. During the initial inflammation phase, *Mmp1*, *Mmp2*, and *Timp* may function to facilitate hemostasis and melanization of the wound site. In response to wounding, Mmp1 is dramatically up-regulated in both the epidermis and the hemocytes, under the control of the JNK pathway. Our investigations into the tissue-specific requirement of *Mmp1* during wound healing demonstrated that *Mmp1* expression specifically in the epidermis is required for re-epithelialization. In the hemocytes, however, we do not have a clear phenotype; Mmp1 is up-regulated in response to wounding in hemocytes, but at most *He>Mmp1-dsRNA* mutants only have delayed re-epithelialization, similar to the wound healing delays observed in mice deficient for MMP-8, a neutrophil MMP (Gutierrez-Fernandez et al., 2007a), suggesting that hematopoietic Mmp1 may play a different function

during wound healing than Mmp1 expressed in the epidermis. Additionally, Mmp1 localization in the epidermis, as well as up-regulation in the hemocytes may require *Mmp2* and *Timp*, as we find disrupted Mmp1 localization in *Mmp2* and *Timp* mutants. The localization phenotype, in conjunction with the shared re-epithelialization phenotypes found in *Mmp1, Mmp2,* and *Timp* mutants provides support for the hypothesis that an Mmp2/Timp/Mmp1 tri-molecular complex may be required for localization of secreted Mmp1, and suggests that this complex may function *in vivo* to facilitate re-epithelialization.

The potential wound healing delays that we observe when we knockdown Mmp1 in the hemocytes, as well as our data that suggests that Mmp1.f2 catalytic activity in the hemocytes is required for re-epithelialization, is somewhat contradictory the current literature, which indicates that hemocytes are not required for wound closure (Babcock et al., 2008; Galko and Krasnow, 2004a; Stramer et al., 2005). Loss of crystal cells, in *lozenge*^{r15} (*lz*^{r15}) mutants, in *Drosophila* larvae has no effect on re-epithelialization, despite scab formation defects (Galko and Krasnow, 2004a). Similar studies ablated most hemocytes by driving *Hid*, a *Drosophila* gene involved in inducing apoptosis (Goyal et al., 2000), with the hemocyte marker peroxidasin (Pxn-Gal4), showed no effect on re-epithelialization (Babcock et al., 2008). However, as with the other hemocyte-specific GAL4 drivers (*He-GAL4* and *Hml-GAL4*), *Pxn-GAL4* is only expressed in a portion of the hemocyte population (Meister, 2004), leaving the possibility that

hemocytes not expressing *Pxn* are able to compensate for the loss of *Pxn*-expressing hemocytes to promote wound healing. Until re-epithelialization can be assessed in animals completely devoid of hemocytes the requirement for functional hemocytes during wound healing in *Drosophila* larvae cannot be adequately determined.

Even if hemocytes are not required for re-epithelialization, our data does suggest that *Mmp1* from the hemocytes may play a role in regulating the wound-induced inflammatory response, as both ERK and JNK signaling are affected when we knockdown Mmp1 is the hemocytes. Similar to the epidermis, we find that wound-induced Mmp1 up-regulation in the hemocytes is controlled by the JNK pathway; however, by Puc^{LacZ}, a transcriptional reporter of *Puc* expression and a readout of JNK signaling, Mmp1 appears to function in a feedback loop, restricting epidermal *Puc* expression in both intensity and spatially limiting *Puc* expression to the vicinity of the wound site. Similarly, Mmp1 expression from the hemocytes may also play a role in limiting wound-induced *dpERK* expression, as we find an expansion, in mutants, in number of epidermal cells near the wound site expressing *dpERK*. A decrease in epidermal expression of both RTK and JNK signaling, which we have shown to induce Mmp1 up-regulation, may contribute to the delayed wound closure phenotype suggested by our *He>Mmp1-dsRNA* data, as both ERK signaling and Mmp1 expression in the epidermis are necessary for re-epithelialization (Stevens and Page-McCaw,

2012; Wu et al., 2009b); providing evidence that there is some form of hemocyte / epidermal cell cross-talk during wound healing that promotes wound healing. Previous studies have shown that the *Drosophila* PDGE/VGEF-like ligand, *Pvf1*, from the hemolymph is required to induce re-epithelialization (Wu et al., 2009b). *In vitro* studies show that MMPs function to cleave chemokines (Overall et al., 2002) effecting inflammation and wound healing (McQuibban et al., 2001). If MMPs perform a similar function *in vivo*, perhaps once hemocytes are recruited to the wound site they release Mmp1, which prototypically-processes a signaling molecule, such as Pvf1, to stimulate epidermal cell migration.

Focusing on the re-epithelialization defects, we propose that the cell migration defects found in *Mmp1* mutants, as seen in the failed cell elongation and actin remodeling, may be secondary to the defects in both baseline ECM maintenance and ECM remodeling post-wounding that we observe in *Mmp1* mutants. A somewhat surprising result, this suggests that during wound healing, a secreted MMP is required not simply to degrade ECM, but plays a role in ECM deposition. In light of the results that indicate that *Mmp1* is also required for baseline ECM maintenance, we propose that *Mmp1* may function to cleave matrix components in order for new ECM components to be inserted into the matrix as it grows, or as the leading edge epidermal cells invade the wound bed. Precedence for an MMP to promote matrix assembly has been shown in *MT1-MMP* null mice, which have weak tendons resulting from an inability to

maintain these collagen-rich connective tissues (Holmbeck et al., 1999). However, it is important to note the structure of the fibrillar matrix composing the structure of the tendons is very different from the non-fibrillar ECM that makes-up the *Drosophila* basement membrane. This is the first evidence that a secreted MMP is required for basement membrane deposition. A necessary part of re-epithelialization is the re-establishment of the ECM that was destroyed during wounding. If the ECM is not repaired, cells will lack the necessary structure support to accommodate migration, resulting in re-epithelialization failures.

While our data indicate that *Mmp2* is required for re-epithelialization, we also find that, *Mmp2* is not required for basement membrane maintenance, at least by Pcan localization, suggesting that the re-epithelialization defects in *Mmp2* mutants are not secondary to a weakened basement membrane. One hypothesis is that *Mmp2* functions in a complex with Mmp1 to tether Mmp1 at the cell surface; therefore, in the absence of *Mmp2*, Mmp1 is mislocalized and does not associate with the necessary substrates to facilitate cell migration. Whether those substrates are ECM components, or other bioactive molecules it is unclear. However, from our work in cultured S2 cells, Mmp1 and Mmp2 do not physically interact, undermining the tri-molecular complex hypothesis. If a complex does form between Mmp2, Timp, and Mmp1, our data indicate that it is context-specific, required for some Mmp1 functions during wound healing, but not all. Alternatively, *Mmp2* could function to proteolytically-process an

unknown molecule that then facilitates Mmp1 localization, a hypothesis that we could test by expressing a catalytically-inactive form of Mmp2 in the epidermis or the hemocytes followed by assessment of Mmp1 localization.

While there are only two MMPs in the *Drosophila* genome, as opposed to the 25 MMPs in vertebrates, suggesting that *Drosophila* should serve as a simple system in which to study MMP function; the function of MMPs in *Drosophila* appears to be more complicated than suggested by the simplicity of their genome. In *Drosophila,* there is only one secreted MMP to potentially perform the functions of seventeen MMPs in vertebrates, just as there is only one membrane-anchored MMP in Drosophila to potentially function as nine do in vertebrates. We have identified roles for both *Mmp1* and *Mmp2*, as well as their endogenous inhibitor, *Timp*, during both the inflammatory and the re-epithelialization phases of wound healing including some shared phenotypes, such as promoting cell elongation and re-epithelialization, and possibly contributing to hemostasis and melanization, as well as independent functions during ECM maintenance and ERK signaling From our studies of MMPs during wound healing we hypotheszie that *Mmp1* and *Mmp2* functions may be finely and differentially regulated in a context-specific manner. For example, we have shown that Mmp1 up-regulation in response to wounding is dependent on JNK signaling, but JNK signaling is not required for Mmp1 expression in unwounded tissues. Whereas, the unwounded epidermis requires *Mmp2* and *Timp* or Mmp1

localization, ECM maintenance only requires *Timp* and *Mmp1*. *Mmp2* and *Timp* may also be required for wound-induced Mmp1 up-regulation, but those results are difficult to interpret as mislocalization and failure in Mmp1 up-regulation would appear the same in our assay; that hypothesis would be better tested with an Mmp1 transcriptional reporter. Additionally, our data suggest that Mmp2, Timp, and Mmp1 may form a tri-molecular complex in order to facilitate hemostasis, scab formation, and re-epithelialization, but such a complex is not required for many processes outside of wound healing, such as trachea elongation (Glasheen et al., 2010a), or wing disc eversion during development. Together, this work demonstrates the importance of *in vivo* analysis, not only to identify the function, but also the regulatory mechanisms that control that function, particularly for highly versatile proteins, such as MMPs. Many MMPs are up-regulated in wound healing in vertebrates, but they are frequently separated spatially and temporally (Gill and Parks, 2008), suggesting that each MMP has a unique function during wound healing, which may become clear if we understand the context-specific mechanisms regulating that MMP. Understanding the functions and complex mechanisms that regulate MMPs during wound healing could provide insight into MMP functions during pathological states, such as chronic wounds, arthritis, and cancer.

CHAPTER VII

FUTURE DIRECTIONS

As with any line of research, there are always more questions. Studying MMPs in *Drosophila* provides an *in vivo* system to study the functions and regulatory mechanisms of each class of MMP. We have identified several shared phenotypes between *Mmp1* and *Mmp2* during wound healing, as well as a few independent phenotypes, indicating that MMPs in *Drosophila* play multiple roles during wound healing. *Mmp1*, *Mmp2*, and *Timp,* are each required for re-epithelialization, but how each promotes wound healing is unclear. We have suggested that the ERK signaling, actin remodeling, and cell elongation defects observed in *Mmp1* mutants are secondary to the ECM defects found in this genetic background, but an alternative possibility is that each represents an independent function of Mmp1 elicited after unique *Mmp1*-dependent proteolytic events. Further research is required to fully comprehend precisely how MMPs are involved during wound healing *in vivo.*

Extensive research has clearly elucidated the mechanism of hemostasis in mammals, but the same cannot be said of the mechanisms of hemostasis in arthropods, such as *Drosophila melanogaster*. The specific components of the clotting mechanism are different between mammalian and arthropod systems, outcome of the two pathways are similar. By more thoroughly understanding

the individual components of the clotting mechanisms and their functions in *Drosophila*, we can potentially identify parallels between the mammalian and insect pathways. Our studies have shown that both *Drosophila Mmp1* and *Mmp2* play a role in promoting hemostasis and scab formation. However, further research is required to understand specifically what role MMPs play in the melanization cascade, whether they directly or indirectly facilitate clotting and scab formation. We propose two different mechanisms for the relationship between Mmp1 and Mmp2 during scab formation. First, that Mmp1 and Mmp2 function independently, but have opposing functions: Mmp1 promotes melanization, while Mmp2 inhibits melanization. A second model could be that Mmp2, Timp, and Mmp1 form a tri-molecular complex on cell surface, of presumably crystal cells, where they function together to restrict Mmp1 activity, thus promoting melanization at the wound site. Our wounding assay does not address a response to septic wounding, or response to a real immune threat, where melanization would be required to neutralize said pathogen. To determine if *Mmp1* or *Mmp2* is also required for melanization following infection, melanin deposition following septic wounding, as well as exposure to actual *Drosophila* pathogens, such as parasitic wasps, should be assayed in *Mmp1* and *Mmp2* mutant backgrounds. If *Mmp1* and/or *Mmp2* are only required to for melanization at the wound site, then we would not expect any defects in pathogen encapsulation in response to infection. Further research is need to understand the extent of the melanization phenotype presented here, to

determine if MMP functions are limited to hemostasis, or if they extend to the innate immune response.

During wound healing, hemocytes dramatically up-regulate Mmp1 not just when found in the wound bed, but in a systemic response to wounding. Our data suggest that Mmp1 may play a role in limiting both JNK and ERK signaling to the vicinity of the wound site. However, this is merely an observation from preliminary experiments, which need to be confirmed through replication and quantification. While we show that *Mmp1* is promotes RTK signaling, we do not know if *Mmp1* directly, or indirectly participates in RTK signaling. To further establish a specific function of Mmp1 during wound healing, research should be conducted to elucidate Mmp1 substrates *in vivo* during wound healing, perhaps by co-immunoprecipitation assays of lysates from wounded epidermal samples, followed by mass spectrometry analysis to identify proteins that co-IP with anti-Mmp1.

Intriguingly, we observe several subpopulations of hemocytes in the wound bed, including those that express high levels of Mmp1 and those that do not, some that express *He*, a plasmatocyte marker, and some morphological plasmatocytes that do not express *Hemese*. These observations suggest that there may be unique subpopulations of plasmatocytes involved in wound healing. Characterizing these various plasmatocytes subpopulation would be an interesting new avenue to pursue, as most of the work in *Drosophila*

hematopoiesis has been focused on the three major types of hemocyte, crystal cell, lamellocytes, and plasmatocytes (Kurucz et al., 2007; Meister and Lagueux, 2003), but little is known about the subpopulations within each class, or the precise function and regulation of hemocytes during wound healing.

We also show data that suggest that the *Mmp1* isoform, Mmp1.f2, may be required in the hemocytes to promote wound healing, which is contradictory to the literature that suggests that hemocytes in general are not required for re-epithelialization. However, those experiments were either done in embryos, which may repair tissue damage by regeneration mechanisms, not canonical wound healing mechanisms (Martin, 1997), or they were performed in 3rd instar devoid of only a subpopulation of hemocytes (Wu et al., 2009b). To more stringently determine if hemocytes are essential for wound healing in *Drosophila*, the common hemocyte-specific drivers should be combined in the same animal, to effect hemocyte gene expression in multiple hemocyte populations simultaneously. If it turns out that hemocytes are not required for re-epithelialization, then our Mmp1.f2 results could be a consequence of overexpressing a secreted protease that, while catalytically-inactive, may induce extraneous functions unrelated to endogenous Mmp1.f2 function. As with all our Mmp1 isoform data, isoform-specific RNA interfering (RNAi) constructs should be made to confirm our with the dominant-negative, catalytically-inactive Mmp1 constructs, the requirement for Mmp1.f1 in the epidermis and Mmp1.f2 in

the hemocytes for re-epithelialization, as well as potentially identify additional isoform-specific functions.

In zebrafish, MMP-13 plays a role in macrophage recruitment to wounds (Zhang et al., 2008). In *Mmp1* mutants we actually observe an opposite phenotype, where there may be an increased number of hemocytes found in wound sites, suggesting that either in the absence of *Mmp1* the inflammatory response is enhanced, allowing recruitment of more hemocytes to the wound, or in the absence of *Mmp1* hemocytes once captured at the wound site, are unable to release adhesions are a subsequently retained within the wound. MMPs have also been shown to function to modify integrins (Pal-Ghosh et al., 2011; Vaisar et al., 2009), if such modifications are required to release hemocytes from the wound, then if we were to knock down both Mmp1 and an integrin using RNAi in the hemocytes simultaneously, then we would expect to find a decrease in the number of hemocytes retained in the wound site. We have not analyzed wound-induced hemocyte dynamics in an *Mmp2* or *Timp* mutant background, so it is possible that *Mmp2* or *Timp* may also play a role in either recruiting or releasing hemocytes from the wound site.

Based on our wound closure assays, *Mmp1*, *Mmp2*, and *Timp* may function together to promote re-epithelialization; however, it is presently unclear if *Mmp1*, *Mmp2*, and *Timp* function together, perhaps as a complex, or if they function individually to promote wound healing. Information regarding the *in vivo*

localization of Mmp2 and Timp could be very informative; however, the tools to assess Mmp2 and Timp localization are currently unavailable. Our attempts at generating antibodies against either Mmp2 or Timp were unsuccessful. An alternative tactic would be to generate flies with fluorescently-tagged *Mmp2* or *Timp* at the endogenous locus by homologous recombination, in order to visualize endogenous Mmp2 or Timp. If Mmp2 and Timp were tagged with unique fluorophores, such as CFP and YFP, then physical interactions between Mmp2 and Timp could be assessed by fluorescence resonance energy transfer (FRET). Fluorescently-tagged proteins provide the added benefit of the potential for live-imaging, to monitor expression changes in real-time *in vivo*. We have attempted to determine if Mmp1, Mmp2, and Timp physically interact *in vivo* by co-immunoprecipitation using an anti-Mmp1 antibody combined with mass spectrometry to identify any binding partners of Mmp1; however, these attempts have been unsuccessful, as we have not been able to recover enough product for larval lysates following IP with anti-Mmp1 to detect Mmp1, let alone any binding partners. Further protocol optimization, perhaps by scaling up the concentration of both crude protein and antibody, may generate improved results.

Now that we have an *in vivo* model in which to study MMP functions during normal wound healing, it would be informative to adapt the system in order to study the functions of MMPs during abnormal wound healing, chronic

ulcerated wounds in diabetic patients. Recent work has established *Drosophila* as a diabetes model by identifying animals that are mutant in the insulin/IGF pathway (Baker and Thummel, 2007). By performing our wounding assays is such a mutant background we could potentially understand how MMPs are involved in wound healing under abnormal or chronic wound conditions. Further research into the functions and regulation of *Drosophila* MMPs, by either the aforementioned experiments, or along other avenues, is necessary to provide more detailed insight into the *in vivo* functions of each class of MMP during wound healing. By understanding how MMPs function during normal wound healing, we may be able to design therapeutic treatments to improve the outcome of abnormal wound healing, to induce healing in non-healing wounds.

APPENDIX A

SEQUENCE COMPARISON BETWEEN *MMP1* ISOFORMS

The *Drosophila* genome has been shown to encode 1 secreted MMP, *Mmp1* (Llano et al., 2000) and 1 membrane-anchored MMP, *Mmp2 (Llano et al., 2002)*. According to the National Center for Biotechnology Information (NCBI), there are 9 predicted isoforms of *Mmp1* and 2 predicted isoforms of *Mmp2.* Sequence alignment between the two predicted Mmp2 isoforms shows that both sequences encode an identical polypeptide, indicating that while there might be differences in the untranslated regions (UTRs) of the two predicted forms of Mmp2, only one Mmp2 polypeptide is transcribed. For *Mmp1*, on the other hand, sequence comparison suggests that out of the 9 predicted isoforms, 5 unique polypeptides are generated. We have grouped the predicted isoforms into 4 groups based on sequence similarity (Fig. A.1). For all the isoforms, the differences are at the C-terminal end of the hemopexin domain (Fig. A.1), suggesting that each isoform may recognize a unique set of substrates. Mmp1 form C (hereafter referred to as Mmp1.f3a) and Mmp1 form H (hereafter called Mmp1.f3b) are grouped together because they share 53 amino acids (aa) at the end of the hemopexin domain, but differ by 28aa which Mmp1.f3a shares with Mmp1.f1, but not Mmp1.f3b (green group in Fig. A.1).

Figure A.1: Sequence comparison between predicted *Mmp1* isoforms.
A) Mmp1 amino acid sequence with the conserved region in black and the regions unique to each isoform in color-coded based on designated group shown in (B). The base of the arrow indicates where the sequence of each isoform deviates from the conserved sequence, or in the case of Mmp1.f3a, from the unique region of Mmp1.f1. **B)** Table showing how the 9 predicted Mmp1 isoforms are grouped into 4 groups. Color shading of each group corresponds to the colored sequences in (A). Also included in the table is the number of amino acids for each predicted polypeptide, the number of unique amino acids for each class, the domain that contains the unique sequence, and the new name that we assigned to each unique polypeptide. Mmp1.f1 has 12 unique amino acids + 28 amino acids that are only shared with Mmp1.f3a. Mmp1.f2 and Mmp1.f4 has 11 and 26 unique amino acids, respectively. Group 3 has two members, Mmp1.f3a and Mmp1.f3b, which differ only by the 28 amino acids that Mmp1.f3a shares with Mmp1.f1, which Mmp1.f3b does not contain.

A **Conserved Mmp1 sequence**

MTNCQSSVFIVVGTLFSIMAAAQSAPVSTTTQAEIYLSQFGYLP
ASARNPASSGLHDQRTWVSAIEEFQSFAGLNITGELDAETMKLMSLPRCGVRDRVGTG
DSRSKRYALQGSRWRVKNLTYKISKYPKRLKRVDVDAEIGRAFAVWSEDTDLTFTRKT
SGPVHIEIKFVESEHGDGDAFDGQGGTLAHAFFPVFGGDAHFDDAELWTIGSPRGTNL
FQVAAHEFGHSLGLSHSDQSSALMAPFYRGFEPVFKLDEDDKAAIQSLYGRKTNQLRP
TNVYPATTQRPYSPPKVPLDDSICKDSKVDTLFNSAQGETYAFKGDKYYKLTTDSVEE
GYPQLISKGWPGLPGNIDAAFTYKNGKTYFFKGTQYWRYQGRQMDGVYPKEISEGFTG
IPDHLDAAMVWGGNGKIYFFKGSKFWRFDPAKRPPVKASYPKPISNWEGVPNNLDAAL
KYTNGYTYFFKGDKYYRFHDARFAVDSATPPFPRPTAHWWFGCKNTPSSTG

NIVEGSDNEFEQHSMIPHADDGNGDDFDAGEWDRLSGSFV
Isoform 1 (aka D, F, E, G)

FKRRGYKNKNN
Isoform 2 (aka J)

AVGDHQSNDEPIVPEVAERTGNGASQSKLTSSSAVSTVITTILMCLVSKSIVS
Isoform 3a (aka C)

AVGDHQSNDEPIVPEVAERTGNGASQSKLTSSSAVSTVITTILMCLVSKSIVS
Isoform 3b (aka H)

APQVPSLNPNPNQGILPSWMWGLYNRFF
Isoform 4 (aka I, K)

B

Isoform	Predicted Length	Sequence Identical to Isoform	Approx. # Unique aa *	Unique Region	Alternative Names
Mmp1-G	541aa	D, F, E	12 (+ 28**)	hemopexin	Mmp1.f1
Mmp1-F	541aa	D, E, G			
Mmp1-D	541aa	E, F, G			
Mmp1-E	542aa	D, F, G			
Mmp1-J	512aa		11	hemopexin	Mmp1.f2
Mmp1-C	584aa	H,D,E, F,G	53 (+ 28***)	hemopexin	Mmp1.F3a
Mmp1-H	554aa	C	53****	hemopexin	Mmp1.f3b
Mmp1-K	528aa	I	26	hemopexin	Mmp1.f4
Mmp1-I	528aa	K			

* Number of amino acids unique to this group
**Mmp1.f1 has 12 unique amino acids and 28aa shared only with Mmp1.C
*** Mmp1.C has 53 amino acids shared between Mmp1.C and Mmp1.H and 28 amino acids shared only with Mmp1.f1
**** Mmp1.H has 53 aa in common with Mmp1.C only, but it lacks the 28aa region homologous with Mmp1.f1

Once we determined the sequence similarity between the isoforms, we need to determine which if any of these predicted Mmp1 isoforms actually exist. Mmp1.f1 and Mmp1.f2 cDNA has been previously isolated from screening embryo, larval, and pupal libraries (Page-McCaw et al., 2003b), demonstrating that both Mmp1.f1 and Mmp1.f2 are at least translated in *Drosophila.* As for the other isoforms, only Mmp1.C (which we call Mmp1.f3a in Fig. A.1) is strongly supported, according the *Drosophila* database, Flybase (Flybase.org), by the existence of 3 cDNA clones that contain a full length Mmp1.C transcript. This strongly suggests that Mmp1.f3a exists *in vivo*. There is only weak evidence suggesting the existence of either Mmp1.hMmp1.K or Mmp1.I, which we classify as Mmp1.f3b or Mmp1.f4, respectively. For these three predicted isoforms there are end sequence only cDNA sequences that contain a portion of Mmp1.H, Mmp.I, or Mmp1.K, with 5 expressed sequence tags (ESTs) recognizing Mmp1.H and Mmp1.K, but not Mmp1.I. However, there are no cDNAs that contain full length transcripts of Mmp1.H, Mmp1.K or Mmp1.I, calling into the question the existence of these isoforms. Together, this analysis suggests that there are at least three Mmp1 isoforms that may have recognize a unique set of substrates and perform independent functions *in vivo*.

Methods

Sequence analysis.

Amino acid sequences were gathered for each predicted isoform from the NCBI database and imported into SerialCloner v.2.1. Sequences were aligned using the Local align feature and then scanned by eye to identify the start and stop of each open reading frame.

APPENDIX B

ECM DEFECTS MAY NOT BE SUFFICIENT TO INDUCE RE-EPITHELIALIZATION DEFECTS

Introduction

Often thought of as a static extracellular structure, the ECM plays an important role in facilitating cell mobility and regulating signaling events during development, inflammation, and repair processes (Dobaczewski et al., 2010; Kirmse et al., 2011a; Wang et al., 2008). Similar to vertebrates, the basement membrane in *Drosophila* is composed of primarily type IV collagen, laminin, an entactin, Nidogen, and a heparan-sulfate proteoglycan, Perlecan (Pcan), (Fessler and Fessler, 1989). Type IV collagen forms heterotrimers between a combination of two subfamilies, α1-like, encoded by *Collagen at 25C* (*Cg25C*) in *Drosophila*, and α2-like, encoded by *Viking* (*Vkg*) (Le Parco et al., 1986; Yasothornsrikul et al., 1997). Perlecan is encoded by *trol* in *Drosophila*, which has previously been shown to be expressed in hemocytes (Lin, 2004; Lindner et al., 2007), and our previous studies suggest that Pcan may be produced by the epidermis (Chapter V). *Trol* has been shown to be involved in several growth factor signaling pathways, including PDGF/VEGF, and when mutated results in a decreased number of circulating plasmatocytes (Lindner et al., 2007), both of which are phenotypes that could lead to impaired wound healing. However, in this

appendix, we report that ECM defects may not be sufficient to induce re-epithelialization defects.

Methods

Fly lines.

The following lines from the Vienna Drosophila RNAi center (VDRC) were used: *UAS-Vkg-dsRNA* (VDRC transformant 106812), *UAS-Cg25C-dsRNA* (VDRC transformants 104536 and 28369), *UAS-trol-dsRNA* (VDRC transformants 22642 and 24549). Other fly lines used were *A58-Gal4* (M. Galko), and *Hml-Gal4, UAS-eGFP* (J. Royet), and *C564-GAL4* (FlybaseID FBst0006982). w^{1118} was used as wild type.

Wounding assay and immunohistochemistry.

The wounding assay follows the protocol described in Stevens and Page-McCaw (2012). Wounded animals were collected 18h post-wounding for wound closure analysis. Dissections, fixation, and immunohistochemistry was done according to protocol described in Stevens and Page-McCaw (2012). Primary antibodys used were mouse monoclonal IgG2a anti-FasIII (DSHB) used at 1:10 and a 1:1 cocktail of mouse monoclonal IgG1 ant Mmp1 clones 5H7 and 3B8 (DSHB) used at 1:100. Secondary antibodies used were Cy3-labeled goat anti-mouse IgG1 (Jackson Immuno) and DyeLight 649-labeled goat anti-mouse IgG2a

(Jackson Immuno) both used at 1:300. Tissue was mounted onto slides in Vectashield mounting media + DAPI.

Microscopy.

Optical sectioning was performed with a Zeiss Apotome mounted on an Axio imager Z1 or M2, with the 20X/0.8 Plan-Apochromat objective. Fluorescent images were acquired with an Axiocam MRm (Zeiss) camera paired with Axiovision 4.8 (Zeiss). Z-stacks were compressed into 2-deminsional XY projections using the Orthoview function in Axiovision. All images were exported from their acquisition programs as 16-bit, grayscale, TIFF files for post-processing in Adobe Photoshop CS4, or ImageJ v.1.43u.

Wound area measurements.

Closure and wound area were assessed based on the presence of both FasIII staining at cell borders and epidermal polyploid nuclei as stained with DAPI. To calculate wound area, the outline tool in Axiovision (Zeiss) was used to manually outline the wound edge. This feature automatically calculates the area of the outlined region using image acquisition specifications. Statstical anaylses were performed with the analysis tools available in GraphPad Prism v. 5.01 to

compare mutant and wild-type wound area by One-way ANOVA. Error bars represent the standard error of the mean.

Results and Discussion

We have previously reported that *Mmp1* is required for both wound healing and deposition of ECM components into the basement membrane (Stevens and Page-McCaw, 2012) and we hypothesized that the re-epithelialization defects are secondary to the ECM defects that we observe in *Mmp1* mutants. To test this hypothesis, we knocked-down expression of *trol*, *Cg25C*, or *Vkg* using double-stranded RNA constructs. There is some debate over which tissue, epidermis, hemocyte, or fat body, is important for the production of ECM components (Bunt et al., 2010; Lin, 2004; Pastor-Pareja and Xu, 2011b), so we utilized three different drivers to knockdown expression in the hemocytes with *Hemolectin-GAL4* (*Hml-GAL4*), the epidermis with *A58-GAL4*, or the fat body with *C564-GAL4*. To assess re-epithelialization ability, wound area was measured 18h post-wounding. In wild type larvae 18h post-wounding, wounds have closed in 84% of animals tested (Fig. B.1A-C). When Cg25C, or α1-like collagen IV, is knocked down using a *UAS-Cg25C-dsRNA* construct expressed specifically in the fat body (*C564>Cg25C-dsRNA*) wounds remained open in 2 out of 3 (67%) animals tested, with a wound area that is not significantly larger than wild type 18h post-wounding (Fig. B.1A-A'). These

preliminary data suggest that Cg25C expression in the fat body is not required for re-epithelialization. When we knocked down Cg25C in either the hemocytes (*Hml>Cg25C-dsRNA*), or in the epidermis (*A58>Cg25C-dsRNAi*), however, wounds remained open in 2 of 4 (50%), and 2 of 3 (67%), respectively (Fig. B.1A), but there was no significant difference in wound area between mutant and wild type 18h post-wounding (Fig. B.1A'). When we knocked down Vkg, or α2-like collagen IV, with the three drivers, wounds closed in 2 of 2 (100%) *C564>Vkg-dsRNA* mutants, while wounds remained open in 4 of 7 (57%) *Hml>Vkg-dsRNA* and 2 of 4 (50%) *A58>Vkg-dsRNA* mutants 18h post-wounding (Fig. B.1B). In *Vkg-dsRNA* mutant backgrounds, there was no significant difference in average wound area 18h post-wounding between mutant and wild type (Fig. B.1B'), suggesting that tissue-specific knockdown of *Vkg* is not sufficient to cause re-epithelialization defects. Similarly, interfering with *trol* expression had no effect on re-epithelialization in 2 of 2 (100%) *C564>trol-dsRNA* mutants, but caused wounds to remain open in 2 of 6 (33%) *Hml>trol-dsRNA* and 2 of 5 (40%) *A58>trol-dsRNA* mutants 18h post-wounding (Fig B.1C); in all *trol-dsRNA* mutants backgrounds there was no significant difference in wound area 18h post-wounding relative to wild type (Fig. B.1C'). Together, these results suggest that tissue-specific knockdown of *trol* is not sufficient to cause re-epithelialization defects.

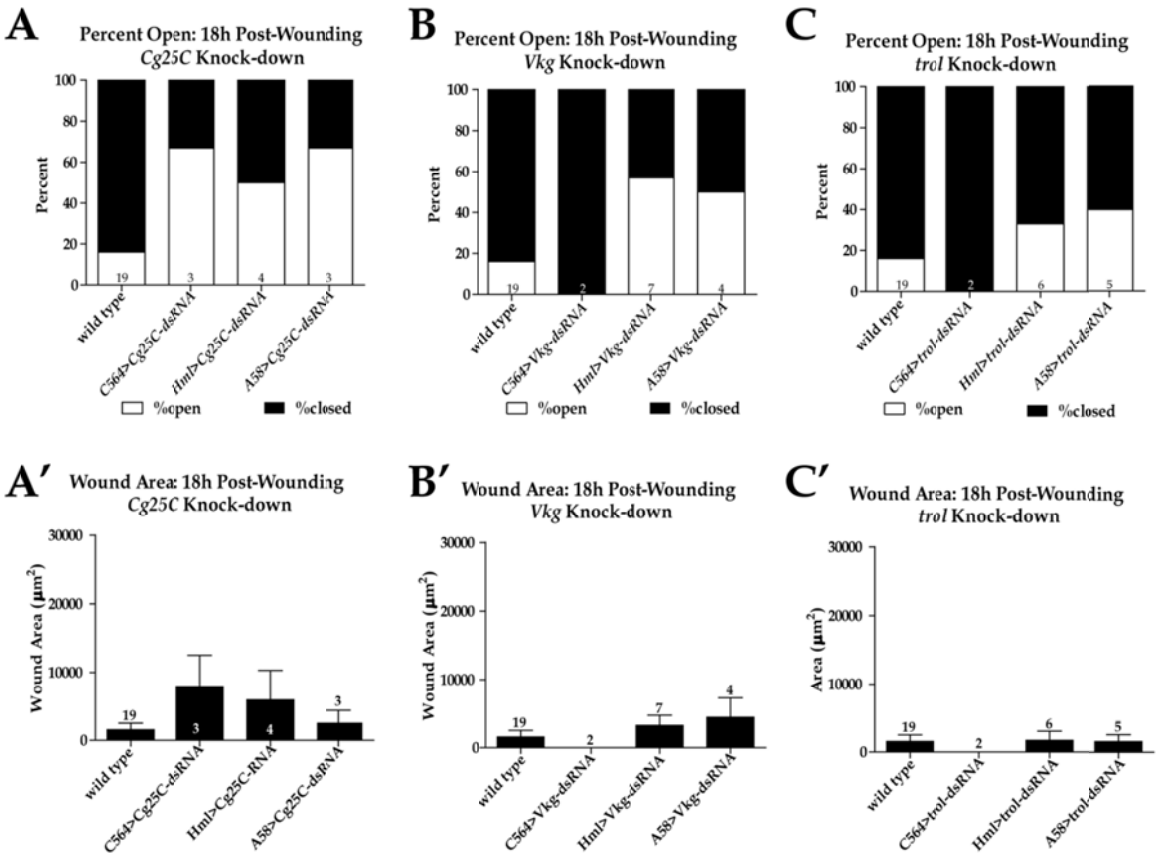

Figure B.1: ECM defects may not be sufficient to cause re-epithelialization defects.
A-C) Graphs showing percent of wounds that are open (white) versus closed (black) 18h post-wounding in tissue-specific knock-down of *Cg25C* (A), *Vkg* (B), and *trol* (C). **A′-C′)** Graph of wound area 18h post-wounding in designated genotypes. There is no significant difference in wound area at 18h post-wounding in any mutant background relative to wild type by One-way ANOVA. All *Cg25C* and *Trol* mutant data represents the combination of two independent dsRNA constructs for each gene. Numbers on each bar indicate the number of wounded animals tested in each group. Error bars indicate the standard error of the mean.

Based on these preliminary results, ECM defects may not be sufficient to cause re-epithelialization defects, undermining our hypothesis that the re-epithelialization defects observed in *Mmp1* mutants are a secondary to the ECM remodeling defects that we observe in this mutant background. However, as these are preliminary results, there are several questions that need to be addresses before conclusions can really be drawn. First, the efficiency of our

RNAi lines needs to be confirmed. Two independent UAS-*Cg25C-dsRNA* and *UAS-trol-dsRNA* lines used for the re-epithelialization experiments, with equivalent results, which suggest that we are not observing off-target effects, but we have not measured, by qPCR, the amount of *CG25C* or *trol* knockdown that we actually obtained. It is plausible that the dsRNA constructs that we used do not cause sufficient expression knockdown to produce a phenotype. When these experiments were performed, there was only one *UAS-Vkg-dsRNA* line available, so we were not able to control for off-target effects, and like the other ECM RNAi lines, the efficacy of *Vkg* expression interference induced by this *UAS-Vkg-dsRNA* line was not measured. Assuming that these RNAi lines cause significant expression knockdown and do not have off-target effects, it is also possible that knocking down either *Vkg*, *Cg25C*, or *trol* in just one tissue is not enough to induce a basement membrane defects, this experiment assumes that ECM components are only produced from one tissue source, but it is possible that either multiple tissues contribute to basement membrane production, or other tissue are able to compensate for loss of ECM component expression from a primary source, by producing and secreting the necessary ECM component. We could test this hypothesis by driving *Cg25C-dsRNA*, *Vkg-dsRNA*, or *Trol-dsRNA* with a more ubiquitous driver, such as *tubulin-GAL4* (*Tub-GAL4*), eliminating the need to know specifically which tissue is required for basement membrane production. The finding that ECM defects may not lead to re-epithelialization defects post-wounding is surprising and more research is required both to

confirm this result, as well as to determine the specific role of the basement membrane during wound healing.

REFERENCES

Abe, R., S.C. Donnelly, T. Peng, R. Bucala, and C.N. Metz. 2001. Peripheral blood fibrocytes: differentiation pathway and migration to wound sites. *Journal of immunology*. 166:7556-7562.

Allan, J.A., A.J. Docherty, P.J. Barker, N.S. Huskisson, J.J. Reynolds, and G. Murphy. 1995. Binding of gelatinases A and B to type-I collagen and other matrix components. *The Biochemical journal*. 309 (Pt 1):299-306.

Ando, B., T. Wiedmer, K.K. Hamilton, and P.J. Sims. 1988. Complement proteins C5b-9 initiate secretion of platelet storage granules without increased binding of fibrinogen or von Willebrand factor to newly expressed cell surface GPIIb-IIIa. *The Journal of biological chemistry*. 263:11907-11914.

Babcock, D.T., A.R. Brock, G.S. Fish, Y. Wang, L. Perrin, M.A. Krasnow, and M.J. Galko. 2008. Circulating blood cells function as a surveillance system for damaged tissue in Drosophila larvae. *Proc Natl Acad Sci U S A*. 105:10017-10022.

Bai, S., R. Thummel, A.R. Godwin, H. Nagase, Y. Itoh, L. Li, R. Evans, J. McDermott, M. Seiki, and M.P. Sarras, Jr. 2005. Matrix metalloproteinase expression and function during fin regeneration in zebrafish: analysis of MT1-MMP, MMP2 and TIMP2. *Matrix biology : journal of the International Society for Matrix Biology*. 24:247-260.

Baker, K.D., and C.S. Thummel. 2007. Diabetic larvae and obese flies-emerging studies of metabolism in Drosophila. *Cell Metab*. 6:257-266.

Barrientos, S., O. Stojadinovic, M.S. Golinko, H. Brem, and M. Tomic-Canic. 2008. Growth factors and cytokines in wound healing. *Wound repair and regeneration : official publication of the Wound Healing Society [and] the European Tissue Repair Society*. 16:585-601.

Beaucher, M., E. Hersperger, A. Page-McCaw, and A. Shearn. 2007a. Metastatic ability of Drosophila tumors depends on MMP activity. *Dev Biol*. 303:625-634.

Beaucher, M., E. Hersperger, A. Page-McCaw, and A. Shearn. 2007b. Metastatic ability of Drosophila tumors depends on MMP activity. *Developmental biology*. 303:625-634.

Bergers, G., R. Brekken, G. McMahon, T.H. Vu, T. Itoh, K. Tamaki, K. Tanzawa, P. Thorpe, S. Itohara, Z. Werb, and D. Hanahan. 2000. Matrix metalloproteinase-9 triggers the angiogenic switch during carcinogenesis. *Nat Cell Biol*. 2:737-744.

Bidla, G., M. Lindgren, U. Theopold, and M.S. Dushay. 2005. Hemolymph coagulation and phenoloxidase in Drosophila larvae. *Dev Comp Immunol*. 29:669-679.

Bode, W., F.X. Gomis-Ruth, and W. Stockler. 1993. Astacins, serralysins, snake venom and matrix metalloproteinases exhibit identical zinc-binding environments (HEXXHXXGXXH and Met-turn) and topologies and should be grouped into a common family, the 'metzincins'. *FEBS letters*. 331:134-140.

Brancato, S.K., and J.E. Albina. 2011. Wound macrophages as key regulators of repair: origin, phenotype, and function. *Am J Pathol*. 178:19-25.

Brandt, E., F. Petersen, A. Ludwig, J.E. Ehlert, L. Bock, and H.D. Flad. 2000. The beta-thromboglobulins and platelet factor 4: blood platelet-derived CXC chemokines with divergent roles in early neutrophil regulation. *J Leukoc Biol*. 67:471-478.

Braun, A., J.A. Hoffmann, and M. Meister. 1998. Analysis of the Drosophila host defense in domino mutant larvae, which are devoid of hemocytes. *Proc Natl Acad Sci U S A*. 95:14337-14342.

Brenner, D.A., M. O'Hara, P. Angel, M. Chojkier, and M. Karin. 1989. Prolonged activation of jun and collagenase genes by tumour necrosis factor-alpha. *Nature*. 337:661-663.

Brew, K., and H. Nagase. 2010. The tissue inhibitors of metalloproteinases (TIMPs): an ancient family with structural and functional diversity. *Biochimica et biophysica acta*. 1803:55-71.

Brockes, J.P., and A. Kumar. 2002. Plasticity and reprogramming of differentiated cells in amphibian regeneration. *Nature reviews. Molecular cell biology*. 3:566-574.

Broughton, G., 2nd, J.E. Janis, and C.E. Attinger. 2006. A brief history of wound care. *Plast Reconstr Surg*. 117:6S-11S.

Bucala, R., L.A. Spiegel, J. Chesney, M. Hogan, and A. Cerami. 1994. Circulating fibrocytes define a new leukocyte subpopulation that mediates tissue repair. *Mol Med*. 1:71-81.

Bullard, K.M., M.T. Longaker, and H.P. Lorenz. 2003. Fetal wound healing: current biology. *World J Surg*. 27:54-61.

Bullard, K.M., L. Lund, J.S. Mudgett, T.N. Mellin, T.K. Hunt, B. Murphy, J. Ronan, Z. Werb, and M.J. Banda. 1999a. Impaired wound contraction in stromelysin-1-deficient mice. *Ann Surg*. 230:260-265.

Bullard, K.M., L. Lund, J.S. Mudgett, T.N. Mellin, T.K. Hunt, B. Murphy, J. Ronan, Z. Werb, and M.J. Banda. 1999b. Impaired wound contraction in stromelysin-1-deficient mice. *Ann Surg*. 230:260-265.

Bunt, S., C. Hooley, N. Hu, C. Scahill, H. Weavers, and H. Skaer. 2010. Hemocyte-secreted type IV collagen enhances BMP signaling to guide renal tubule morphogenesis in Drosophila. *Developmental cell*. 19:296-306.

Burrage, P.S., K.S. Mix, and C.E. Brinckerhoff. 2006. Matrix metalloproteinases: role in arthritis. *Front Biosci*. 11:529-543.

Butler, G.S., M.J. Butler, S.J. Atkinson, H. Will, T. Tamura, S. Schade van Westrum, T. Crabbe, J. Clements, M.P. d'Ortho, and G. Murphy. 1998. The TIMP2 membrane type 1 metalloproteinase "receptor" regulates the concentration and efficient activation of progelatinase A. A kinetic study. *The Journal of biological chemistry*. 273:871-880.

Cao, J., A. Rehemtulla, W. Bahou, and S. Zucker. 1996. Membrane type matrix metalloproteinase 1 activates pro-gelatinase A without furin cleavage of the N-terminal domain. *The Journal of biological chemistry*. 271:30174-30180.

Cavani, A., G. Zambruno, A. Marconi, V. Manca, M. Marchetti, and A. Giannetti. 1993. Distinctive integrin expression in the newly forming epidermis during wound healing in humans. *The Journal of investigative dermatology*. 101:600-604.

Cerenius, L., and K. Soderhall. 2004. The prophenoloxidase-activating system in invertebrates. *Immunol Rev*. 198:116-126.

Chesney, J., C. Metz, A.B. Stavitsky, M. Bacher, and R. Bucala. 1998. Regulated production of type I collagen and inflammatory cytokines by peripheral blood fibrocytes. *Journal of immunology*. 160:419-425.

Choi, W.S., O.H. Jeon, H.H. Kim, and D.S. Kim. 2008. MMP-2 regulates human platelet activation by interacting with integrin alphaIIbbeta3. *J Thromb Haemost*. 6:517-523.

Coover, H.N., Joyner, F.B., Sheerer,N.H. ,Wicker, T.H. 1959. Chemistry and performance of cyanoacrylate adhesive. *J Soc Plast Surg Engl*. 15:5-6.

Crozatier, M., J.M. Ubeda, A. Vincent, and M. Meister. 2004. Cellular immune response to parasitization in Drosophila requires the EBF orthologue collier. *PLoS biology*. 2:E196.

Daley, J.M., S.K. Brancato, A.A. Thomay, J.S. Reichner, and J.E. Albina. 2010. The phenotype of murine wound macrophages. *J Leukoc Biol*. 87:59-67.

De Gregorio, E., S.J. Han, W.J. Lee, M.J. Baek, T. Osaki, S. Kawabata, B.L. Lee, S. Iwanaga, B. Lemaitre, and P.T. Brey. 2002. An immune-responsive Serpin regulates the melanization cascade in Drosophila. *Dev Cell*. 3:581-592.

Desmouliere, A. 1995. Factors influencing myofibroblast differentiation during wound healing and fibrosis. *Cell biology international*. 19:471-476.

Discher, D.E., P. Janmey, and Y.-L. Wang. 2005a. Tissue cells feel and respond to the stiffness of their substrate. *Science (New York, N.Y.)*. 310:1139-1143.

Discher, D.E., P. Janmey, and Y.L. Wang. 2005b. Tissue cells feel and respond to the stiffness of their substrate. *Science*. 310:1139-1143.

Dobaczewski, M., C. Gonzalez-Quesada, and N.G. Frangogiannis. 2010. The extracellular matrix as a modulator of the inflammatory and reparative response following myocardial infarction. *Journal of molecular and cellular cardiology*. 48:504-511.

Doehn, U., C. Hauge, S.R. Frank, C.J. Jensen, K. Duda, J.V. Nielsen, M.S. Cohen, J.V. Johansen, B.R. Winther, L.R. Lund, O. Winther, J. Taunton, S.H. Hansen, and M. Fr√∂din. 2009a. RSK Is a Principal Effector of the RAS-ERK Pathway for Eliciting a Coordinate Promotile/Invasive Gene Program and Phenotype in Epithelial Cells. *Molecular Cell*. 35:511-522.

Doehn, U., C. Hauge, S.R. Frank, C.J. Jensen, K. Duda, J.V. Nielsen, M.S. Cohen, J.V. Johansen, B.R. Winther, L.R. Lund, O. Winther, J. Taunton, S.H. Hansen, and M. Frodin. 2009b. RSK is a principal effector of the RAS-ERK pathway for eliciting a coordinate promotile/invasive gene program and phenotype in epithelial cells. *Molecular cell*. 35:511-522.

Dovi, J.V., L.K. He, and L.A. DiPietro. 2003. Accelerated wound closure in neutrophil-depleted mice. *J Leukoc Biol*. 73:448-455.

Egeblad, M., and Z. Werb. 2002a. New functions for the matrix metalloproteinases in cancer progression. *Nature reviews. Cancer*. 2:161-174.

Egeblad, M., and Z. Werb. 2002b. New functions for the matrix metalloproteinases in cancer progression. *Nature Rev Cancer*. 2:161-174.

Eming, S.A., T. Krieg, and J.M. Davidson. 2007. Inflammation in wound repair: molecular and cellular mechanisms. *J Invest Dermatol*. 127:514-525.

Engelhardt, E., A. Toksoy, M. Goebeler, S. Debus, E.B. Brocker, and R. Gillitzer. 1998. Chemokines IL-8, GROalpha, MCP-1, IP-10, and Mig are

sequentially and differentially expressed during phase-specific infiltration of leukocyte subsets in human wound healing. *Am J Pathol*. 153:1849-1860.

Fernandez-Catalan, C., W. Bode, R. Huber, D. Turk, J.J. Calvete, A. Lichte, H. Tschesche, and K. Maskos. 1998. Crystal structure of the complex formed by the membrane type 1-matrix metalloproteinase with the tissue inhibitor of metalloproteinases-2, the soluble progelatinase A receptor. *The EMBO journal*. 17:5238-5248.

Fessler, J.H., and L.I. Fessler. 1989. Drosophila extracellular matrix. *Annu Rev Cell Biol*. 5:309-339.

Fessler, L.I., R.E. Nelson, and J.H. Fessler. 1994. Drosophila extracellular matrix. *Methods in enzymology*. 245:271-294.

Franc, N.C., J.L. Dimarcq, M. Lagueux, J. Hoffmann, and R.A. Ezekowitz. 1996. Croquemort, a novel Drosophila hemocyte/macrophage receptor that recognizes apoptotic cells. *Immunity*. 4:431-443.

Franc, N.C., P. Heitzler, R.A. Ezekowitz, and K. White. 1999. Requirement for croquemort in phagocytosis of apoptotic cells in Drosophila. *Science*. 284:1991-1994.

Friedrich, M.V., M. Schneider, R. Timpl, and S. Baumgartner. 2000. Perlecan domain V of Drosophila melanogaster. Sequence, recombinant analysis and tissue expression. *European journal of biochemistry / FEBS*. 267:3149-3159.

Furie, B., and B.C. Furie. 1992. Molecular and cellular biology of blood coagulation. *The New England journal of medicine*. 326:800-806.

Gabay, L., R. Seger, and B.Z. Shilo. 1997. In situ activation pattern of Drosophila EGF receptor pathway during development. *Science*. 277:1103-1106.

Gajewski, K.M., R.P. Sorrentino, J.H. Lee, Q. Zhang, M. Russell, and R.A. Schulz. 2007. Identification of a crystal cell-specific enhancer of the black cells prophenoloxidase gene in Drosophila. *Genesis*. 45:200-207.

Galko, M.J., and M.A. Krasnow. 2004a. Cellular and genetic analysis of wound healing in Drosophila larvae. *PLoS biology*. 2:E239.

Galko, M.J., and M.A. Krasnow. 2004b. Cellular and genetic analysis of wound healing in Drosophila larvae. *PLoS Biol*. 2:E239.

Gearing, A., P. Beckett, M. Christodoulou, M. Churchill, J. Clements, M. Crimmin, A. Davidson, A. Drummond, W. Galloway, R. Gilbert, and a. et. 1995. Matrix metalloproteinases and processing of pro-TNF-alpha. *J Leukoc Biol*. 57:774-777.

Gilbert, G.E., P.J. Sims, T. Wiedmer, B. Furie, B.C. Furie, and S.J. Shattil. 1991. Platelet-derived microparticles express high affinity receptors for factor VIII. *The Journal of biological chemistry*. 266:17261-17268.

Gill, S.E., S.Y. Kassim, T.P. Birkland, and W.C. Parks. 2010. Mouse models of MMP and TIMP function. *Methods Mol Biol*. 622:31-52.

Gill, S.E., and W.C. Parks. 2008. Metalloproteinases and their inhibitors: regulators of wound healing. *Int J Biochem Cell Biol*. 40:1334-1347.

Gillitzer, R., and M. Goebeler. 2001. Chemokines in cutaneous wound healing. *J Leukoc Biol*. 69:513-521.

Gipson, I.K., S.J. Spurr-Michaud, and A.S. Tisdale. 1988. Hemidesmosomes and anchoring fibril collagen appear synchronously during development and wound healing. *Developmental biology*. 126:253-262.

Glasheen, B.M., A.T. Kabra, and A. Page-McCaw. 2009a. Distinct functions for the catalytic and hemopexin domains of a Drosophila matrix metalloproteinase. *Proceedings of the National Academy of Sciences of the United States of America*. 106:2659-2664.

Glasheen, B.M., A.T. Kabra, and A. Page-McCaw. 2009b. Distinct functions for the catalytic and hemopexin domains of a Drosophila matrix metalloproteinase. *Proc Natl Acad Sci U S A*. 106:2659-2664.

Glasheen, B.M., R.M. Robbins, C. Piette, G.J. Beitel, and A. Page-McCaw. 2010a. A matrix metalloproteinase mediates airway remodeling in Drosophila. *Dev Biol*. 344:772-783.

Glasheen, B.M., R.M. Robbins, C. Piette, G.J. Beitel, and A. Page-McCaw. 2010b. A matrix metalloproteinase mediates airway remodeling in Drosophila. *Developmental biology*. 344:772-783.

Godenschwege, T.A., N. Pohar, S. Buchner, and E. Buchner. 2000a. Inflated wings, tissue autolysis and early death in tissue inhibitor of metalloproteinases mutants of Drosophila. *Eur J Cell Biol*. 79:495-501.

Godenschwege, T.A., N. Pohar, S. Buchner, and E. Buchner. 2000b. Inflated wings, tissue autolysis and early death in tissue inhibitor of metalloproteinases mutants of Drosophila. *European journal of cell biology*. 79:495-501.

Goldberg, G.I., A. Strongin, I.E. Collier, L.T. Genrich, and B.L. Marmer. 1992. Interaction of 92-kDa type IV collagenase with the tissue inhibitor of metalloproteinases prevents dimerization, complex formation with interstitial collagenase, and activation of the proenzyme with stromelysin. *The Journal of biological chemistry*. 267:4583-4591.

Goldberg, S.R., and R.F. Diegelmann. 2010. Wound healing primer. *Surg Clin North Am*. 90:1133-1146.

Gomis-Ruth, F.X., K. Maskos, M. Betz, A. Bergner, R. Huber, K. Suzuki, N. Yoshida, H. Nagase, K. Brew, G.P. Bourenkov, H. Bartunik, and W. Bode. 1997. Mechanism of inhibition of the human matrix metalloproteinase stromelysin-1 by TIMP-1. *Nature*. 389:77-81.

Goto, A., T. Kadowaki, and Y. Kitagawa. 2003. Drosophila hemolectin gene is expressed in embryonic and larval hemocytes and its knock down causes bleeding defects. *Developmental biology*. 264:582-591.

Goto, A., T. Kumagai, C. Kumagai, J. Hirose, H. Narita, H. Mori, T. Kadowaki, K. Beck, and Y. Kitagawa. 2001. A Drosophila haemocyte-specific protein,

hemolectin, similar to human von Willebrand factor. *The Biochemical journal*. 359:99-108.

Goyal, L., K. McCall, J. Agapite, E. Hartwieg, and H. Steller. 2000. Induction of apoptosis by Drosophila reaper, hid and grim through inhibition of IAP function. *The EMBO journal*. 19:589-597.

Grinnell, F. 1994. Fibroblasts, myofibroblasts, and wound contraction. *The Journal of cell biology*. 124:401-404.

Guha, A., L. Lin, and T.B. Kornberg. 2009. Regulation of Drosophila matrix metalloprotease Mmp2 is essential for wing imaginal disc:trachea association and air sac tubulogenesis. *Developmental biology*. 335:317-326.

Guinea-Viniegra, J., R. Zenz, H. Scheuch, D. Hnisz, M. Holcmann, L. Bakiri, H.B. Schonthaler, M. Sibilia, and E.F. Wagner. 2009. TNFalpha shedding and epidermal inflammation are controlled by Jun proteins. *Genes & development*. 23:2663-2674.

Gum, R., H. Wang, E. Lengyel, J. Juarez, and D. Boyd. 1997. Regulation of 92 kDa type IV collagenase expression by the jun aminoterminal kinase- and the extracellular signal-regulated kinase-dependent signaling cascades. *Oncogene*. 14:1481-1493.

Gurtner, G.C., S. Werner, Y. Barrandon, and M.T. Longaker. 2008. Wound repair and regeneration. *Nature*. 453:314-321.

Gutierrez-Fernandez, A., M. Inada, M. Balbin, A. Fueyo, A.S. Pitiot, A. Astudillo, K. Hirose, M. Hirata, S.D. Shapiro, A. Noel, Z. Werb, S.M. Krane, C. Lopez-Otin, and X.S. Puente. 2007a. Increased inflammation delays wound healing in mice deficient in collagenase-2 (MMP-8). *The FASEB journal : official publication of the Federation of American Societies for Experimental Biology*. 21:2580-2591.

Gutierrez-Fernandez, A., M. Inada, M. Balbin, A. Fueyo, A.S. Pitiot, A. Astudillo, K. Hirose, M. Hirata, S.D. Shapiro, A. Noel, Z. Werb, S.M. Krane, C. Lopez-Otin, and X.S. Puente. 2007b. Increased inflammation delays

wound healing in mice deficient in collagenase-2 (MMP-8). *FASEB J*. 21:2580-2591.

Hartenstein, B., B.T. Dittrich, D. Stickens, B. Heyer, T.H. Vu, S. Teurich, M. Schorpp-Kistner, Z. Werb, and P. Angel. 2006. Epidermal development and wound healing in matrix metalloproteinase 13-deficient mice. *The Journal of investigative dermatology*. 126:486-496.

Hartlapp, I., R. Abe, R.W. Saeed, T. Peng, W. Voelter, R. Bucala, and C.N. Metz. 2001. Fibrocytes induce an angiogenic phenotype in cultured endothelial cells and promote angiogenesis in vivo. *The FASEB journal : official publication of the Federation of American Societies for Experimental Biology*. 15:2215-2224.

Hattori, N., S. Mochizuki, K. Kishi, T. Nakajima, H. Takaishi, J. D'Armiento, and Y. Okada. 2009a. MMP-13 plays a role in keratinocyte migration, angiogenesis, and contraction in mouse skin wound healing. *Am J Pathol*. 175:533-546.

Hattori, N., S. Mochizuki, K. Kishi, T. Nakajima, H. Takaishi, J. D'Armiento, and Y. Okada. 2009b. MMP-13 plays a role in keratinocyte migration, angiogenesis, and contraction in mouse skin wound healing. *Am J Pathol*. 175:533-546.

Hebda, P.A., M.A. Collins, and M.D. Tharp. 1993. Mast cell and myofibroblast in wound healing. *Dermatol Clin*. 11:685-696.

Helman, A., and Z. Paroush. 2010. Detection of RTK pathway activation in Drosophila using anti-dpERK immunofluorescence staining. *Methods Mol Biol*. 661:401-408.

Hess, C.T., and R.S. Kirsner. 2003. Orchestrating wound healing: assessing and preparing the wound bed. *Adv Skin Wound Care*. 16:246-257; quiz 258-249.

Hiller, O., A. Lichte, A. Oberpichler, A. Kocourek, and H. Tschesche. 2000. Matrix metalloproteinases collagenase-2, macrophage elastase, collagenase-3, and membrane type 1-matrix metalloproteinase impair clotting by degradation

of fibrinogen and factor XII. *The Journal of biological chemistry*. 275:33008-33013.

Holmbeck, K., P. Bianco, J. Caterina, S. Yamada, M. Kromer, S.A. Kuznetsov, M. Mankani, P.G. Robey, A.R. Poole, I. Pidoux, J.M. Ward, and H. Birkedal-Hansen. 1999. MT1-MMP-deficient mice develop dwarfism, osteopenia, arthritis, and connective tissue disease due to inadequate collagen turnover. *Cell*. 99:81-92.

Hotary, K., X.Y. Li, E. Allen, S.L. Stevens, and S.J. Weiss. 2006. A cancer cell metalloprotease triad regulates the basement membrane transmigration program. *Genes & development*. 20:2673-2686.

Hynes, R.O. 2002. Integrins: bidirectional, allosteric signaling machines. *Cell*. 110:673-687.

Hynes, R.O., and Q. Zhao. 2000. The evolution of cell adhesion. *J Cell Biol*. 150:F89-96.

Igaki, T., H. Kanda, H. Okano, T. Xu, and M. Miura. 2011. Eiger and wengen: the Drosophila orthologs of TNF/TNFR. *Adv Exp Med Biol*. 691:45-50.

Igaki, T., H. Kanda, Y. Yamamoto-Goto, H. Kanuka, E. Kuranaga, T. Aigaki, and M. Miura. 2002a. Eiger, a TNF superfamily ligand that triggers the Drosophila JNK pathway. *The EMBO journal*. 21:3009-3018.

Igaki, T., H. Kanda, Y. Yamamoto-Goto, H. Kanuka, E. Kuranaga, T. Aigaki, and M. Miura. 2002b. Eiger, a TNF superfamily ligand that triggers the Drosophila JNK pathway. *EMBO J*. 21:3009-3018.

Igaki, T., J.C. Pastor-Pareja, H. Aonuma, M. Miura, and T. Xu. 2009. Intrinsic tumor suppression and epithelial maintenance by endocytic activation of Eiger/TNF signaling in Drosophila. *Dev Cell*. 16:458-465.

Imai, K., E. Ohuchi, T. Aoki, H. Nomura, Y. Fujii, H. Sato, M. Seiki, and Y. Okada. 1996. Membrane-type matrix metalloproteinase 1 is a gelatinolytic

enzyme and is secreted in a complex with tissue inhibitor of metalloproteinases 2. *Cancer Res*. 56:2707-2710.

Ingvarsen, S., D.H. Madsen, T. Hillig, L.R. Lund, K. Holmbeck, N. Behrendt, and L.H. Engelholm. 2008. Dimerization of endogenous MT1-MMP is a regulatory step in the activation of the 72-kDa gelatinase MMP-2 on fibroblasts and fibrosarcoma cells. *Biol Chem*. 389:943-953.

Itoh, Y., A. Takamura, N. Ito, Y. Maru, H. Sato, N. Suenaga, T. Aoki, and M. Seiki. 2001. Homophilic complex formation of MT1-MMP facilitates proMMP-2 activation on the cell surface and promotes tumor cell invasion. *The EMBO journal*. 20:4782-4793.

Juhasz, I., G.F. Murphy, H.C. Yan, M. Herlyn, and S.M. Albelda. 1993. Regulation of extracellular matrix proteins and integrin cell substratum adhesion receptors on epithelium during cutaneous human wound healing in vivo. *Am J Pathol*. 143:1458-1469.

Kauppila, S., W.S. Maaty, P. Chen, R.S. Tomar, M.T. Eby, J. Chapo, S. Chew, N. Rathore, S. Zachariah, S.K. Sinha, J.M. Abrams, and P.M. Chaudhary. 2003. Eiger and its receptor, Wengen, comprise a TNF-like system in Drosophila. *Oncogene*. 22:4860-4867.

Kaur, H., S.S. Chaurasia, V. Agrawal, C. Suto, and S.E. Wilson. 2009. Corneal myofibroblast viability: opposing effects of IL-1 and TGF beta1. *Exp Eye Res*. 89:152-158.

Kazes, I., I. Elalamy, J.D. Sraer, M. Hatmi, and G. Nguyen. 2000. Platelet release of trimolecular complex components MT1-MMP/TIMP2/MMP2: involvement in MMP2 activation and platelet aggregation. *Blood*. 96:3064-3069.

Kinoshita, T., H. Sato, A. Okada, E. Ohuchi, K. Imai, Y. Okada, and M. Seiki. 1998. TIMP-2 promotes activation of progelatinase A by membrane-type 1 matrix metalloproteinase immobilized on agarose beads. *The Journal of biological chemistry*. 273:16098-16103.

Kirmse, R., H. Otto, and T. Ludwig. 2011a. Interdependency of cell adhesion, force generation and extracellular proteolysis in matrix remodeling. *Journal of cell science*. 124:1857-1866.

Kirmse, R., H. Otto, and T. Ludwig. 2011b. Interdependency of cell adhesion, force generation and extracellular proteolysis in matrix remodeling. *Journal of Cell Science*. 124:1857-1866.

Koshikawa, N., S. Schenk, G. Moeckel, A. Sharabi, K. Miyazaki, H. Gardner, R. Zent, and V. Quaranta. 2004. Proteolytic processing of laminin-5 by MT1-MMP in tissues and its effects on epithelial cell morphology. *FASEB J*. 18:364-366.

Krampert, M., W. Bloch, T. Sasaki, P. Bugnon, T. Rulicke, E. Wolf, M. Aumailley, W.C. Parks, and S. Werner. 2004. Activities of the matrix metalloproteinase stromelysin-2 (MMP-10) in matrix degradation and keratinocyte organization in wounded skin. *Molecular Biology of the Cell*. 15:5242-5254.

Kreider, T., R.M. Anthony, J.F. Urban, Jr., and W.C. Gause. 2007. Alternatively activated macrophages in helminth infections. *Curr Opin Immunol*. 19:448-453.

Krummel, T.M., J.M. Nelson, R.F. Diegelmann, W.J. Lindblad, A.M. Salzberg, L.J. Greenfield, and I.K. Cohen. 1987. Fetal response to injury in the rabbit. *J Pediatr Surg*. 22:640-644.

Kurucz, E., B. Vaczi, R. Markus, B. Laurinyecz, P. Vilmos, J. Zsamboki, K. Csorba, E. Gateff, D. Hultmark, and I. Ando. 2007. Definition of Drosophila hemocyte subsets by cell-type specific antigens. *Acta Biol Hung*. 58 Suppl:95-111.

Kuzuya, M., S. Kanda, T. Sasaki, N. Tamaya-Mori, X.W. Cheng, T. Itoh, S. Itohara, and A. Iguchi. 2003. Deficiency of gelatinase a suppresses smooth muscle cell invasion and development of experimental intimal hyperplasia. *Circulation*. 108:1375-1381.

Kyriakides, T.R., D. Wulsin, E.A. Skokos, P. Fleckman, A. Pirrone, J.M. Shipley, R.M. Senior, and P. Bornstein. 2009a. Mice that lack matrix metalloproteinase-9 display delayed wound healing associated with delayed reepithelization and disordered collagen fibrillogenesis. *Matrix Biol*. 28:65-73.

Kyriakides, T.R., D. Wulsin, E.A. Skokos, P. Fleckman, A. Pirrone, J.M. Shipley, R.M. Senior, and P. Bornstein. 2009b. Mice that lack matrix metalloproteinase-9 display delayed wound healing associated with delayed reepithelization and disordered collagen fibrillogenesis. *Matrix biology : journal of the International Society for Matrix Biology*. 28:65-73.

Lanot, R., D. Zachary, F. Holder, and M. Meister. 2001. Postembryonic hematopoiesis in Drosophila. *Developmental biology*. 230:243-257.

Larsen, E., A. Celi, G.E. Gilbert, B.C. Furie, J.K. Erban, R. Bonfanti, D.D. Wagner, and B. Furie. 1989. PADGEM protein: a receptor that mediates the interaction of activated platelets with neutrophils and monocytes. *Cell*. 59:305-312.

Larson, B.J., M.T. Longaker, and H.P. Lorenz. 2010. Scarless fetal wound healing: a basic science review. *Plast Reconstr Surg*. 126:1172-1180.

Lauffenburger, D.A., and A.F. Horwitz. 1996. Cell migration: a physically integrated molecular process. *Cell*. 84:359-369.

Le Parco, Y., J.P. Cecchini, B. Knibiehler, and C. Mirre. 1986. Characterization and expression of collagen-like genes in Drosophila melanogaster. *Biology of the cell / under the auspices of the European Cell Biology Organization*. 56:217-226.

Leclerc, V., N. Pelte, L. El Chamy, C. Martinelli, P. Ligoxygakis, J.A. Hoffmann, and J.M. Reichhart. 2006. Prophenoloxidase activation is not required for survival to microbial infections in Drosophila. *EMBO Rep*. 7:231-235.

Lehti, K., J. Lohi, M.M. Juntunen, D. Pei, and J. Keski-Oja. 2002. Oligomerization through hemopexin and cytoplasmic domains regulates the activity and

turnover of membrane-type 1 matrix metalloproteinase. *The Journal of biological chemistry*. 277:8440-8448.

Leibovich, S.J., and R. Ross. 1975. The role of the macrophage in wound repair. A study with hydrocortisone and antimacrophage serum. *Am J Pathol*. 78:71-100.

Leiper, L.J., P. Walczysko, R. Kucerova, J. Ou, L.J. Shanley, D. Lawson, J.V. Forrester, C.D. McCaig, M. Zhao, and J.M. Collinson. 2006. The roles of calcium signaling and ERK1/2 phosphorylation in a Pax6+/- mouse model of epithelial wound-healing delay. *BMC Biol*. 4:27.

Lemmon, M.A., and J. Schlessinger. 2010. Cell signaling by receptor tyrosine kinases. *Cell*. 141:1117-1134.

Levenson, S.M., E.F. Geever, L.V. Crowley, J.F. Oates, 3rd, C.W. Berard, and H. Rosen. 1965. The Healing of Rat Skin Wounds. *Ann Surg*. 161:293-308.

Levi, E., R. Fridman, H.Q. Miao, Y.S. Ma, A. Yayon, and I. Vlodavsky. 1996. Matrix metalloproteinase 2 releases active soluble ectodomain of fibroblast growth factor receptor 1. *Proc Natl Acad Sci U S A*. 93:7069-7074.

Li, Q., P.W. Park, C.L. Wilson, and W.C. Parks. 2002. Matrilysin shedding of syndecan-1 regulates chemokine mobilization and transepithelial efflux of neutrophils in acute lung injury. *Cell*. 111:635-646.

Ligoxygakis, P., N. Pelte, C. Ji, V. Leclerc, B. Duvic, M. Belvin, H. Jiang, J.A. Hoffmann, and J.M. Reichhart. 2002. A serpin mutant links Toll activation to melanization in the host defence of Drosophila. *The EMBO journal*. 21:6330-6337.

Lin, X. 2004. Functions of heparan sulfate proteoglycans in cell signaling during development. *Development*. 131:6009-6021.

Lindner, J.R., P.R. Hillman, A.L. Barrett, M.C. Jackson, T.L. Perry, Y. Park, and S. Datta. 2007. The Drosophila Perlecan gene trol regulates multiple

signaling pathways in different developmental contexts. *BMC Dev Biol*. 7:121.

Llano, E., G. Adam, A.M. Pendas, V. Quesada, L.M. Sanchez, I. Santamaria, S. Noselli, and C. Lopez-Otin. 2002. Structural and Enzymatic Characterization of Drosophila Dm2-MMP, a Membrane-bound Matrix Metalloproteinase with Tissue-specific Expression. *J. Biol. Chem.* 277:23321-23329.

Llano, E., A.M. Pendas, P. Aza-Blanc, T.B. Kornberg, and C. Lopez-Otin. 2000. Dm1-MMP, a Matrix Metalloproteinase from Drosophila with a Potential Role in Extracellular Matrix Remodeling during Neural Development. *J. Biol. Chem.* 275:35978-35985.

Luo, D., B. Mari, I. Stoll, and P. Anglard. 2002. Alternative splicing and promoter usage generates an intracellular stromelysin 3 isoform directly translated as an active matrix metalloproteinase. *The Journal of biological chemistry*. 277:25527-25536.

Luster, A.D., R. Alon, and U.H. von Andrian. 2005. Immune cell migration in inflammation: present and future therapeutic targets. *Nature immunology*. 6:1182-1190.

Majno, G. 1975. The Healing Hand: Man and Wound in the Ancient World. Harvard University Press, Cambridge, Massachusettes.

Mann, K.G., R.J. Jenny, and S. Krishnaswamy. 1988. Cofactor proteins in the assembly and expression of blood clotting enzyme complexes. *Annu Rev Biochem*. 57:915-956.

Martin-Blanco, E., A. Gampel, J. Ring, K. Virdee, N. Kirov, A.M. Tolkovsky, and A. Martinez-Arias. 1998. puckered encodes a phosphatase that mediates a feedback loop regulating JNK activity during dorsal closure in Drosophila. *Genes & development*. 12:557-570.

Martin, P. 1997. Wound healing--aiming for perfect skin regeneration. *Science*. 276:75-81.

Martin, P., D. D'Souza, J. Martin, R. Grose, L. Cooper, R. Maki, and S.R. McKercher. 2003. Wound healing in the PU.1 null mouse--tissue repair is not dependent on inflammatory cells. *Current biology : CB*. 13:1122-1128.

Martin, P., and S.J. Leibovich. 2005. Inflammatory cells during wound repair: the good, the bad and the ugly. *Trends Cell Biol*. 15:599-607.

Martin, P., and C.D. Nobes. 1992. An early molecular component of the wound healing response in rat embryos--induction of c-fos protein in cells at the epidermal wound margin. *Mechanisms of development*. 38:209-215.

Martinez Arias, A. 1993a. Development and Patterning of the Larval Epidermis of *Drosophila*. *In* The Development of *Drosophla melanogaster*. Cold Spring Harbor Laboratory Press. 517-608.

Martinez Arias, A. 1993b. Development and patterning of the larval epidermis of Drosophila. *In* The Development of Drosophila melanogaster. Vol. 1. M. Bate and A. Martinez Arias, editors. Cold Spring Harbor Laboratory Press, Plainview, New York. 517-608.

Maskos, K., and W. Bode. 2003. Structural basis of matrix metalloproteinases and tissue inhibitors of metalloproteinases. *Mol Biotechnol*. 25:241-266.

Massova, I., L.P. Kotra, R. Fridman, and S. Mobashery. 1998. Matrix metalloproteinases: structures, evolution, and diversification. *The FASEB journal : official publication of the Federation of American Societies for Experimental Biology*. 12:1075-1095.

Matsubayashi, Y., M. Ebisuya, S. Honjoh, and E. Nishida. 2004a. ERK activation propagates in epithelial cell sheets and regulates their migration during wound healing. *Current biology : CB*. 14:731-735.

Matsubayashi, Y., M. Ebisuya, S. Honjoh, and E. Nishida. 2004b. ERK activation propagates in epithelial cell sheets and regulates their migration during wound healing. *Current biology : CB*. 14:731-735.

McGuire, J.K., Q. Li, and W.C. Parks. 2003. Matrilysin (matrix metalloproteinase-7) mediates E-cadherin ectodomain shedding in injured lung epithelium. *Am J Pathol*. 162:1831-1843.

McQuibban, G.A., G.S. Butler, J.H. Gong, L. Bendall, C. Power, I. Clark-Lewis, and C.M. Overall. 2001. Matrix metalloproteinase activity inactivates the CXC chemokine stromal cell-derived factor-1. *The Journal of biological chemistry*. 276:43503-43508.

McQuibban, G.A., J.H. Gong, E.M. Tam, C.A. McCulloch, I. Clark-Lewis, and C.M. Overall. 2000. Inflammation dampened by gelatinase A cleavage of monocyte chemoattractant protein-3. *Science*. 289:1202-1206.

McQuibban, G.A., J.H. Gong, J.P. Wong, J.L. Wallace, I. Clark-Lewis, and C.M. Overall. 2002. Matrix metalloproteinase processing of monocyte chemoattractant proteins generates CC chemokine receptor antagonists with anti-inflammatory properties in vivo. *Blood*. 100:1160-1167.

Medzhitov, R. 2008. Origin and physiological roles of inflammation. *Nature*. 454:428-435.

Meister, M. 2004. Blood cells of Drosophila: cell lineages and role in host defence. *Curr Opin Immunol*. 16:10-15.

Meister, M., and M. Lagueux. 2003. Drosophila blood cells. *Cell Microbiol*. 5:573-580.

Menke, N.B., K.R. Ward, T.M. Witten, D.G. Bonchev, and R.F. Diegelmann. 2007. Impaired wound healing. *Clinics in Dermatology*. 25:19-25.

Meszaros, A.J., J.S. Reichner, and J.E. Albina. 2000. Macrophage-induced neutrophil apoptosis. *Journal of immunology*. 165:435-441.

Miller, C.M., A. Page-McCaw, and H.T. Broihier. 2008. Matrix metalloproteinases promote motor axon fasciculation in the Drosophila embryo. *Development*. 135:95-109.

Mitchison, T.J., and L.P. Cramer. 1996. Actin-based cell motility and cell locomotion. *Cell*. 84:371-379.

Miyamori, H., T. Takino, Y. Kobayashi, H. Tokai, Y. Itoh, M. Seiki, and H. Sato. 2001. Claudin promotes activation of pro-matrix metalloproteinase-2 mediated by membrane-type matrix metalloproteinases. *The Journal of biological chemistry*. 276:28204-28211.

Mogilner, A., and K. Keren. 2009a. The shape of motile cells. *Curr Biol*. 19:R762-771.

Mogilner, A., and K. Keren. 2009b. The shape of motile cells. *Current biology : CB*. 19:R762-771.

Mohammed, F.F., D.S. Smookler, S.E. Taylor, B. Fingleton, Z. Kassiri, O.H. Sanchez, J.L. English, L.M. Matrisian, B. Au, W.C. Yeh, and R. Khokha. 2004. Abnormal TNF activity in Timp3-/- mice leads to chronic hepatic inflammation and failure of liver regeneration. *Nat Genet*. 36:969-977.

Mohan, R., S.K. Chintala, J.C. Jung, W.V. Villar, F. McCabe, L.A. Russo, Y. Lee, B.E. McCarthy, K.R. Wollenberg, J.V. Jester, M. Wang, H.G. Welgus, J.M. Shipley, R.M. Senior, and M.E. Fini. 2002. Matrix metalloproteinase gelatinase B (MMP-9) coordinates and effects epithelial regeneration. *The Journal of biological chemistry*. 277:2065-2072.

Morgunova, E., A. Tuuttila, U. Bergmann, M. Isupov, Y. Lindqvist, G. Schneider, and K. Tryggvason. 1999. Structure of human pro-matrix metalloproteinase-2: activation mechanism revealed. *Science*. 284:1667-1670.

Morin, X., R. Daneman, M. Zavortink, and W. Chia. 2001. A protein trap strategy to detect GFP-tagged proteins expressed from their endogenous loci in Drosophila. *Proc Natl Acad Sci U S A*. 98:15050-15055.

Mosser, D.M., and X. Zhang. 2008. Activation of murine macrophages. *Curr Protoc Immunol*. Chapter 14:Unit 14 12.

Mott, J.D., and Z. Werb. 2004. Regulation of matrix biology by matrix metalloproteinases. *Current opinion in cell biology*. 16:558-564.

Murphy, M.J. 2011. Wound Healing Disorders: Chronic Wounds and Keloids
Molecular Diagnostics in Dermatology and Dermatopathology. M.J. Murphy, editor. Humana Press. 359-368.

Murray, M.J., L.I. Fessler, and J. Palka. 1995. Changing distributions of extracellular matrix components during early wing morphogenesis in Drosophila. *Dev. Biol.* 168:150-165.

Nappi, A.J., F. Frey, and Y. Carton. 2005. Drosophila serpin 27A is a likely target for immune suppression of the blood cell-mediated melanotic encapsulation response. *Journal of insect physiology*. 51:197-205.

Niethammer, P., C. Grabher, A.T. Look, and T.J. Mitchison. 2009. A tissue-scale gradient of hydrogen peroxide mediates rapid wound detection in zebrafish. *Nature*. 459:996-999.

Noselli, S. 1998. JNK signaling and morphogenesis in Drosophila. *Trends Genet*. 14:33-38.

Oblander, S.A., Z. Zhou, B.G. Galvez, B. Starcher, J.M. Shannon, M. Durbeej, A.G. Arroyo, K. Tryggvason, and S.S. Apte. 2005. Distinctive functions of membrane type 1 matrix-metalloprotease (MT1-MMP or MMP-14) in lung and submandibular gland development are independent of its role in pro-MMP-2 activation. *Dev Biol*. 277:255-269.

Olson, M.W., M.M. Bernardo, M. Pietila, D.C. Gervasi, M. Toth, L.P. Kotra, I. Massova, S. Mobashery, and R. Fridman. 2000. Characterization of the monomeric and dimeric forms of latent and active matrix metalloproteinase-9. Differential rates for activation by stromelysin 1. *The Journal of biological chemistry*. 275:2661-2668.

Osterud, B., and S.I. Rapaport. 1977. Activation of factor IX by the reaction product of tissue factor and factor VII: additional pathway for initiating blood coagulation. *Proceedings of the National Academy of Sciences of the United States of America*. 74:5260-5264.

Overall, C.M., A.E. King, H.F. Bigg, A. McQuibban, J. Atherstone, D.K. Sam, A.D. Ong, T.T. Lau, U.M. Wallon, Y.A. DeClerck, and E. Tam. 1999. Identification of the TIMP-2 binding site on the gelatinase A hemopexin C-domain by site-directed mutagenesis and the yeast two-hybrid system. *Annals of the New York Academy of Sciences*. 878:747-753.

Overall, C.M., G.A. McQuibban, and I. Clark-Lewis. 2002. Discovery of chemokine substrates for matrix metalloproteinases by exosite scanning: a new tool for degradomics. *Biol Chem*. 383:1059-1066.

Overall, C.M., E. Tam, G.A. McQuibban, C. Morrison, U.M. Wallon, H.F. Bigg, A.E. King, and C.R. Roberts. 2000. Domain interactions in the gelatinase A.TIMP-2.MT1-MMP activation complex. The ectodomain of the 44-kDa form of membrane type-1 matrix metalloproteinase does not modulate gelatinase A activation. *The Journal of biological chemistry*. 275:39497-39506.

Pack-Chung, E., P.T. Kurshan, D.K. Dickman, and T.L. Schwarz. 2007. A Drosophila kinesin required for synaptic bouton formation and synaptic vesicle transport. *Nature neuroscience*. 10:980-989.

Page-McCaw, A., A.J. Ewald, and Z. Werb. 2007. Matrix metalloproteinases and the regulation of tissue remodelling. *Nat Rev Mol Cell Biol*. 8:221-233.

Page-McCaw, A., J. Serano, J.M. Sante, and G.M. Rubin. 2003a. Drosophila matrix metalloproteinases are required for tissue remodeling, but not embryonic development. *Dev Cell*. 4:95-106.

Page-McCaw, A., J. Serano, J.M. Sante, and G.M. Rubin. 2003b. Drosophila matrix metalloproteinases are required for tissue remodeling, but not embryonic development. *Developmental cell*. 4:95-106.

Pal-Ghosh, S., T. Blanco, G. Tadvalkar, A. Pajoohesh-Ganji, A. Parthasarathy, J.D. Zieske, and M.A. Stepp. 2011. MMP9 cleavage of the {beta}4 integrin ectodomain leads to recurrent epithelial erosions in mice. *J Cell Sci*. 124:2666-2675.

Parks, W.C., C.L. Wilson, and Y.S. Lopez-Boado. 2004. Matrix metalloproteinases as modulators of inflammation and innate immunity. *Nat Rev Immunol*. 4:617-629.

Pastor-Pareja, J.C., and T. Xu. 2011a. Shaping Cells and Organs in Drosophila by Opposing Roles of Fat Body-Secreted Collagen IV and Perlecan. *Developmental cell*. 21:245-256.

Pastor-Pareja, J.C., and T. Xu. 2011b. Shaping cells and organs in Drosophila by opposing roles of fat body-secreted Collagen IV and perlecan. *Developmental cell*. 21:245-256.

Pilcher, B.K., J.A. Dumin, B.D. Sudbeck, S.M. Krane, H.G. Welgus, and W.C. Parks. 1997. The activity of collagenase-1 is required for keratinocyte migration on a type I collagen matrix. *The Journal of cell biology*. 137:1445-1457.

Ra, H.J., and W.C. Parks. 2007. Control of matrix metalloproteinase catalytic activity. *Matrix Biol*. 26:587-596.

Ramet, M., R. Lanot, D. Zachary, and P. Manfruelli. 2002. JNK signaling pathway is required for efficient wound healing in Drosophila. *Dev Biol*. 241:145-156.

Rao, S., C. Lang, E.S. Levitan, and D.L. Deitcher. 2001. Visualization of neuropeptide expression, transport, and exocytosis in Drosophila melanogaster. *J Neurobiol*. 49:159-172.

Razzell, W., W. Wood, and P. Martin. 2011. Swatting flies: modelling wound healing and inflammation in Drosophila. *Disease models & mechanisms*. 4:569-574.

Rebustini, I.T., C. Myers, K.S. Lassiter, A. Surmak, L. Szabova, K. Holmbeck, V. Pedchenko, B.G. Hudson, and M.P. Hoffman. 2009. MT2-MMP-Dependent Release of Collagen IV NC1 Domains Regulates Submandibular Gland Branching Morphogenesis. *Dev Cell*. 17:482-493.

Rizki, M.T., and R.M. Rizki. 1959. Functional significance of the crystal cells in the larva of Drosophila melanogaster. *J Biophys Biochem Cytol*. 5:235-240.

Rudolph-Owen, L.A., D.L. Hulboy, C.L. Wilson, J. Mudgett, and L.M. Matrisian. 1997. Coordinate expression of matrix metalloproteinase family members in the uterus of normal, matrilysin-deficient, and stromelysin-1-deficient mice. *Endocrinology*. 138:4902-4911.

Saarialho-Kere, U., E. Kerkela, T. Jahkola, S. Suomela, J. Keski-Oja, and J. Lohi. 2002. Epilysin (MMP-28) expression is associated with cell proliferation during epithelial repair. *The Journal of investigative dermatology*. 119:14-21.

Sabeh, F., X.Y. Li, T.L. Saunders, R.G. Rowe, and S.J. Weiss. 2009. Secreted versus membrane-anchored collagenases: relative roles in fibroblast-dependent collagenolysis and invasion. *The Journal of biological chemistry*. 284:23001-23011.

Sanchez Alvarado, A. 2006. Planarian regeneration: its end is its beginning. *Cell*. 124:241-245.

Santavicca, M., A. Noel, H. Angliker, I. Stoll, J.P. Segain, P. Anglard, M. Chretien, N. Seidah, and P. Basset. 1996. Characterization of structural determinants and molecular mechanisms involved in pro-stromelysin-3 activation by 4-aminophenylmercuric acetate and furin-type convertases. *The Biochemical journal*. 315 (Pt 3):953-958.

Sawicki, G., E. Salas, J. Murat, H. Miszta-Lane, and M.W. Radomski. 1997. Release of gelatinase A during platelet activation mediates aggregation. *Nature*. 386:616-619.

Scherfer, C., C. Karlsson, O. Loseva, G. Bidla, A. Goto, J. Havemann, M.S. Dushay, and U. Theopold. 2004. Isolation and characterization of hemolymph clotting factors in Drosophila melanogaster by a pullout method. *Current biology : CB*. 14:625-629.

Schneider, I. 1972. Cell lines derived from late embryonic stages of Drosophila melanogaster. *J Embryol Exp Morphol*. 27:353-365.

Schneider, M., A.A. Khalil, J. Poulton, C. Castillejo-Lopez, D. Egger-Adam, A. Wodarz, W.M. Deng, and S. Baumgartner. 2006. Perlecan and Dystroglycan act at the basal side of the Drosophila follicular epithelium to maintain epithelial organization. *Development*. 133:3805-3815.

Schultz, G.S., and A. Wysocki. 2009. Interactions between extracellular matrix and growth factors in wound healing. *Wound Repair Regen*. 17:153-162.

Sela-Passwell, N., G. Rosenblum, T. Shoham, and I. Sagi. 2010. Structural and functional bases for allosteric control of MMP activities: can it pave the path for selective inhibition? *Biochimica et biophysica acta*. 1803:29-38.

Sharma, G.D., J. He, and H.E. Bazan. 2003. p38 and ERK1/2 coordinate cellular migration and proliferation in epithelial wound healing: evidence of cross-talk activation between MAP kinase cascades. *The Journal of biological chemistry*. 278:21989-21997.

Shaw, T.J., and P. Martin. 2009. Wound repair at a glance. *J Cell Sci*. 122:3209-3213.

Shephard, P., G. Martin, S. Smola-Hess, G. Brunner, T. Krieg, and H. Smola. 2004. Myofibroblast differentiation is induced in keratinocyte-fibroblast co-cultures and is antagonistically regulated by endogenous transforming growth factor-beta and interleukin-1. *Am J Pathol*. 164:2055-2066.

Silverthorn, D.U. 2004. Human Physiology: An Integrated Approach. Pearson Education, Inc., San Francisco, CA.

Sims, P.J., E.M. Faioni, T. Wiedmer, and S.J. Shattil. 1988. Complement proteins C5b-9 cause release of membrane vesicles from the platelet surface that are enriched in the membrane receptor for coagulation factor Va and express prothrombinase activity. *The Journal of biological chemistry*. 263:18205-18212.

Singer, A.J., and R.A. Clark. 1999. Cutaneous wound healing. *N Engl J Med*. 341:738-746.

Singh, P., C. Chen, S. Pal-Ghosh, M.A. Stepp, D. Sheppard, and L. Van De Water. 2009. Loss of integrin alpha9beta1 results in defects in proliferation, causing poor re-epithelialization during cutaneous wound healing. *The Journal of investigative dermatology*. 129:217-228.

Sluss, H.K., Z. Han, T. Barrett, D.C. Goberdhan, C. Wilson, R.J. Davis, and Y.T. Ip. 1996. A JNK signal transduction pathway that mediates morphogenesis and an immune response in Drosophila. *Genes & development*. 10:2745-2758.

Smith, A.V., and T.L. Orr-Weaver. 1991. The regulation of the cell cycle during Drosophila embryogenesis: the transition to polyteny. *Development*. 112:997-1008.

Spicer, E.K., R. Horton, L. Bloem, R. Bach, K.R. Williams, A. Guha, J. Kraus, T.C. Lin, Y. Nemerson, and W.H. Konigsberg. 1987. Isolation of cDNA clones coding for human tissue factor: primary structure of the protein and cDNA. *Proceedings of the National Academy of Sciences of the United States of America*. 84:5148-5152.

Srivastava, A., J.C. Pastor-Pareja, T. Igaki, R. Pagliarini, and T. Xu. 2007. Basement membrane remodeling is essential for Drosophila disc eversion and tumor invasion. *Proc Natl Acad Sci U S A*. 104:2721-2726.

Steffensen, B., U.M. Wallon, and C.M. Overall. 1995. Extracellular matrix binding properties of recombinant fibronectin type II-like modules of human 72-kDa gelatinase/type IV collagenase. High affinity binding to native type I collagen but not native type IV collagen. *The Journal of biological chemistry*. 270:11555-11566.

Stevens, L.J., and A. Page-McCaw. 2012. A Secreted MMP Is Required for Re-epithelialization during Wound Healing. *Molecular Biology of the Cell*.

Stramer, B., W. Wood, M.J. Galko, M.J. Redd, A. Jacinto, S.M. Parkhurst, and P. Martin. 2005. Live imaging of wound inflammation in Drosophila embryos reveals key roles for small GTPases during in vivo cell migration. *J Cell Biol*. 168:567-573.

Stramer, B.M., R. Mori, and P. Martin. 2007. The inflammation-fibrosis link? A Jekyll and Hyde role for blood cells during wound repair. *The Journal of investigative dermatology*. 127:1009-1017.

Strongin, A.Y., I. Collier, G. Bannikov, B.L. Marmer, G.A. Grant, and G.I. Goldberg. 1995. Mechanism of cell surface activation of 72-kDa type IV collagenase. Isolation of the activated form of the membrane metalloprotease. *The Journal of biological chemistry*. 270:5331-5338.

Sung, Y.J., Z. Sung, C.L. Ho, M.T. Lin, J.S. Wang, S.C. Yang, Y.J. Chen, and C.H. Lin. 2003. Intercellular calcium waves mediate preferential cell growth toward the wound edge in polarized hepatic cells. *Experimental cell research*. 287:209-218.

Suzuki, M., G. Raab, M.A. Moses, C.A. Fernandez, and M. Klagsbrun. 1997. Matrix metalloproteinase-3 releases active heparin-binding EGF-like growth factor by cleavage at a specific juxtamembrane site. *J Biol Chem*. 272:31730-31737.

Theilgaard-Monch, K., S. Knudsen, P. Follin, and N. Borregaard. 2004. The transcriptional activation program of human neutrophils in skin lesions supports their important role in wound healing. *Journal of immunology*. 172:7684-7693.

Tholozan, F.M.D., C. Gribbon, Z. Li, M.W. Goldberg, A.R. Prescott, N. McKie, and R.A. Quinlan. 2007. FGF-2 Release from the Lens Capsule by MMP-2 Maintains Lens Epithelial Cell Viability. *Molecular Biology of the Cell*. 18:4222-4231.

Thomas, G. 2002. Furin at the cutting edge: from protein traffic to embryogenesis and disease. *Nature reviews. Molecular cell biology*. 3:753-766.

Tschesche, H., A. Lichte, O. Hiller, A. Oberpichler, F.H. Buttner, and E. Bartnik. 2000. Matrix metalloproteinases (MMP-8, -13, and -14) interact with the clotting system and degrade fibrinogen and factor XII (Hagemann factor). *Adv Exp Med Biol*. 477:217-228.

Uhlirova, M., and D. Bohmann. 2006. JNK- and Fos-regulated Mmp1 expression cooperates with Ras to induce invasive tumors in Drosophila. *EMBO J.* 25:5294-5304.

Vaisar, T., S.Y. Kassim, I.G. Gomez, P.S. Green, S. Hargarten, P.J. Gough, W.C. Parks, C.L. Wilson, E.W. Raines, and J.W. Heinecke. 2009. MMP-9 sheds the beta2 integrin subunit (CD18) from macrophages. *Mol Cell Proteomics*. 8:1044-1060.

Van Wart, H.E., and H. Birkedal-Hansen. 1990. The cysteine switch: a principle of regulation of metalloproteinase activity with potential applicability to the entire matrix metalloproteinase gene family. *Proceedings of the National Academy of Sciences of the United States of America*. 87:5578-5582.

Verkhusha, V.V., S. Tsukita, and H. Oda. 1999. Actin dynamics in lamellipodia of migrating border cells in the Drosophila ovary revealed by a GFP-actin fusion protein. *FEBS Lett*. 445:395-401.

Vyalov, S., A. Desmouliere, and G. Gabbiani. 1993. GM-CSF-induced granulation tissue formation: relationships between macrophage and myofibroblast accumulation. *Virchows Arch B Cell Pathol Incl Mol Pathol*. 63:231-239.

Wang, Q., M. Uhlirova, and D. Bohmann. 2010. Spatial restriction of FGF signaling by a matrix metalloprotease controls branching morphogenesis. *Developmental cell*. 18:157-164.

Wang, X., R.E. Harris, L.J. Bayston, and H.L. Ashe. 2008. Type IV collagens regulate BMP signalling in Drosophila. *Nature*. 455:72-77.

Wang, Y., and M.A. McNiven. 2012. Invasive matrix degradation at focal adhesions occurs via protease recruitment by a FAK-p130Cas complex. *The Journal of cell biology*. 196:375-385.

Wang, Z., R. Juttermann, and P.D. Soloway. 2000. TIMP-2 is required for efficient activation of proMMP-2 in vivo. *The Journal of biological chemistry*. 275:26411-26415.

Weber, B.H., G. Vogt, R.C. Pruett, H. Stohr, and U. Felbor. 1994. Mutations in the tissue inhibitor of metalloproteinases-3 (TIMP3) in patients with Sorsby's fundus dystrophy. *Nat Genet*. 8:352-356.

Wei, S., Z. Xie, E. Filenova, and K. Brew. 2003. Drosophila TIMP is a potent inhibitor of MMPs and TACE: similarities in structure and function to TIMP-3. *Biochemistry*. 42:12200-12207.

Weiss, S.J. 1989. Tissue destruction by neutrophils. *The New England journal of medicine*. 320:365-376.

Werner, S., and R. Grose. 2003. Regulation of wound healing by growth factors and cytokines. *Physiological reviews*. 83:835-870.

Will, H., S.J. Atkinson, G.S. Butler, B. Smith, and G. Murphy. 1996a. The soluble catalytic domain of membrane type 1 matrix metalloproteinase cleaves the propeptide of progelatinase A and initiates autoproteolytic activation. Regulation by TIMP-2 and TIMP-3. *J Biol Chem*. 271:17119-17123.

Will, H., S.J. Atkinson, G.S. Butler, B. Smith, and G. Murphy. 1996b. The soluble catalytic domain of membrane type 1 matrix metalloproteinase cleaves the propeptide of progelatinase A and initiates autoproteolytic activation. Regulation by TIMP-2 and TIMP-3. *The Journal of biological chemistry*. 271:17119-17123.

Wood, W., C. Faria, and A. Jacinto. 2006. Distinct mechanisms regulate hemocyte chemotaxis during development and wound healing in Drosophila melanogaster. *J Cell Biol*. 173:405-416.

Wood, W., A. Jacinto, R. Grose, S. Woolner, J. Gale, C. Wilson, and P. Martin. 2002a. Wound healing recapitulates morphogenesis in Drosophila embryos. *Nat Cell Biol*. 4:907-912.

Wood, W., A. Jacinto, R. Grose, S. Woolner, J. Gale, C. Wilson, and P. Martin. 2002b. Wound healing recapitulates morphogenesis in Drosophila embryos. *Nat Cell Biol*. 4:907-912.

Wu, Y., A.R. Brock, Y. Wang, K. Fujitani, R. Ueda, and M.J. Galko. 2009a. A blood-borne PDGF/VEGF-like ligand initiates wound-induced epidermal cell migration in Drosophila larvae. *Curr Biol*. 19:1473-1477.

Wu, Y., A.R. Brock, Y. Wang, K. Fujitani, R. Ueda, and M.J. Galko. 2009b. A blood-borne PDGF/VEGF-like ligand initiates wound-induced epidermal cell migration in Drosophila larvae. *Current biology : CB*. 19:1473-1477.

Wulff, B.C., A.E. Parent, M.A. Meleski, L.A. Dipietro, M.E. Schrementi, and T.A. Wilgus. 2012. Mast Cells Contribute to Scar Formation during Fetal Wound Healing. *The Journal of investigative dermatology*. 132:458-465.

Yasothornsrikul, S., W.J. Davis, G. Cramer, D.A. Kimbrell, and C.R. Dearolf. 1997. viking: identification and characterization of a second type IV collagen in Drosophila. *Gene*. 198:17-25.

Yasunaga, K., T. Kanamori, R. Morikawa, E. Suzuki, and K. Emoto. 2010. Dendrite reshaping of adult Drosophila sensory neurons requires matrix metalloproteinase-mediated modification of the basement membranes. *Developmental cell*. 18:621-632.

Yu, Q., and I. Stamenkovic. 2000. Cell surface-localized matrix metalloproteinase-9 proteolytically activates TGF-beta and promotes tumor invasion and angiogenesis. *Genes Dev*. 14:163-176.

Zeitlinger, J., and D. Bohmann. 1999. Thorax closure in Drosophila: involvement of Fos and the JNK pathway. *Development*. 126:3947-3956.

Zenz, R., H. Scheuch, P. Martin, C. Frank, R. Eferl, L. Kenner, M. Sibilia, and E.F. Wagner. 2003. c-Jun regulates eyelid closure and skin tumor development through EGFR signaling. *Developmental cell*. 4:879-889.

Zhang, S., G.M. Dailey, E. Kwan, B.M. Glasheen, G.E. Sroga, and A. Page-McCaw. 2006. An MMP liberates the Ninjurin A ectodomain to signal a loss of cell adhesion. *Genes Dev*. 20:1899-1910.

Zhang, Y., X.T. Bai, K.Y. Zhu, Y. Jin, M. Deng, H.Y. Le, Y.F. Fu, Y. Chen, J. Zhu, A.T. Look, J. Kanki, Z. Chen, S.J. Chen, and T.X. Liu. 2008. In vivo interstitial migration of primitive macrophages mediated by JNK-matrix metalloproteinase 13 signaling in response to acute injury. *J Immunol*. 181:2155-2164.

Zhou, Z., S.S. Apte, R. Soininen, R. Cao, G.Y. Baaklini, R.W. Rauser, J. Wang, Y. Cao, and K. Tryggvason. 2000a. Impaired endochondral ossification and angiogenesis in mice deficient in membrane-type matrix metalloproteinase I. *Proceedings of the National Academy of Sciences of the United States of America*. 97:4052-4057.

Zhou, Z., S.S. Apte, R. Soininen, R. Cao, G.Y. Baaklini, R.W. Rauser, J. Wang, Y. Cao, and K. Tryggvason. 2000b. Impaired endochondral ossification and angiogenesis in mice deficient in membrane-type matrix metalloproteinase I. *PNAS*. 97:4052-4057.